

2015

# A Silylation-Based Kinetic Resolution of Hydroxy Lactones and Lactams with Subsequent Mechanistic Investigations

Robert W. Clark  
*University of South Carolina*

Follow this and additional works at: <https://scholarcommons.sc.edu/etd>

 Part of the [Chemistry Commons](#)

---

## Recommended Citation

Clark, R. W.(2015). *A Silylation-Based Kinetic Resolution of Hydroxy Lactones and Lactams with Subsequent Mechanistic Investigations*. (Doctoral dissertation). Retrieved from <https://scholarcommons.sc.edu/etd/3662>

This Open Access Dissertation is brought to you by Scholar Commons. It has been accepted for inclusion in Theses and Dissertations by an authorized administrator of Scholar Commons. For more information, please contact [dillarda@mailbox.sc.edu](mailto:dillarda@mailbox.sc.edu).

A Silylation-Based Kinetic Resolution of Hydroxy Lactones and  
Lactams with Subsequent Mechanistic Investigations

by

Robert W. Clark

Bachelor of Science  
The Citadel, The Military College of South Carolina, 2009

---

Submitted in Partial Fulfillment of the Requirements

For the Degree of Doctor of Philosophy in

Chemistry

College of Arts and Sciences

University of South Carolina

2015

Accepted by:

Sheryl L. Wiskur, Major Professor

John J. Lavigne, Committee Member

Andrew B. Greytak, Committee Member

Mike D. Wyatt, Committee Member

Lacy Ford, Senior Vice Provost and Dean of Graduate Studies

© Copyright by Robert W. Clark, 2015  
All Rights Reserved.

## Acknowledgements

It is impossible to mention all of the people that have had an impact on my life up until this point. First and foremost I must thank my advisor Dr. Sheryl Wiskur for the countless hours of personal attention and mentorship. Thanks to all those that provided new and interesting research goals during my graduate tenure. Dr. Cody Sheppard was instrumental in the seminal works that eventually led to the studies herein. To Max Deaton, in the end, you taught me more than I taught you. It was a pleasure to mentor you and to be a spectator of your excitement for science. Dr. Ravish Akhani, our fruitful and meaningful discussions both in and outside of the lab will be remembered. To those in the Wiskur group, keep your heads up you will have accomplished so much before you even realize it. My passion for scientific study began long before my arrival at the University of South Carolina. I know I would not be here without the passion for synthetic organic chemistry instilled upon me while working in the lab with Dr. Randy Blanton and the scientific interest inspired from another exceptional teacher, Mrs. Sherry Arledge. I am fortunate to have an extremely supportive family. My parents both set the example of hard work and dedication that have unquestionably led to my success thus far. Words cannot express my gratitude for all your love and support. Finally to my wife Taylor, you are the foundation upon which I have built all of my success. You have been with me and for me through the good times and the bad. I am so thankful and feel blessed to have you in my life. You have supported me with a smile on your face, and I love you for that. Can you believe it? We finally made it.

## Abstract

The work contained herein focuses on the methodology and design of new reactions for the production of stereoenriched compounds. The primary focus of research discussed is kinetic resolution, a classic and powerful methodology for the separation of a single enantiomer from a racemic mixture. In 2011, a silylation-based resolution catalyzed by a chiral isothioureia produced synthetically useful selectivity factors for mono-functional secondary alcohols. In chapter 2, this methodology was subsequently expanded to include  $\alpha$ -hydroxy lactones with selectivity factors up to 100. This study resulted in the most selective reaction reported to date for the aforementioned silylation-based resolution. In addition to lactones,  $\alpha$ -hydroxy lactams, amides and esters were resolved with synthetically useful enantioselectivity. This is notably the first successful non-enzymatic resolution of hydroxy lactams ever reported.

In an effort to remove chromatography completely from the kinetic resolution process, an alternate polymer-supported version of the reaction was studied. The successful use of polymer-bound triphenylsilyl chloride to eliminate chromatographic purification steps is contained in Chapter 3. The polymer-supported reagent was utilized to produce useful selectivities for the resolution of benzylic alcohols and  $\alpha$ -hydroxy lactones. The polymer-bound silyl source was also successfully recycled without loss in enantioselectivity.

In Chapter 4, our attempts to elucidate the mechanism of the kinetic resolution via reaction progress kinetic analysis will be demonstrated. Preliminary results of this

investigation suggest the reaction is very sensitive to silyl chloride concentration. This finding suggests a more complex reaction than our previous hypothesis. Additionally, a stereoenriched silyl chloride was tested in the silylation reaction. The overall inversion of stereochemistry observed in these experiments does not support our previously proposed double inversion mechanism. Results of the kinetic studies and chiral probe reactions will be utilized to propose a plausible mechanistic cycle for the silylation reaction.

Finally, research to expand silylation-based resolutions to include an asymmetric borane Lewis acid catalyzed silicon-oxygen coupling will be highlighted. A variety of stereogenic at silicon silanes were prepared and tested in the reaction. The low diastereoselectivity of these reactions does not support the ability to affect resolution of racemic alcohols via this method. The reaction was further complicated by reactivity that appeared substrate-dependent. The results of the silicon-oxygen coupling kinetic resolution of substrates to include secondary alcohols and propargylic alcohols will be discussed in Chapter 5.

## Table of Contents

Acknowledgements.....	iii
Abstract.....	iv
List of Tables .....	x
List of Schemes.....	xi
List of Figures.....	xv
Chapter 1 Foundations and Current Outlook of Enantioselective Methodologies .....	1
1.1. Introduction and Scope .....	1
1.2. Chirality and its Implications to Biology.....	1
1.3. Methods of Obtaining Enantiopure Molecules .....	4
1.4. Organocatalyzed Resolutions.....	15
1.5. Silylation-Based Resolution Methods for the Preparation of Non-Racemic Alcohols.....	21
1.6. Conclusions and Outlook.....	27
1.7. References .....	29
Chapter 2 Silylation-Based Kinetic Resolution of $\alpha$ -Hydroxy Lactones and Lactams ....	36
2.1. Introduction and Scope.....	36

2.2. Initial Investigations and Optimization.....	40
2.3. Synthesis of Hydroxy Lactones .....	44
2.4. Examining the Lactones in the Silylation-Based Kinetic Resolution .....	48
2.5. Synthesis of Hydroxy Lactams .....	50
2.6. Testing the Lactams in the Silylation-Based Kinetic Resolution .....	51
2.7. Synthesis of Amides and Esters .....	54
2.8. Testing Amides and Esters in the Silylation-Based Resolution.....	55
2.9. Conclusions and Outlook.....	56
2.10. Experimental .....	58
2.11. References .....	135
 Chapter 3 Polymer-Bound Triphenylsilyl Chloride for the Kinetic Resolution of Secondary Alcohols .....	 142
3.1 Introduction and Scope.....	142
3.2 Polymerization-Based Kinetic Resolutions .....	146
3.3 Enzymatic Kinetic Resolutions on Polymer Supports .....	149
3.4 Silylation-Based Kinetic Resolutions on Polymer Supports.....	151
3.5 Synthesis of Polystyrene Supported Triphenylsilyl Chloride .....	153
3.6 Optimization of the Polymer-Bound Silyl Source .....	155



3.7 Substrate Scope of the Resolution Utilizing Polymer-Bound Silyl-Chloride.....	156
3.8 Recycling and Subsequent Reuse of Polymer-Bound Silyl Chlorides in Kinetic Resolution .....	158
3.9 Conclusion and Outlook.....	159
3.10 Experimental .....	161
3.11 References .....	186
<b>Chapter 4 Mechanistic Investigations of a Silylation-Based Kinetic Resolution: Reaction Progress Kinetic Analysis.....</b>	<b>191</b>
4.1. Introduction and Scope.....	191
4.2. Reaction Progress Kinetic Analysis: an Overview .....	196
4.3. Turnover Frequency Study: Determination of Catalyst Reaction Order .....	208
4.4. Different Excess Studies of Alcohol and Silyl Chloride.....	211
4.5. Same Excess Study: Implications for Catalyst Degradation.....	218
4.6. A Case of Zeroth Order with Respect to Base: Initial Rate Investigations .....	219
4.7. Stereogenic at Silicon Silyl Chlorides as Chiral Probes .....	222
4.8. Overall Mechanistic Picture Based on Kinetic Investigations and Other Mechanistic Studies .....	231
4.9. Conclusions and Outlook.....	234
4.10. Experimental .....	239

4.11. References .....	262
Chapter 5 Kinetic Resolution of Secondary Alcohols via Borane	
Lewis Acid Catalyzed Silylation .....	269
5.1 Introduction and Scope .....	269
5.2 Preliminary Data .....	273
5.3 Synthesis of Stereogenic Silanes.....	274
5.4 Substrate Scope Investigations.....	279
5.5 Conclusions and Outlook .....	283
5.6 Experimental .....	284
5.7 References.....	293

## List of Tables

Table 2.1 Reaction Optimization Conditions for Pantolactone .....	41
Table 2.2 Alternating the Silyl Source for the Kinetic Resolution .....	42
Table 2.3 Exploring the Effect of Base on Selectivity.....	43
Table 2.4 Testing the Effect of Solvent on Selectivity .....	44
Table 2.5 Substrate Scope of the Silylation-Based Kinetic Resolution of $\alpha$ -Hydroxy Lactones .....	49
Table 2.6 Scope of the Silylation-Based Kinetic Resolution of $\alpha$ -Hydroxy Lactams .....	52
Table 2.7 Scope of the Silylation Kinetic Resolution of Amides and Esters .....	56
Table 3.1 Noyori's Polystyrene-Supported Asymmetric Hydrogenation.....	144
Table 3.3 Enantioselective Ziegler-Natta Polymerization of Olefins.....	147
Table 3.4 Optimization of the Polystyrene-Supported Kinetic Resolution .....	155
Table 3.5 Substrate Scope of the Polymer-Bound Silylchloride Method.....	157
Table 3.6 Molecular weight parameters of polymers characterized from GPC and $^1\text{H}$ NMR .....	164
Table 3.7 Silylation-based Kinetic Resolution of 4-Chromanol Varying the Molecular Weight of Polymer Supported Silyl Source.....	167
Table 4.1 Monitoring the Enantioenrichment throughout the Reaction .....	261
Table 5.1 Initial Conditions for the Lewis Acid Catalyzed Silylation.....	274
Table 5.2 Borane Lewis Acid Catalyzed Silylation of Alcohols .....	281
Table 5.3 Further Investigations: Results with Alternate Nucleophiles .....	282

## List of Schemes

Scheme 1.1 Resolution of ( <i>S</i> )-Phenylethylamine via the L-Tartrate salt.....	7
Scheme 1.2 The CBS Asymmetric Reduction of Acetophenone .....	8
Scheme 1.3 Phosphoramidate Catalyzed Asymmetric Aldol Reaction .....	9
Scheme 1.4 Organocatalyzed Desymmetrization of Meso Diols .....	10
Scheme 1.5 A Simple Chiral Alcohol as a Building Block for a Bioactive Agent.....	16
Scheme 1.6 Chiral Pyridiniums for the Resolution of Alcohols.....	18
Scheme 1.7 Vedejs' Bicyclic Phosphine Catalyzed Kinetic Resolution .....	19
Scheme 1.8 Fu's Acylation-Based Kinetic Resolution.....	20
Scheme 1.9 Birman's Isothiourea Catalyzed Acylation-Based Kinetic Resolution .....	21
Scheme 1.10 Chiral Silanes for the Kinetic Resolution of Secondary Alcohols .....	22
Scheme 1.11 Silylation-Based Kinetic Resolution of Diols .....	23
Scheme 1.12 Tan's Regiodivergent Kinetic Resolution .....	24
Scheme 1.13 Silylation-Based Kinetic Resolution of Indanol Developed by Ishikawa.....	25
Scheme 1.14 Isothiourea Catalyzed Silylation-Based Resolution Developed by Wiskur.....	26
Scheme 1.15 One-Pot Enantiomeric Excess Polishing Sequence of Tetralol .....	27
Scheme 2.1 Silylation-Based Resolutions of Cyclic 2° Benzylic Alcohols and Potential Application to Hydroxy Lactones .....	37
Scheme 2.2 Kinetic Resolution of $\alpha$ -Hydroxy Lactones by Acyl Transfer .....	38
Scheme 2.3 Copper Catalyzed Asymmetric Carbamoylation of Pantolactone.....	39

Scheme 2.4 Synthesis of $\beta,\beta$ -Disubstituted Hydroxy Lactones .....	45
Scheme 2.5 Davis' Oxidation of $\beta,\beta$ -Dimethyl Valerolactone .....	46
Scheme 2.6 Carbonyl-Ene Reaction Route to a $\gamma, \gamma$ -Substituted Lactone .....	47
Scheme 2.7 Hetero Diels-Alder Preparation of Bicyclic Lactones.....	47
Scheme 2.8 Microwave Assisted Synthesis of Lactams from Lactones with Aryl Amines.....	51
Scheme 2.9 Direct Oxidation Route to Hydroxy Lactams .....	51
Scheme 2.10 Proposed Carbonyl- $\pi$ Interaction of N-Aryl Lactams .....	54
Scheme 2.11 Synthesis of a Benzyl Ester from Lactic Acid .....	54
Scheme 2.12 Synthesis of Hydroxy Amides.....	55
Scheme 2.13 Silylation-Based Resolution of 2-Arylcyclohexanols .....	57
Scheme 3.1 Approaches to Kinetic Resolutions on Polymer Supports .....	145
Scheme 3.2 Enantioselective Ring-Opening Polymerization of Propene Oxide.....	148
Scheme 3.3 Kinetic Resolution via Ring Opening Metathesis .....	149
Scheme 3.4 Enzyme Induced Deprotection of Polymer-Bound Alcohols.....	150
Scheme 3.5 Enzymatic Acylation of Alcohols Utilizing a Polymer Support .....	151
Scheme 3.6 Kinetic Resolution via Silicon-Oxygen Coupling on a Polymeric Support.....	152
Scheme 3.7 Design of the Polymer-Supported Silylation-Based Resolution.....	153
Scheme 3.8 Synthesis of Polystyrene-Supported Triphenylsilylchloride.....	154
Scheme 3.9 Recycling procedure and Large Scale Resolution using Polystyrene-Bound Triphenylsilyl Chloride .....	159
Scheme 3.10 Employing a Linker on the Polymer Support.....	160
Scheme 3.11 Nitroxide Mediated Polymerization to Generate Polymer-Bound Silane.	163

Scheme 4.1 Acylation-Based Kinetic Resolution Developed by Birman including Proposed Transition State .....	192
Scheme 4.2 General Approach to Linear-Free Energy Relationship Studies.....	194
Scheme 4.3 General Reaction for Kinetic Experiments .....	202
Scheme 4.4 General Reaction for Turnover Frequency Experiments .....	209
Scheme 4.5 General Reaction for “Different Excess” Experiments.....	212
Scheme 4.6 General Reaction Conditions for the “Same Excess” Studies.....	218
Scheme 4.7 General Reaction for Rate Determination with Respect to Base .....	220
Scheme 4.8 Proposed Double Inversion Pathway at Silicon .....	223
Scheme 4.9 Synthesis of Enantioenriched Silane Precursor.....	224
Scheme 4.10 Classical Resolution of Stereogenic Silanes .....	224
Scheme 4.11 Stereoretentive Reduction of Silyl Ether with $\text{LiAlH}_4$ .....	225
Scheme 4.12 Stereoretentive Chlorination with Sulfuryl Chloride .....	225
Scheme 4.13 Attempted Chlorination with Chlorine Gas .....	226
Scheme 4.14 Stereoenriched Chlorosilanes for the Silylation of ( <i>R</i> )-Tetralol .....	227
Scheme 4.15 Stereoretentive Reduction of a Diastereomeric Silyl Ether .....	228
Scheme 4.16 Stereoenriched Chlorosilanes for the Silylation of Cyclohexanol .....	229
Scheme 4.17 Plausible Explanation for Inversion of Configuration at Silicon .....	230
Scheme 4.18 Hypothetical Intermediates to Explain Order in Silyl Chloride.....	232
Scheme 4.19 Removal of Chloride with a Non-Coordinating Anion.....	233
Scheme 4.20 Chloride Containing Additive in the Silylation Reaction .....	234
Scheme 4.21 Evaluating the Kinetics of Alternate Silyl Sources.....	237
Scheme 4.22 Alternate Triphenylsilyl Sources in the Kinetic Resolution.....	238
Scheme 5.1 Proposed Lewis Acid Catalyzed Kinetic Resolution .....	269

Scheme 5.2 Synthesis of a Stereoenriched Silane from ( <i>S</i> )-BINOL .....	275
Scheme 5.3 Synthesis of Stereogenic at Silicon Silanes.....	276
Scheme 5.4 Preparation of Sterically Hindered <i>tert</i> -butylmethylphenylsilane .....	277
Scheme 5.5 Cyclic Silanes via a Two-Step Protocol.....	278
Scheme 5.6 Use of Racemic Silanes in Initial Investigations.....	279
Scheme 5.7 Asymmetric Silicon-Oxygen Coupling Catalyzed by an Axillary Chiral Borane .....	284

## List of Figures

Figure 1.1 A Simple Pair of Enantiomers .....	2
Figure 1.2 Differing Biological Activities of Asparagine Enantiomers .....	3
Figure 1.3 Anti-Cancer Natural Product Taxol.....	5
Figure 1.4 Dependency of $k_{rel}$ on the Transition State Energy Differences .....	12
Figure 1.6 Two-Point Binding in Oestreich's Silylation-Based Resolution.....	25
Figure 3.1 GPC trace of polymers of varying $M_n$ .....	163
Figure 3.2 $^1H$ NMR spectrum of the polymer synthesized.....	164
Figure 4.1 Mechanistic Cycle for the Asymmetric Acylation of 2-Arylcyclohexanols.....	195
Figure 4.2 Proposed Mechanistic Cycle for the Silylation Reaction .....	196
Figure 4.3 Employing the Pre-Equilibrium Approximation.....	197
Figure 4.4 Employing NMR Analysis to Determine IR Concentration Data .....	204
Figure 4.5 Verifying the Conversion from IR Data with NMR Analysis.....	205
Figure 4.6 Simple Graphical Rate of the Silylation-Based Resolution Reaction .....	208
Figure 4.7 Demonstration of Positive Order in Catalyst.....	210
Figure 4.8 Overlay of Turnover Frequency versus Alcohol Concentration .....	211
Figure 4.9 Determining the Order with Respect to Alcohol with "Different Excess" Protocol.....	214
Figure 4.10 Demonstrated Positive Order in Silyl Chloride.....	215
Figure 4.11 Determining the Order with Respect to Silyl Chloride with "Different Excess" Protocol.....	216



Figure 4.12 Overlay of Data with Higher Order in Silyl Chloride .....	217
Figure 4.13 Time-Adjusted “Same Excess” Experiment.....	219
Figure 4.14 Initial Rate Investigations with Various Base Concentrations .....	221
Figure 4.15 Graphical Rate Equation with Varied Base Concentration .....	222
Figure 4.16 Overall Mechanistic Picture after Mechanistic Investigations .....	235
Figure 4.17 Determination of Conversion from Aliquots and NMR Analysis.....	241
Figure 5.1 Detailed Mechanism for Borane Catalyzed Silicon-Oxygen Couplings.....	271
Figure 5.2 Diastereomeric Transition States in the Borane Catalyzed Silylation.....	272

# Chapter 1 Foundations and Current Outlook of Enantioselective Methodologies

## 1.1. Introduction and Scope

Stereochemistry and asymmetry is ubiquitous in chemistry. The primary focus herein is the development of novel methods for the production of stereochemically interesting and relevant classes of organic molecules. The information introduced in this section will provide important terminology as well as provide the driving force for subsequent research contained within.

## 1.2. Chirality and its Implications to Biology

Chirality is derived from the Greek word for “hand” and refers to the easily observed body part.<sup>1</sup> An ordinary person’s hands are three dimensional and lack any form of symmetry. As a result, the hand is asymmetric. Moreover, holding a mirror up to a person’s left hand would result in the appearance of a right hand in the mirror. The right and left hands are mirror images of one another, but the two cannot be superimposed upon each other. This phenomenon is also possible when molecules are asymmetric. The principle concern for the research herein will focus almost exclusively on molecules with tetrahedral geometry, although asymmetry can occur in other geometries. It is relatively

simple to envision an asymmetric, tetrahedral molecule by placing four different substituents on a single carbon. This asymmetric carbon-center is also termed a stereocenter at carbon. This asymmetric molecule possesses the same properties demonstrated by the pair of hands *vide supra*. These two mirror image molecules are specifically termed enantiomers<sup>2</sup> (Figure 1.1). A pair of enantiomers exhibits the same physical properties: boiling point, solubility, melting point, etc. This attribute presents a daunting challenge to separate a pair of racemates, a 50:50 mixture of enantiomers.

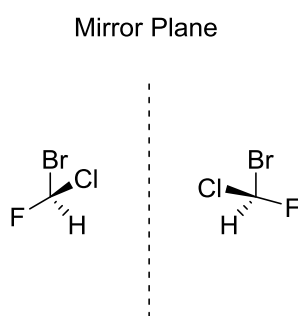


**Figure 1.1 A Simple Pair of Enantiomers**

Fortunately for life on earth, nature has developed a method for selectively preparing and utilizing chiral molecules in a single enantiomer or unichiral form. Life as we know it would not be possible without this ability, and much chemical and even philosophical debate exists to determine the origins of this selectivity. For example nature has, selected L-amino acids and D-sugars for unknown reasons. As a direct consequence, a racemic mixture of chiral, small molecules from natural and artificial sources can have differing effects on biological function.<sup>3</sup> Since biologically active or therapeutic agents are often chiral compounds, this difference in biological function may require the agent be prepared in single enantiomer form. An example of differing activities in biological

systems is D- and L-asparagine. The D-enantiomer of this amino acid is sweet; the natural L enantiomer has no taste<sup>4</sup> (Figure 1.2).

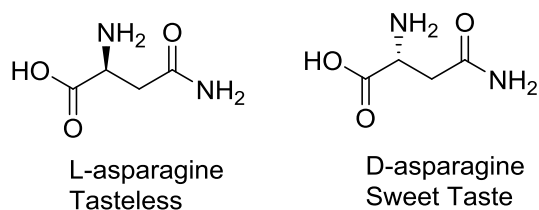


**Figure 1.2 Differing Biological Activities of Asparagine Enantiomers**

The example of D- and L-Asparagine was the first discovery of enantioselectivity at a human biological receptor.<sup>5-6</sup> This difference in physiological activity can be exploited when a chiral molecule is utilized as a therapeutic agent.<sup>7</sup> Often, one enantiomer of a drug will have the ideal biological affect, whereas the other enantiomer will have no or lower activity or worse, toxic activity.<sup>8</sup> For example, *S*-naproxen, sold under the trade name Aleve, is sold as a single enantiomer, because *R*-naproxen is less active and causes significant liver damage.<sup>9</sup> Due to the potential differences in physiological activity, a drug for sale in the American market is thus regulated by the FDA in order to avoid disastrous side effects.<sup>10</sup> These regulations require the minor enantiomer be rigorously tested to verify the stereoisomer is inert, before it can be sold as a racemic mixture. Moreover, the level of enantiopurity must be maintained for samples used in vitro through clinical trials and eventual marketing. Obviously, the multi-billion dollar per year pharmacy industry relies heavily on a number of methods to prepare enantiomers in high and consistent enantiomeric excess.<sup>11</sup> In the year 2000, 15% of the pharmaceutical market consisted of chiral drugs and 80% of the developing drugs were

chiral. Thus, the drive to develop newer and more efficient methods of producing chiral molecules as a single stereoisomer is lucrative and vital to drug development.

As a result of this importance, the analysis of the stereochemical makeup of non-racemic mixtures is vital. The term enantiomeric excess (ee) is frequently used as an expression for the level of enantioenrichment (Equation 1.1). The ee is a useful value since it is directly related to optical rotation, itself a historically common and important physical property of non-racemic mixtures. The recent advent of other methods of analyzing non-racemic mixtures and the added complexity of ee in subsequent calculations<sup>12</sup> has caused enantiomeric ratio (e.r.) to be preferred, however. The enantiomeric ratio is simply the ratio of each enantiomer in the total mixture.

$$\text{enantiomeric excess} = \left[ \frac{|[R]-[S]|}{[R]+[S]} \right] \times 100\%$$

**Equation 1.1**

### **1.3. Methods of Obtaining Enantiopure Molecules**

#### **1.3.1. Enantioenriched Compounds from Natural Sources**

For centuries man has inadvertently utilized enantiomerically enriched small molecules for the treatment of a variety of ailments. A classic example from history is the extractions from the bark of the Cinchona trees local to South America. These crude extractions were originally believed to be cures for a variety of fevers. After the advent of more advanced science, the enantiomerically pure alkaloid quinine was proven to possess antimalarial activity.<sup>3</sup>

There are, however, several disadvantages that make natural sources for bioactive compounds unfeasible. The number, quantity and variety of bioactive compounds that exist in nature are limited. The natural products produced by the plant are designed for a specific purpose within the plant itself. The bioactivity in the human body is merely a coincidence, and these compounds are not designed for a specific pharmaceutical application. Additionally, the methods for obtaining these compounds from nature often rely on crude extractions and require large amounts of the natural source. These problems have led to increased cost and undue stress on natural resources. A classic example is the anti-cancer compound Taxol<sup>13</sup> (Figure 1.3). Demand for Taxol led to the near extinction of the Pacific yew tree from which the compound is extracted from the bark. The process of obtaining the bark kills the tree. Luckily, the development of manmade synthetic approaches<sup>14-16</sup> saved the trees from extinction and was reproduced on industrial scale by Bristol-Myers Squibb. This example highlights the need to develop synthetic methods to produce compounds in single enantiomer form as opposed to dependency upon nature. In a response to this need, organic chemists have developed a variety of such methodologies.

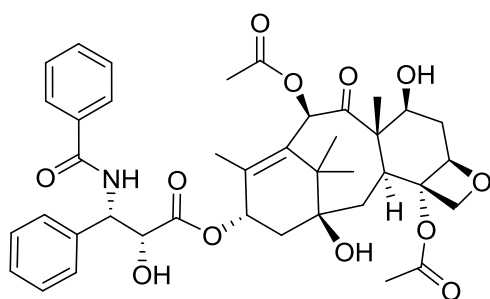
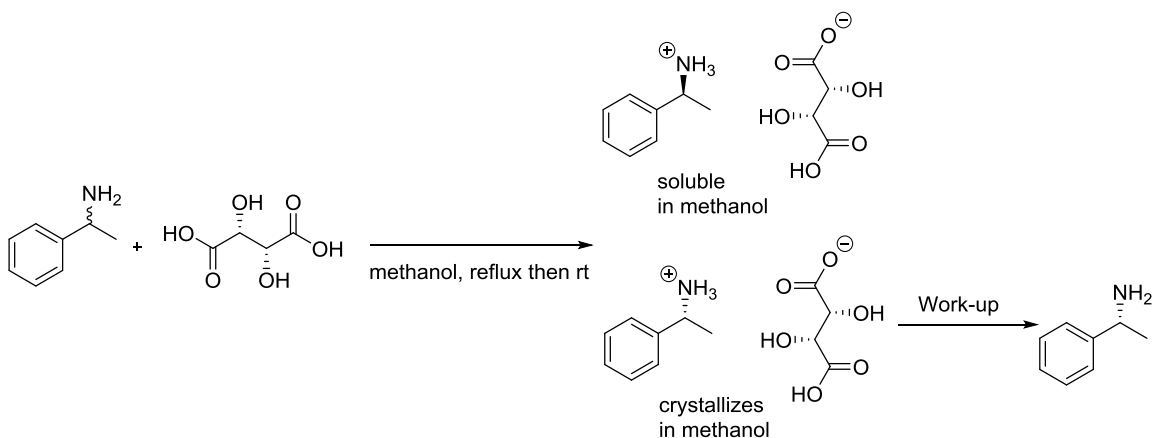


**Figure 1.3 Anti-Cancer Natural Product Taxol**

### 1.3.2. Classical Resolution

One of the oldest synthetic approaches to enantioenriched molecules is the classical resolution, which is the separation of enantiomers usually through a crystallization event. These chemical resolutions typically rely on a chiral, enantioenriched auxiliary to generate diastereomers from racemic mixtures. Chemical resolutions are not the most effective method as they rely on an enantiopure auxiliary in a stoichiometric ratio and can only achieve a 50% theoretical yield. Also, this method relies on a significant difference in properties of the newly formed diastereomeric products, such as solubility of one of the diastereomers. These physical properties are not predictable and if they are not significantly different poor separation will result. Readily available L-tartrate is a common carboxylic acid found in nature and is commonly employed as a chiral auxiliary in classical resolutions through the formation of diastereomeric salts by protonating racemic amines. In the below example,<sup>17</sup> the racemic amine, 1-phenylethylamine, is reacted with the enantiopure carboxylic acid via a Brønsted acid-base reaction (Scheme 1.1). The resulting diastereomeric salts exhibit different solubilities in methanol resulting in the selective precipitation of one diastereomeric salt. The precipitate is isolated, and after a work-up with aqueous NaOH, the desired enriched amine is obtained.



**Scheme 1.1 Resolution of (S)-Phenylethylamine via the L-Tartrate salt**

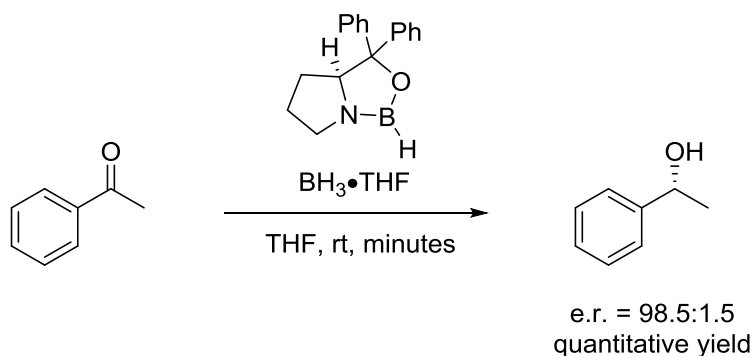
### 1.3.3. Chromatographic Resolution

It is possible to chromatographically separate a mixture of enantiomers.<sup>2</sup> For most stationary phases, a polar stationary phase (silica) is coated with a chiral, enriched material such as a cyclodextrin. The racemic mixture to be resolved is dissolved in a non-polar mobile phase. The interaction of the racemic mixture with the enriched stationary phase induces different retention times between the stereoisomers. This method has the distinct advantage of obtaining both stereoisomers as a single enantiomer after the separation. It is also the modern method of determining the enantiomeric purity of non-racemic compounds. Despite the advantages, the overall cost of this method including cost of stationary phases and solvents limits its application. The scale of chromatographic separation is also limited. Most HPLC columns can only effectively separate enantiomers up to the gram scale. Thus, this costly method when utilized on pharmaceutical industrial scale is not feasible.



### 1.3.4. Asymmetric Catalysis

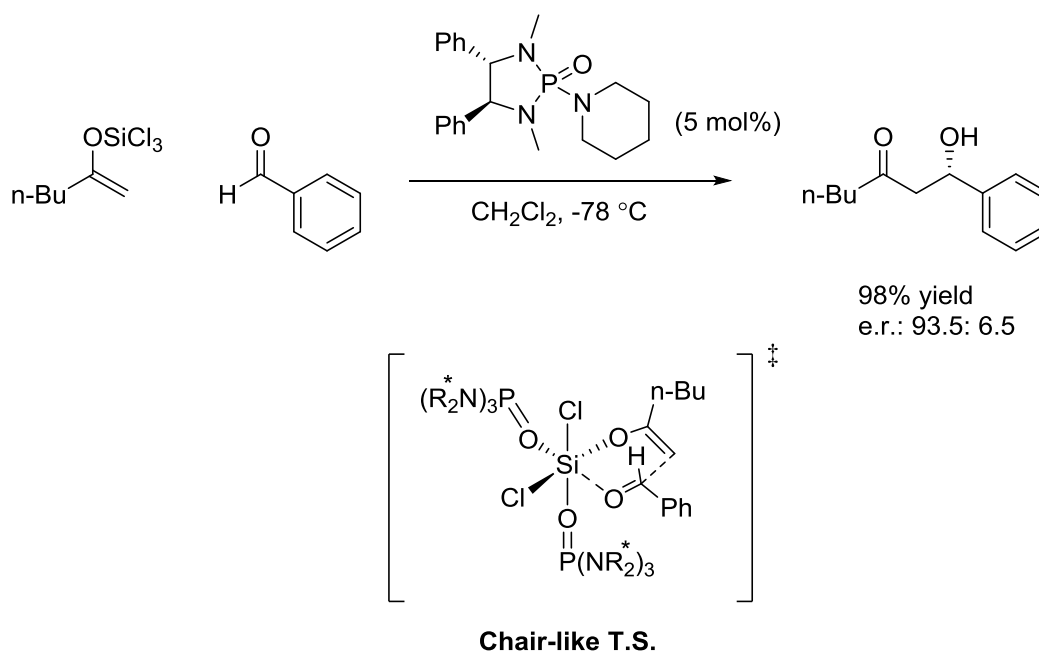
Due to the disadvantages of the aforementioned methods, chemists have developed more direct synthetic routes to enantioenriched compounds. In this way, a stereochemically enriched compound is synthesized outright as opposed to the above separation techniques. One of most direct methods is asymmetric catalysis, whereby a single enantiomer is selectively formed from an achiral starting material. Such starting materials are prochiral and can typically be made into a tetrahedral stereocenter in a single step through preferential attack on one face of the molecule, termed either Re or Si. A basic example of this methodology is the asymmetric reduction of a prochiral ketone. The Corey-Bakshi-Shibata (CBS) reduction<sup>18</sup> of acetophenone (Scheme 1.2) is highly selective and produces the enantioenriched secondary alcohol with very high enantiomeric ratios (98.5:1.5).



**Scheme 1.2 The CBS Asymmetric Reduction of Acetophenone**

Another important example of asymmetric reaction of a prochiral molecule is the aldol reaction developed by Denmark (Scheme 1.3).<sup>19</sup> The reaction uses a silyl enol ether as the nucleophile bearing a trichlorosilyl group and an aldehyde bearing no  $\alpha$ -protons such as benzaldehyde. The reaction is performed at  $-78\text{ }^{\circ}\text{C}$  in dichloromethane. Two

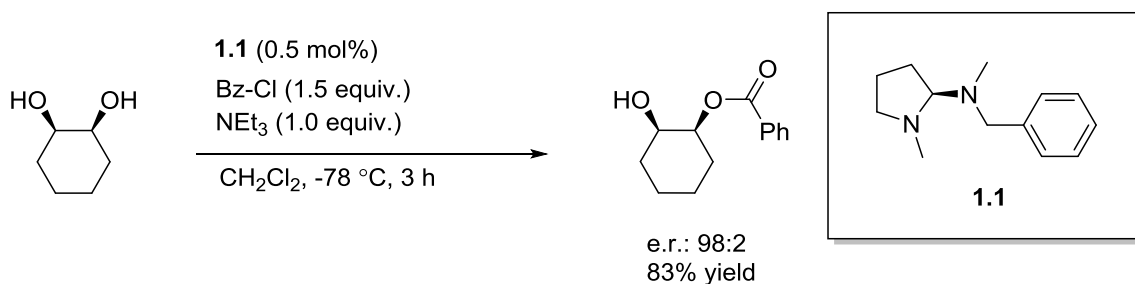
chiral phosphoramidate catalysts coordinate with the silicon thus activating it via Lewis-base activation and generating a hexavalent silicon center.<sup>20</sup> The aldol is proposed to proceed through a 6-membered, chair-like transition state (Scheme 1.3). In this mechanism, the Re face attack of the aldehyde is preferred in a 93.5:6.5 ratio. Interestingly, less electrophilic silyl groups led to reduced selectivity presumably due to changes in coordination of the silicon during the reaction.



**Scheme 1.3 Phosphoramidate Catalyzed Asymmetric Aldol Reaction**

Another more specific form of asymmetric catalysis involves desymmetrization of a meso molecule.<sup>21-22</sup> A meso molecule is a diastereomer which as a result of symmetry is achiral; these molecules also have at least diastereomer that is chiral. This method is mentioned here due to the relation to subsequent research contained in this work. Often, meso compounds can be converted into enantiomerically enriched compounds in a single step. One excellent example is the desymmetrization of meso diols.<sup>21, 23</sup> The reaction

developed by Oriyama selectively acylates one of the alcohols in the presence of the chiral diamine catalyst<sup>24</sup> **1.1** (Scheme 1.4) thus generating a chiral, enantioenriched molecule. The level of optical purity is controlled by the acylation ratio of the two alcohols as opposed to the facial discrimination discussed previously. The reaction is not trivial since the benzoyl acyl group is stable to harsh conditions, thus the stereocenter can be maintained while the non-protected alcohol is modified permanently. This method is not to be confused with kinetic resolutions, to be discussed below, just because it is based on the derivatization of alcohols. It is an example of asymmetric catalysis and is reported as such.



#### Scheme 1.4 Organocatalyzed Desymmetrization of Meso Diols

Unfortunately, the level of enantioenrichment in all of these methods remains constant throughout the reaction and is dependent upon, in the case of the CBS reduction, the ratio of Re to Si face attack by the borane. The asymmetric catalysis must be re-optimized in order to achieve the desired enantiomeric ratio. This reoptimization includes changes to reaction temperature, catalyst or reagents. This leads to additional cost and delays in production. The reaction may even be abandoned for another method if the level of enrichment does not meet requirements for the e.r. of the product after reoptimization.

### 1.3.5. Kinetic Resolution and Related Methods

The final method is yet another example of resolution of a racemic mixture.<sup>25</sup> This methodology is distinctly different from the aforementioned classical resolution using chiral auxiliaries. In these resolutions, one enantiomer is transformed to an entirely different functional group, leaving the other enantiomer alone. The now transformed enantiomer has different physical properties and can be separated from the unreacted starting material via column chromatography, distillation, or another physical method. Generally, the reactions are stopped around 50-60% conversion in order to maximize the yield of the enriched, unreacted starting material. Highly efficient resolutions can provide both products and starting materials in enantioenriched form; however, most resolutions target the remaining starting material for isolation. This is due in part to the fact that the e.r. of products generally decrease with increasing conversion, while the e.r. of the starting material increases with conversion. Less efficient kinetic resolutions targeting the enantioenriched products achieve very little conversion and low isolated yields. A kinetic resolution, as the name suggests, proceeds under kinetic control. A significant difference in energy must exist between the transition states ( $\Delta\Delta G^\ddagger$ ) of the two enantiomers in efficient resolutions (Figure 1.4).<sup>26</sup> This is usually accomplished upon action of an enantioenriched catalyst or reagent to generate diastereomeric transition states. Since these reactions are performed under kinetic control, it is advantageous to maintain cool temperatures; therefore, reaction temperatures ranging from 0 to -78 °C are common.

Unlike asymmetric reactions, the efficiency of a resolution is impossible to determine based on enantiomeric ratios, since the enantioenrichment of the unreacted

starting material is directly dependent upon conversion. Therefore, a different parameter, selectivity factor ( $s$ ), is used for the purpose of quantifying the efficiency of kinetic resolutions. A selectivity factor is essentially the relative rate of the two enantiomers ( $k_{\text{fast}}/k_{\text{slow}}$ , see Equation 1.2).<sup>26</sup> The selectivity factor is related directly to the difference in energies of the diastereomeric transition states and determined by analyzing both enantiomeric excess of the starting material and product ( $ee_{\text{SM}}$  and  $ee_{\text{P}}$ , respectively). With these values determined, the fraction conversion ( $\text{conv}$ , Equation 1.3) can be obtained. The  $s$ -factor can then be obtained from the  $ee$  of the starting material and fraction conversion (Equation 1.4). In a perfectly effective resolution, the slower reacting enantiomer is slow enough to prevent conversion resulting in an  $s$ -value of infinity, but examples of nearly perfect resolutions ( $s > 1000$ ) are extraordinarily rare.<sup>26</sup> In reality, kinetic resolutions vary in their ability to resolve enantiomers. Generally, a resolution is considered efficient in synthetic applications if  $s \geq 10$ .

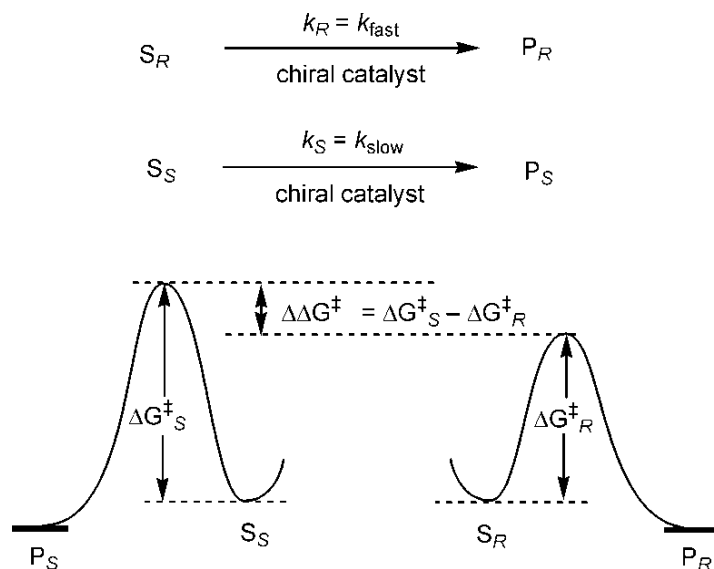


**Figure 1.4 Dependency of  $k_{\text{rel}}$  on the Transition State Energy Differences (Reprinted with Permission of Publisher)<sup>26</sup>**

$$k_{\text{rel}} = s = k_{\text{fast}}/k_{\text{slow}} = e^{\Delta\Delta G^\ddagger/RT}$$

### Equation 1.2

$$\text{conv} = \frac{ee_{\text{SM}}}{ee_{\text{SM}} + ee_{\text{P}}}$$

### Equation 1.3

$$s = \frac{\ln[(1-\text{conv})(1-ee_{\text{SM}})]}{\ln[(1-\text{conv})(1+ee_{\text{SM}})]}$$

### Equation 1.4

An excellent example of a kinetic resolution is the enantioselective derivatization of a racemic alcohol with a protecting group. Alcohols are more polar than the protected alcohol. Resultantly, the products are readily separable from the unreacted starting material via column chromatography. The protecting group can be removed in a non-stereoselective fashion post separation so as to isolate both the enriched starting material and product.

The primary disadvantage of kinetic resolution is the limitation of yield; the starting material can only be isolated in a maximum of 50% yield under ideal conditions if the starting material is a racemic mixture. This drawback is somewhat alleviated by the fact that high levels of enantioenrichment can be obtained simply by controlling conversion. Even if the reaction is not very selective ( $s = 5$ ), enantioenriched material can be obtained (e.r.: 99:1) from a racemic starting material by driving the reaction to higher conversion to 75% (Equation 1.5). As long as  $s$ -factor is known for a resolution, the conversion needed to achieve a desired enrichment level can be calculated using the starting material e.r. ( $S_{\text{min}}^0 : S_{\text{maj}}^0$ ; 50:50 for racemic mixtures) and desired e.r. for the major and minor enantiomer ( $S_{\text{min}}$  and  $S_{\text{maj}}$ ), respectively.<sup>27</sup>

$$\text{conv} = 1 - \left[ \left( \frac{S_{\min}}{S_{\min}^o} \right) \left( \frac{S_{\text{maj}}^o}{S_{\text{maj}}} \right)^s \right]^{1/(s-1)}$$

### Equation 1.5

Other related methods to kinetic resolutions exist, but all still rely on the basic kinetics discussed previously. These methods include: dynamic kinetic resolutions, parallel kinetic resolutions, and regiodivergent kinetic resolutions. In a dynamic kinetic resolution (DKR),<sup>28</sup> the starting material must be racemizable under the reaction conditions. The efficiency is still related to selectivity factor; however, the relative rate of enantiomers corresponds to the e.r. of the products. If the racemization occurs faster than the stereoselective transformation, a yield of up to 100% is possible. As a result, a DKR type resolution is more similar to asymmetric catalysis, and the enantiomeric ratio of products and yields are consequently reported. Alternatively in a parallel kinetic resolution<sup>29</sup> (PKR) both enantiomers undergo a transformation to a different product at similar rates. The theoretical maximum yield is 50%, but the enrichment level of products is independent of conversion. The final example is the regiodivergent resolution<sup>30</sup> of racemic mixtures. This resolution is similar to the PKR; two parallel pathways to product occur simultaneously. In this process, two separate regioisomers are formed from each enantiomer upon action of a chiral catalyst or reagent. Like the PKR the regiodivergent resolution has a maximum yield of 50% and the enantioenrichment is independent of reaction conversion. All of these related transformations do not conform to the selectivity factor calculations mentioned previously for the classical kinetic resolution.<sup>26</sup> As discussed the drawback of these resolutions is the same level of enantioenrichment is

maintained throughout the reaction, eliminating the opportunity to increase enrichment by furthering reaction progress.

#### 1.4. Organocatalyzed Resolutions

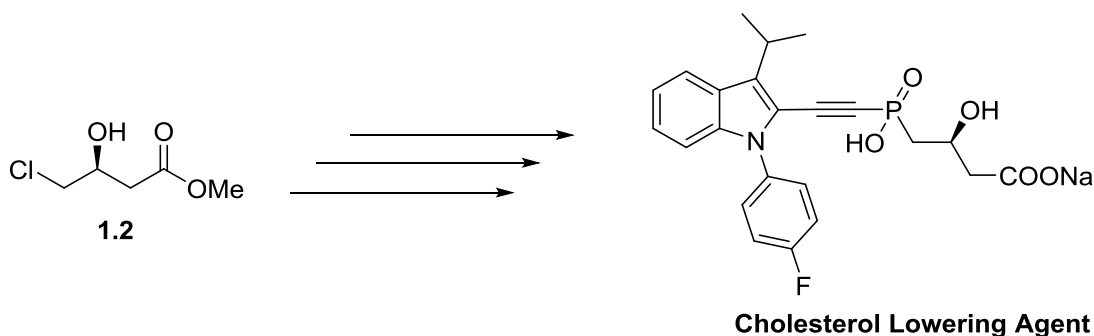
Over the last one hundred years, numerous kinetic resolutions have been developed to generate stereochemically challenging products.<sup>25-26, 30</sup> Therefore, the broad field of this method is beyond the scope of this document. However, due to the types of novel resolutions reported herein, a review of the most relevant asymmetric reactions is required. A variety of metal or enzymatically catalyzed reactions are very successful, but many of these approaches will not be discussed in great detail. In an attempt to narrow the scope, the reactions below will generally be limited to organocatalysis. An organocatalyzed reaction can be characterized as a reaction facilitated by purely organic, small-molecules. Most of these catalysts function through the donation of electrons or protons. Thus, all reactions catalyzed in this way are either Brønsted or Lewis acid-base reactions. These general reactions have led to asymmetric reactions for a plethora of functional groups.

Small-molecule catalysts offer several advantages over transition metal and enzyme catalysts. Transition metals can be very expensive. Additionally, these transition metals must be ligated with chiral organic molecules in order to achieve stereinduction. Metals are also toxic and often difficult to remove from the desired product. This is of particular concern where human consumption of the product is expected, and therefore, regulated.<sup>31-32</sup> Enzymes, on the other hand, are typically very efficient and typically require environmentally friendly alcoholic or aqueous solvents.<sup>33-34</sup> However, these biocatalysts are frequently too selective for a particular substrate class, functional group



or specific molecule.<sup>35</sup> Attempts to make enzymatic resolutions and reactions more general are frequently unsuccessful. Conversely, organic molecules are relatively easy to synthesize, moisture insensitive and are inexpensive.<sup>36-37</sup> These positives help to alleviate the negative aspect of the larger catalyst loadings common to organocatalyzed reactions as compared to metal catalyzed reactions. As a result of these advantages, organic molecule induced reactions have become routine synthetic processes in industrial applications.<sup>31</sup> In corollary to this, the introduction will focus primarily on small-molecule catalyzed resolutions of secondary alcohols.

While a variety of structures and functional groups can be resolved via resolutions this review will focus on the resolutions of secondary alcohols an important class of molecules for various pharmaceutical applications. Chiral secondary alcohols are important building blocks and intermediates for pharmaceuticals. For example, the single enantiomer alcohol **1.2** can be utilized as a starting material to generate the cholesterol lowering aminophosphate (Scheme 1.5).<sup>38</sup> Note the only stereogenic center of this bioactive compound is at the alcohol functionalized carbon.

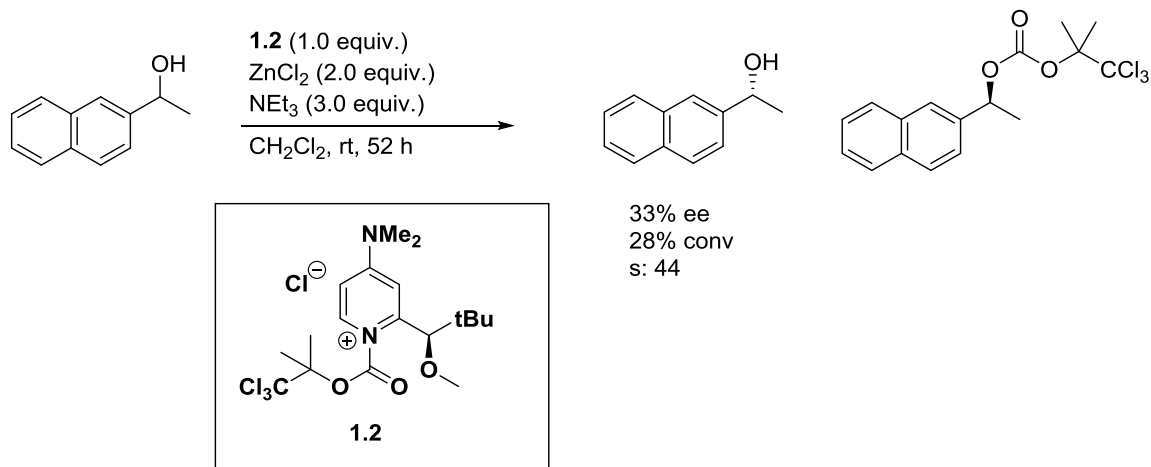


**Scheme 1.5 A Simple Chiral Alcohol as a Building Block for a Bioactive Agent**

Kinetic resolutions of alcohols have benefited from the relatively recent renaissance in small-molecule catalysis. The organocatalyzed acyl transfer reactions are

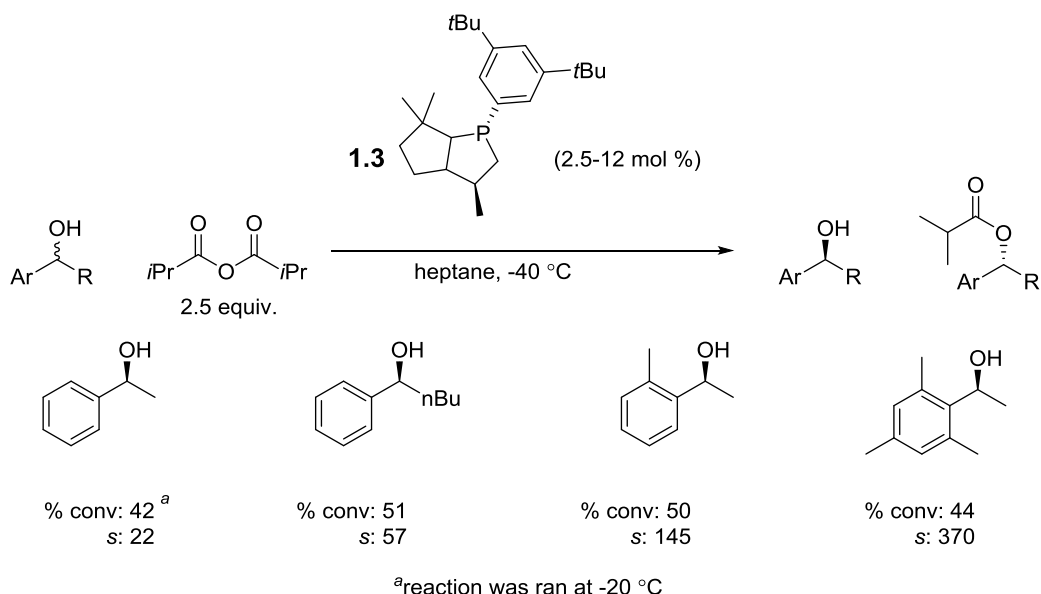
of particular interest to subsequent investigations. Several successful methods exist including reactions catalyzed by chiral amines,<sup>23-24</sup> (dialkylamino)pyridines (DMAP),<sup>39</sup> *N*-heterocyclic carbenes,<sup>40</sup> phosphines,<sup>41-42</sup> and isothioureas,<sup>43-45</sup> among others. The investigations into asymmetric acylation of secondary alcohols by Lewis base catalysis: i.e. chiral DMAP and isothiourea catalysts are of particular interest in regards to the subsequent research to be discussed.

Nearly all chiral amine, phosphorus or pyridine derivatives form a covalent bond with the acylating derivatizing agent thus activating these nascent species for attack by an alcohol.<sup>19</sup> An excellent example of this is Vedejs' chiral DMAP pyridinium **1.2** which is formed from a chiral pyridine and a chloroformate.<sup>39</sup> The chloride is displaced upon reaction with the Lewis basic pyridine. These chiral pyridiniums are acyl sources in the presence of super stoichiometric quantities of Lewis acid ( $ZnCl_2$  or  $MgBr_2$ ) and a stoichiometric quantity of tertiary amine base to control HCl byproduct. The reaction is sluggish at room temperature with only modest conversions achieved. The methodology produces resolved benzylic alcohols and allylic alcohols with excellent *s*-factors ranging from 11-53. For example the benzylic alcohol 1-naphthylethanol is resolved with a selectivity factor of 44 albeit with low conversion of only 28% (Scheme 1.6). The major drawback to this approach is the stoichiometric quantity the chiral acylation source. This disadvantage has led to significant research in acylation reactions that are catalytic with respect to the source of chirality.



**Scheme 1.6 Chiral Pyridiniums for the Resolution of Alcohols**

The bicyclic phosphine catalysts developed by Vedejs were some of the first organocatalysts for the asymmetric, catalytic acylation of secondary alcohols.<sup>42</sup> This kinetic resolution is most selective with isobutyric anhydride as the acyl source in relatively non-polar solvents such as heptane or toluene at cold temperatures (-20 to -40 °C). The original study produced some of the highest selectivity factors for an organocatalyzed resolution. Simple benzylic alcohols were resolved with *s*-factors ranging from 22 to an incredible 370 for the sterically demanding 1-mesitylethanol. This method has also resolved allylic alcohols using catalyst **1.3** and similar conditions to those shown in Scheme 1.7.<sup>41</sup>

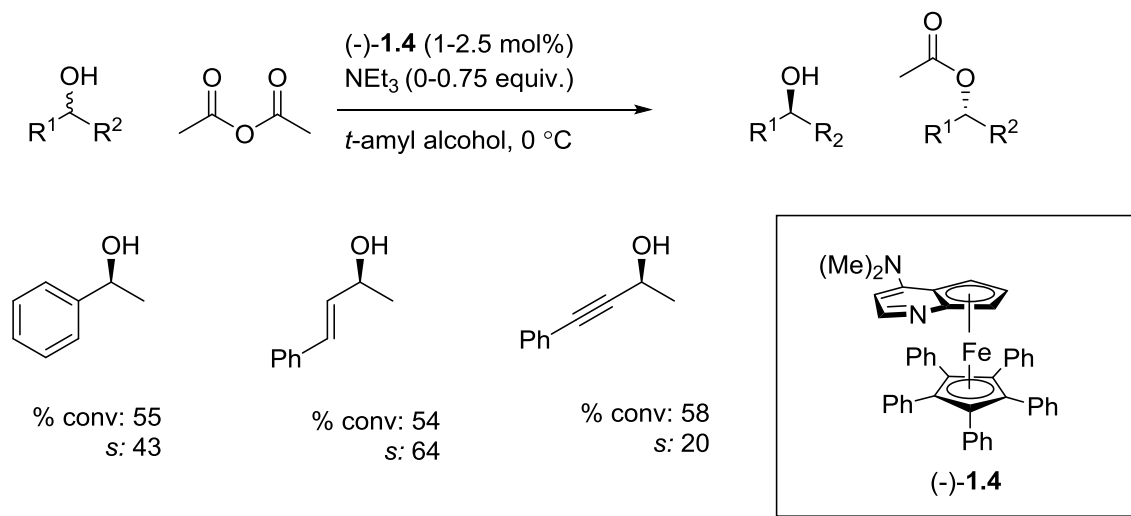


### Scheme 1.7 Vedejs' Bicyclic Phosphine Catalyzed Kinetic Resolution

The pyridine derivative DMAP is an excellent acyl-transfer catalyst as demonstrated in the above reactive pyridiniums (Figure 1.5). This molecule readily forms an active acyl species not only from acid chlorides but from acid anhydrides as well. However, DMAP is a planar molecule, thus it possesses two planes of symmetry without appendages like those in Vedejs' pyridiniums. A symmetrical molecule with two planes of symmetry cannot induce a selective asymmetric reaction. This problem was solved by Fu and coworkers. By installing a pyridine derivative onto FeCpCl or FeCp\*Cl (Note Cp is cyclopentadiene; Cp\* is the pentaphenylcyclopentadiene ligand) an asymmetric and stable catalyst is produced ( $\pm$ -**1.4**).<sup>46</sup> This produces a racemic mixture which can be enriched via HPLC chromatography on chiral stationary phase or classical resolution.

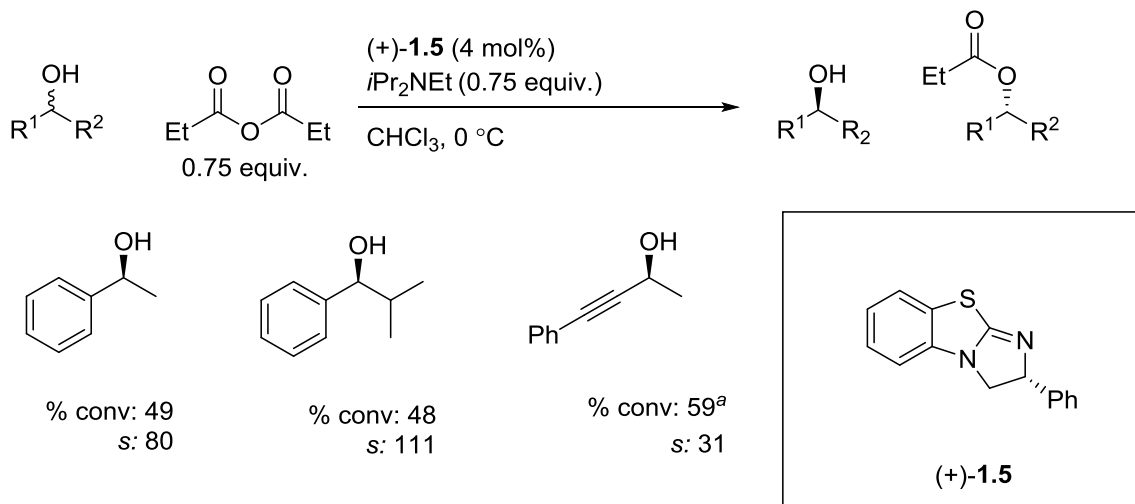
The catalysts developed by Fu<sup>47</sup> have successfully resolved a variety of secondary alcohols including allylic<sup>48</sup>, propargylic<sup>49</sup>, and benzylic alcohols<sup>50</sup> (Scheme 1.8). Note that the iron center does not serve as a reactive site in these reactions. Thus, these

reactions are more accurately described as organocatalyzed despite containing a transition metal. The catalyst **1.4** acylates all three of the aforementioned alcohol classes with excellent selectivities. Additionally, these catalysts facilitate other reactions such as the enantioselective formation of esters from ketenes,<sup>51</sup> among others.



**Scheme 1.8** Fu's Acylation-Based Kinetic Resolution

Another excellent example of an acylation-based kinetic resolution is the isothiourea catalyzed acylation of secondary alcohols developed by Birman. The most efficient catalyst was found to be benzoctetramisole (**1.5**)<sup>43</sup> (Scheme 1.9). The reaction utilized acetic acid anhydride as the acyl source and proceeded under relatively mild conditions (0 °C in chloroform). This system represents a highly selective organocatalyzed resolutions, and it achieves synthetically useful selectivities for simple benzylic alcohols,<sup>43</sup> propargylic alcohols,<sup>52</sup> and 2-arylcyclohexanols.<sup>44</sup> The methodology was also extended to include the dynamic kinetic resolution of azlactones.<sup>45</sup>



<sup>a</sup>propargylic alcohols required no *iPr*<sub>2</sub>NEt

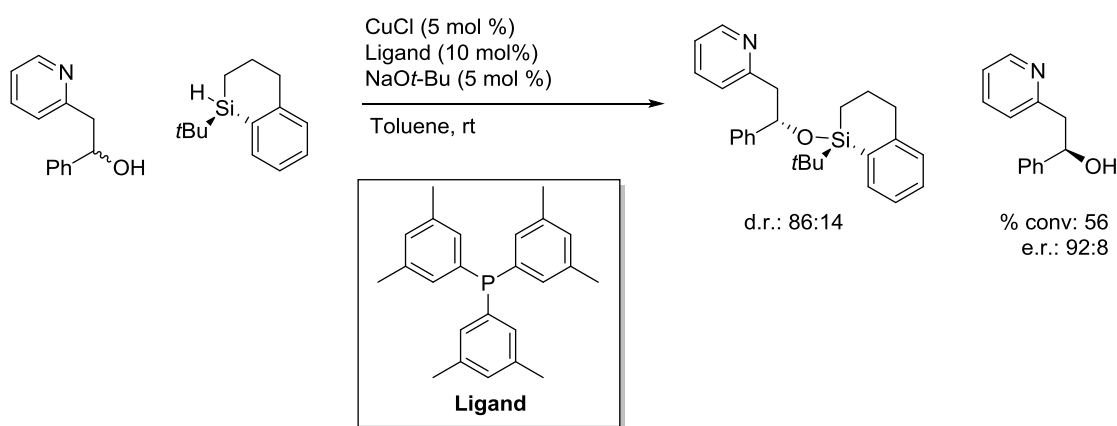
### Scheme 1.9 Birman's Isothiourea Catalyzed Acylation-Based Kinetic Resolution

#### 1.5. Silylation-Based Resolution Methods for the Preparation of Non-Racemic Alcohols

The silyl ether protecting group is arguably the most frequently utilized protecting group for synthetic applications. Some advantages of the silyl ether include tenability, mild installment conditions and orthogonal protection and deprotection.<sup>53</sup> The silylated alcohol can usually be selectively deprotected with mild tetrabutylammonium fluoride (TBAF) in minutes depending on specific silyl group. Despite these advantages, until 10 years ago no examples of asymmetric silylation existed. A silyl group can be installed on an alcohol using a variety of methods including catalysis by Lewis acids and Lewis bases or transition metals.

Asymmetric dehydrogenative silicon-oxygen couplings have been successfully employed in kinetic resolutions. These reactions utilized a stereogenic at silicon chiral derivatizing reagent.<sup>54</sup> The reaction is catalyzed by an inexpensive copper catalyst in low catalyst loadings (5 mol %) and in the presence of a phosphine ligand (Scheme 1.10).

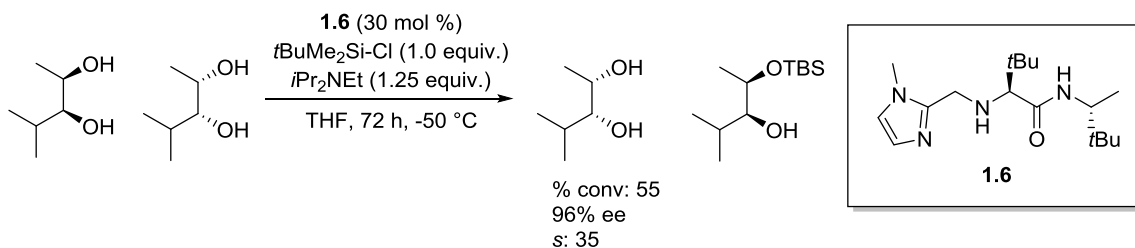
Synthetically useful selectivities were only achieved whenever a donating pyridine group was part of the alcohol substrate, which offered two-point binding on the metal catalyst. The only disadvantages to the system are the preparation of the enriched silane and the limited substrate scope.<sup>55-56</sup> An alternate method using chiral taddol-based ligands and achiral silanes was developed,<sup>57</sup> and similar selectivities were observed for donor functionalized alcohols like those shown in Scheme 1.10.



**Scheme 1.10 Chiral Silanes for the Kinetic Resolution of Secondary Alcohols**

Racemic diols have also been resolved via a silylation-based kinetic resolution employing a unique amino acid- based catalyst **1.6** in the reaction.<sup>58</sup> The bi-functional catalyst was presumed to activate the silyl chloride (*tert*-butyldimethylsilyl chloride) via the Lewis basic imidazole site. The diol was then oriented via hydrogen bonding, to achieve excellent selectivities (Scheme 1.11). The reaction is also regioselective, with silylation predominately occurring on the less sterically encumbered alcohol. The amino acid-based catalyst **1.6** effectively catalyzes the desymmetrization of diols<sup>59</sup> and 1,2,3-triols.<sup>60</sup> Unfortunately, the reaction required long reaction times, around 72 h at -50 °C.

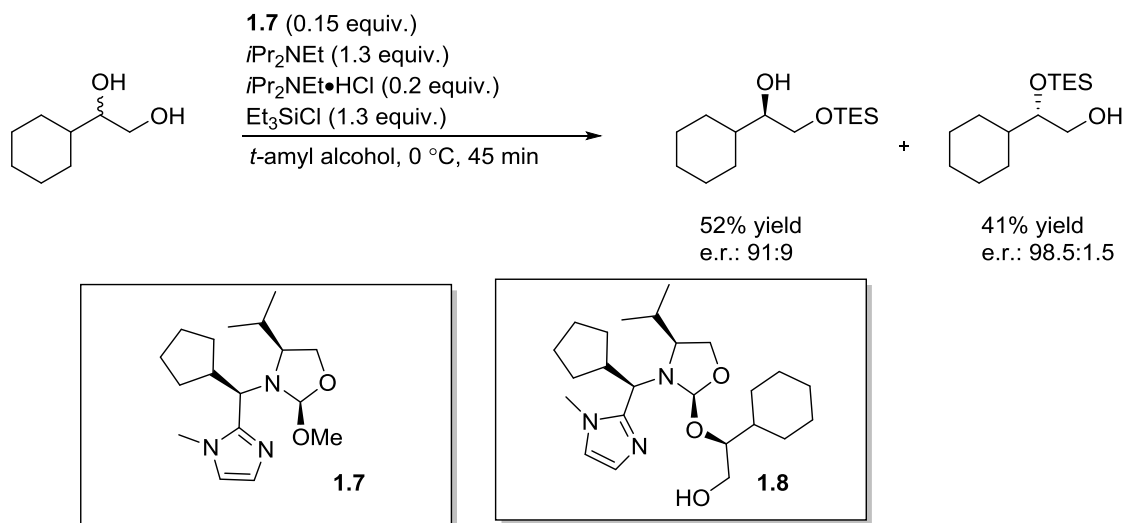
This drawback was recently solved by adding a more nucleophilic co-catalyst<sup>61</sup> as the Lewis base activator. The rate was accelerated affording complete reaction in a fraction of the time. This study demonstrated that the originally proposed intramolecular activation was inaccurate; therefore, it is likely the reaction is activated and directed by two separate molecules of **1.6**.



### Scheme 1.11 Silylation-Based Kinetic Resolution of Diols

Another enantioselective silylation is the regiodivergent kinetic resolution of racemic mixture reported by Tan.<sup>62</sup> Recall this reaction is a form of parallel kinetic resolution where two enantioselective pathways occur simultaneously (See section 1.3.5). In this case, the parallel pathways are the silylation of the primary alcohol versus the secondary alcohol in the presence of **1.7**, a bi-functional catalyst (Scheme 1.12). Both regioselective reactions occurred with excellent and opposite enantioselectivity achieving an e.r. of 91:9 for the silylation of the primary alcohol and 98.5:1.5 for the secondary alcohol. This reaction is particularly different from other approaches that rely solely on transition metal or Lewis base activation of a derivatizing reagent. The bi-functional catalyst **1.7** can form a covalent reversible bond to the alcohol via the imidazole ring to form intermediate **1.8**. This catalyst-substrate binding<sup>63</sup> allows for excellent regioselectivity. The internal imidazole then activates the silyl source for enantioselective and regio-selective protection.





### Scheme 1.12 Tan's Regiodivergent Kinetic Resolution

All of the previous examples of silylation-based kinetic resolutions have been dependent upon a catalyst-substrate two point binding mechanism in order to achieve enantioselective protection. For example, Oestreich's kinetic resolutions (Scheme 1.10) require a donating pyridine group on the substrate. The donating group allows for a more stable transition state<sup>64</sup> and efficient transfer of chiral information from the enriched silane to the substrate (Figure 1.5). Selecting a single enantiomer for silylation in an alcohol which lacks additional functionality is a significant challenge. This system and many others cannot overcome this problem.

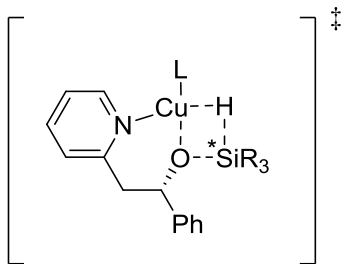
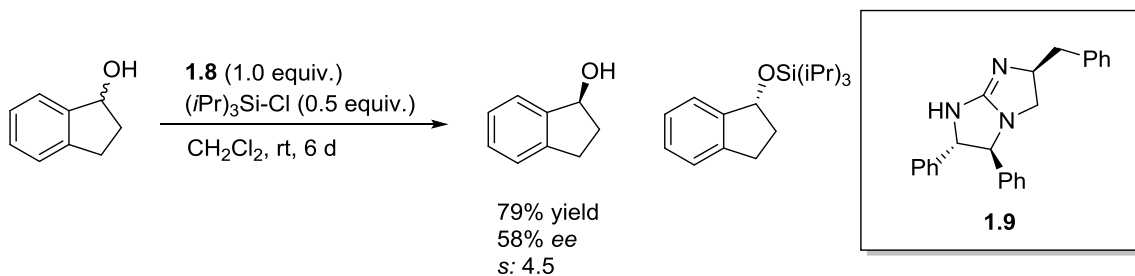


**Figure 1.5 Two-Point Binding in a Silylation-Based Resolution Developed by Oestreich**

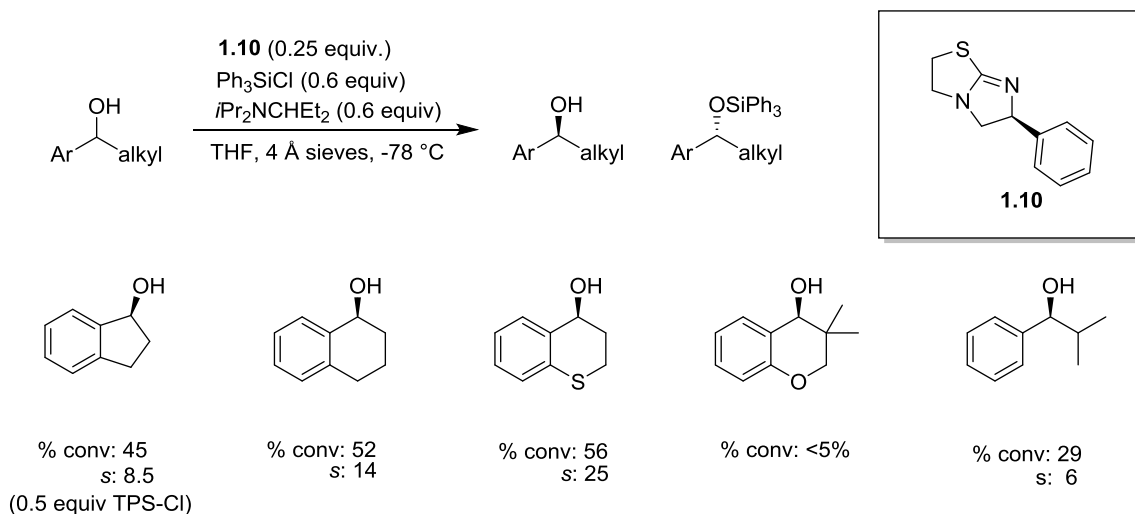
Ishikawa demonstrated a moderately selective kinetic resolution of a mono-functional alcohol catalyzed by chiral guanidine **1.9** (Scheme 1.13).<sup>65</sup> The bulky silyl source triisopropylsilyl chloride required six days of reaction time, obtaining a conversion of 21%, based upon isolated yield. Additionally, a stoichiometric quantity of catalyst was needed due to its Brønsted basic guanidine functionality. The selectivity was poor with an estimated  $s = 4.5$  using the yield and enantiomeric excess of the recovered alcohol. While this example is obviously not synthetically viable, the reaction has inspired other silylation-based approaches to the kinetic resolution of simple benzylic alcohols.



**Scheme 1.13 Silylation-Based Kinetic Resolution of Indanol Developed by Ishikawa**

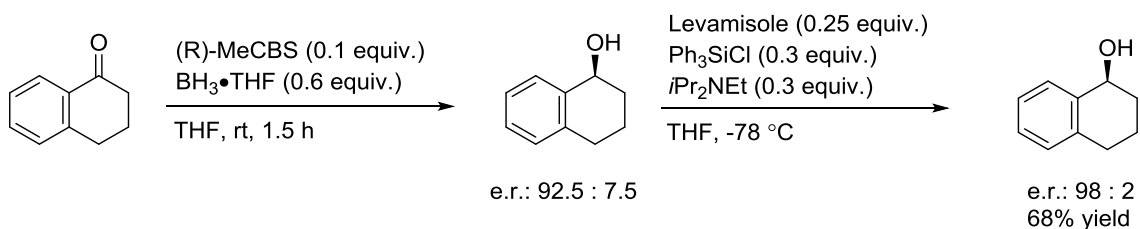
Fortunately, a successful silylation-based resolution of these challenging benzylic alcohols has been reported by Wiskur<sup>66</sup> (Scheme 1.14). A variety of cyclic, benzylic

secondary alcohols were resolved with selectivity factors ranging from 5-25. The most selective substrate was thiochromanol which was resolved to an e.r. of 94:6 and had a selectivity factor of 25. Notably, indanol was also resolved obtaining the highest selectivity ( $s = 8.5$ ) for that substrate in an organocatalyzed kinetic resolution. The method was particularly advantageous since all of the reagents were commercially available. Additionally, levamisole **1.10** is a very inexpensive pharmaceutical<sup>67</sup> with veterinary applications that has been utilized in acylations<sup>43</sup> as a Lewis base catalyst. The bulky base, diisopropylisopentylamine ( $i\text{Pr}_2\text{NCHEt}_2$ ), removes the HCl byproduct formed during the reaction. The method has several limitations, however. Acyclic alcohols were significantly less selective ( $s = 14$  for cyclic alcohol  $\alpha$ -tetralol vs  $s = 6$  for 1-phenyl-2-methylpropanol), and sterically large groups in the 2-position failed to form silyl ethers.



**Scheme 1.14 Isothiourea Catalyzed Silylation-Based Resolution Developed by Wiskur**

Since this seminal report, the levamisole-triphenylsilyl chloride methodology has successfully been employed in a one-pot ee polishing sequence<sup>27</sup> (Scheme 1.15). Tetralone was reduced asymmetrically using the CBS-borane reduction.<sup>18</sup> The borane was decomposed with methanol and dried under vacuum. The crude, partially enriched alcohol (92.5:7.5 e.r.) was then further enriched via the silylation-based kinetic resolution to an e.r. of 98:2 with an overall yield of 68%. The primary advantages were the avoidance of chromatography until after the silylation and achieving high levels of enantioenrichment not possible in the asymmetric reduction. Additionally, the disadvantageous 50% maximum yield inherent to kinetic resolutions of racemic compounds is overcome in these reactions. Thus, the tandem use of an asymmetric reaction and a kinetic resolution is quite powerful.



**Scheme 1.15 One-Pot Enantiomeric Excess Polishing Sequence of Tetralol**

## 1.6. Conclusions and Outlook

The isothioureia catalyzed silylation-based kinetic resolution at this time was very limited in substrate scope and utility. As a result, research presented here has focused significantly on the expansion of the substrate scope to include molecular structures other than secondary benzylic alcohols. Mechanistic investigations into the origins of selectivity and transition state structure will be paramount to these investigations as well.

Initial studies focused primarily on expanding the structures capable of being resolved by the triphenylsilylchloride-isothiourea methodology. In chapter two, the testing of  $\alpha$ -hydroxy carbonyl compounds in the silylation-based kinetic resolution will be described.<sup>68</sup> Successes and conclusions about the general structures capable of being resolved using the methodology will be made. In the third chapter, the methodology was expanded to include a homogenous polymer solid support as the silyl source. The advantages of such a system will be highlighted and hypotheses about future directions for polymer-based methods will be made. Mechanistic investigations into the silylation based reaction will be discussed in detail in chapter four. This will include a review of previous mechanistic studies: catalyst-isothiourea NMR and linear free energy relationship (LFER) studies.<sup>69</sup> The combination of this knowledge and subsequent kinetic data will attempt to propose a plausible mechanism for the asymmetric silylation. Finally, the use of borane Lewis acid catalysts for asymmetric silicon-oxygen couplings will be discussed. Particular focus will be on the transfer of chiral information from stereogenic at silicon compounds to racemic secondary alcohols.

## 1.7. References

1. Smith, M. B.; March, J., *March's Advanced Organic Chemistry: Reactions, Mechanisms, and Structure*. 5th ed.; John Wiley and Sons: New York, 2001; p 125.
2. Eliel, E. L.; Wilen, S. H., *Stereochemistry of Organic Compounds*. John Wiley and Sons: New York, 1994; p 249.
3. Gal, J.; Cintas, P. Early History of the Recognition of Molecular Biochirality. *Top. Curr. Chem.* **2013**, *333*, 1.
4. Mazur, R. H.; Schlatter, J. M.; Goldkamp, A. H. Structure-Taste Relationships of Some Dipeptides. *J. Am. Chem. Soc.* **1969**, *91*, 2684.
5. Gal, J. The Discovery of Stereoselectivity at Biological Receptors: Arnaldo Piutti and the Taste of the Asparagine Enantiomers-History and Analysis on the 125th Anniversary. *Chirality* **2012**, *24*, 959.
6. Easson, L. H.; Stedman, E. Studies on the Relationship Between Chemical Constitution and Physiological action: Molecular Dissymmetry and Physiological Activity. *Biochem. J.* **1933**, *27*, 1257.
7. Testa, B.; Vistoli, G.; Pedretti, A.; Caldwell, J. Organic Stereochemistry Part 5. *Helv. Chim. Acta* **2013**, *96*, 747.
8. Shah, R. R.; Midgley, J. M.; Branch, S. K. Stereochemical Origin of Some Clinically Significant Drug Safety Concerns: Lessons for Future Drug Development. *Adverse Drug React. Toxicol. Rev.* **1998**, *17*, 145.
9. Kean, W. F.; Lock, C. J. L.; Rischke, J.; Butt, R.; Buchanan, W. W.; Howard-Lock, H. Effect of R and S Enantiomers of Naproxen on Aggregation and Thromboxane Production in Human Platelets. *J. Pharm. Sci.* **1989**, *78*, 324.
10. FDA.  
<http://www.fda.gov/drugs/GuidanceComplianceRegulatoryInformation/Guidances/ucm122883.htm>.

11. Breuer, M.; Ditrach, K.; Habicher, T.; Hauer, B.; Kessler, M.; Sturmer, R.; Zelinski, T. Industrial Methods for the Production of Optically Active Intermediates. *Angew. Chem., Int. Ed.* **2004**, *43*, 788.
12. Gawley, R. E. Do the Terms "% ee" and "% de" Make Sense as Expressions of Stereoisomer Composition or Stereoselectivity? *J. Org. Chem.* **2006**, *71*, 2411.
13. Ottaggio, L.; Bestoso, F.; Armirotti, A.; Balbi, A.; Damonte, G.; Mazzei, M.; Sancandi, M.; Miele, M. Taxanes from Shells and Leaves of *Corylus Avellana*. *J. Nat. Prod.* **2008**, *71*, 58.
14. Holton, R. A.; Kim, H. B.; Somoza, C.; Liang, F.; Biediger, R. J.; Boatman, P. D.; Shindo, M.; Smith, C. C.; Kim, S. First Total Synthesis of Taxol. 2. Completion of the C and D Rings. *J. Am. Chem. Soc.* **1994**, *116*, 1599.
15. Holton, R. A.; Somoza, C.; Kim, H. B.; Liang, F.; Biediger, R. J.; Boatman, P. D.; Shindo, M.; Smith, C. C.; Kim, S. First Total Synthesis of Taxol. 1. Functionalization of the B Ring. *J. Am. Chem. Soc.* **1994**, *116*, 1597.
16. Nicolaou, K. C.; Yang, Z.; Liu, J. J.; Ueno, H.; Nantermet, P. G.; Guy, R. K.; Claiborne, C. F.; Renaud, J.; Couladouros, E. A.; Paulvannan, K.; et al. Total Synthesis of Taxol. *Nature* **1994**, *367*, 630.
17. Ault, A. R. (+)- and (-)-1-Phenylethylamine. *Org. Synth.* **1969**, *49*, 93.
18. Corey, E. J.; Bakshi, R. K.; Shibata, S. Highly Enantioselective Borane Reduction of Ketones Catalyzed by Chiral Oxazaborolidines. Mechanism and Synthetic Implications. *J. Am. Chem. Soc.* **1987**, *109*, 5551.
19. Denmark, S. E.; Beutner, G. L. Lewis Base Catalysis in Organic Synthesis. *Angew. Chem., Int. Ed.* **2008**, *47*, 1560.
20. Denmark, S. E.; Su, X.; Nishigaichi, Y. The Chemistry of Trichlorosilyl Enolates. 6. Mechanistic Duality in the Lewis Base-Catalyzed Aldol Addition Reaction. *J. Am. Chem. Soc.* **1998**, *120*, 12990.

21. C. Willis, M. Enantioselective Desymmetrisation. *J. Chem. Soc., Perkin Trans. I* **1999**, 1765.
22. Eliel, E. L.; Wilen, S. H., *Stereochemistry of Organic Compounds*. John Wiley and Sons: New York, 1994; p 123.
23. Oriyama, T.; Imai, K.; Hosoya, T.; Sano, T. Asymmetric Acylation of Meso-Diols with Benzoyl Halide in the Presence of a Chiral Diamine. *Tetrahedron Lett.* **1998**, 39, 397.
24. Oriyama, T.; Imai, K.; Sano, T.; Hosoya, T. Highly Efficient Catalytic Asymmetric Acylation of Meso-1,2-Diols with Benzoyl Chloride in the Presence of a Chiral Diamine Combined with Et<sub>3</sub>N. *Tetrahedron Lett.* **1998**, 39, 3529.
25. Kagan, H. B.; Fiaud, J. C., In *Topics in Stereochemistry*, L., E.; Wilen, S. H., Eds. John Wiley and Sons: 1988; pp 249.
26. Keith, J. M.; Larrow, J. F.; Jacobsen, E. N. Practical Considerations in Kinetic Resolution Reactions. *Adv. Synth. Catal.* **2001**, 343, 5.
27. Klauck, M. I.; Patel, S. G.; Wiskur, S. L. Obtaining Enriched Compounds Via a Tandem Enantioselective Reaction and Kinetic Resolution Polishing Sequence. *J. Org. Chem.* **2012**, 77, 3570.
28. Strauss, U. T.; Felfer, U.; Faber, K. Biocatalytic Transformation of Racemates into Chiral Building Blocks in 100% Chemical Yield and 100% Enantiomeric Excess. *Tetrahedron: Asymmetry* **1999**, 10, 107.
29. Eames, J. Parallel Kinetic Resolutions. *Angew. Chem., Int. Ed.* **2000**, 39, 885.
30. Vedejs, E.; Jure, M. Efficiency in Nonenzymatic Kinetic Resolution. *Angew. Chem., Int. Ed.* **2005**, 44, 3974.
31. Sun, B.-F. Total Synthesis of Natural and Pharmaceutical Products Powered by Organocatalytic Reactions. *Tetrahedron Lett.* **2015**, 56, 2133.
32. Yoshimura, T. Catalytic Asymmetric Reactions in Alkaloid and Terpenoid Syntheses. *Tetrahedron Lett.* **2014**, 55, 5109.



33. Rachwalski, M.; Vermue, N.; Rutjes, F. P. J. T. Recent Advances in Enzymatic and Chemical Deracemisation of Racemic Compounds. *Chem. Soc. Rev.* **2013**, *42*, 9268.
34. Koeller, K. M.; Wong, C.-H. Enzymes for Chemical Synthesis. *Nature* **2001**, *409*, 232.
35. Isobe, K.; Tamauchi, H.; Fuhshuku, K.; Nagasawa, S.; Asano, Y. A Simple Enzymatic Method for Production of a Wide Variety of D-Amino Acids Using L-Amino Acid Oxidase from *Rhodococcus* sp. AIU Z-35-1. *Enzyme Res.* **2010**, *2010*, 1.
36. List, B. Introduction: Organocatalysis. *Chem. Rev.* **2007**, *107*, 5413.
37. List, B. *Top. Curr. Chem.* **2009**, *291*.
38. Patel, R. N. Biocatalytic Synthesis of Chiral Alcohols and Amino Acids for Development of Pharmaceuticals. *Biomolecules* **2013**, *3*, 741.
39. Vedejs, E.; Chen, X. Kinetic Resolution of Secondary Alcohols. Enantioselective Acylation Mediated by a Chiral (Dimethylamino)pyridine Derivative. *J. Am. Chem. Soc.* **1996**, *118*, 1809.
40. Marion, N.; Diez-Gonzalez, S.; Nolan, S. P. N-Heterocyclic Carbenes as Organocatalysts. *Angew. Chem., Int. Ed.* **2007**, *46*, 2988.
41. Vedejs, E.; MacKay, J. A. Kinetic Resolution of Allylic Alcohols Using a Chiral Phosphine Catalyst. *Org. Lett.* **2001**, *3*, 535.
42. Vedejs, E.; Daugulis, O. A Highly Enantioselective Phosphabicyclooctane Catalyst for the Kinetic Resolution of Benzylic Alcohols. *J. Am. Chem. Soc.* **2003**, *125*, 4166.
43. Birman, V. B.; Li, X. Benzotetramisole: a Remarkably Enantioselective Acyl Transfer Catalyst. *Org. Lett.* **2006**, *8*, 1351.
44. Birman, V. B.; Li, X. Homobenzotetramisole: an Effective Catalyst for Kinetic Resolution of Aryl-Cycloalkanols. *Org. Lett.* **2008**, *10*, 1115.
45. Yang, X.; Lu, G.; Birman, V. B. Benzotetramisole-Catalyzed Dynamic Kinetic Resolution of Azlactones. *Org. Lett.* **2010**, *12*, 892.

46. Ruble, J. C.; Fu, G. C. Chiral  $\pi$ -Complexes of Heterocycles with Transition Metals: A Versatile New Family of Nucleophilic Catalysts. *J. Org. Chem.* **1996**, *61*, 7230.
47. Fu, G. C. Enantioselective Nucleophilic Catalysis with “Planar-Chiral” Heterocycles. *Acc. Chem. Res.* **2000**, *33*, 412.
48. Bellemin-Laponnaz, S.; Tweddell, J.; Ruble, J. C.; Breitling, F. M.; Fu, G. C. The Kinetic Resolution of Allylic Alcohols by a Non-Enzymatic Acylation Catalyst; Application to Natural Product Synthesis. *Chem. Commun.* **2000**, 1009.
49. Tao, B.; Ruble, J. C.; Hoic, D. A.; Fu, G. C. Nonenzymatic Kinetic Resolution of Propargylic Alcohols by a Planar-Chiral DMAP Derivative: Crystallographic Characterization of the Acylated Catalyst. *J. Am. Chem. Soc.* **1999**, *121*, 5091.
50. Ruble, J. C.; Latham, H. A.; Fu, G. C. Effective Kinetic Resolution of Secondary Alcohols with a Planar-Chiral Analogue of 4-(Dimethylamino)pyridine. Use of the Fe(C<sub>5</sub>Ph<sub>5</sub>) Group in Asymmetric Catalysis. *J. Am. Chem. Soc.* **1997**, *119*, 1492.
51. Wiskur, S. L.; Fu, G. C. Catalytic Asymmetric Synthesis of Esters from Ketenes. *J. Am. Chem. Soc.* **2005**, *127*, 6176.
52. Birman, V. B.; Guo, L. Kinetic Resolution of Propargylic Alcohols Catalyzed by Benzotetramisole. *Org. Lett.* **2006**, *8*, 4859.
53. Greene, T. W.; Wuts, P. G. M., *Protective Groups in Organic Synthesis*. 3 ed.; John Wiley and Sons: New York, USA, 1999.
54. Oestreich, M. Silicon-Stereogenic Silanes in Asymmetric Catalysis. *Synlett* **2007**, *2007*, 1629.
55. Oestreich, M.; Königs, C. Shortened Synthesis of a Silicon-Stereogenic Cyclic Silane. *Synthesis* **2011**, *2011*, 2062.
56. Oestreich, M.; Schmid, U. K.; Auer, G.; Keller, M. A Convergent Method for the Synthesis of Highly Enantiomerically Enriched Cyclic Silanes with Silicon-Centered Chirality. *Synthesis* **2003**, 2725.

57. Weickgenannt, A.; Mewald, M.; Muesmann, T. W. T.; Oestreich, M. Catalytic Asymmetric Si-O Coupling of Simple Achiral Silanes and Chiral Donor-Functionalized Alcohols. *Angew. Chem., Int. Ed.* **2010**, *49*, 2223.
58. Zhao, Y.; Mitra, A. W.; Hoveyda, A. H.; Snapper, M. L. Kinetic Resolution of 1,2-Diols Through Highly Site and Enantioselective Catalytic Silylation. *Angew. Chem., Int. Ed.* **2007**, *46*, 8471.
59. Zhao, Y.; Rodrigo, J.; Hoveyda, A. H.; Snapper, M. L. Enantioselective Silyl Protection of Alcohols Catalysed by an Amino-Acid-Based Small Molecule. *Nature* **2006**, *443*, 67.
60. You, Z.; Hoveyda, A. H.; Snapper, M. L. Catalytic Enantioselective Silylation of Acyclic and Cyclic Triols: Application to Total Syntheses of Cleroindicins D, F, and C. *Angew. Chem., Int. Ed.* **2009**, *48*, 547.
61. Manville, N.; Alite, H.; Haeffner, F.; Hoveyda, A. H.; Snapper, M. L. Enantioselective Silyl Protection of Alcohols Promoted by a Combination of Chiral and Achiral Lewis Basic Catalysts. *Nat. Chem.* **2013**, *5*, 768.
62. Worthy, A. D.; Sun, X.; Tan, K. L. Site-Selective Catalysis: Toward a Regiodivergent Resolution of 1,2-Diols. *J. Am. Chem. Soc.* **2012**, *134*, 7321.
63. Sammakia, T.; Hurley, T. B. 2-Formyl-4-pyrrolidinopyridine (FPP): A New Catalyst for the Hydroxyl-Directed Methanolysis of Esters. *J. Am. Chem. Soc.* **1996**, *118*, 8967.
64. Weickgenannt, A.; Mewald, M.; Oestreich, M. Asymmetric Si-O Coupling of Alcohols. *Org. Biomol. Chem.* **2010**, *8*, 1497.
65. Isobe, T.; Fukuda, K.; Araki, Y.; Ishikawa, T. Modified Guanidines as Chiral Superbases: the First Example of Asymmetric Silylation of Secondary Alcohols. *Chem. Commun.* **2001**, 243.
66. Sheppard, C. I.; Taylor, J. L.; Wiskur, S. L. Silylation-Based Kinetic Resolution of Monofunctional Secondary Alcohols. *Org. Lett.* **2011**, *13*, 3794.
67. *The Merck Index*. 14 ed.; 2006; p 5460.

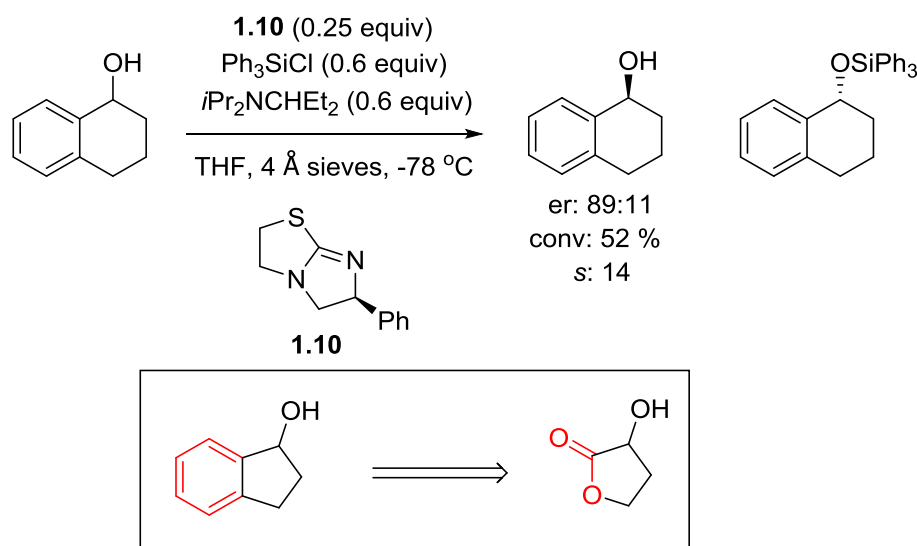
68. Clark, R. W.; Deaton, T. M.; Zhang, Y.; Moore, M. I.; Wiskur, S. L. Silylation-Based Kinetic Resolution of  $\alpha$ -Hydroxy Lactones and Lactams. *Org. Lett.* **2013**, *15*, 6132.
69. Akhani, R. K.; Moore, M. I.; Pribyl, J. G.; Wiskur, S. L. Linear free-energy relationship and rate study on a silylation-based kinetic resolution: mechanistic insights. *J. Org. Chem.* **2014**, *79*, 2384.

## Chapter 2 Silylation-Based Kinetic Resolution of $\alpha$ -Hydroxy Lactones and Lactams

### 2.1. Introduction and Scope

Herein, substrate scope expansion of the silylation-based kinetic resolution developed in the Wiskur laboratory beyond the previously discovered mono-functional alcohol class of compounds<sup>1</sup> will be discussed. The use of silicon in asymmetric reactions is an emerging field. As discussed in Chapter 1, the use of silicon-based reagents for the production of chiral secondary alcohols was previously limited to asymmetric hydrosilylation of a prochiral ketone.<sup>2-4</sup> An alternate and powerful method to produce enantioenriched secondary alcohols is the kinetic resolution of racemic alcohols,<sup>5-7</sup> but relatively few examples of silylation-based kinetic resolutions have been explored,<sup>8-9</sup> despite the many synthetic advantages (tunable reactivity, ease of protection, and selective deprotection).<sup>10</sup> The substrates that have been targeted with enantioselective silylation thus far include diols,<sup>11-13</sup> 1,2,3-triols,<sup>14</sup> pyridyl substituted alcohols,<sup>15-18</sup> simple alcohols,<sup>19</sup> and  $\beta$ -hydroxy esters.<sup>20</sup> Recently, the Wiskur group reported a synthetically useful silylation-based kinetic resolution of secondary cyclic alcohols (Scheme 2.3).<sup>1</sup> This methodology utilizes the chiral isothioureia levamisole (**1.10**) as a chiral Lewis base to activate triphenylsilyl chloride.<sup>21</sup> Moderate to high selectivity factors (*s* up to 25) were obtained for a variety of mono-functional, cyclic, secondary alcohols. Unfortunately,

when acyclic secondary alcohols such as 1-phenylethanol were attempted nearly all selectivity was lost. Note: reprinted with permission from Clark, R.W.; Deaton, T.M.; Zhang, Y.; Moore, M.I.; Wiskur, S.L. *Org. Lett.* **2013**, *15*, 6132. Copyright 2013 American Chemical Society.



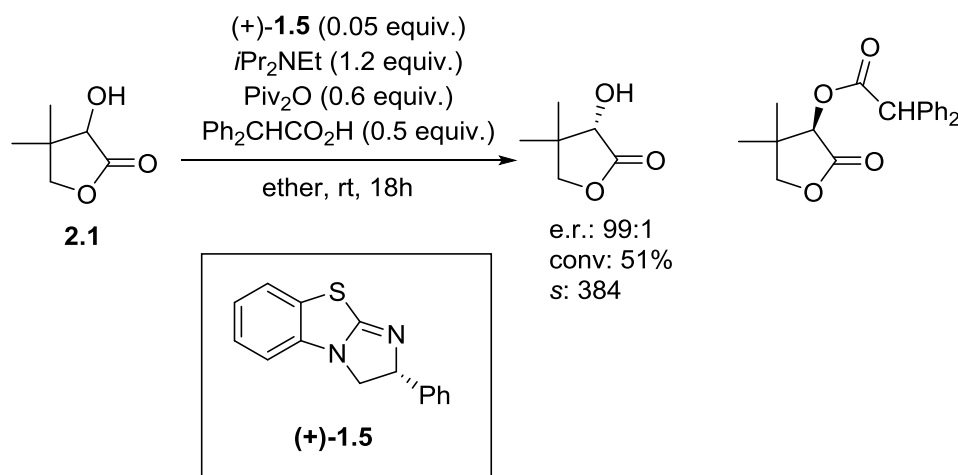
**Scheme 2.1 Silylation-Based Resolutions of Cyclic 2° Benzylic Alcohols and Potential Application to Hydroxy Lactones**

In order to expand the substrate scope of our silylation-based kinetic resolution, we concluded that a successful substrate class would possess many of the same topologies as cyclic benzylic alcohols: a relatively planar substrate with a pi system adjacent to the alcohol. We hypothesized  $\alpha$ -hydroxy lactones or lactams could be amenable to resolution based on the position of the carbonyl and inherit conformational rigidity (Scheme 2.1).

Enantiomerically pure  $\alpha$ -hydroxy lactones and lactams are highly desirable chiral building blocks for the synthesis of biologically active compounds<sup>22-25</sup> and natural products<sup>26</sup> and have been used as chiral auxiliaries in a variety of reactions.<sup>27</sup> While a

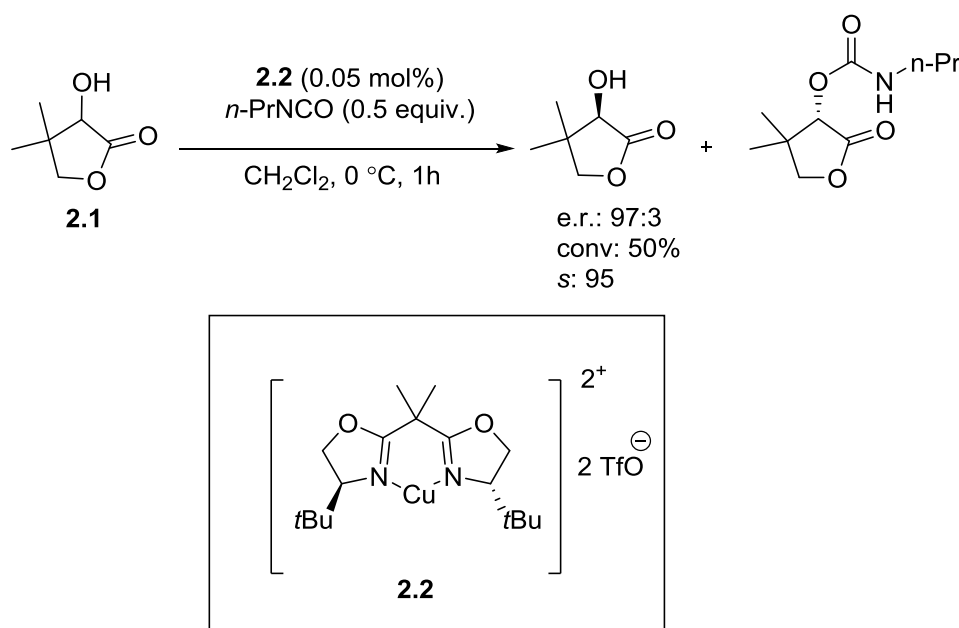
number of asymmetric synthetic methods<sup>27-30</sup> have been developed to produce these compounds, including enzymatic kinetic resolutions,<sup>31-32</sup> until recently there has been very little work with non-enzymatic kinetic resolutions of these substrates. Currently, there are two examples of non-enzymatic kinetic resolutions of lactones which include a copper catalyzed carbamoylation<sup>33</sup> and an isothioureia catalyzed acylation.<sup>34</sup>

The acyl-transfer kinetic resolution of these lactones utilized reaction conditions similar to those developed by Birman<sup>35</sup> (Scheme 2.2) by employing benzotetramisole (**1.5**) as the acylating catalyst. One major difference between this resolution and previous benzotetramisole catalyzed acylations is the acyl source.<sup>36-37</sup> The reaction conditions in this case form a mixed anhydride in situ from pivalic anhydride (Piv<sub>2</sub>O) and diphenylacetic acid. The reaction was most useful for lactones possessing sterically large groups in the β-position. Pantolactone (**2.1**), for example, was resolved with a selectivity factor of 384. Very impressive selectivities up to 1000 were obtained using this anhydride at ambient temperatures for twelve examples.



**Scheme 2.2 Kinetic Resolution of α-Hydroxy Lactones by Acyl Transfer**

The asymmetric carbamoylation resolution developed by Okhuma was also highly selective when employing Cu (II) catalysts bearing chiral bis(oxazoline) ligands (Scheme 2.3). The most efficient kinetic resolutions were observed with catalyst **2.2** and propyl isocyanate as the isocyanate source. The resolution of pantolactone was achieved with 50% conversion in 1 hour at 0 °C in dichloromethane. An impressive selectivity factor of 95 was observed for pantolactone **2.1** and selectivities into the 200s were obtained for lactones possessing sterically demanding groups in the  $\beta$ -position. However, attempts to resolve structurally related lactams were less successful, only achieving an *s*-factor of up to 3.



**Scheme 2.3 Copper Catalyzed Asymmetric Carbamoylation of Pantolactone**

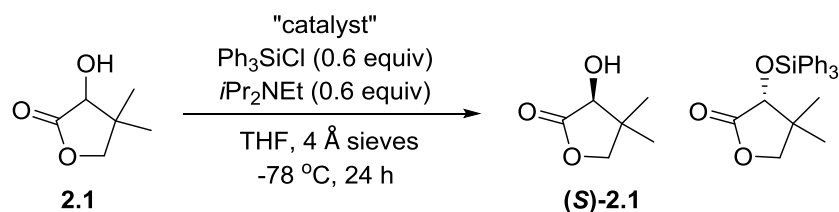
To the best of our knowledge, a successful non-enzymatic resolution of  $\alpha$ -hydroxy lactams remains unreported. In this chapter, the expansion of the substrates employed in silylation-based kinetic resolutions to include  $\alpha$ -hydroxy lactones and



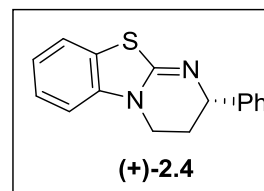
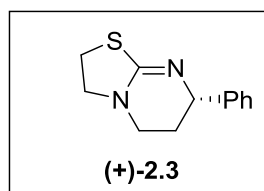
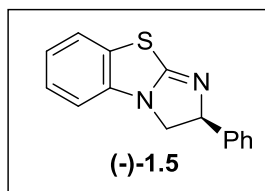
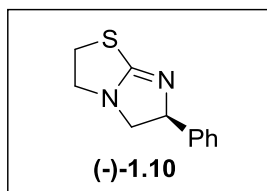
lactams, as well as a few amides and esters is discussed.<sup>38</sup> The method employs commercially available reagents to resolve a variety of synthetically useful substrates and achieves selectivity factors<sup>39</sup> up to 100.

## 2.2. Initial Investigations and Optimization

Initially, reaction conditions were developed using commercially available pantolactone (**2.1**) as the model substrate. Conditions similar to our previous work were employed, with the exception of a change in the base from diisopropyl-3-pentyl amine to Hünig's base because of the limited availability of the former. When catalysts **1.10** and (-)-benzotetramisole<sup>35</sup> (**1.5**) were tested, little to no conversion was observed (Table 2.1, Entries 1 and 2). When the reaction was warmed from -78 to -40 °C using **1.5** as the catalyst, only minor amounts of product formed, but some selectivity was achieved (Entry 3). Utilizing catalyst **1.5**, the concentration was almost tripled which led to an increase in conversion to about 40% and an impressive selectivity factor of 28 (Entry 4). In an attempt to increase the conversion further, the catalyst loading was increased to 25 mol%, resulting in a slight increase in conversion to 52% and a selectivity factor of 36 (Entry 5). After observing the significant effect of isothiourea structure on conversion, two additional catalysts were synthesized<sup>40</sup> and utilized in the kinetic resolution. When catalysts **1.10**, **2.3**, and **2.4** were employed under similar conditions to Entry 5, the resolutions failed to achieve conversions above 10% (Entries 6-8). Warming the reaction to 0°C in presence of **2.4** also failed to produce appreciable quantities of silyl ether product. Therefore, catalyst **1.5** and the conditions in Table 2.1 Entry 5 were chosen for subsequent studies.

**Table 2.1 Reaction Optimization Conditions for Pantolactone**

entry	catalyst (equiv)	conc. [M] <sup>a</sup>	% conv <sup>b</sup>	s <sup>b</sup>
1	<b>1.10</b> (0.2)	0.16	<5%	--
2	<b>1.5</b> (0.2)	0.16	<5%	--
3 <sup>c</sup>	<b>1.5</b> (0.2)	0.16	9%	<b>18</b>
4	<b>1.5</b> (0.2)	0.42	41%	<b>28</b>
5	<b>1.5</b> (0.25)	0.42	52%	<b>36</b>
6	<b>1.10</b> (0.25)	0.42	6%	--
7	<b>2.3</b> (0.2)	0.42	10%	--
8	<b>2.4</b> (0.2)	0.42	<5%	--
9 <sup>d</sup>	<b>2.4</b> (0.2)	0.42	7%	--



<sup>a</sup>Concentration with respect to substrate. <sup>b</sup>See ref.41 <sup>c</sup>Reaction was run at -40 °C. <sup>d</sup>Reaction was run at 0 °C.

An investigation into the effect of different silyl groups, solvents, and bases revealed that the previously determined conditions were still the optimum choice (triphenylsilyl chloride, THF, and Hünig's base). As was seen previously, the phenyl groups on the silyl chloride play a critical role in effecting the selectivity of the reaction (Table 2.2, Entries 2 and 3 versus Entry 1). When silyl chlorides were employed that contained fewer or no phenyl groups, the selectivity of the reaction dramatically

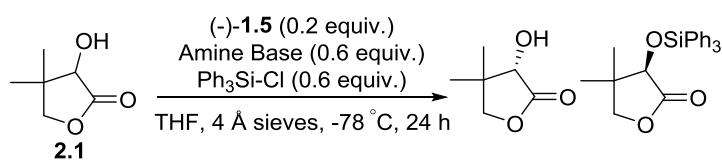
decreased from 36 to 2.9 and 4.6 for diphenylmethyl and phenyldimethylsilyl chloride, respectively. When a silyl source containing no aryl groups, triethylsilyl chloride, was employed very little silyl ether was formed with a low selectivity factor as well (Entry 4).

**Table 2.2 Alternating the Silyl Source for the Kinetic Resolution**

Entry	"silyl"	% conv <sup>a</sup>	<i>s</i> <sup>a</sup>
1	Ph <sub>3</sub> Si- (a)	52%	36
2	Ph <sub>2</sub> MeSi- (b)	56%	2.9
3	PhMe <sub>2</sub> Si- (c)	42%	4.6
4	Et <sub>3</sub> Si- (d)	25% <sup>b</sup>	2.9

<sup>a</sup>See ref. 41. <sup>b</sup>Conversion determined by <sup>1</sup>H NMR.

Alternative bases to *i*Pr<sub>2</sub>NEt were next investigated (Yan Zhang). Triethylamine produced the most comparable results to Hunig's base over the range of bases tested (Table 2.3, Entry 1 and 2) with only a slight decrease in conversion observed for the former. More sterically demanding bases triisobutylamine, and tribenzylamine resulted in a decrease in product formation (Table 2.3 Entry 3 and 4). Employing tributylamine resulted in similar conversions as compared to Hunig's base albeit with a significant decrease in selectivity (Entry 5). It was also demonstrated that the base is vital for conversion; experiments ran without base resulted in little to no silyl ether formation (Entry 6).

**Table 2.3 Exploring the Effect of Base on Selectivity**

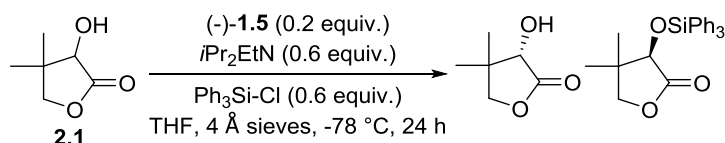
Entry	Base	Conv (%) <sup>a</sup>	s <sup>a</sup>	er SM
1	triethyl amine	43	31	84:16
2	<i>N,N</i> -diisopropylethyl amine	45	31	88:12
3	tribenzyl amine	21	31	62:38
4	triisobutyl amine	23	31	65:35
5	tributyl amine	39	25	70:30
6 <sup>b</sup>	no base	<5	--	--

<sup>a</sup>See ref. 41. <sup>b</sup>Conversion determined by <sup>1</sup>H NMR.

Next attention was focused on solvents other than THF, the solvent found to be optimal for benzylic alcohols<sup>1</sup> (Yan Zhang). The solvents dichloromethane, DMF, DME, and toluene provided high conversions, but selectivity factors were significantly decreased compared to THF (*s*: 7, 2, 5 and, 10 respectively; Table 2.4; Note DMF and DME were ran at  $-40^\circ\text{C}$  due to the high melting point of these solvents). Interestingly, toluene and dichloromethane resulted in improved conversion (Entries 2 and 5). A few mixed solvent systems were thus explored. A 10%  $\text{CH}_2\text{Cl}_2$  solution in THF produced a higher conversion to the detriment of selectivity as compared to THF (Entry 6). When reactions employing 5 and 10% toluene in THF were tested a similar increase in conversion was observed; however, the selectivity when compared to pure THF was again slightly decreased (Entries 7 and 8). Employing the optimal conditions (Table 2.1, Entry 5) on a preparative scale kinetic resolution of **2.1** showed similar results to the

smaller scale runs. Over a gram of alcohol was tested in the kinetic resolution, and a selectivity factor of 28 was observed with 50% conversion. This reaction had only a minor reduction in selectivity (Table 2.1, Entry 5;  $s = 36$ ) and demonstrated the applicability of the reaction to preparatory scale synthesis.

**Table 2.4 Testing the Effect of Solvent on Selectivity**



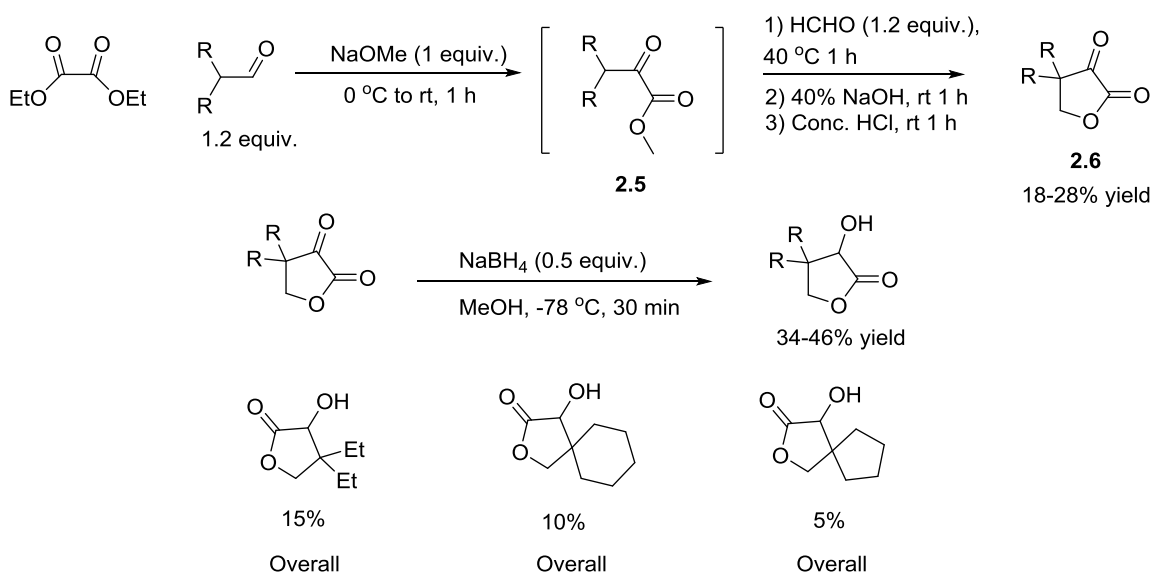
Entry	Solvent	Temp °C	Conv. % <sup>a</sup>	$s^a$	er SM
1	THF	-78	46	27	86:14
2	CH <sub>2</sub> Cl <sub>2</sub>	-78	53	7	83:17
3	DMF	-40	43	2	57:43
4	DME	-40	41	5	57:43
5	Toluene	-78	56	10	89:11
6	10% CH <sub>2</sub> Cl <sub>2</sub> in THF	-78	51	19	90:10
7	10% Toluene in THF	-78	51	25	95:5
8	5% Toluene in THF	-78	59	26	89:11

<sup>a</sup>See ref. 41.

### 2.3. Synthesis of Hydroxy Lactones

With the optimized reaction conditions obtained from the resolution of **2.1**, the substrate scope was explored. We wanted to explore the effect of the steric bulk at the  $\beta$ -position, therefore a variety of lactones possessing sterically hindered groups in the  $\beta$ -position were synthesized.<sup>42</sup> Several lactones with varying  $\beta,\beta$ -substitution including  $\beta,\beta$ -diethyl and  $\beta$ -spirocyclic lactones derivatized with five and six-membered rings were

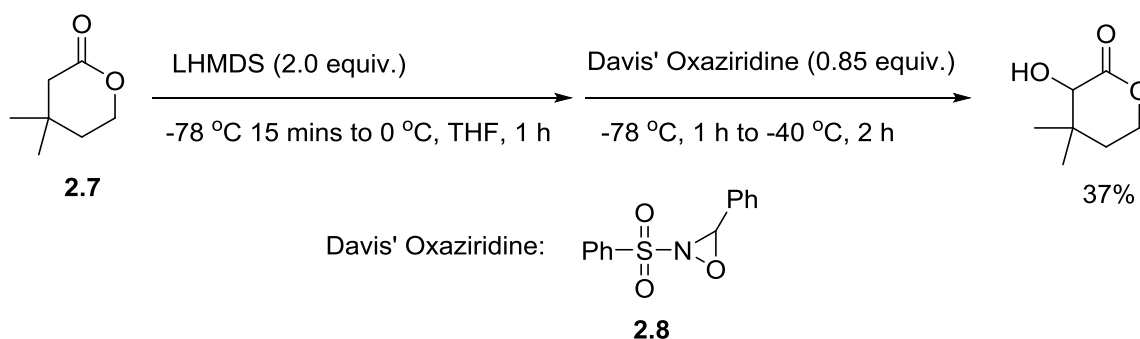
prepared utilizing the method outlined in Scheme 2.4. First, furandiones of the general structure **2.6** were prepared via a four step synthesis in one pot. The pyruvate derivative **2.5** is obtained from degradation of the Claisen adduct of diethyloxalate and an aldehyde formed upon sodium methoxide catalysis. An aldol reaction with formaldehyde followed by cyclization affords the desired diketones **2.6** in modest yield after vacuum distillation. Subsequently, the desired  $\alpha$ -hydroxy lactones were obtained after sodium borohydride reduction at  $-78\text{ }^\circ\text{C}$  in order to control rates of over-reduction.



### Scheme 2.4 Synthesis of $\beta,\beta$ -Disubstituted Hydroxy Lactones

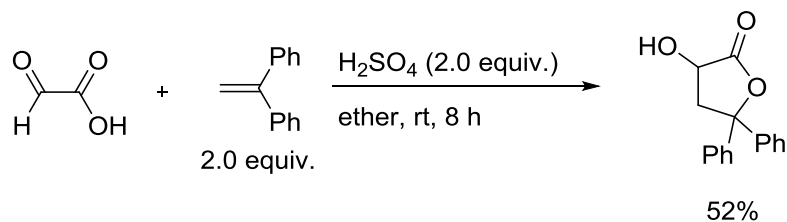
The preparation of six-membered ring lactones cannot be achieved from the approach highlighted in Scheme 2.4. Alternatively, the  $\alpha$ -hydroxy lactone was obtained more directly from  $\alpha$ -oxidation of the corresponding lactone (Scheme 2.5). The enolate of starting material **2.7** is formed using lithium hexamethyldisilazane (LHMDS) as the base. This base is needed because the oxidant, Davis' oxaziridine (**2.8**), is reactive with other more common bases used for this purpose such as lithium diisopropylamine.<sup>43</sup> The

oxidation with **2.8** afforded the desired lactone in modest yield from  $\beta,\beta$ -dimethyl lactone **2.7**. More general oxidants, such as *m*-chloroperoxybenzoic acid<sup>44</sup> (MCPBA) cannot be utilized with lactones since its nucleophilic nature facilitates ring opening. Unfortunately, numerous attempts to oxidize valerolactone, the same lactone as **2.7** but lacking beta substitution, were unsuccessful.



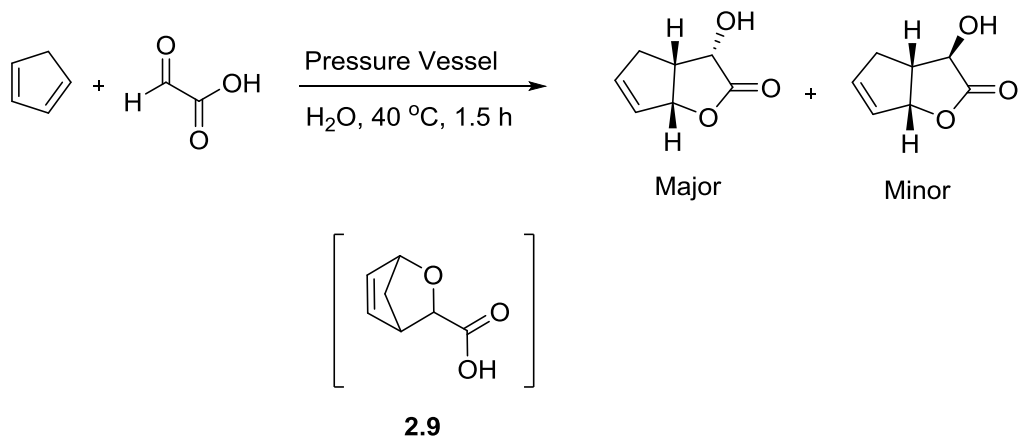
### Scheme 2.5 Davis' Oxidation of $\beta,\beta$ -Dimethyl Valerolactone

The study of 5-membered ring lactones possessing disubstitution in the gamma position was also of interest. This class of compounds presented a significant challenge, and very few methods of production were available. An interesting carbonyl-ene reaction was attempted<sup>45</sup> (Scheme 2.6). Gratifyingly, reaction of glyoxylic acid with 1,1-diphenylethene under sulfuric acid catalysis afforded the desired lactone in good yield. In this reaction, the alkene attacks the activated aldehyde prompting cyclization via bond formation between the nascent carbocation and carboxylic acid.



### Scheme 2.6 Carbonyl-Ene Reaction Route to a $\gamma, \gamma$ -Substituted Lactone

A bicyclic  $\alpha$ -hydroxy lactone was prepared via a hetero Diels-Alder reaction. Freshly prepared cyclopentadiene was reacted with the aldehyde of the glyoxylic acid electrophile in a pressure vessel with water as the solvent (Scheme 2.7). The Diels-Alder adduct **2.9** is not stable and rapidly undergoes a carbocation-forming rearrangement to a diastereomeric mixture of lactones under the reaction conditions. The diastereomers were successfully separated by column chromatography. The major, cis product was utilized in the kinetic resolution since the sterics in the  $\beta$ -position are cis to the alcohol, essentially providing more sterics than the trans isomer.



### Scheme 2.7 Hetero Diels-Alder Preparation of Bicyclic Lactones



## 2.4. Examining the Lactones in the Silylation-Based Kinetic Resolution

With a variety of lactones prepared for study the substrate scope was next tested using the previously optimized conditions (Table 2.5). When the commercially available  $\alpha$ -hydroxy- $\gamma$ -butyrolactone was investigated a significant decrease in selectivity was observed (Entry 1). This led us to hypothesize that sterically large groups in the  $\beta$ -position are highly important to selectivity. As predicted, changing the  $\beta,\beta$ -dimethyl group in **2.1** to a larger  $\beta,\beta$ -diethyl group resulted in a dramatic increase in selectivity to an *s* of 100 (Table 2.5, Entry 3). This result is the highest selectivity factor obtained to date for the triphenyl silylation-based kinetic resolution of secondary alcohols.<sup>1, 46</sup> Spiro cyclic lactones (Table 2.5, Entries 4 and 5) were also resolved with a high degree of selectivity. The cyclohexane substituted spiro lactone (Entry 5) was more selective than the cyclopentane substituted one (Entry 4), presumably due to the increased sterics of the six membered ring. The fused bicyclic lactone was also explored with moderate selectivity (Entry 6). Interestingly, when the lactone was substituted in the  $\gamma$ -position with sterically large phenyl groups (Table 2.5, Entry 7) nearly all selectivity was lost. Finally, when the  $\beta,\beta$ -disubstituted lactone ring was expanded from a 5 to a 6 membered ring (Entry 8) the substrate became too sterically hindered and no conversion was obtained. Unfortunately, the corresponding unsubstituted 6-membered ring lactone, obtained commercially, decomposed under the reaction conditions and therefore could not be examined (Entry 9). This decomposition presumably could explain the failed synthetic attempts for this substrate using the method shown in Scheme 2.5.

**Table 2.5 Substrate Scope of the Silylation-Based Kinetic Resolution of  $\alpha$ -Hydroxy Lactones**

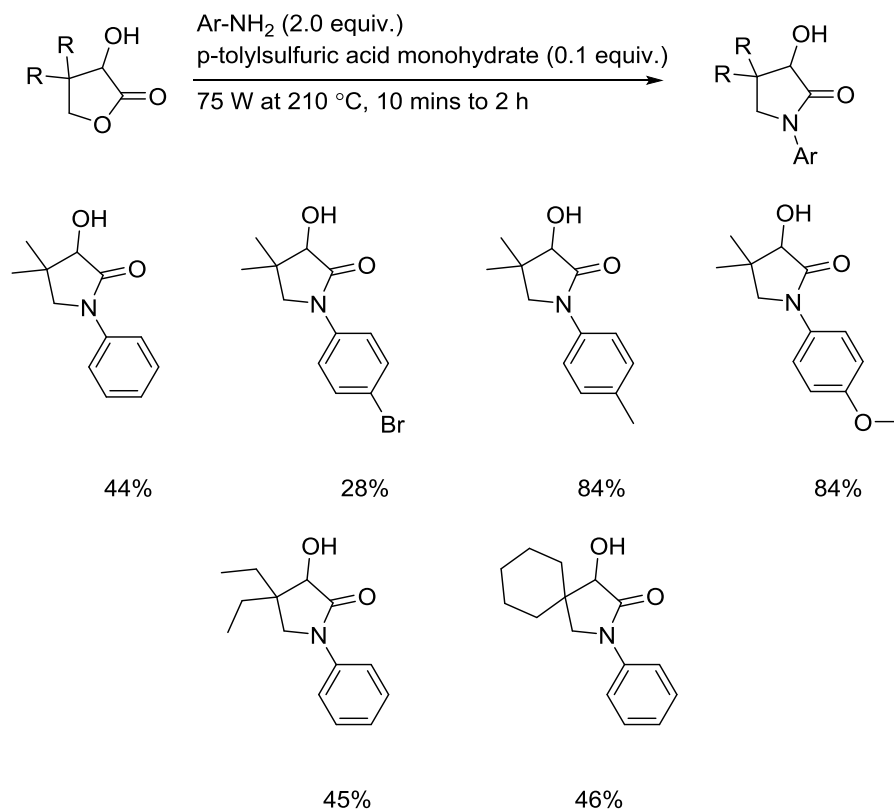
entry	recovered alcohol	<i>t</i> (h)	er of recovered alcohol	% conv <sup>a</sup>	<i>s</i> <sup>a</sup>
1		24	82:18	57	5.8
2		24	96:4	52	36
3		48	82:18	40	100
4		48	94:6	53	23
5		48	98:2	53	48
6		48	90:10	58	7.8
7		24	53:47	56	1.2
8		48	--	<5 <sup>b</sup>	--
9		24	--	decomp <sup>b</sup>	--

<sup>a</sup>See ref. 41. <sup>b</sup>Conversion determined by <sup>1</sup>H NMR.

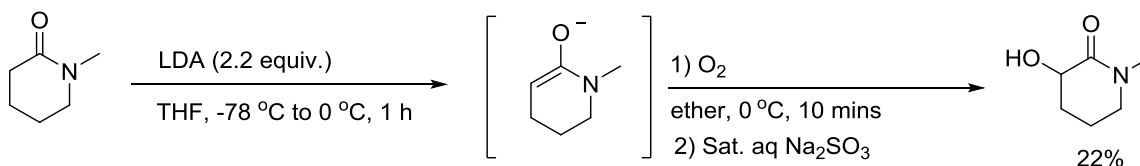
## 2.5. Synthesis of Hydroxy Lactams

In order to examine  $\alpha$ -hydroxy lactams they needed to be synthesized. The simplest approach for 5-membered ring lactams is amidation and cyclization of the lactones prepared previously. The microwave was utilized since the irradiation affords a faster dehydration and cyclization reaction as compared to conventional approaches. *N*-aryl substituted lactams could thus be prepared in one step from the corresponding lactone and an aryl amine<sup>47</sup> (Scheme 2.8). In most cases, the lactam was formed in 10 minutes under 75W constant microwave irradiation with catalytic quantities (0.1 equiv.) of *p*-tolylsulfuric acid. The lactams were obtained in excellent yields using more electron-rich anilines and good to moderate with aniline as the amine source. When an aryl amine possessing an electron withdrawing bromine was prepared in a similar fashion significantly lower yields were obtained with additional reaction time.

Hydroxy lactams with rings larger than five members are difficult to prepare using the approach shown in Scheme 2.8. However, these lactams can be prepared from direct oxidation of the enolate in a similar fashion to the Davis' oxidation of lactones (Scheme 2.9). However, the lactams generally require stronger oxidizing reagents than Vedejs'<sup>48</sup> or Davis' reagent.<sup>43</sup> In our approach, the enolate is formed via deprotonation with LDA and oxidized with oxygen gas. The reaction yields an  $\alpha$ -organic peroxide which is reduced with Na<sub>2</sub>SO<sub>3</sub> to the desired alcohol upon work-up. As with any organic peroxide, care was taken not to allow the unstable intermediate to warm above 0 °C. Although the yield was low, this method offers a simple approach to 6-membered ring hydroxy lactams.



**Scheme 2.8 Microwave Assisted Synthesis of Lactams from Lactones with Aryl Amines**



**Scheme 2.9 Direct Oxidation Route to Hydroxy Lactams**

### 2.6. Testing the Lactams in the Silylation-Based Kinetic Resolution

The lactams were universally less selective than their lactone counterparts. Unfortunately, complete loss of enantioselectivity was observed for the *N*-phenyl lactam with no substituents in the  $\beta$ -position (Table 2.6, Entry 1). Even though amides are known to catalyze silylation reactions,<sup>10</sup> no product was detected when the reaction was

run with the same unsubstituted substrate in the absence of catalyst **1.5**. This shows that the lack of selectivity is not due to an uncontrolled background reaction.

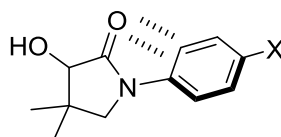
**Table 2.6 Scope of the Silylation-Based Kinetic Resolution of  $\alpha$ -Hydroxy Lactams**

entry	recovered alcohol	<i>t</i> (h)	er of recovered alcohol	% conv <sup>a</sup>	<i>s</i> <sup>a</sup>
1		24	rac	57 <sup>b</sup>	1.0
2		48	84:16	47	14
3		48	60:40	22	7.1
4		48	66:34	32	6.8
5		48	62:38	34	3.3
6		48	60:40	20	20
7 <sup>c</sup>		72	97:3	56	24

<sup>a</sup>See ref. 41. <sup>b</sup>Conversion determined by <sup>1</sup>H NMR. <sup>c</sup>Reaction performed with 0.75 equiv of Ph<sub>3</sub>SiCl and *i*Pr<sub>2</sub>NEt.

Similarly to the lactones, increasing sterics in the  $\beta$ -position of the lactams increased the selectivity. As the substituents were changed from methyl to ethyl to a 6-membered spiro ring (Table 2.6, Entries 2, 6, and 7), the selectivity factors increased from 14 to 20 to 24 respectively. However, the reactions became sluggish as the sterics increased in the  $\beta$ -position; therefore, more equivalents of silyl chloride and base were employed to force higher conversions (Entry 7). The effect of electronics on the *N*-aryl group was investigated by substituting electron donating (methyl, methoxy) and an electron withdrawing group (bromo) in the para position (Table 2.6, Entries 3-5). Surprisingly, a decrease in selectivity was observed for both electron withdrawing and electron donating substituents. The selectivity factor for electron donating groups dropped by a factor of 2, while electron withdrawing groups decreased the selectivity factor even further ( $s = 7.1, 6.8, \text{ and } 3.3, \text{ respectively}$ ).

As shown in Table 2.5 (Entry 3 versus 7), the reaction is sensitive to the position of sterics on the substrates. Substituents in the  $\beta$ -position are advantageous to selectivity, whereas sterics in the  $\gamma$ -position are detrimental. The *N*-aryl group<sup>49-50</sup> on the lactams also seems to alter the selectivity of the reaction resulting in a decrease in enantio-discrimination as compared to the lactone counterparts. Presumably, this is the result of a change in sterics on the substrates due to the phenyl group rotating out of the lactam plane to form a carbonyl- $\pi$  interaction (Scheme 2.10).<sup>50</sup> The interaction would be more pronounced with the bromo substituted phenyl group, resulting in the low selectivity observed.

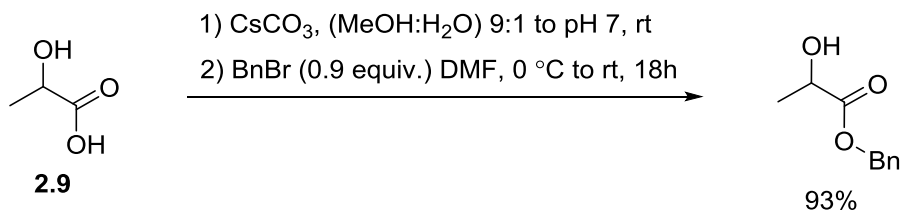


X = OMe, Me, Br

### Scheme 2.10 Proposed Carbonyl- $\pi$ Interaction of N-Aryl Lactams

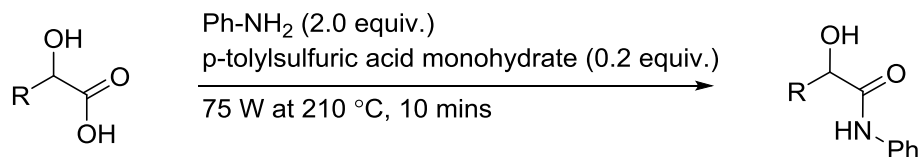
#### 2.7. Synthesis of Amides and Esters

In order to determine the triphenylsilyl chloride-based resolutions efficiency on acyclic substrates, a variety of amides and esters were synthesized. A benzyl ester was prepared employing simple esterification of lactic acid **2.9** (Scheme 2.11). First, the cesium salt was isolated upon deprotonation with cesium carbonate and work-up. The salt was then reacted with benzyl bromide in dimethylformamide (DMF) at room temperature to yield the benzyl ester from a nucleophilic substitution in excellent yield.



### Scheme 2.11 Synthesis of a Benzyl Ester from Lactic Acid

The preparation of amides was much more general (Scheme 2.12) and used a similar approach to that utilized for lactams (Scheme 2.8). The  $\alpha$ -hydroxy amides were obtained via microwave assisted and acid catalyzed amidation. Reaction of an  $\alpha$ -hydroxy acid and aniline after microwave irradiation at 75 W for 10 minutes afforded desired products in excellent yields in all cases utilizing this approach.



**Scheme 2.12 Synthesis of Hydroxy Amides**

### 2.8. Testing Amides and Esters in the Silylation-Based Resolution

Acyclic esters and amides were also explored employing the previously developed standard reaction conditions (Table 2.7). Previously, acyclic substrates, such as 1-phenylethanol, were slow to silylate and displayed no enantio-discrimination.<sup>1</sup> The *N*-phenyl amides and *O*-phenyl and *O*-benzyl ester in Table 4 did show a small amount of selectivity with decent conversions. The small improvement of the amides over previous acyclic substrates is presumably due to the high energy barrier of rotation around the nitrogen-carbon bond providing some degree of planarity.<sup>51</sup> The amides showed no sensitivity to substituents next to the alcohol (Entries 1-3), but were slightly more selective than the esters (Entries 4 and 5). This is probably the result of the increased barrier of rotation for the amides versus the esters.



**Table 2.7 Scope of the Silylation Kinetic Resolution of Amides and Esters**

X = NH, O

entry	recovered alcohol	t (h)	er of recovered alcohol	% conv <sup>a</sup>	s <sup>a</sup>
1		24	81:19	47	8.5
2		24	83:17	54	6.6
3		24	79:21	49	7.3
4		24	83:17	57	3.9
5		24	81:19	53	5.6

<sup>a</sup>See ref 41.

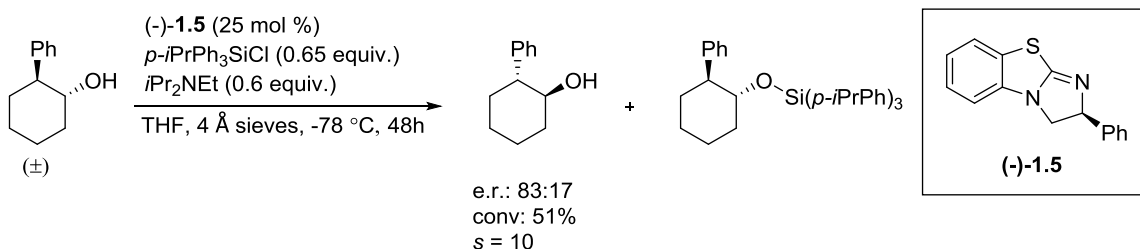
## 2.9. Conclusions and Outlook

In conclusion, silylation-based kinetic resolutions have been expanded to include synthetically valuable  $\alpha$ -hydroxy carbonyl compounds employing an isothiourea catalyst and commercially available reagents. This is one of the few non-enzymatic kinetic resolutions of  $\alpha$ -hydroxy lactones and the first non-enzymatic kinetic resolution of  $\alpha$ -hydroxy lactams. Selectivity factors up to 100 were obtained by including sterically demanding groups adjacent to the alcohol. Spirocenter containing lactones and lactams were efficiently resolved under these conditions. It was discovered that sterics elsewhere

on the ring proved detrimental, and acyclic amides and esters were tolerated in this system although with limited selectivity.

Future investigations to make the methodology more synthetically viable are paramount. Application of the reaction at temperatures closer to ambient temperature would be beneficial to practical applications on large scale. Lactones that have been demonstrated to be highly selective ( $s > 30$ ; i.e. Table 2.5, Entries 2, 3, and 5) could be tested in the reaction at higher temperatures. The selectivities of these reactions would undoubtedly be lower but may be synthetically useful at higher temperatures at  $-40\text{ }^{\circ}\text{C}$  or room temperature. These studies should test one substrate to demonstrate the maximum temperature at which an  $s$ -factor greater than ten can be achieved.

Additional substrate scope expansion studies have been accomplished (Li Wang) The general core structures investigated in this chapter have provided critical guidance to further expand the substrate scope of the silylation-based kinetic resolution. Recently, 2-arylcyclohexanols were successfully resolved using similar conditions to those employed for  $\alpha$ -hydroxy lactones.<sup>46</sup> These substrates are undoubtedly selective in this methodology as a result of the conformationally rigid cyclohexane featuring a  $\pi$ -system in close proximity to the alcohol (Scheme 2.3).



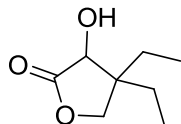
**Scheme 2.13 Silylation-Based Resolution of 2-Arylcyclohexanols**

Understanding the mechanism involved in the transfer of chirality from isothioureia to alcohol is inevitably required to fully understand and evaluate the future directions of this methodology. Further studies to elucidate the mechanism have been done including a linear free energy relationship (LFER) study<sup>52</sup> (Ravish Akhani). These mechanistic investigations have directly impacted the application of the triphenylsilyl chloride based resolution. For instance, the LFER study indicated electron-donating groups on the phenyl rings of the silylsource have a significant, favorable effect on selectivity. Therefore, these modified triarylsilyl chlorides were utilized to resolve 2-arylclohexanols (Scheme 2.13).<sup>46</sup> This substrate class would otherwise be much less easily resolved by the triphenylsilyl chloride-based method due to lower selectivities. Insights into the mechanism will provide new and interesting directions for the kinetic resolution. Further work included mechanistic study through the use of a kinetic evaluation using in situ analytical techniques. Results of these kinetic studies and other mechanistic investigations into silylation-based kinetic resolutions will be discussed in Chapter 4.

## 2.10. Experimental

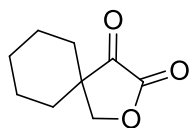
### Racemic Lactone and Lactam Syntheses

Pantolactone was purchased from TCI and recrystallized from ether and hexanes prior to use.  $\alpha$ -Hydroxy- $\gamma$ -butyrolactone was purchased from Acros and used without further purification. Phenyl-2-hydroxypropanoate<sup>53</sup> and ( $\pm$ )-4-endo-hydroxy-2-oxabicyclo[3.3.0]oct-7-en-3-one<sup>54</sup> can be prepared from known literature procedures.



#### 4,4-Diethyl-3-hydroxydihydrofuran-2(3H)-one<sup>55</sup>

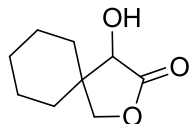
To a 50 mL round bottom flask was added 4,4-diethyl-4,5-dihydrofuran-2,3-dione<sup>42</sup> (1.1 g, 7.0 mmol) and the flask was equipped with a stir bar. The solid was dissolved in 10 mL of methanol with stirring, then cooled to -78 °C in a dry ice/acetone bath for 15 mins. Sodium borohydride (132 mg, 3.5 mmol) was added in portions. The progress of the reaction was monitored by TLC. After 30 mins, conversion was complete and the reaction was quenched with a saturated aqueous NH<sub>4</sub>Cl solution (2 mL) and allowed to warm to room temperature for 30 mins. The contents of the flask were transferred to a separatory funnel and diluted with ether. Water was added to dissolve the precipitate and the aqueous layer was extracted with ether (4 x 25 mL) and combined. The organic layers were washed with brine and dried over sodium sulfate. Filtration and concentration yielded an oil which was further purified on silica gel column chromatography (25% EtOAc in hexanes) to afford the hydroxy lactone as a white solid, 710 mg, 64 % yield. <sup>1</sup>H NMR: (400 MHz, CDCl<sub>3</sub>) δ 4.22 (s, 1 H), 4.16 (d, *J* = 9.3 Hz, 1 H), 3.87 (d, *J* = 9.3, 1 H), 1.67-1.39 (m, 4 H), 0.99 (t, *J* = 7.5 Hz, 3 H), 0.91 (t, *J* = 7.5 Hz, 3 H). <sup>13</sup>C NMR (101 MHz, CDCl<sub>3</sub>) δ 178.3, 74.7, 73.1, 46.6, 28.1, 21.4, 8.5, 8.0.



#### 2-Oxaspiro[4.5]decane-3,4-dione

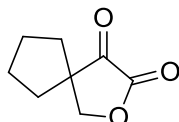
An oven dried 250 mL round bottom flask was fitted with stir bar and septum and purged with argon. Sodium methoxide in methanol (5.9 mL, 5.4 M) was added via syringe. The

solution was then cooled to 0 °C in an ice bath for 15 mins. Diethyl oxalate (4.3 mL, 32 mmol) was added via syringe followed by cyclohexane carboxaldehyde (4.7 mL, 38.4 mmol) slowly via syringe. The resulting mixture was allowed to warm to ambient temperature with stirring for 1 h. The mixture was warmed to 40 °C in a sand bath and an aqueous solution of formaldehyde (3.12 g, 37% w/w) was added. The resulting mixture was left to stir at 40 °C for 1 h. Upon cooling to room temperature, 3.5 g of a 40% aqueous sodium hydroxide solution was added and the mixture was allowed to stir an additional hour. Finally, 6.4 mL of concentrated HCl was added and the mixture was left to stir for 1 h producing salt as a precipitate. The salt was filtered away and the resulting aqueous mixture was concentrated via rotovap to remove methanol. The resulting biphasic mixture was diluted with 50 mL of EtOAc and transferred to a separatory funnel. The aqueous layer was extracted with EtOAc (3 x 50 mL) and the combined organic layers were washed with brine. Further drying over sodium sulfate, filtration and concentration yielded a yellow oil. This oil was fractionally distilled under reduced pressure with the product distilling at 85 °C, 4 mm Hg. The resulting oil rapidly solidified to produce an oily white solid. Further purification by recrystallization (ether and hexanes) afforded the desired product as white crystals, 1.23 g, 22.9 % yield **mp** range = 67-69 °C. **<sup>1</sup>H NMR:** (400 MHz, CDCl<sub>3</sub>) δ ppm 4.53 (s, 1H), 1.84-1.80 (m, 2H), 1.74-1.62 (m, 5H), 1.49-1.31 (m, 3H). **<sup>13</sup>C NMR** (101 MHz, CDCl<sub>3</sub>) δ ppm 197.6, 160.9, 75.1, 45.5, 31.2, 24.6, 21.4. **IR** (neat, cm<sup>-1</sup>) 2934, 2860, 1774, 1449, 1299, 1228, 1115, 993, 973, 898, 820, 740. **HRMS** (ESI) calculated for (C<sub>9</sub>H<sub>12</sub>O<sub>3</sub><sup>+</sup>) (M<sup>+</sup>): 168.0780, Observed: 168.0782.



#### 4-Hydroxy-2-oxaspiro[4.5]decan-3-one

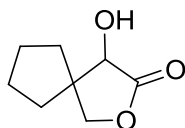
To a 50 mL round bottom flask was added 2-oxaspiro[4.5]decane-3,4-dione (1.23 g, 7.3 mmol) and the flask was equipped with a stir bar. The solid was dissolved in 10 mL of methanol with stirring then cooled to  $-78\text{ }^{\circ}\text{C}$  in a dry ice/acetone bath for 15 mins. Sodium borohydride (140 mg, 3.7 mmol) was added in portions. The progress of the reaction was monitored by TLC. After 30 mins conversion was complete and the reaction was quenched with a saturated aqueous  $\text{NH}_4\text{Cl}$  solution (2 mL) and allowed to warm to room temperature for 30 mins. The contents of the flask were transferred to a separatory funnel and diluted with ether. Water was added to dissolve the precipitate and the aqueous layer was extracted with ether (4 x 25 mL) and combined. The organic layer was washed with brine and dried over sodium sulfate. Filtration and concentration yielded an oil which was further purified on silica gel column chromatography (25% EtOAc in hexanes) to afford the hydroxy lactone as a white solid, 573 mg, 46.2% yield, **mp** range =  $57\text{-}58\text{ }^{\circ}\text{C}$ .  **$^1\text{H NMR}$** : (400 MHz,  $\text{CDCl}_3$ )  $\delta$  ppm 4.34 (d,  $J = 9.2$ , 1H), 4.09 (d,  $J = 3.6$ , 1H), 3.89 (dd,  $J = 1.4, 7.8$ , 1H), 2.82 (d,  $J = 3.8$ , 1H), 1.74-1.57 (m, 6H), 1.44-1.20 (m, 4H).  **$^{13}\text{C NMR}$**  (101 MHz,  $\text{CDCl}_3$ )  $\delta$  ppm 177.7, 75.7, 73.6, 44.1, 33.7, 25.8, 25.3, 22.9, 21.7. **IR** (neat,  $\text{cm}^{-1}$ ) 3417, 2930, 2853, 1771, 1455, 1161, 1108, 1001, 980, 933, 850, 730. **HRMS** (ESI) calculated for  $(\text{C}_9\text{H}_{14}\text{O}_3)^+$  ( $\text{M}^+$ ): 170.0937, Observed: 170.0944.



### 2-Oxaspiro[4.4]nonane-3,4-dione

An oven dried 250 mL round bottom flask was fitted with a stir bar and septum and purged with argon. Sodium methoxide in methanol (6.2 mL, 5.4 M) was added via syringe. The solution was then cooled to 0 °C in an ice bath for 15 mins. Diethyl oxalate (4.5 mL, 33 mmol) was added via syringe followed by cyclopentane carboxaldehyde (4.4 mL, 40 mmol) slowly via syringe. The resulting mixture was allowed to warm to ambient temperature with stirring for 1 h. The mixture was warmed to 40 °C in a sand bath and an aqueous solution of formaldehyde (3.2 g, 37% w/w) was added. The resulting mixture was left to stir at 40 °C for 1 h. Upon cooling to room temperature, 3.6 g of a 40% aqueous sodium hydroxide solution was added and the mixture was allowed to stir an additional hour. Finally, 6.6 mL of concentrated HCl was added and the mixture was left to stir for 1 h producing salt as a precipitate. The salt was filtered away and the resulting aqueous mixture was concentrated via rotovap to remove methanol. The resulting biphasic mixture was diluted with 50 mL of EtOAc and transferred to a separatory funnel. The aqueous layer was extracted with EtOAc (3 x 50 mL) and the combined organic layers were washed with brine. Further drying over sodium sulfate, filtration and concentration yielded a yellow oil. This oil was fractionally distilled under reduced pressure with the product distilling at 155 °C, 4 mm Hg. The resulting oil rapidly solidified to produce an oily white solid. Further purification by recrystallization (ether and hexanes) afforded the desired product as white crystals, 1.56 g, 25% yield, **mp** range 54-55 °C. <sup>1</sup>H NMR: (400 MHz, CDCl<sub>3</sub>) δ ppm 4.55 (s, 2H), 2.09-1.75 (m, 8H). <sup>13</sup>C

**NMR** (101 MHz, CDCl<sub>3</sub>) δ ppm 198.0, 160.7, 76.7, 52.8, 36.5, 25.8. **IR** (neat, cm<sup>-1</sup>) 2966, 2872, 1779, 1768, 1446, 1386, 1322, 1266, 1110, 991, 931, 889. **HRMS** (ESI) calculated for (C<sub>8</sub>H<sub>10</sub>O<sub>3</sub>)<sup>+</sup> (M<sup>+</sup>): 154.0624, Observed: 154.0624.

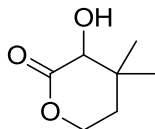


#### **4-Hydroxy-2-oxaspiro[4.4]nonan-3-one**

To a 50 mL round bottom flask was added 2-oxaspiro[4.4]nonane-3,4-dione (1.5 g, 10 mmol) and the flask was equipped with a stir bar. The solid was dissolved in 10 mL of methanol with stirring then cooled to -78 °C in a dry ice acetone bath for 15 mins. Sodium borohydride (190 mg, 5.0 mmol) was added in portions. The progress of the reaction was monitored by TLC. After 30 mins of reaction time conversion was complete and the reaction was quenched with a saturated aqueous NH<sub>4</sub>Cl solution (2 mL) and allowed to warm to room temperature for 30 mins. The contents of the flask were transferred to a separatory funnel and diluted with ether. Water was added to dissolve the precipitate and the aqueous layer was extracted with ether (4 x 25 mL) and combined. The organic layer was washed with brine and dried over sodium sulfate. Filtration and concentration yielded an oil which was further purified on silica gel column chromatography (25% EtOAc in hexanes) to afford the hydroxyl lactone as a white solid, 1.57 g, 25% **mp** range = 70-72 °C. **<sup>1</sup>H NMR:** (400 MHz, CDCl<sub>3</sub>) δ ppm 4.32 (s, 1 H), 4.13 (d, *J* = 8.8 Hz, 1 H), 4.03 (dd, *J* = 7.8, 1.0 Hz, 1 H), 3.43 (br, 1 H), 2.05-1.58 (m, 7 H), 1.46-1.39 (m, 1 H). **<sup>13</sup>C NMR:** (101 MHz, CDCl<sub>3</sub>) δ ppm 177.9, 76.1, 73.6, 51.6, 33.6, 29.1, 25.0, 24.9. **IR** (neat, cm<sup>-1</sup>) 3378, 2951, 2868, 1759, 1426, 1287, 1199, 1131,



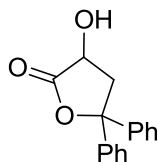
1095, 988, 873, 722. **HRMS** (ESI) calculated for (C<sub>8</sub>H<sub>12</sub>O<sub>3</sub>) (M<sup>+</sup>): 156.0780, Observed: 156.0780.



### **3-Hydroxy-4,4-dimethyltetrahydro-2H-pyran-2-one**

A 250 mL schlenk flask was fitted with a stir bar and a septum and purged with argon. Into this flask, bis(trimethylsilyl)amine (0.95 mL, 4.5 mmol) was added via syringe and dissolved in 15 mL of THF. The solution was cooled to -78 °C in a dry ice acetone bath. *n*BuLi in hexanes (1.9 mL, 4.5 mmol) was added drop wise via syringe, then the mixture was left to stir for 1 h. A solution of 5-hydroxy-3,3-dimethylpentanoic acid lactone<sup>56</sup> (374 mg, 2.9 mmol) was prepared in 20 mL of THF under argon and the resulting solution added slowly via syringe to the reaction vessel. The reaction was allowed to proceed at -78 °C for 15 mins then warmed to 0 °C in an ice bath over 1 h. The reaction mixture was again cooled to -78 °C. A solution of Davis' oxaziridine<sup>57</sup> (1.1 g, 3.8 mmol) was prepared under argon in 20 mL of THF and added to the reaction slowly via syringe. The reaction was stirred at -78 °C for 1 h then warmed to -40 °C in a dry ice/acetonitrile bath over a 2 h period. The reaction was quenched with 36 mL of a 1 M aqueous NH<sub>4</sub>Cl solution, and the mixture was left to warm to ambient temperature. The resulting biphasic mixture was transferred to a separatory funnel and diluted with ether (50 mL). The aqueous layer was extracted with ether (4 x 25 mL) and the organic layers combined. The ethereal mixture was then washed with brine, dried over sodium sulfate and filtered. Concentration of the crude gave an oily white solid. The crude was purified on silica gel column chromatography (10% EtOAc in hexanes gradient to 30% EtOAc in hexanes gradient to

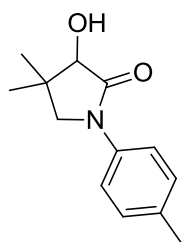
50% EtOAc in hexanes) affording the product with oxaziridine decomposition products. The impurities were removed via trituration with a hot 1:1 ether: hexanes solution, and the insoluble Davis' degradation products filtered away. Concentration of the filtrate gave the desired product with only minor impurities as a colorless oil, 240 mg, 57% yield. **<sup>1</sup>H NMR:** (400 MHz, CDCl<sub>3</sub>) δ ppm 4.37 (dd, *J* = 5.9, 1.0, 2H), 4.01 (s, 1H) 1.97-1.90 (m, 1H), 1.84-1.77 (m, 1H), 1.21 (s, 3H), 1.02 (s, 3H). **<sup>13</sup>C NMR** (101 MHz, CDCl<sub>3</sub>) δ ppm 175.2, 75.0, 65.9, 36.3, 34.6, 27.7, 21.1. **IR** (neat, cm<sup>-1</sup>) 3478, 2960, 1731, 1469, 1258, 1162, 1108, 1066, 996, 883, 755. **HRMS** (M<sup>+</sup>) calculated for (C<sub>7</sub>H<sub>12</sub>O<sub>3</sub>)<sup>+</sup> (M<sup>+</sup>): 144.0780, Observed: 144.0776.



### 3-Hydroxy-5,5-diphenyldihydrofuran-2(3H)-one

A 50 mL round bottom flask was equipped with stir bar and charged with 6 mL of ether. Glyoxylic acid monohydrate (920 mg, 10 mmol) was added and the mixture stirred vigorously to produce a suspension. Concentrated sulfuric acid (1.1 mL, 20 mmol) was added resulting in immediate solvation of the monohydrate. 1,1-Diphenylethene (3.5 mL, 20 mmol) was added drop wise via syringe and the mixture was left to stir at ambient temperature for 8 h. The reaction was quenched by adding 30 mL of a saturated aqueous sodium bicarbonate solution and the biphasic mixture was transferred to a separatory funnel. The aqueous layer was extracted with EtOAc (3 x 25 mL), and the resulting organic layers were combined and dried over sodium sulfate. After filtration and concentration, the crude was subjected to silica gel chromatography (10% EtOAc in

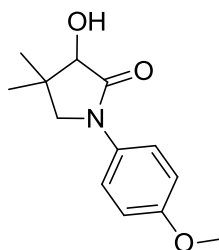
hexanes gradient to 40% EtOAc in hexanes) to afford the product as a white solid, 1.3 g, 52 %, **mp** range = 90 – 93 °C. **<sup>1</sup>H NMR**: (400 MHz, CDCl<sub>3</sub>) δ ppm 7.42-7.24 (m, 10H), 4.49 (t, *J* = 8.7, 1H), 3.47 (dd, *J* = 7.8, 4.8, 1H), 3.26 (br, 1H), 2.77 (dd, *J* = 11.3, 1.2, 1H). **<sup>13</sup>C NMR** (101 MHz, CDCl<sub>3</sub>) δ ppm 176.7, 143.0, 141.7, 128.8, 128.5, 128.2, 128.1, 125.3, 125.2, 86.7, 68.3, 43.3. **IR** (neat, cm<sup>-1</sup>) 3472, 1770, 1493, 1448, 1288, 1226, 1206, 1124, 961, 938, 751, 696. **HRMS** (ESI) calculated for (C<sub>16</sub>H<sub>14</sub>O<sub>3</sub><sup>+</sup>) (M<sup>+</sup>): 254.0937, Observed: 254.0941.



### 3-Hydroxy-4,4-dimethyl-1-(p-tolyl)pyrrolidin-2-one

Pantolactone (294 mg, 2.1 mmol) was added to a 10 mL microwave vessel equipped with a stir bar. Solid *p*-tolylsulfuric acid monohydrate (40 mg, 0.21 mmol) was added followed by *p*-methylaniline (450 mg, 4.2 mmol). The vessel was then purged with argon and sealed with a septum. The mixture was then microwaved at 75 W with a maximum temperature of 235 °C for 10 mins. The mixture was monitored by <sup>1</sup>H NMR which indicated complete conversion. The mixture was allowed to cool to ambient temperature. The crude was taken up in 100 mL of EtOAc and transferred to a separatory funnel. The organic layer was washed with 1 M HCl (2 x 20 mL), dried over sodium sulfate, filtered and concentrated. The product was purified by silica gel chromatography (25% EtOAc in hexanes gradient to 66% EtOAc in hexanes), affording the product as a tan solid 386 mg, 84 % **mp** range = 95-98 °C. **<sup>1</sup>H NMR** (400 MHz, CDCl<sub>3</sub>) δ ppm 7.49 (d, *J* = 8.5 Hz, 2

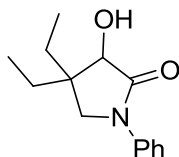
H), 7.18 (d,  $J = 8.8$  Hz, 2 H), 4.11 (d,  $J = 2.4$  Hz, 1 H), 3.53 (d,  $J = 9.6$  Hz, 1 H), 3.50 (d,  $J = 2.7$  Hz, 1 H), 3.42 (d,  $J = 9.6$  Hz, 1 H), 2.33 (s, 3 H), 1.32 (s, 3 H), 1.09 (s, 3 H).  $^{13}\text{C}$  NMR (101 MHz,  $\text{CDCl}_3$ )  $\delta$  ppm 173.6, 136.6, 134.6, 129.5, 119.5, 78.4, 57.8, 38.5, 24.6, 20.9, 19.9. IR (neat,  $\text{cm}^{-1}$ ) 3353, 2869, 1687, 1514, 1427, 1338, 1270, 1103, 1026, 815. HRMS (ESI) calculated for  $(\text{C}_{13}\text{H}_{17}\text{NO}_2^+)$  ( $\text{M}^+$ ): 219.1253, Observed: 219.1252.



### 3-Hydroxy-1-(4-methoxyphenyl)-4,4-dimethylpyrrolidin-2-one

Pantolactone (294 mg, 2.1 mmol) was added to a 10 mL microwave vessel equipped with stir bar. Solid *p*-tolylsulfuric acid monohydrate (40, mg, 0.21 mmol) was added followed by *p*-methoxyaniline (517 mg, 4.2 mmol). The vessel was then purged with argon and sealed with a septum. The mixture was then microwaved at 75 W with a maximum temperature of 260 °C for 10 mins. The mixture was monitored by  $^1\text{H}$  NMR which indicated complete conversion. The mixture was allowed to cool to ambient temperature. The crude was taken up in 100 mL of EtOAc and transferred to a separatory funnel. The organic layer was washed with 1 M HCl (2 x 20 mL), dried over sodium sulfate, filtered and concentrated. The product was purified by silica gel chromatography (25% EtOAc in hexanes gradient to 66% EtOAc in hexanes), affording the product as a tan solid 416 mg, 84 % mp range = 98-100 °C.  $^1\text{H}$  NMR (400 MHz,  $\text{CDCl}_3$ )  $\delta$  ppm 7.52 (d,  $J = 9.2$  Hz, 2 H), 6.92 (d,  $J = 9.2$  Hz, 2 H), 4.11 (s, 1 H), 3.81 (s, 3 H), 5.25 (d,  $J = 9.6$  Hz, 1 H), 3.40 (d,  $J = 9.6$  Hz, 1 H), 3.18 (br, 1 H), 1.33 (s, 3 H), 1.10 (s, 3 H).  $^{13}\text{C}$  NMR (101 MHz,

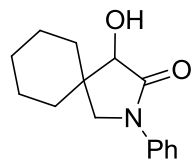
CDCl<sub>3</sub>)  $\delta$  ppm 173.4, 156.9, 132.5, 121.4, 121.4, 114.3, 78.5, 58.3, 55.7, 38.8, 24.8, 24.8, 20.2. **IR** (neat, cm<sup>-1</sup>) 3350, 2963, 1686, 1510, 1434, 1271, 1247, 1130, 1025, 830, 729. **HRMS** (ESI) calculated for (C<sub>13</sub>H<sub>17</sub>NO<sub>3</sub><sup>+</sup>) (M<sup>+</sup>): 235.1201, Observed: 235.1202.



#### 4,4-Diethyl-3-hydroxy-1-phenylpyrrolidin-2-one

To a 10 mL microwave vessel equipped with stir bar, 4,4-Diethyl-3-hydroxydihydrofuran-2(3H)-one (1.64 g, 10.3 mmol) was added. Next, Solid *p*-tolylsulfuric acid monohydrate (195, mg, 1.03 mmol) was added and the vessel was purged with argon and sealed with a septum. Aniline (1.88 mL, 20.7 mmol) was added via syringe and the mixture was stirred at ambient temperature for 15 min to solubilize the solid starting materials. The mixture was then microwaved at 75 W with a maximum temperature of 210 °C for 4.5 h. The mixture was monitored by <sup>1</sup>H NMR which indicated > 60% conversion. The crude was taken up in 100 mL of EtOAc and transferred to a separatory funnel. The organic layer was washed with 1 M HCl (2 x 20 mL), dried over sodium sulfate, filtered and concentrated. The resulting solid was triturated with ether to yield a tan solid, 1.1 g, 45 %, **mp** range = 103-105 °C. **<sup>1</sup>H NMR** (400 MHz, CDCl<sub>3</sub>)  $\delta$  ppm 7.63 (d, *J* = 8.1 Hz, 2 H), 7.37 (t, *J* = 7.7 Hz, 2 H), 7.16 (t, *J* = 7.3 Hz, 1 H), 4.24 (s, 1 H), 3.77 (br, 1 H), 3.55 (d, *J* = 9.9 Hz, 1 H), 3.44 (d, *J* = 9.9 Hz, 1 H), 1.70-1.50 (m, 4 H), 1.03 (t, *J* = 7.5 Hz, 3 H), 0.87 (t, *J* = 7.5 Hz, 3 H). **<sup>13</sup>C NMR** (101 MHz, CDCl<sub>3</sub>)  $\delta$  ppm 174.6, 139.0, 128.9, 124.8, 119.6, 77.4, 54.0, 43.9, 29.7, 22.8, 8.9, 8.5. **IR** (neat, cm<sup>-1</sup>)

) 3383, 2960, 2878, 1676, 1595, 1498, 1404, 1282, 1221, 1100, 914, 797, 758. **HRMS** (ESI) calculated for (C<sub>14</sub>H<sub>19</sub>NO<sub>2</sub>) (M<sup>+</sup>): 233.1410, Observed: 233.1413.



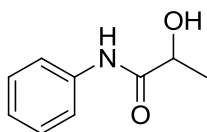
#### **4-Hydroxy-2-phenyl-2-azaspiro[4.5]decan-3-one**

To a 10 mL microwave vessel equipped with stir bar 4-Hydroxy-2-oxaspiro[4.5]decan-3-one (573 mg, 3.37 mmol) was added. Next, Solid *p*-tolylsulfuric acid monohydrate (64, mg, 0.337 mmol) was added and the vessel was purged with argon and sealed with a septum. Aniline (0.31 mL, 6.75 mmol) was added via syringe and the mixture was stirred at ambient temperature for 15 min to solubilize the solid starting materials. The mixture was then microwaved at 75 W with a maximum temperature of 210 °C for 40 mins. The mixture was monitored by <sup>1</sup>H NMR which indicated partial conversion. The mixture was allowed to cool to ambient temperature and aniline (0.31 mL, 6.75 mmol) was added via syringe. The mixture was then subjected to the previously mentioned microwave conditions for an additional 70 mins, at which point <sup>1</sup>H NMR indicated nearly complete conversion. The crude was taken up in 100 mL of EtOAc and transferred to a separatory funnel. The organic layer was washed with 1 M HCl (2 x 20 mL), dried over sodium sulfate, filtered and concentrated. The resulting solid was triturated with cold ether to yield a tan solid, 382 mg, 46 %, **mp** range = 124-127 °C. **<sup>1</sup>H NMR** (400 MHz, CDCl<sub>3</sub>) δ ppm 7.64 (d, *J* = Hz, 2 H), 7.39 (t, *J* = Hz, 2 H), 7.18 (t, *J* = Hz, 1 H), 4.09 (s, 1 H), 3.77 (d, *J* = Hz, 1 H), 3.43 (d, *J* = Hz, 1 H), 1.88-1.64 (m, 6 H), 1.39-1.28 (m, 4 H). **<sup>13</sup>C NMR** (101 MHz, CDCl<sub>3</sub>) δ ppm 173.8, 139.2, 128.9, 124.8, 119.5, 78.5, 54.0, 41.6, 35.0, 26.5,

25.6, 23.1, 22.0. **IR** (neat,  $\text{cm}^{-1}$ ) 3345, 2932, 2853, 1682, 1595, 1493, 1403, 1305, 1272, 1152, 1109, 898, 764, 692. **HRMS** (ESI) calculated for ( $\text{C}_{15}\text{H}_{19}\text{NO}_2$ ) ( $\text{M}^+$ ): 245.1408, Observed: 245.1410.

### General Procedure for the Preparation of $\alpha$ -Hydroxy Amides (GP1)

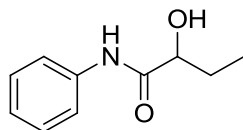
The  $\alpha$ -hydroxy carboxylic acid, was added to a 10 mL microwave vessel equipped with stir bar. Solid *p*-tolylsulfuric acid monohydrate (0.2 equiv.) was added followed by aniline (2.0 equiv.). The vessel was then purged with argon and sealed with a septum. The mixture was then microwaved at 75 W with a maximum temperature of 210 °C for 10 mins. The mixture was monitored by  $^1\text{H}$  NMR which indicated complete conversion. The mixture was allowed to cool to ambient temperature. The crude was taken up in 100 mL of EtOAc and transferred to a separatory funnel. The organic layer was washed with 1 M HCl (2 x 20 mL), dried over sodium sulfate, filtered and concentrated. The product was purified by silica gel chromatography (EtOAc and hexanes) or recrystallized affording the desired hydroxy amides.



### 2-Hydroxy-N-phenylpropanamide

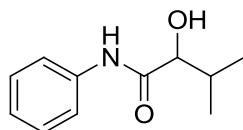
The product was prepared from (D,L)-lactic acid (3.0 mmol) according to **GP1**. The desired product was isolated after column chromatography (25% EtOAc in hexanes gradient to 66% EtOAc in hexanes) as a tan solid, 388 mg, 78 % yield.  $^1\text{H}$  NMR (400 MHz,  $\text{CDCl}_3$ )  $\delta$  ppm 8.53 (br, 1 H), 7.54 (d,  $J = 7.8$  Hz, 2 H), 7.32 (t,  $J = 7.8$  Hz, 2 H),

7.12 (t,  $J = 7.4$  Hz, 1 H), 4.34 (q,  $J = 6.8$  Hz, 1 H), 3.29 (br, 1 H), 1.51 (d,  $J = 6.8$  Hz, 3 H).  $^{13}\text{C}$  NMR (101 MHz,  $\text{CDCl}_3$ )  $\delta$  ppm 172.6, 137.1, 129.0, 124.6, 119.8, 68.8, 21.2.



### 2-Hydroxy-N-phenylbutanamide

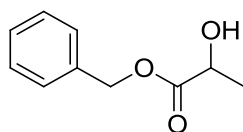
The product was prepared from (D,L)-2-hydroxybutyric acid (5.0 mmol) according to **GP1**. The desired product was obtained as a white solid after extractions with no further purification required, 792 mg, 88 % yield.  $^1\text{H}$  NMR (400 MHz,  $\text{CDCl}_3$ )  $\delta$  ppm 8.37 (br, 1 H), 7.59-7.57 (m, 2 H), 7.36-7.32 (m, 2 H), 7.15-7.11 (m, 1 H), 4.26-4.22 (m, 1 H), 2.49 (br, 1 H), 2.05-1.94 (m, 1 H), 1.81 (dddd,  $J = 14.6, 14.6, 7.3, 7.3$  Hz, 1 H), 1.05 (t,  $J = 7.3$  Hz, 3 H).  $^{13}\text{C}$  NMR (101 MHz,  $\text{CDCl}_3$ )  $\delta$  ppm 171.9, 137.2, 129.0, 124.5, 119.7, 73.6, 27.9, 9.2.



### 2-Hydroxy-3-methyl-N-phenylbutanamide

The product was prepared from 2-hydroxy-3-methylbutyric acid (3.0 mmol) according to **GP1**. The desired product was obtained as a tan solid after recrystallization from  $\text{CH}_2\text{Cl}_2$ , 415 mg, 72 % yield..  $^1\text{H}$  NMR (400 MHz,  $\text{CDCl}_3$ )  $\delta$  ppm 8.53 (br, 1 H), 7.55-7.53 (m, 2 H), 7.33-7.31 (m, 2 H), 7.13-7.09 (m, 1 H), 4.08 (d,  $J = 3.2$  Hz, 1 H), 3.36 (br, 1 H), 2.27 (dddd,  $J = 20.8, 13.7, 6.9, 3.2$  Hz, 1 H), 1.05 (d,  $J = 6.9$  Hz, 3 H), 0.90 (d,  $J = 6.9$  Hz, 3 H).  $^{13}\text{C}$  NMR (101 MHz,  $\text{CDCl}_3$ )  $\delta$  ppm 171.8, 137.1, 129.0, 124.5, 119.9, 76.6, 31.9, 19.2, 15.5.





### Benzyl-2-hydroxypropanoate

The product was prepared from a modified procedure to that described in the literature.<sup>58</sup>

A 50 mL round bottom flask was equipped with a stir bar and a septum. (D,L)-lactic acid (313 mg, 3.45mmol) was added followed by 7 mL of a MeOH:H<sub>2</sub>O (1:9) solution. The solution was then treated with a 20% CsCO<sub>3</sub> solution drop wise until a pH of 7 was achieved. The solvent was then removed under reduced pressure. DMF (4 mL) was added to the flask and removed under reduced pressure revealing the cesium salt of lactic acid. The salt was suspended in DMF (4.0 mL) and cooled to 0 °C and benzyl bromide (560 mg, 3.11 mmol) was added drop wise. The mixture was then allowed to warm to ambient temperature and stirred for 18 h. The crude was extracted with ether (50 mL) and partitioned with 50 mL of water. The aqueous layer was then extracted with ether (3x 50 mL) and the organic layers combined and washed with sat. NaHCO<sub>3</sub>, brine, and dried over sodium sulfate. Filtration followed by solvent removal under reduced pressure gave the desired product as a colorless oil, 523 mg, 93% yield. <sup>1</sup>H NMR (400 MHz, CDCl<sub>3</sub>) δ ppm 7.40-7.33 (m, 5 H), 5.22 (s, 2 H), 4.32 (q, *J* = 6.8 Hz, 1 H), 2.89 (br, 1 H), 1.43 (d, *J* = 6.8 Hz, 3 H). <sup>13</sup>C NMR (101 MHz, CDCl<sub>3</sub>) δ ppm 175.5, 135.2, 128.6, 128.2, 128.1, 67.3, 66.7, 20.4.

### General Procedure for the Kinetic Resolution of $\alpha$ -Hydroxy Lactones and Lactams (GP2)

Into a 1-dram vial equipped with a stir bar and activated 4Å molecular sieves, racemic substrate (0.5 mmol) and catalyst (0.125 mmol) was added. The vial was then purged

with argon and sealed with a septum. The starting materials were then dissolved in 0.9 mL of THF. Base (0.3 mmol) was added via syringe and the vial was cooled to -78 °C in a cryocool for 30 mins. The cooled mixture was then treated with 0.3 mL of a freshly prepared 1M silyl chloride solution in THF. The reaction was left to stir a set amount of time at -78 °C then quenched with 0.3 mL of methanol. The solution was left to warm to room temperature then the contents of the vial were extracted into a 4-dram vial with ether. Concentration gave an oil which was subjected to column chromatography (10% EtOAc in hexanes gradient to 50% EtOAc in hexanes) to separate the starting material from products. Starting material that coeluted with catalyst was purified by washing with 5% HCl and extracted with ether (3 x 5 mL) followed by drying over sodium sulfate. Filtration and removal of the solvent afforded the starting material suitable for conversion to the benzoate ester or separation on chiral stationary phase HPLC.

### **General Procedure for Product Deprotection (GP3)**

The silyl-protected alcohol was weighed into a 4 dram vial. The vial was then equipped with a stir bar and a septum. The solid was then dissolved in 1 mL of THF with stirring. To this solution TBAF (1 mL) was added. The reaction was monitored via TLC (1:3 EtOAc: hexanes). The reactions were generally complete in less than 2 h. The reaction was then quenched with brine, extracted with diethyl ether three times and dried over a sodium sulfate silica gel mixture and filtered. Concentration via rotovap afforded an oil. Subsequent purification on silica gel column chromatography (10% EtOAc in hexanes gradient to 50% EtOAc in hexanes) afforded the deprotected products suitable for conversion to the benzoate ester or separation on chiral stationary phase HPLC.

#### **General Procedure for Benzoylation of Alcohols for HPLC Analysis (GP4)**

A 4-dram vial containing the lactone or lactam was fitted with a stir bar and a septum. DMAP (0.1 equiv.) was weighed and added to the vial. The mixture was then dissolved in 2 mL of dichloromethane with stirring. Triethyl amine (2.0 equivalents) was added via syringe and the vessel was cooled to 0 °C in an ice bath. Benzoyl chloride (1.4 equivalents) was then added drop wise via syringe and the reaction was left to stir for 30 mins at which point TLC of the crude indicated reaction was complete. The reaction was quenched with saturated sodium bicarbonate and extracted three times with dichloromethane. The combined organic layers were then dried over sodium sulfate. After concentration the crude was then purified via silica gel column chromatography (1:9 EtOAc: hexanes) to obtain the desired benzoylated lactone or lactam. The benzoate esters were then analyzed by HPLC using chiral stationary phases.

#### **General Procedure for the silylation of alcohols for HPLC Analysis (GP5)**

A 4-dram vial containing the lactone or lactam was fitted with a stir bar and a septum and then dissolved in 2 mL of THF with stirring. *N*-methyl imidazole (0.25 equiv.) was added to the solution via syringe. Next, Hünig's base (2.0 equivalents) was added via syringe. Triphenylsilyl chloride (1.1 equivalents) was then added in portions and the reaction was left to stir for 2 h at ambient temperature. TLC of the crude indicated the reaction was complete in 2 h or less in all cases. The reaction was quenched with sat NH<sub>4</sub>Cl (1 mL) and extracted three times with ether (5 mL). The combined organic layers were then dried over sodium sulfate. After concentration the crude was then purified via silica gel column chromatography (1:9 EtOAc: hexanes) to obtain the desired triphenyl silylated lactone or lactam. The silyl ethers were then analyzed by HPLC using chiral stationary phases.

## Analytical Data and HPLC Traces for Kinetic Resolutions

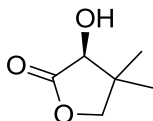
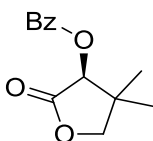
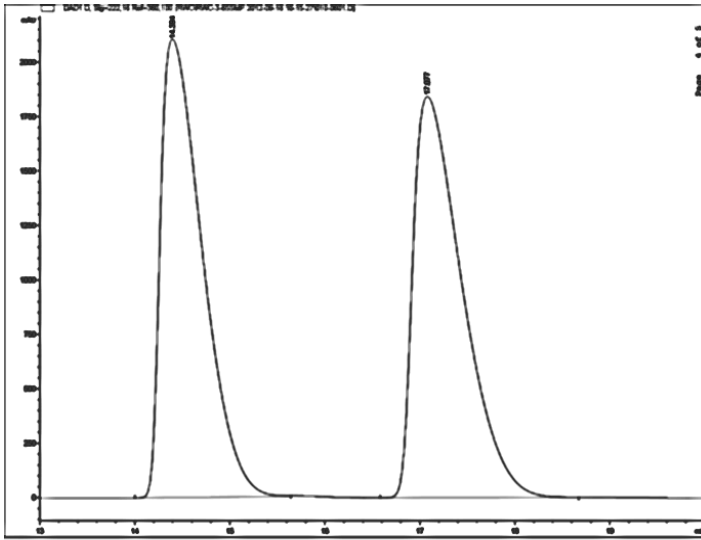


**Table 2.1, Entry 5:** Recovered starting material: 20 mg, 31%.  $^1\text{H}$  NMR (400 MHz,  $\text{CDCl}_3$ )  $\delta$  ppm 4.13 (s, 1H), 4.03 (d,  $J = 8.9$  Hz 1H), 3.95 (d,  $J = 8.9$  Hz 1H), 2.93 (br, 1H), 1.24 (s, 3H), 1.09 (s, 3H).  $^{13}\text{C}$  NMR (101 MHz,  $\text{CDCl}_3$ )  $\delta$  ppm 177.5, 76.4, 75.7, 40.8, 22.9, 18.8.

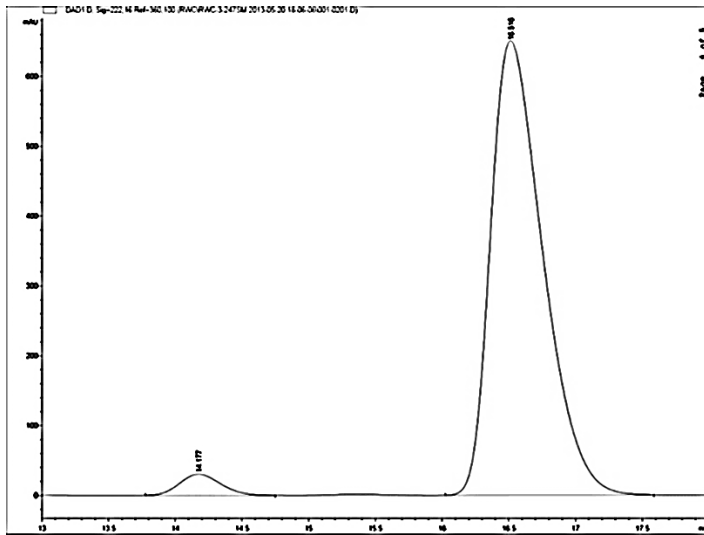


$^1\text{H}$  NMR (400 MHz,  $\text{CDCl}_3$ )  $\delta$  ppm 8.12-8.09 (m, 2 H), 7.64-7.60 (m, 1 H), 7.50-7.46 (m, 2 H), 5.63 (s, 1 H), 4.12 (dd,  $J = 9.0, 3.6$  Hz, 2 H), 1.29 (s, 3 H), 1.23 (s, 3 H).  $^{13}\text{C}$  NMR (101 MHz,  $\text{CDCl}_3$ )  $\delta$  ppm 172.3, 165.3, 133.8, 130.0, 128.7, 128.6, 76.2, 75.4, 40.6, 23.1, 20.1.

HPLC separation conditions and stereochemical assignment<sup>59</sup> made after conversion to the corresponding benzoate ester. Chiralpak OD-H Column 6% isopropyl alcohol in hexane, flow rate: 1 mL/min, 25 °C;  $t_R$  14.7 min for (R)-enantiomer (minor) and 16.8 min for (S)-enantiomer (major). (er = 96:4).



Peak #	RetTime [min]	Type	Width [min]	Area [mAU*s]	Height [mAU]	Area %
1	14.394	BB	0.4725	6.40074e4	2106.32520	49.3149
2	17.077	BB	0.5504	6.57859e4	1843.21606	50.6851



Peak #	RetTime [min]	Type	Width [min]	Area [mAU*s]	Height [mAU]	Area %
1	14.177	BB	0.3361	657.05231	30.40471	3.5786
2	16.516	BB	0.4193	1.77036e4	650.90228	96.4214

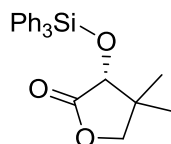


**Table 2.1, Entry 5:** Recovered product: 87 mg, 44% white solid. **mp range** = 90-93 °C.

**<sup>1</sup>H NMR** (400 MHz, CDCl<sub>3</sub>) δ ppm 7.74-7.71 (m, 6H), 7.48-7.37 (m, 9H), 4.15 (s, 1H),

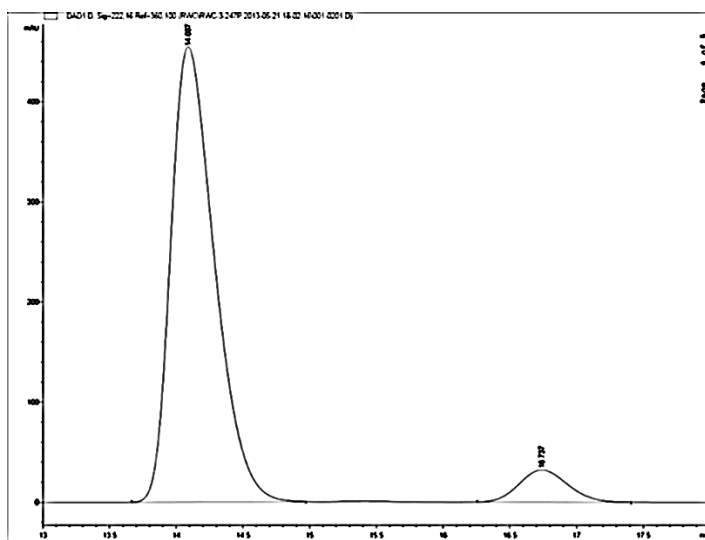
3.95 (d, *J* = 8.9 Hz, 1H), 3.76 (d, *J* = 8.9 Hz, 1 H), 1.18 (s, 3H), 0.86 (s, 3H) **<sup>13</sup>C NMR** (101 MHz, CDCl<sub>3</sub>) δ ppm 175.2, 135.7, 133.4, 130.3, 127.9, 77.25, 75.4, 41.1, 22.6, 19.6.

**Optical Rotation** [α]<sub>D</sub><sup>25</sup>: = +6.0 (c = 0.86) CHCl<sub>3</sub> **IR** (neat, cm<sup>-1</sup>) 3000, 2929, 2852,

1789, 1428, 1197, 1117, 1009, 857, 744, 712. **HRMS** (ESI) Calculated for (M<sup>+</sup>)

(C<sub>24</sub>H<sub>24</sub>O<sub>3</sub>Si<sup>+</sup>): 388.1489 Observed: 388.1480.

HPLC data is of the desilylated products followed by conversion to the corresponding benzoate ester. The same conditions as the benzoate ester of the starting material were utilized. (er = 93:7).



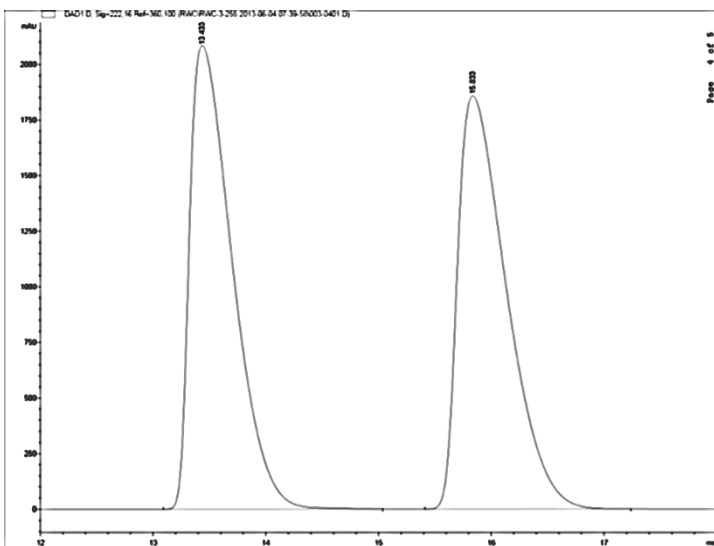
Peak #	RetTime [min]	Type	Width [min]	Area [mAU*s]	Height [mAU]	Area %
1	14.087	BB	0.3491	1.03334e4	454.84186	92.6570
2	16.737	BB	0.3965	818.91858	32.22737	7.3430

### Kinetic Resolution Data for Table 2.1 Entry 5

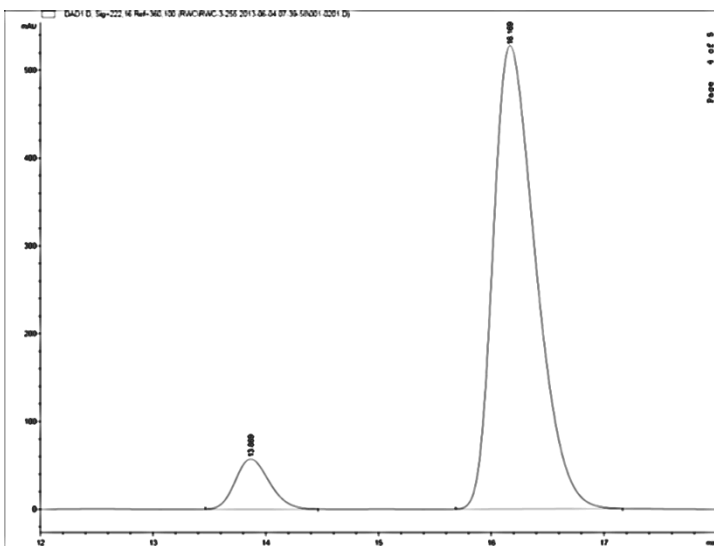
#	er SM	er P	% conv	s	s AVG
1	96:4	93:7	52.1	42	<b>36</b>
2	87:13	93:7	46.2	30	

#### Procedure for the Kinetic Resolution of Pantolactone, **3** (8.0 mmol Scale)

Into an oven dried 50 mL round bottom flask equipped with a stir bar and activated 4Å molecular sieves, pantolactone **3** (1.04 g, 8.0 mmol) and (-)-benzotetramisole (505 mg, 2.0 mmol) was added. The vial was then purged with argon and sealed with a septum. The starting materials were then dissolved in 14.25 mL of THF. Hünig's base (836 µL, 4.8 mmol) was added via syringe and the vial was cooled to -78 °C in a cryocool for 30 mins. The cooled mixture was then treated with 4.8 mL of a freshly prepared 1M triphenylsilyl chloride solution in THF. The reaction was left to stir for 24 h at -78 °C then quenched with 2 mL of methanol. The solution was left to warm to room temperature, then the flasks contents were extracted with ether. Concentration of the mixture gave an oil which was subjected to column chromatography (10% EtOAc in hexanes gradient to 50% EtOAc in hexanes) to separate the starting material from products. The starting material that coeluted with catalyst was purified by washing with 5% HCl (20 mL) and extraction with ether (5 x 20 mL) followed by drying over sodium sulfate. Filtration and removal of the solvent afforded the starting material (383 mg, 37%) suitable for conversion to the benzoate ester for separation on chiral stationary phase HPLC. The silylated product (1.45 g, 47%) that was isolated was deprotected according to the general procedure and converted to the corresponding benzoate ester for separation on chiral stationary phase HPLC.



Peak #	RetTime [min]	Type	Width [min]	Area [mAU*s]	Height [mAU]	Area %
1	13.433	BB	0.4059	5.46973e4	2086.11157	49.5461
2	15.833	BB	0.4616	5.56995e4	1858.80469	50.4539

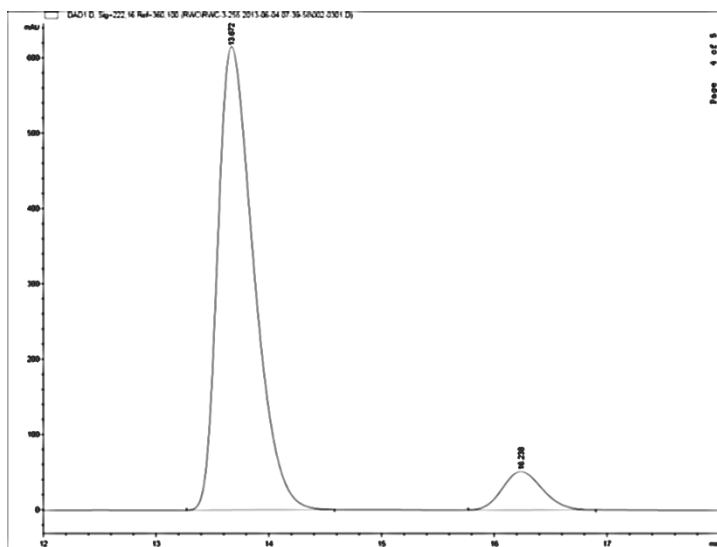


Peak #	RetTime [min]	Type	Width [min]	Area [mAU*s]	Height [mAU]	Area %
1	13.869	BB	0.3283	1209.76379	57.30398	8.0396
2	16.169	BB	0.4057	1.38379e4	528.05005	91.9604

The benzoate ester of the starting materials were separated Chiralpak OD-H Column 6% isopropyl alcohol in hexane, flow rate: 1 mL/min, 25 °C;  $t_R$  13.6 min for (R)-enantiomer (minor) and 16.2 min for (S)-enantiomer (major). (er = 92:8).



The benzoate ester of the deprotected product was run on chiral stationary phase HPLC under the same conditions as the starting materials. (er = 92:8).



Peak #	RetTime [min]	Type	Width [min]	Area [mAU*s]	Height [mAU]	Area %
1	13.672	BB	0.3399	1.36084e4	615.69922	91.5003
2	16.238	BB	0.3845	1264.12463	51.11473	8.4997

#### Kinetic Resolution Data for the Resolution of 2.1 (8.0 mmol scale)

#	er SM	er P	% conv	<i>s</i>
1	92:8	92:8	50.3	<b>28</b>

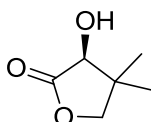
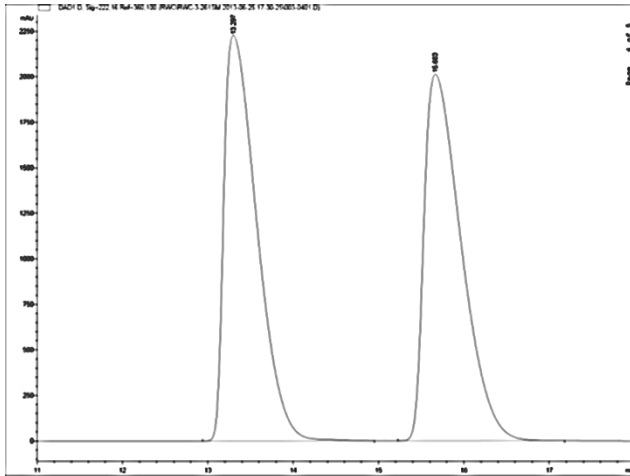
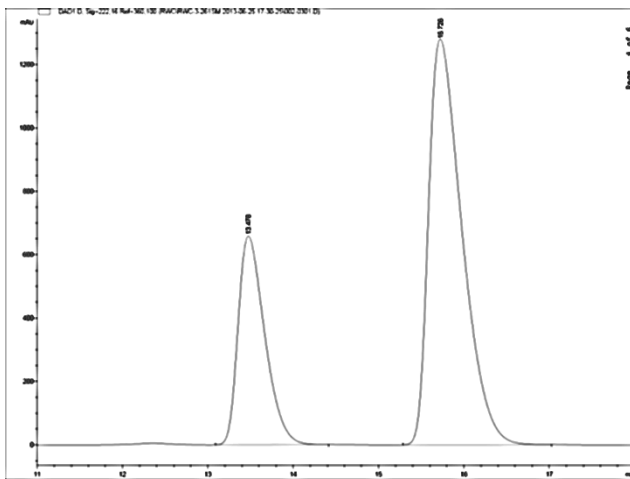


**Table 2.2, Entry 2:** Recovered starting material: 19 mg, 29 %. <sup>1</sup>H NMR (400 MHz, CDCl<sub>3</sub>) δ ppm 4.13 (s, 1H), 4.03 (d, *J* = 8.9 Hz 1H), 3.95 (d, *J* = 8.9 Hz 1H), 2.93 (br, 1H), 1.24 (s, 3H), 1.09 (s, 3H). <sup>13</sup>C NMR (101 MHz, CDCl<sub>3</sub>) δ ppm 177.5, 76.4, 75.7, 40.8, 22.9, 18.8.

HPLC conditions for the starting material was as follows using the corresponding benzoate ester of the starting material: Chiralpak OD-H Column 6% isopropyl alcohol in hexane, flow rate: 1 mL/min, 25 °C;  $t_R$  14.3 min for (R)-enantiomer (minor) and 15.6 min for (S)-enantiomer (major). (er = 71:29).



Peak #	RetTime [min]	Type	Width [min]	Area [mAU*s]	Height [mAU]	Area %
1	13.297	BB	0.4147	5.93742e4	2229.21802	49.4095
2	15.663	BB	0.4683	6.07932e4	2013.26929	50.5905



Peak #	RetTime [min]	Type	Width [min]	Area [mAU*s]	Height [mAU]	Area %
1	13.478	BB	0.3332	1.43015e4	659.05975	29.1196
2	15.726	BB	0.4171	3.48115e4	1280.91016	70.8804

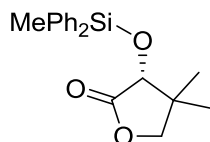
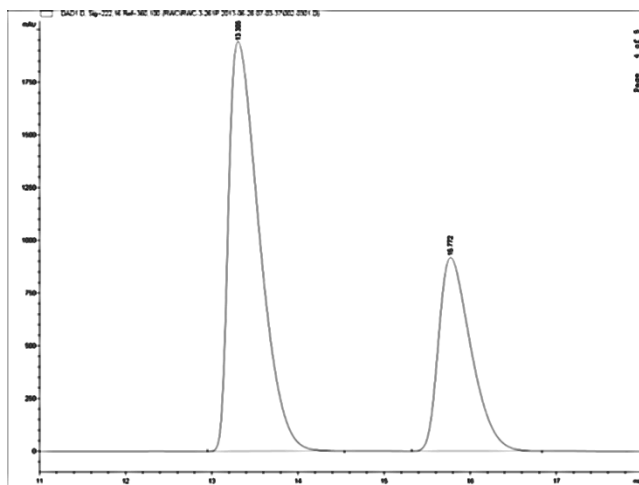


**Table 2.2, Entry 2:** Recovered product: 62 mg, 38 % colorless oil.  $^1\text{H NMR}$  (400 MHz,  $\text{CDCl}_3$ )  $\delta$  ppm 7.67-7.64 (m, 3 H), 7.45-7.36 (m, 5 H), 4.03 (s, 1 H), 3.95 (d,  $J = 8.9$  Hz, 1 H), 3.79 (d,  $J = 8.9$  Hz, 1 H), 1.12 (s, 3 H), 0.98 (s, 3 H), 0.80 (s, 3 H).  $^{13}\text{C NMR}$  (101 MHz,  $\text{CDCl}_3$ )  $\delta$  ppm 175.5, 135.3, 134.9, 134.7, 134.4, 130.2, 130.0, 127.9, 127.8, 75.6, 40.9, 22.8, 19.4, -2.1. **Optical Rotation**  $[\alpha]_D^{25}$ : +18.0 ( $c = 0.90$ )  $\text{CHCl}_3$ . **IR** (neat,  $\text{cm}^{-1}$ ) 3070, 2963, 1791, 1464, 1428, 1201, 1118, 1010, 861, 773, 725. **HRMS** (ESI) Calculated for  $(\text{C}_{19}\text{H}_{22}\text{O}_3\text{Si}^+)$  (M-Ph $^+$ ): 326.1332 Observed: 326.1320.

HPLC data is of the desilylated products followed by conversion to the corresponding benzoate ester. The same conditions as the benzoate ester of the starting material were utilized. (er = 67:34).



Peak #	RetTime [min]	Type	Width [min]	Area [mAU*s]	Height [mAU]	Area %
1	13.305	BB	0.3807	4.81189e4	1944.50085	66.7389
2	15.772	BB	0.4005	2.39814e4	918.86115	33.2611

### Kinetic Resolution Data for Table 2.2, Entry 2

#	er SM	er P	% conv	s	s AVG
1	71:29	67:33	55.5	2.8	<b>2.9</b>
2	65:35	68:32	46.4	2.9	

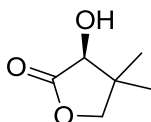
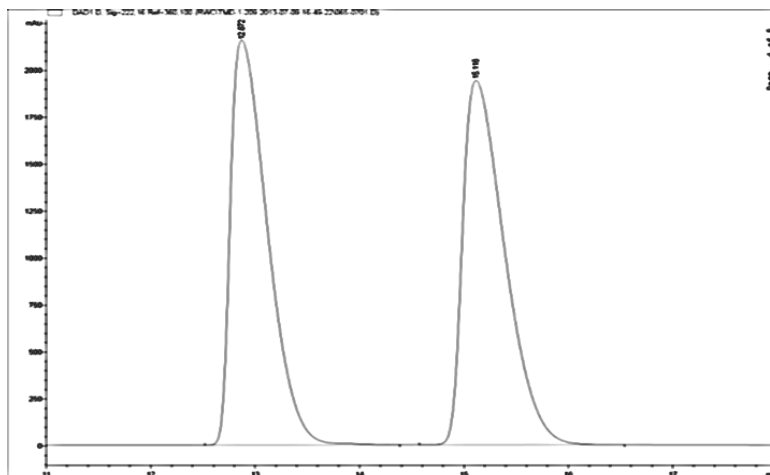
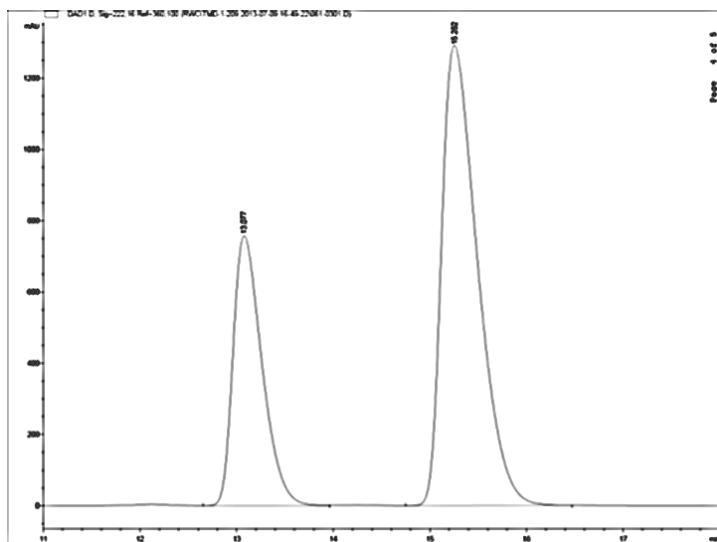


**Table 2.2, Entry 3:** Recovered starting material: 30 mg, 46 %.  $^1\text{H NMR}$  (400 MHz,  $\text{CDCl}_3$ )  $\delta$  ppm 4.13 (s, 1H), 4.03 (d,  $J = 8.9$  Hz 1H), 3.95 (d,  $J = 8.9$  Hz 1H), 2.93 (br, 1H), 1.24 (s, 3H), 1.09 (s, 3H).  $^{13}\text{C NMR}$  (101 MHz,  $\text{CDCl}_3$ )  $\delta$  ppm 177.5, 76.4, 75.7, 40.8, 22.9, 18.8.

HPLC conditions for the starting material was as follows using the corresponding benzoate ester of the starting material: Chiralpak OD-H Column 6% isopropyl alcohol in hexane, flow rate: 1 mL/min, 25 °C;  $t_R$  13.1 min for (R)-enantiomer (minor) and 15.2 min for (S)-enantiomer (major). (er = 68:32).



Peak #	RetTime [min]	Type	Width [min]	Area [mAU*s]	Height [mAU]	Area %
1	12.872	BB	0.3816	5.28144e4	2157.74219	49.3934
2	15.116	BB	0.4311	5.41116e4	1942.03601	50.6066



Peak #	RetTime [min]	Type	Width [min]	Area [mAU*s]	Height [mAU]	Area %
1	13.077	VB	0.3200	1.57115e4	757.53796	32.0921
2	15.252	VB	0.3962	3.32461e4	1292.12537	67.9079

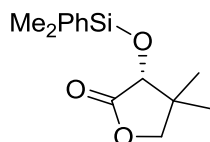
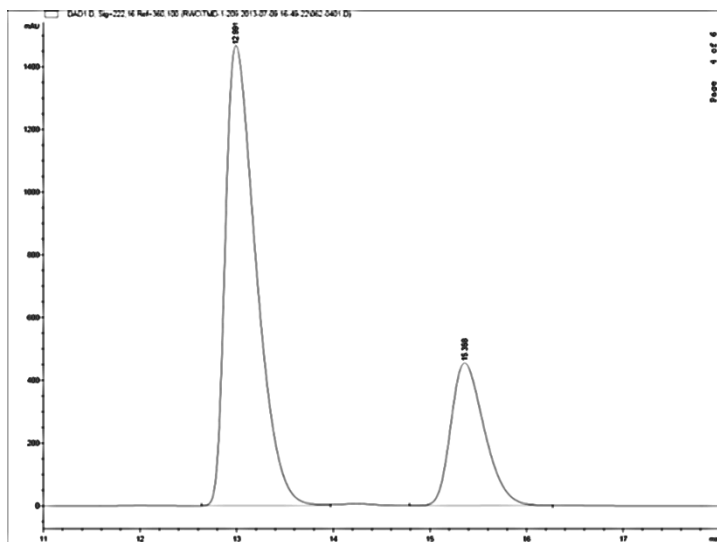


**Table 2.2, Entry 3:** Recovered product: 53 mg, 40 % colorless oil.  $^1\text{H NMR}$  (400 MHz,  $\text{CDCl}_3$ )  $\delta$  ppm 7.64-7.61 (m, 2 H), 7.42-7.37 (m, 3 H), 3.97-3.95 (m, 2 H), 3.82 (d,  $J = 8.9$  Hz, 1 H), 1.06 (s, 3 H), 1.01 (s, 3 H), 0.51 (s, 3 H), 0.48 (s, 3 H).  $^{13}\text{C NMR}$  (101 MHz,  $\text{CDCl}_3$ )  $\delta$  ppm 175.7, 136.7, 133.7, 129.9, 127.9, 75.7, 40.8, 22.8, 19.2, -0.9, -1.5. **Optical Rotation**  $[\alpha]_D^{25}$ : +21.2 ( $c = 1.0$ )  $\text{CHCl}_3$ . **IR** (neat,  $\text{cm}^{-1}$ ) 2962, 1792, 1464, 1428, 1252, 1201, 1116, 1010, 992, 868, 830, 785, 699. **HRMS** (ESI) Calculated for  $(\text{C}_{13}\text{H}_{17}\text{O}_3\text{Si}^+)$  (M-Me $^+$ ): 249.0941 Observed: 249.0943.

HPLC data is of the desilylated products followed by conversion to the corresponding benzoate ester. The same conditions as the benzoate ester of the starting material were utilized. (er = 75:25).



Peak #	RetTime [min]	Type	Width [min]	Area [mAU*s]	Height [mAU]	Area %
1	12.991	BB	0.3362	3.22446e4	1468.22314	74.6792
2	15.358	VB	0.3704	1.09328e4	454.92160	25.3208

### Kinetic Resolution Data for Table 2.2, Entry 3

#	er SM	er P	% conv	<i>s</i>	<i>s</i> AVG
1	68:32	75:25	42.0	4.1	<b>4.6</b>
2	66:34	79:21	35.8	5.0	

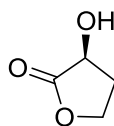
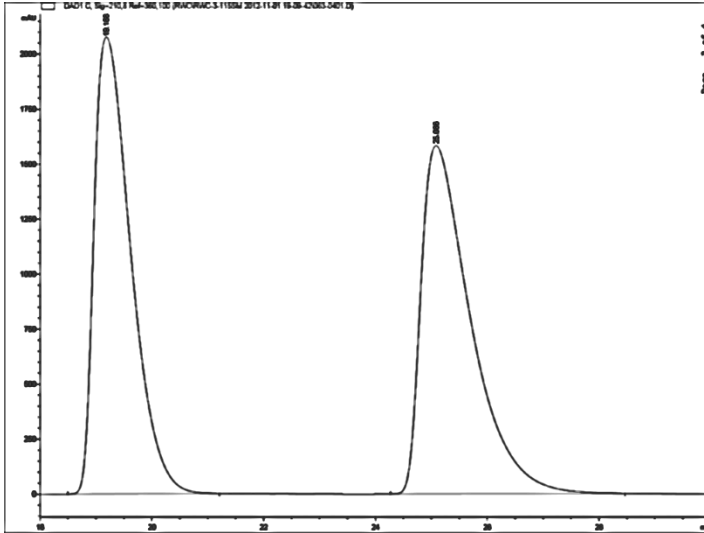


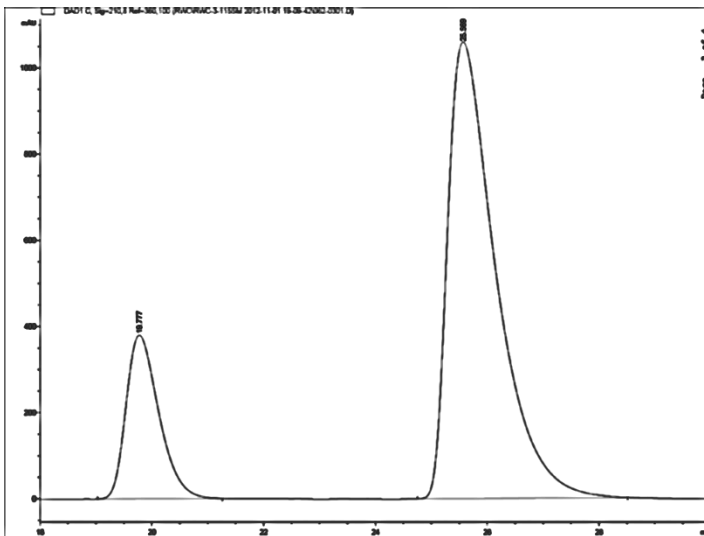
**Table 2.5, Entry 1:** Recovered starting material: 13 mg, 25 %  $^1\text{H}$  NMR (400 MHz,  $\text{CDCl}_3$ )  $\delta$  ppm 4.52 (dd,  $J = 8.3, 1.8$  Hz, 1 H), 4.45 (td, 8.9, 2.0 Hz, 1 H), 3.31 (br, 1 H), 2.66-2.59 (m, 1 H), 2.35-2.25 (m, 1 H).  $^{13}\text{C}$  NMR (101 MHz,  $\text{CDCl}_3$ )  $\delta$  ppm 177.9, 67.4, 65.2, 30.9. **Optical Rotation:**  $[\alpha]_{\text{D}}^{25} = -51.8$  ( $c = 1.07$ )  $\text{CHCl}_3$

Stereochemical assignment made based on optical rotation comparison of the recovered starting materials to the literature.<sup>60</sup> HPLC separation conditions made after conversion to

the triphenylsilyl protected alcohol. Chiralpak OD-H Column 3% isopropyl alcohol in hexane, flow rate: 1 mL/min, 25 °C;  $t_R$  19.7 min for (R)-enantiomer (minor) and 25.5 min for (S)-enantiomer (major). (er = 80:20).



Peak #	RetTime [min]	Type	Width [min]	Area [mAU*s]	Height [mAU]	Area %
1	19.188	BB	0.7043	9.44429e4	2077.63525	49.2276
2	25.086	BB	0.9228	9.74066e4	1583.24609	50.7724



Signal 2: DAD1 C, Sig=210,8 Ref=360,100

Peak #	RetTime [min]	Type	Width [min]	Area [mAU*s]	Height [mAU]	Area %
1	19.777	BB	0.6253	1.54840e4	380.03409	19.6289
2	25.569	BB	0.8959	6.33997e4	1059.83704	80.3711

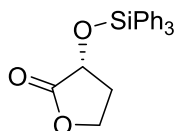
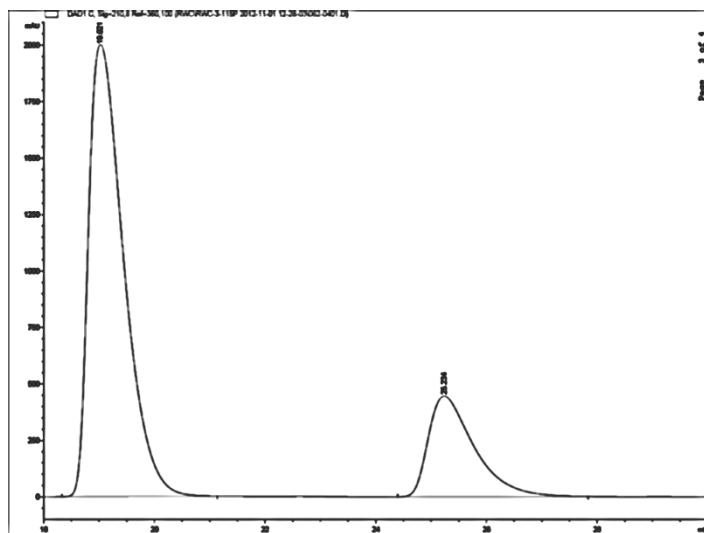


**Table 2.5, Entry 1:** Recovered product: 70 mg, 39%, white solid. **mp range** = 112-115 °C. **<sup>1</sup>H NMR** (400 MHz, CDCl<sub>3</sub>) δ ppm 7.69 (d, *J* = 6.5 Hz, 6 H), 7.46-7.37 (m, 9H), 4.51 (t, *J* = 8.3 Hz, 1H), 4.30. (td, *J* = 8.5, 3.4 Hz, 1 H), 4.05-3.99 (m, 1 H), 2.28-2.21 (m, 2 H). **<sup>13</sup>C NMR** (101 MHz, CDCl<sub>3</sub>) δ ppm 175.3, 135.4, 133.0, 130.4, 128.0, 68.6, 64.4, 32.0. **Optical Rotation** [α]<sub>D</sub><sup>25</sup>: = +13.0 (c = 0.85) CHCl<sub>3</sub> **IR** (neat, cm<sup>-1</sup>) 3013, 2945, 2853, 1781, 1428, 1219, 1150, 1116, 996, 846, 745, 706. **HRMS** (ESI) Calculated for (C<sub>22</sub>H<sub>20</sub>O<sub>3</sub>Si<sup>+</sup>) (M<sup>+</sup>): 360.1176 Observed: 360.1175.

HPLC data is of the silylated products. The same conditions as the silylated starting material were utilized. (er = 77:23).



Peak #	RetTime [min]	Type	Width [min]	Area [mAU*s]	Height [mAU]	Area %
1	19.021	BB	0.6475	8.79426e4	2001.75708	77.4192
2	25.234	BB	0.8595	2.56502e4	445.63168	22.5808



### Kinetic Resolution Data for Table 2.5 Entry 1

#	er SM	er P	% conv	<i>s</i>	<i>s</i> AVG
1	82:18	74:26	56.9	5.5	<b>5.8</b>
2	80:20	77:23	52.5	6.2	

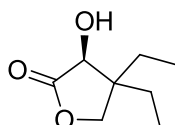
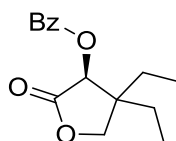


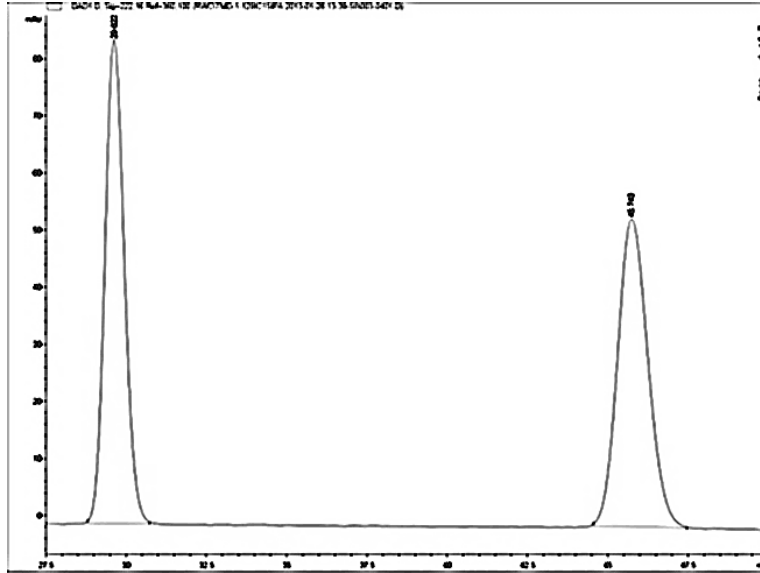
**Table 2.5, Entry 3:** Recovered starting material: 45 mg, 57 % <sup>1</sup>H NMR: (400 MHz, CDCl<sub>3</sub>) δ ppm 4.22 (s, 1 H), 4.16 (d, *J* = 9.3 Hz, 1 H), 3.88 (d, *J* = 9.3 Hz, 1 H), 1.66-1.42 (m, 4 H), 0.99 (t, *J* = 7.4 Hz, 3 H), 0.91 (t, *J* = 7.4, 3 H). <sup>13</sup>C NMR: (101 MHz, CDCl<sub>3</sub>) δ ppm 178.3, 74.7, 73.1, 46.6, 28.1, 21.4, 8.5, 8.09.



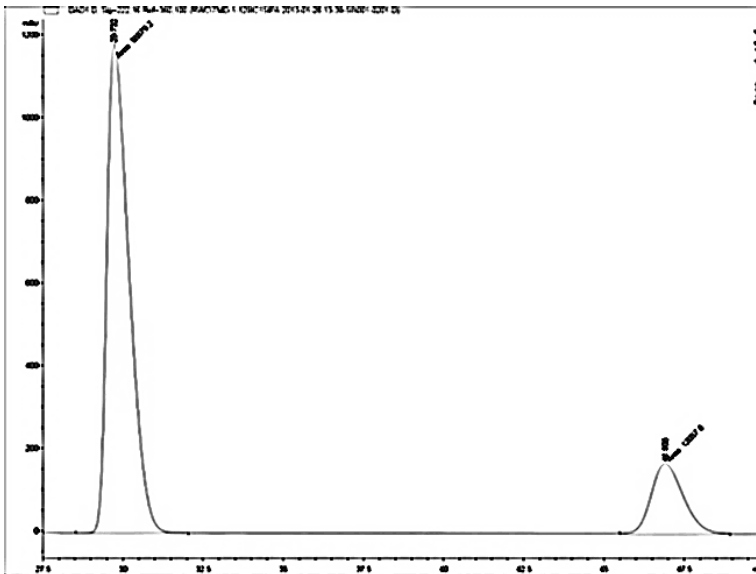
<sup>1</sup>H NMR: (400 MHz, CDCl<sub>3</sub>) δ ppm 8.10-8.07 (m, 2 H), 7.62 (tt, *J* = 7.4, 1.3 Hz, 1 H), 7.50-7.46 (m, 2 H), 5.78 (s, 1 H), 4.25 (d, *J* = 9.4 Hz, 1 H) 4.08 (d *J* = 9.4 Hz, 1 H) 1.75-1.60 (m, 4 H), 1.02 (t, *J* = 7.5 Hz, 3 H) 0.94 (t, *J* = 7.5 Hz, 3 H). <sup>13</sup>C NMR: (101 MHz, CDCl<sub>3</sub>) δ ppm 172.9, 165.2, 133.7, 130.0, 128.9, 128.6, 73.7, 72.9, 46.1, 27.9, 23.5, 8.3, 8.2. **Optical Rotation** [α]<sub>D</sub><sup>25</sup>: = -12.2 (c = 1.2) CHCl<sub>3</sub>

Stereochemical assignment made based on comparison of optical rotation data for the benzoate ester to that in the literature.<sup>34</sup> HPLC separation conditions made after conversion to the corresponding benzoate ester. Chiralpak IC Column 15% isopropyl

alcohol in hexane, flow rate: 1 mL/min, 25 °C;  $t_R$  28.3 min for (S)-enantiomer (major) and 44.6 min for (R)-enantiomer (minor). (er = 82:18).



Peak #	RetTime [min]	Type	Width [min]	Area [mAU*s]	Height [mAU]	Area %
1	29.622	BB	0.6497	3542.39868	84.74413	50.1067
2	45.743	BB	1.0095	3527.31812	53.89592	49.8933



Peak #	RetTime [min]	Type	Width [min]	Area [mAU*s]	Height [mAU]	Area %
1	29.732	MM	0.7975	5.66792e4	1184.51624	82.4581
2	46.906	MM	1.1726	1.20578e4	171.38118	17.5419

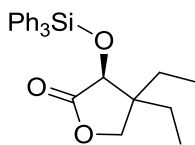
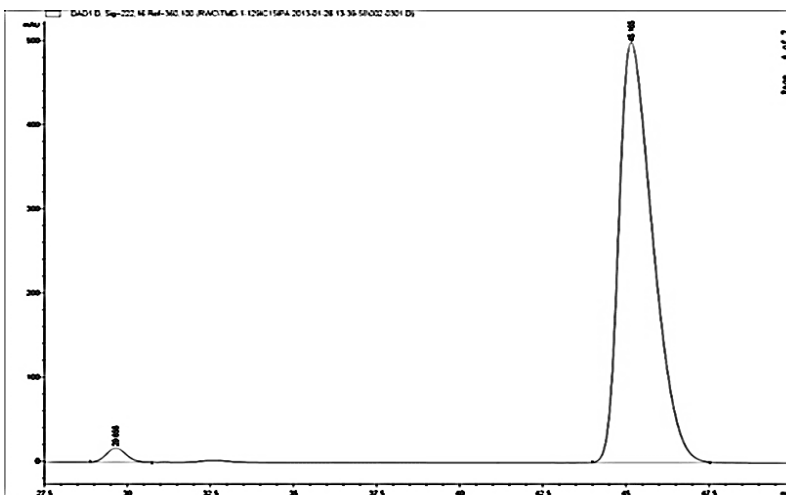


**Table 2.5, Entry 3:** Recovered product: 81 mg, 40 %, white solid. **mp range** = 66-72 °C.

**<sup>1</sup>H NMR:** (400 MHz, CDCl<sub>3</sub>) δ ppm 7.72-7.70 (m, 6 H), 7.45-7.36 (m, 9 H), 4.21 (s, 1 H), 4.06 (d, *J* = 9.3 Hz, 1 H), 3.81 (d, *J* = 9.3 Hz, 1 H), 1.70-1.63 (m, 2 H), 1.38-1.20 (m, 2 H), 0.97 (t, *J* = 7.5 Hz, 3 H), 0.68 (t, *J* = 7.5 Hz, 3 H). **<sup>13</sup>C NMR:** (101 MHz, CDCl<sub>3</sub>) δ ppm 175.9, 135.6, 133.5, 130.2, 127.8, 75.2, 72.0, 46.6, 27.7, 24.1, 8.6, 8.4. **Optical Rotation** [α]<sub>D</sub><sup>25</sup>: +5.1 (c = 0.86) **IR** (neat, cm<sup>-1</sup>) 3071, 2965, 2858, 1788, 1483, 1427, 1190, 1146, 1116, 1012, 856, 742, 711. **HRMS** (ESI) Calculated for (C<sub>20</sub>H<sub>23</sub>O<sub>3</sub>Si<sup>+</sup>) (M-C<sub>6</sub>H<sub>5</sub><sup>+</sup>): 339.1409 Observed: 339.1410.

HPLC data is of the desilylated products followed by conversion to the corresponding benzoate ester. The same conditions as the benzoate ester of the starting material were utilized. (er = 98:2).



Peak #	RetTime [min]	Type	Width [min]	Area [mAU*s]	Height [mAU]	Area %
1	29.656	BB	0.6472	699.28369	16.88456	1.9442
2	45.165	BB	1.0930	3.52682e4	499.92706	98.0558

### Kinetic Resolution Data for Table 2.5, Entry 3

#	er SM	er P	% conv	s	s AVG
1	82:18	98:2	40.3	100	<b>100</b>
2	77:23	98:2	35.8	101	

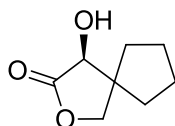
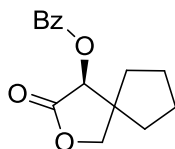


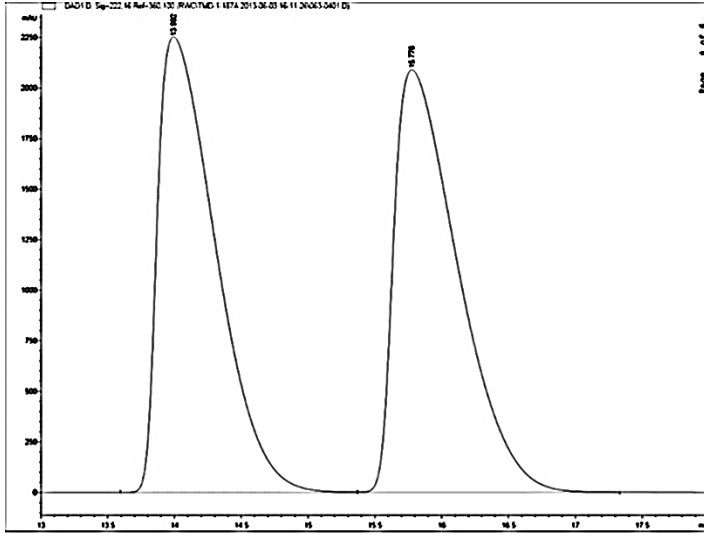
**Table 2.5, Entry 4:** Recovered starting material: 31 mg, 40 %. **<sup>1</sup>H NMR:** (400 MHz, CDCl<sub>3</sub>) δ ppm 4.32 (s, 1 H), 4.13 (d, *J* = 8.8 Hz, 1 H), 4.03 (dd, *J* = 7.8, 1.0 Hz, 1 H), 3.43 (br, 1 H), 2.05-1.58 (m, 7 H), 1.46-1.39 (m, 1 H). **<sup>13</sup>C NMR:** (101 MHz, CDCl<sub>3</sub>) δ ppm 177.9, 76.1, 73.6, 51.6, 33.6, 29.1, 25.0, 24.9. **Optical Rotation** [α]<sub>D</sub><sup>25</sup>: + 6.4 (c = 0.86).



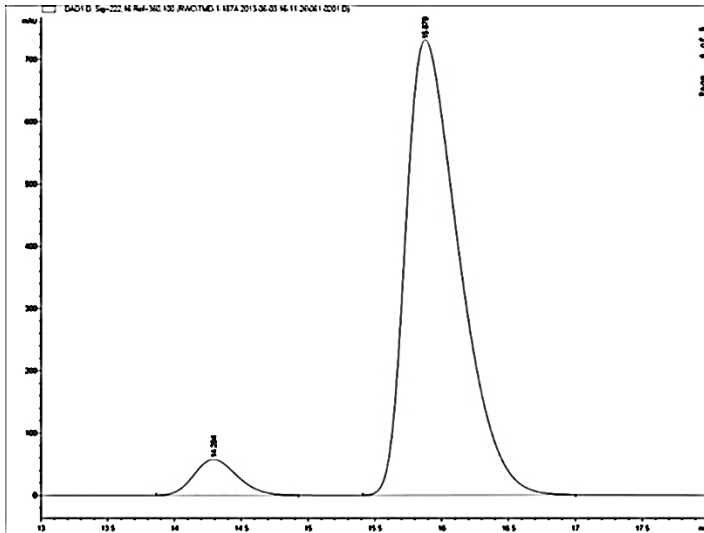
Colorless oil. **<sup>1</sup>H NMR:** (400 MHz, CDCl<sub>3</sub>) δ ppm 8.11-8.08 (m, 2 H), 7.64-7.59 (m, 1 H), 7.5-7.46 (m, 2 H), 5.78 (s, 1 H), 4.23 (d, *J* = 8.9 Hz, 1 H), 4.17 (dd, *J* = 8.1, 0.9 Hz, 1 H), 2.06-1.95 (m, 2 H), 1.78-1.62 (m, 6 H). **<sup>13</sup>C NMR:** (101 MHz, CDCl<sub>3</sub>) δ ppm 172.4, 165.3, 133.8, 130.0, 128.8, 128.6, 75.8, 73.6, 51.1, 33.6, 30.7, 24.8, 24.7. **Optical Rotation** [α]<sub>D</sub><sup>25</sup>: +18.7 (c = 0.82). **IR** (neat, cm<sup>-1</sup>) 2958, 2872, 1789, 1725, 1601, 1451, 1315, 1262, 1096, 998, 706. **HRMS** (ESI) Calculated for (C<sub>15</sub>H<sub>16</sub>O<sub>4</sub>)<sup>+</sup> (M<sup>+</sup>): 260.1043 Observed: 260.1047.

Stereochemical assignment made based on comparison of optical rotation data for the recovered starting material to that in the literature.<sup>61</sup> HPLC separation conditions made

after conversion to the corresponding benzoate ester. Chiralpak OD-H Column 6% isopropyl alcohol in hexane, flow rate: 1 mL/min, 25 °C;  $t_R$  14.3 min for (R)-enantiomer (minor) and 15.9 min for (S)-enantiomer (major). (er = 94:6).



Peak #	RetTime [min]	Type	Width [min]	Area [mAU*s]	Height [mAU]	Area %
1	13.992	BV	0.4712	6.77994e4	2252.36987	49.4661
2	15.776	VB	0.5129	6.92629e4	2088.49219	50.5339



Peak #	RetTime [min]	Type	Width [min]	Area [mAU*s]	Height [mAU]	Area %
1	14.294	BB	0.3506	1308.03906	57.67369	6.0624
2	15.879	BB	0.4252	2.02682e4	731.54596	93.9376

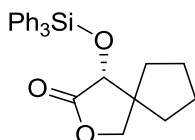
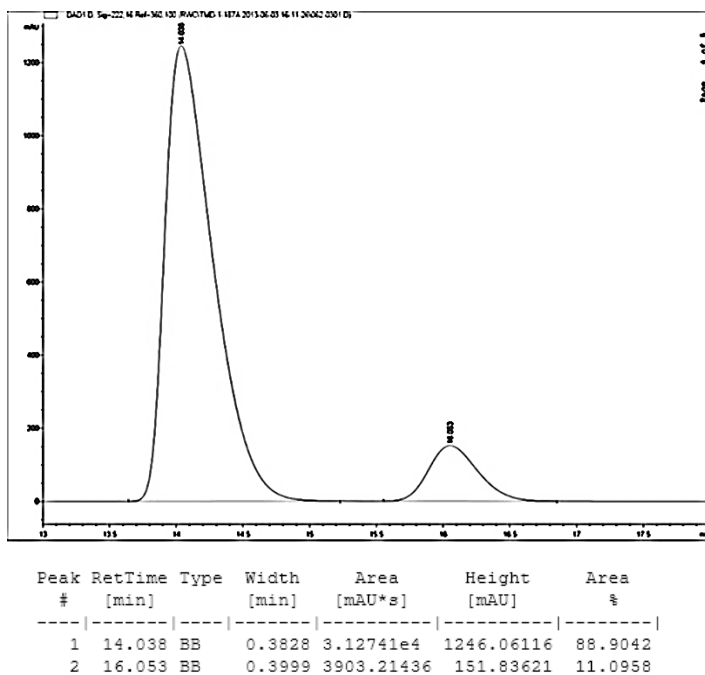


**Table 2.5, Entry 4:** Recovered product: 106 mg, 51 %, white solid. **mp range** = 83-92 °C. **<sup>1</sup>H NMR:** (400 MHz, CDCl<sub>3</sub>) δ ppm 7.72-7.70 (m, 6 H), 7.47-7.37 (m, 9 H), 4.29 (s, 1 H), 4.07 (d, *J* = 8.7 Hz, 1 H), 3.82 (d, *J* = 8.7 Hz, 1 H), 1.69-1.26 (m, 8 H). **<sup>13</sup>C NMR:** (101 MHz, CDCl<sub>3</sub>) δ ppm 175.1, 135.7, 133.4, 130.3, 127.9, 75.4, 74.9, 52.0, 33.0, 22.5, 25.1, 25.0. **Optical Rotation** [ $\alpha$ ]<sub>D</sub><sup>25</sup>: - 5.4 (c = 0.90) CHCl<sub>3</sub>. **IR** (neat, cm<sup>-1</sup>) 3029, 2955, 2898, 1786, 1428, 1191, 1147, 1115, 1100, 989, 862, 744, 699. **HRMS** (ESI) Calculated for (M<sup>+</sup>) (C<sub>26</sub>H<sub>26</sub>O<sub>3</sub>Si<sup>+</sup>): 414.1645 Observed: 414.1663.

HPLC data is of the desilylated products followed by conversion to the corresponding benzoate ester. The same conditions as the benzoate ester of the starting material were utilized. (er = 89:11).



### Kinetic Resolution Data for Table 2.5 Entry 4

#	er SM	er P	% conv	<i>s</i>	<i>s</i> AVG
1	94:6	89:11	53.0	23	<b>23</b>
2	94:6	89:11	53.0	22	

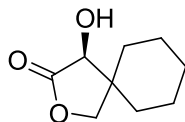
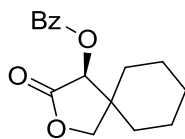


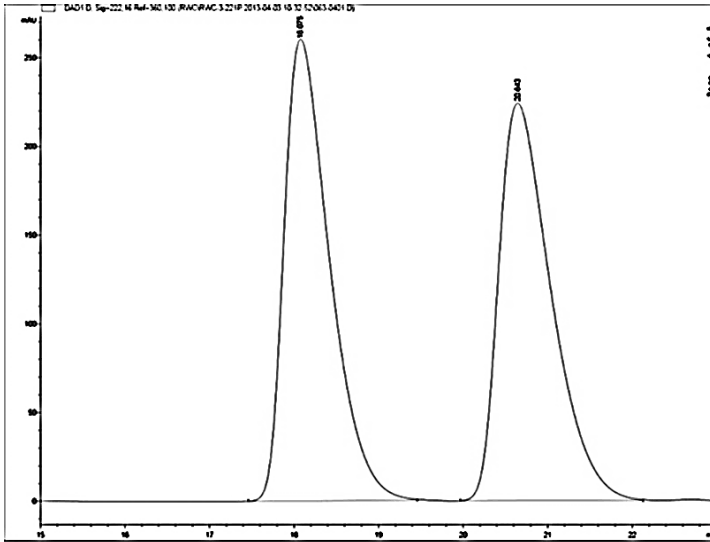
**Table 2.5, Entry 5:** Recovered starting material: 30 mg, 35 %. **<sup>1</sup>H NMR:** (400 MHz, CDCl<sub>3</sub>) δ ppm 4.34 (d, *J* = 9.2 Hz, 1H), 4.09 (d, *J* = 3.6 Hz, 1H), 3.89 (dd, *J* = 1.4, 7.8 Hz, 1H), 2.82 (d, *J* = 3.8 Hz, 1H), 1.74-1.57 (m, 6H), 1.44-1.20 (m, 4H). **<sup>13</sup>C NMR:** (101 MHz, CDCl<sub>3</sub>) δ ppm 177.7, 75.7, 73.6, 44.1, 33.7, 25.8, 25.3, 22.9, 21.7. **Optical Rotation** [α]<sub>D</sub><sup>25</sup>: +12.2 (c = 0.85).



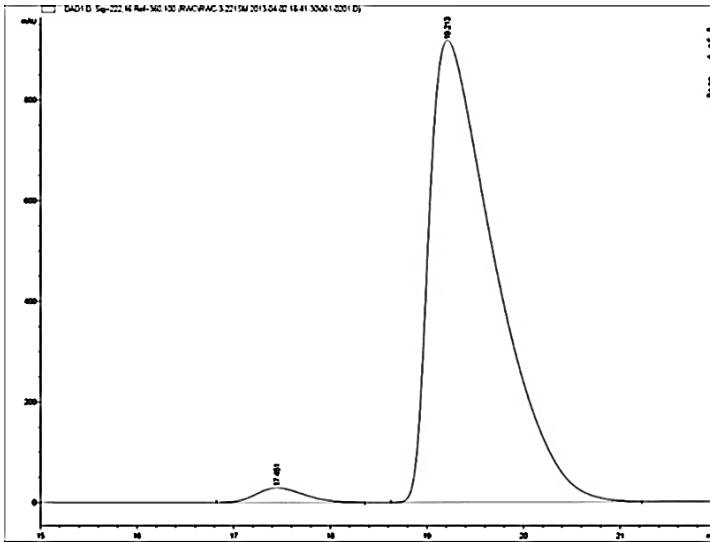
Colorless oil. **<sup>1</sup>H NMR:** (400 MHz, CDCl<sub>3</sub>) δ ppm 8.04-8.02 (m, 2 H), 7.55 (tt, *J* = 7.4, 1.3 Hz, 1 H), 7.43-7.39 (m, 2 H), 5.55 (s, 1 H), 4.38 (d, *J* = 9.2 Hz, 1 H), 4.00 (dd, *J* = 8.2, 1.1 Hz, 1 H), 1.69-1.51 (m, 7 H), 1.43-1.32 (m, 1 H), 1.23-1.11 (m, 2 H). **<sup>13</sup>C NMR:** (101 MHz, CDCl<sub>3</sub>) δ ppm 172.7, 165.5, 133.9, 130.3, 129.0, 128.7, 75.4, 73.6, 44.0, 33.9, 27.4, 25.4, 22.9, 22.0. **Optical Rotation** [α]<sub>D</sub><sup>25</sup>: -25.4 (c = 1.2) **IR** (neat, cm<sup>-1</sup>) 29 26, 2859, 1788, 1727, 1600, 1451, 1382, 1341, 1268, 1112, 1003, 986, 731, 707. **HRMS** (ESI) Calculated for (C<sub>16</sub>H<sub>18</sub>O<sub>4</sub>)<sup>+</sup> (M<sup>+</sup>): 274.1199 Observed: 274.1197.

Stereochemical assignment made based on comparison of optical rotation data for the recovered starting material to that in the literature.<sup>62</sup> HPLC separation conditions made after conversion to the corresponding benzoate ester. Chiralpak OD-H Column 6%

isopropyl alcohol in hexane, flow rate: 1 mL/min, 25 °C;  $t_R$  17.4 min for (R)-enantiomer (minor) and 19.2 min for (S)-enantiomer (major). (er = 98:2).



Peak #	RetTime [min]	Type	Width [min]	Area [mAU*s]	Height [mAU]	Area %
1	18.075	BB	0.5698	9720.57422	260.20248	50.2169
2	20.643	BB	0.6600	9636.58984	223.96283	49.7831



Peak #	RetTime [min]	Type	Width [min]	Area [mAU*s]	Height [mAU]	Area %
1	17.451	BB	0.5326	1000.04388	28.98228	2.2580
2	19.213	BB	0.7081	4.32894e4	918.04187	97.7420



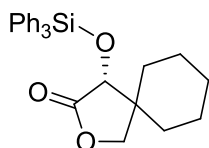
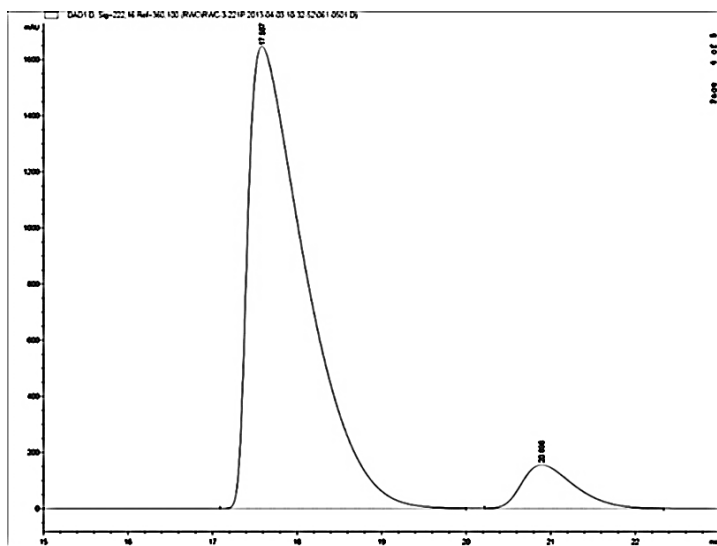


**Table 2.5, Entry 5:** Recovered product: 67 mg, 31 %, white solid. **mp range** = 103-105 °C. **<sup>1</sup>H NMR:** (400 MHz, CDCl<sub>3</sub>) δ ppm 7.73-7.71 (m, 6 H), 7.47-7.37 (m, 9 H), 4.29 (d, *J* = 9.2 Hz, 1 H), 4.09 (s, 1 H), 3.71 (dd, *J* = 7.9, 1.3 Hz, 1 H), 1.74-1.04 (m, 10 H). **<sup>13</sup>C NMR:** (101 MHz, CDCl<sub>3</sub>) δ ppm 175.3, 135.7, 133.4, 130.3, 127.9, 77.1, 72.5, 44.4, 33.1, 26.3, 25.4, 22.8, 21.8. **Optical Rotation** [α]<sub>D</sub><sup>25</sup>: - 8.0 (c = 0.85) **IR** (neat, cm<sup>-1</sup>) 3070, 2920, 2852, 1783, 1428, 1167, 1116, 1105, 1000, 850, 741, 709. **HRMS** (ESI) Calculated for (M<sup>+</sup>) (C<sub>27</sub>H<sub>28</sub>O<sub>3</sub>Si<sup>+</sup>): 428.1802 Observed: 428.1796.

HPLC data is of the desilylated products followed by conversion to the corresponding benzoate ester. The same conditions as the benzoate ester of the starting material were utilized. (er = 92:8).



Peak #	RetTime [min]	Type	Width [min]	Area [mAU*s]	Height [mAU]	Area %
1	17.587	BB	0.7038	7.81929e4	1647.14673	92.0586
2	20.896	BB	0.6639	6745.31689	155.55856	7.9414

### Kinetic Resolution Data for Table 2.5 Entry 5

#	er SM	er P	% conv	<i>s</i>	<i>s</i> AVG
1	98:2	92:8	53.2	43	<b>48</b>
2	97:3	94:6	51.8	52	

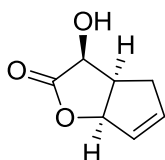
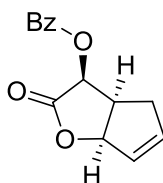


**Table 2.5, Entry 6:** Recovered starting material: 18 mg, 26 %. **<sup>1</sup>H NMR:** (400 MHz, CDCl<sub>3</sub>) δ ppm 6.27 (ddd, *J* = 5.1, 2.8, 2.8 Hz, 1 H), 5.95 (ddd, *J* = 2.8, 2.4, 2.2 Hz, 1 H), 5.35 (ddd, *J* = 6.4, 2.2, 2.1 Hz, 1 H), 4.72 (d, *J* = 9.4 Hz, 1 H), 3.23 (dddd, *J* = 15.3, 9.2, 6.1, 3.1 Hz, 1 H), 2.76 (ddd, *J* = 18.4, 5.5, 3.0 Hz, 1 H), 2.47 (ddd, *J* = 18.4, 9.2, 2.3 Hz, 1 H). **<sup>13</sup>C NMR:** (101 MHz, CDCl<sub>3</sub>) δ ppm 177.3, 141.2, 127.6, 86.6, 69.3, 40.6, 30.8.

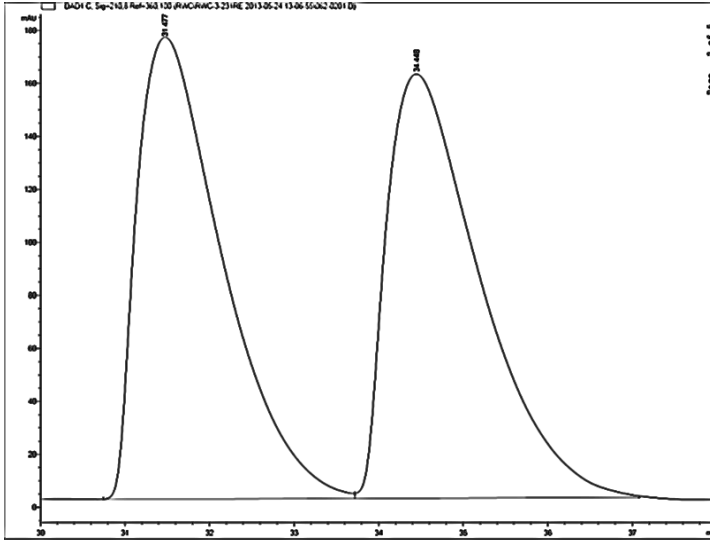
**Optical Rotation** [α]<sub>D</sub><sup>25</sup>: - 72.9 (c = 0.90) CHCl<sub>3</sub>.



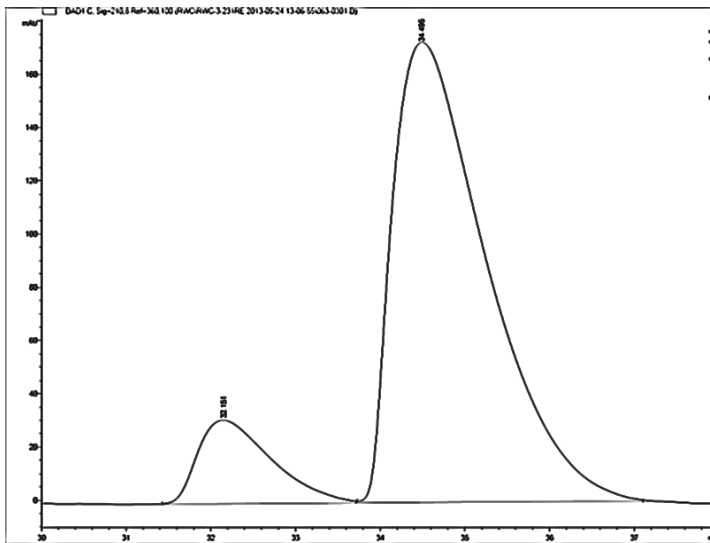
**<sup>1</sup>H NMR:** (400 MHz, CDCl<sub>3</sub>) δ ppm 8.12-8.09 (m, 2 H), 7.64-7.59 (m, 1 H), 7.49-7.46 (m, 2 H), 6.25-6.23 (m, 1 H), 6.01 (ddd, *J* = 7.9, 2.3, 2.3 Hz, 1 H), 5.87 (d, *J* = 9.5 Hz, 1 H), 5.46 (ddd, *J* = 6.6, 2.2, 2.2 Hz, 1 H), 3.51 (dddd, *J* = 12.3, 6.5, 6.5, 5.7 Hz, 1 H), 2.69-2.62 (m, 1 H), 2.52-2.42 (m, 1 H). **<sup>13</sup>C NMR:** (101 MHz, CDCl<sub>3</sub>) δ ppm 172.0, 165.4, 140.1, 133.8, 130.2, 130.0, 128.6, 128.1, 86.4, 70.1, 39.4, 31.6.

Stereochemical assignment made based on comparison of optical rotation data for the recovered starting material to that in the literature. HPLC separation conditions made

after conversion to the corresponding benzoate ester. Chiralpak OJ-H Column 10% isopropyl alcohol in hexane, flow rate: 1 mL/min, 25 °C;  $t_R$  27.9 min for (R)-enantiomer (minor) and 30.2 min for (S)-enantiomer (major). (er = 88:12).



Peak #	RetTime [min]	Type	Width [min]	Area [mAU*s]	Height [mAU]	Area %
1	31.477	BB	1.0696	1.22413e4	174.24312	49.9165
2	34.448	BB	1.1221	1.22823e4	160.08026	50.0835



Peak #	RetTime [min]	Type	Width [min]	Area [mAU*s]	Height [mAU]	Area %
1	32.151	BB	0.8688	1886.36084	31.36052	12.3793
2	34.495	BB	1.1341	1.33516e4	172.86609	87.6207

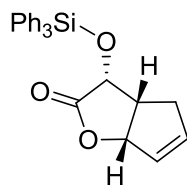
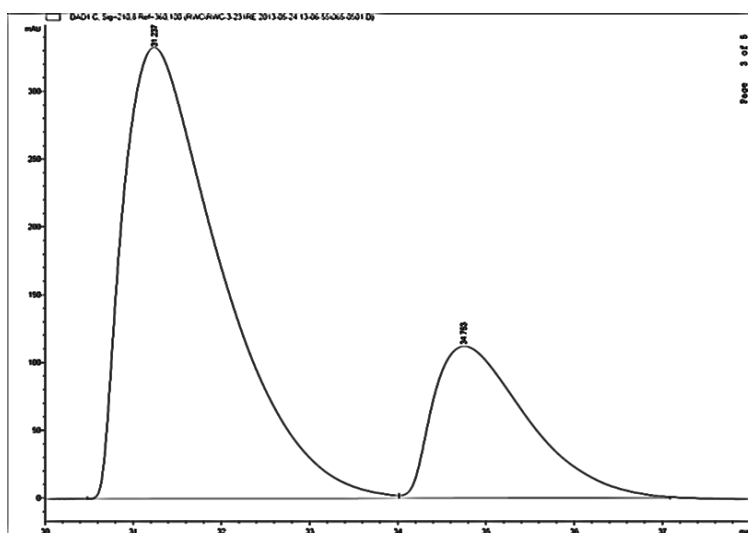


**Table 2.5, Entry 6:** Recovered product: 82 mg, 41 %, white solid. **mp range** = 91-94 °C. **<sup>1</sup>H NMR:** (400 MHz, CDCl<sub>3</sub>) δ ppm 7.74-7.72 (m, 6 H), 7.48-7.38 (m, 9 H), 6.19 (ddd, *J* = 5.6, 2.3, 2.3 Hz, 1 H), 5.88 (ddd, *J* = 7.7, 2.5, 2.5 Hz, 1 H), 5.10 (ddd, *J* = 6.5, 2.2, 2.2 Hz, 1 H), 4.78 (d, *J* = 9.2 Hz, 1 H), 2.91-2.85 (m, 1 H), 2.79-2.72 (m, 1 H), 2.23-2.15 (m, 1 H). **<sup>13</sup>C NMR:** (101 MHz, CDCl<sub>3</sub>) δ ppm 174.7, 140.1, 135.5, 133.1, 130.4, 128.0, 127.9, 84.9, 70.5, 41.1, 31.7. **Optical Rotation** [α]<sub>D</sub><sup>25</sup>: - 2.1 (c = 0.85) CHCl<sub>3</sub>. **IR** (neat, cm<sup>-1</sup>) 3069, 2854, 1771, 1428, 1142, 1116, 1102, 984, 903, 825, 739, 713, 629. **HRMS** (ESI) Calculated for (M-Ph<sup>+</sup>) (C<sub>19</sub>H<sub>17</sub>O<sub>3</sub>Si<sup>+</sup>): 321.0941 Observed: 321.0934.

HPLC data is of the desilylated products followed by conversion to the corresponding benzoate ester. The same conditions as the benzoate ester of the starting material were utilized. (er = 76:24).



Peak #	RetTime [min]	Type	Width [min]	Area [mAU*s]	Height [mAU]	Area %
1	31.237	BB	1.1343	2.57389e4	332.81055	75.6097
2	34.753	BB	1.1163	8302.88477	111.95068	24.3903

### Kinetic Resolution Data for Table 2.5 Entry 6

#	er SM	er P	% conv	<i>s</i>	<i>s</i> AVG
1	88:12	76:24	59.5	6.7	<b>7.8</b>
2	90:10	79:21	57.8	8.8	

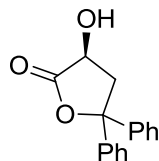
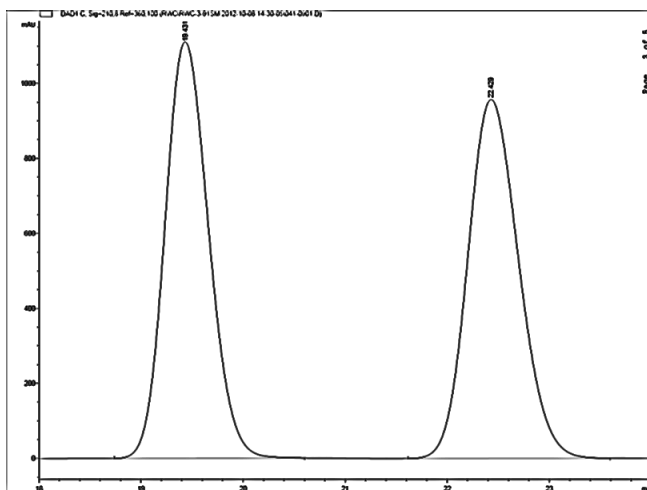


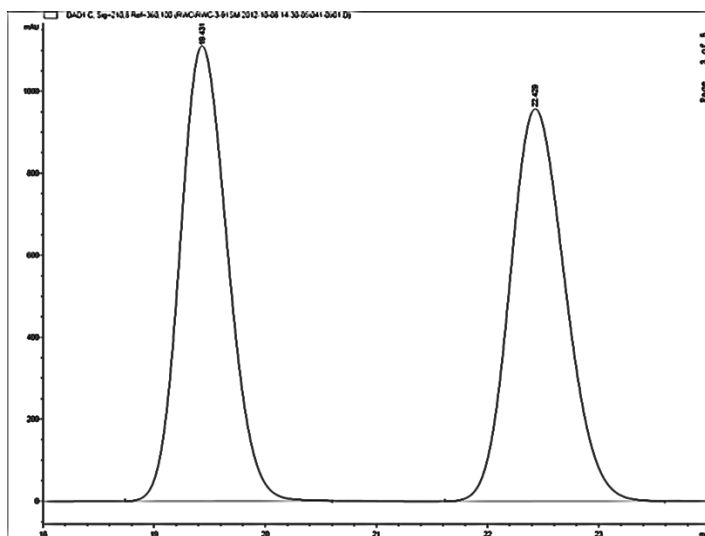
**Table 2.5, Entry 7:** Recovered starting material: 42 mg, 33 %. <sup>1</sup>H NMR: (400 MHz, CDCl<sub>3</sub>) δ ppm 7.42-7.24 (m, 10H), 4.49 (t, *J* = 8.7 Hz, 1H), 3.47 (dd, *J* = 7.8, 4.8 Hz, 1H), 3.26 (br, 1H), 2.77 (dd, *J* = 11.3, 1.2, 1H). <sup>13</sup>C NMR (101 MHz, CDCl<sub>3</sub>) δ ppm 176.7, 143.0, 141.7, 128.8, 128.5, 128.2, 128.1, 125.3, 125.2, 86.7, 68.3, 43.3.

Stereochemical assignment made by analogy to  $\alpha$ -hydroxy- $\gamma$ -butyrolactone (Table 2, Entry 1).



Peak #	RetTime [min]	Type	Width [min]	Area [mAU*s]	Height [mAU]	Area %
1	19.431	BB	0.4664	3.29829e4	1110.90833	49.9062
2	22.429	BB	0.5424	3.31068e4	957.43719	50.0938

Chiral HPLC separation conditions of the purified starting material are as follows: Chiralpak IC Column 10% isopropyl alcohol in hexane, flow rate: 1 mL/min, 25 °C;  $t_R$  19.3 min for (R)-enantiomer (minor) and 22.4 min for (S)-enantiomer (major). (er = 53:47).



Peak #	RetTime [min]	Type	Width [min]	Area [mAU*s]	Height [mAU]	Area %
1	19.431	BB	0.4664	3.29829e4	1110.90833	49.9062
2	22.429	BB	0.5424	3.31068e4	957.43719	50.0938

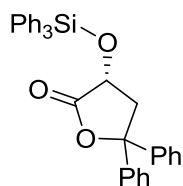
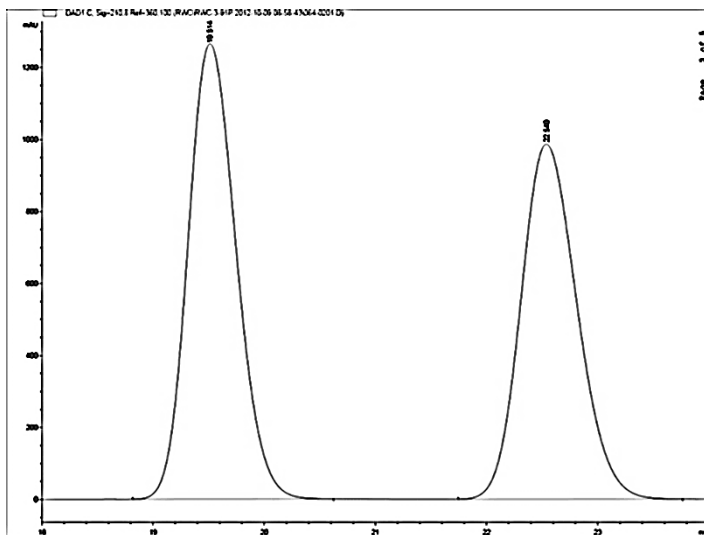


**Table 2.5, Entry 7:** Recovered product 88 mg, 34 %, white solid. **mp range** = 41-43 °C.

**$^1\text{H}$  NMR** (400 MHz,  $\text{CDCl}_3$ )  $\delta$  ppm 7.67-7.63 (m, 6 H), 7.48-7.12 (m, 19 H), 4.51 (dd,  $J = 7.4, 3.2$  Hz, 1 H), 2.96 (dd,  $J = 7.4, 5.2$  Hz, 1 H), 2.67 (dd,  $J = 10.7, 1.9$  Hz, 1 H).  **$^{13}\text{C}$  NMR** (101 MHz,  $\text{CDCl}_3$ )  $\delta$  ppm 174.1, 143.6, 141.4, 135.4, 134.9, 132.9, 130.4, 128.5, 128.4, 128.0, 127.8, 125.4, 125.1, 85.6, 69.8, 44.2. **IR** (neat,  $\text{cm}^{-1}$ ) 3068, 2922, 1785,

1589, 1448, 1428, 1218, 1118, 949, 892, 856, 745, 697. **HRMS** (CI) Calculated for (C<sub>34</sub>H<sub>32</sub>NO<sub>3</sub>Si<sup>+</sup>) (M+NH<sub>4</sub>): 530.2145 Observed: 530.2142.

HPLC data is of the desilylated products. The same conditions as the starting material were utilized. (er = 52:48).



Peak #	RetTime [min]	Type	Width [min]	Area [mAU*s]	Height [mAU]	Area %
1	19.514	BB	0.4712	3.80719e4	1264.83826	52.4163
2	22.540	BB	0.5489	3.45617e4	986.15961	47.5837

**Kinetic Resolution Data for Table 2.5 Entry 7**

#	er SM	er P	% conv	s	s AVG
1	53:47	52:48	56.4	1.2	<b>1.2</b>
2	54:46	55:45	45.2	1.3	

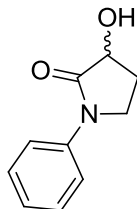


**Table 2.6, Entry 1:** Recovered starting material: 36 mg, 41%. **<sup>1</sup>H NMR:** (CDCl<sub>3</sub>, 400 MHz) δ ppm 7.64 (d, *J* = 8.6 Hz, 2 H), 7.38 (t, *J* = 8.2 Hz, 2 H), 7.18 (t, *J* = 7.5 Hz, 1 H), 4.54-4.47 (m, 1 H), 3.87-3.72 (m, 2 H), 2.64-2.25 (m, 1 H), 2.11 (ddd, *J* = 12.5, 9.4, 3.1 Hz, 1 H). **<sup>13</sup>C NMR:** (CDCl<sub>3</sub>, 101 MHz) δ ppm 174.3, 138.9, 128.2, 125.1, 119.7, 70.7, 44.5, 27.7.

Chiralpak AD-H Column 10% isopropyl alcohol in hexane, flow rate: 1 mL/min, 25 °C; *t<sub>R</sub>* 18.1 min and 20.2 min for each enantiomer. (er = 50:50)

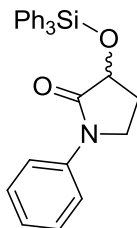


**Table 2.6, Entry 1:** Recovered product: 81 mg, 37%, white solid. **mp range** = 88-92 °C. **<sup>1</sup>H NMR** (400 MHz, CDCl<sub>3</sub>) δ ppm 7.83-7.80 (m, 6 H), 7.65 (d, *J* = 7.4 Hz, 2 H), 7.51-7.35 (m, 11 H), 7.17 (t, *J* = 7.7 Hz, 1 H), 4.61 (t, *J* = 7.9 Hz, 1 H), 3.76-3.78 (m, 1 H), 3.64-3.55 (m, 1 H), 2.31-2.09 (m, 2 H). **<sup>13</sup>C NMR** (101 MHz, CDCl<sub>3</sub>) δ ppm 127.1, 139.3, 135.6, 133.8, 130.2, 128.8, 127.9, 124.7, 119.6, 77.3, 44.0, 29.0. **IR** (neat, cm<sup>-1</sup>) 3256, 2952, 1710, 1495, 1428, 1311, 1115, 997, 904, 834, 710. **HRMS** (ESI) Calculated for (C<sub>22</sub>H<sub>20</sub>NO<sub>2</sub>Si<sup>+</sup>) (M-Ph<sup>+</sup>): 358.1257 Observed: 358.1253.



### Kinetic Resolution Data for Table 2.6, Entry 1

#	er SM	er P	% conv <sup>a</sup>	s	s AVG
1	50:50	ND	45.7	1.0	<b>1.0</b>
2	50:50	ND	47.0	1.0	

<sup>a</sup>- Conversion determined via <sup>1</sup>H NMR of the crude mixture.

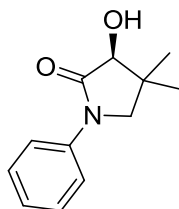
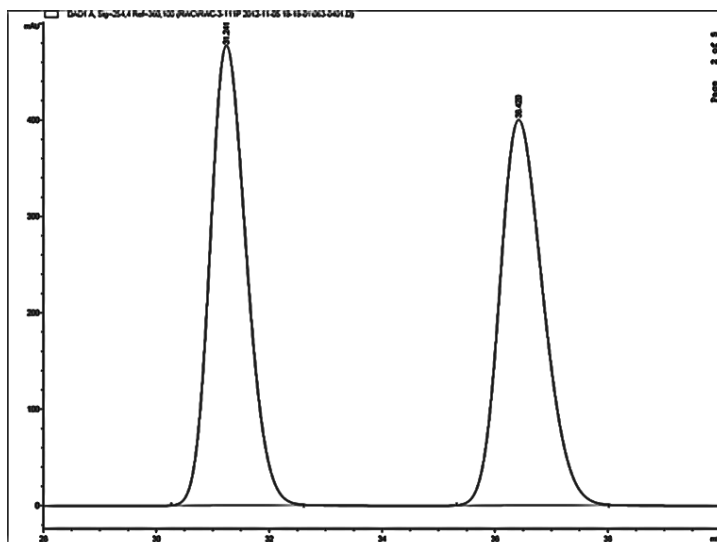
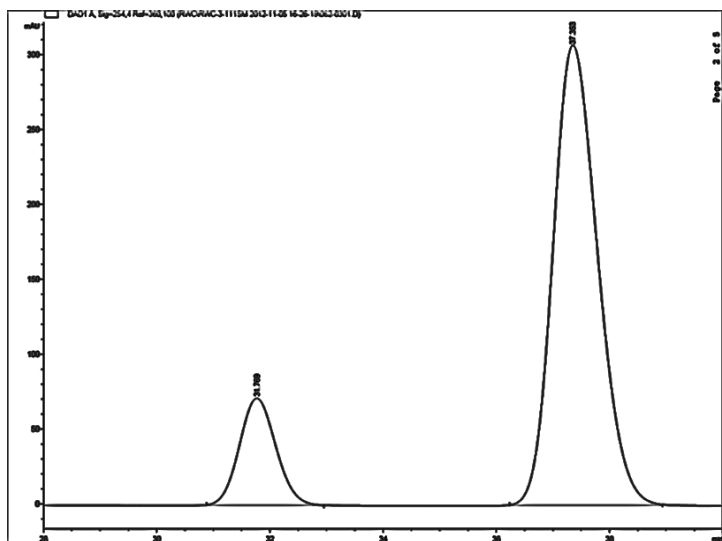


**Table 2.6, Entry 2:** Recovered starting material: 52 mg, 51% <sup>1</sup>H NMR: (CDCl<sub>3</sub>, 400 MHz) δ ppm 7.63-7.61 (m, 2 H), 7.40-7.36 (m, 2 H), 7.19-7.15 (m, 1 H), 4.13 (s, 1 H), 3.59 (br, 1 H), 3.55 (d *J* = 9.6 Hz, 1H), 3.45 (d, *J* = 9.6 Hz, 1 H), 1.33 (s, 3 H), 1.10 (s, 3 H). <sup>13</sup>C NMR: (CDCl<sub>3</sub>, 101 MHz) δ ppm 173.9, 139.1, 128.9, 124.9, 119.5, 78.4, 57.7, 38.4, 24.6, 20.0. **Optical Rotation** [α]<sub>D</sub><sup>25</sup>: - 30.1 (c = 0.91) CHCl<sub>3</sub>.



Peak #	RetTime [min]	Type	Width [min]	Area [mAU*s]	Height [mAU]	Area %
1	31.242	BB	0.7059	2.13375e4	471.59149	49.9140
2	36.420	BB	0.8369	2.14111e4	397.20987	50.0860

Stereochemical assignment made from comparison to the literature. Chiralpak AD-H Column 10% isopropyl alcohol in hexane, flow rate: 1 mL/min, 25 °C;  $t_R$  18.1 min for (R)-enantiomer (minor) and 37.3 min for (S)-enantiomer (major). (er = 84:16).



Peak #	RetTime [min]	Type	Width [min]	Area [mAU*s]	Height [mAU]	Area %
1	31.769	BB	0.6855	3206.80200	71.46523	16.0072
2	37.353	BB	0.8480	1.68267e4	307.21069	83.9928

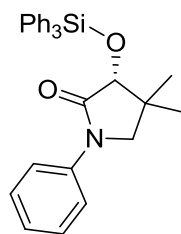
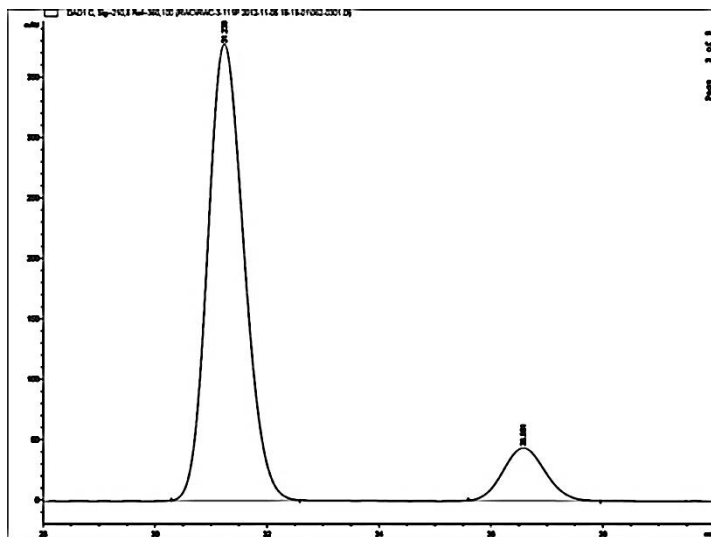


**Table 2.6, Entry 2:** Recovered product: 89 mg, 38%, white solid. **mp range** = 105-108 °C.  **$^1\text{H NMR}$**  (400 MHz,  $\text{CDCl}_3$ )  $\delta$  ppm 7.78 (d,  $J = 6.2$  Hz, 6 H), 7.58 (d,  $J = 7.6$  Hz, 2H), 7.44-7.31 (m, 11H), 7.11 (t,  $J = 7.4$  Hz, 1 H), 4.20 (s, 1 H), 3.38 (dd,  $J = 9.5, 5.0$  Hz, 1 H), 1.20 (s, 3 H), 0.96 (s, 3H).  **$^{13}\text{C NMR}$**  (101 MHz,  $\text{CDCl}_3$ )  $\delta$  ppm 171.9, 139.5, 135.8, 134.0, 130.0, 128.8, 127.8, 124.4, 119.4, 80.2, 56.9, 38.5, 24.3, 20.9. **Optical Rotation**  $[\alpha]_D^{25} = +64.6$  (c = 0.87) **IR** (neat,  $\text{cm}^{-1}$ ) 3066, 2931, 1709, 1597, 1143, 1114,

868, 709, 691. **HRMS** (CI) Calculated for (C<sub>30</sub>H<sub>30</sub>NO<sub>2</sub>Si<sup>+</sup>) (M+H): 464.2040 Observed: 464.2041.

HPLC data is of the desilylated product. The same conditions as the recovered starting materials were utilized. (er = 88:12).



Peak #	RetTime [min]	Type	Width [min]	Area [mAU*s]	Height [mAU]	Area %
1	31.238	BB	0.6949	1.69683e4	380.03403	88.2541
2	36.581	BB	0.8078	2258.34155	43.06859	11.7459

### Kinetic Resolution Data for Table 2.6 Entry 2

#	er SM	er P	% conv	s	s AVG
1	81:19	87:13	45.7	13	<b>14</b>
2	84:16	88:12	47.0	15	

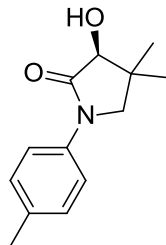
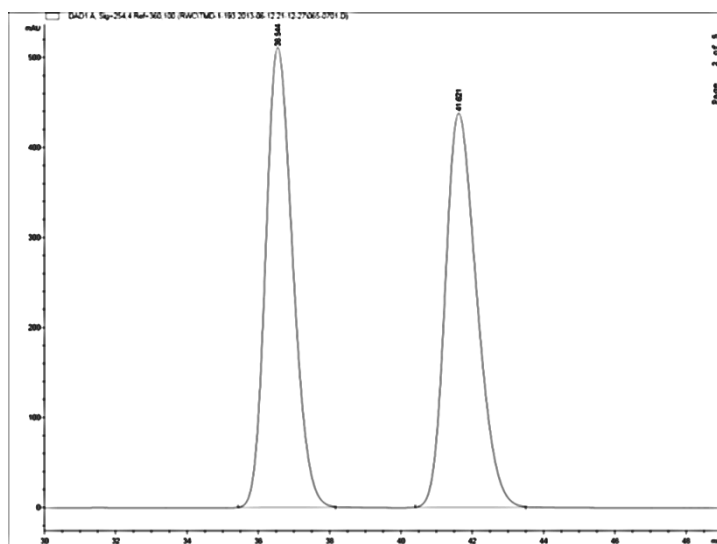
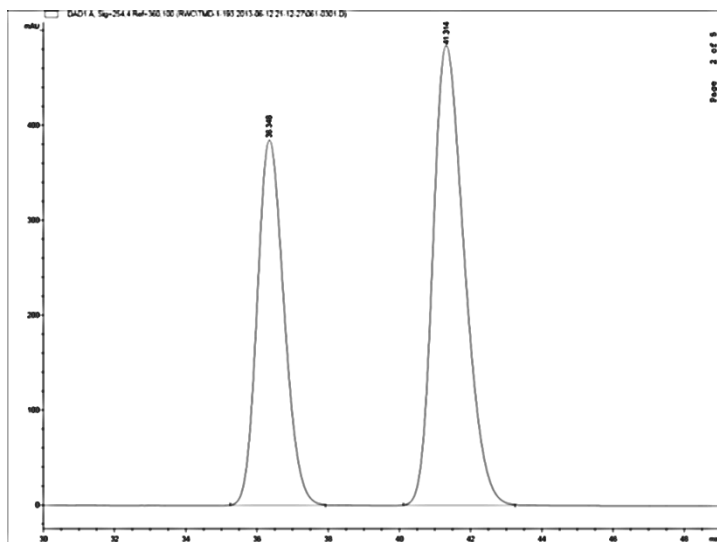


**Table 2.6, Entry 3:** Recovered starting material: mg, %  $^1\text{H NMR}$ : ( $\text{CDCl}_3$ , 400 MHz)  $\delta$  ppm 7.49 (d,  $J = 8.5$  Hz, 2 H), 7.18 (d,  $J = 8.5$  Hz, 2 H), 4.11 (d,  $J = 2.4$  Hz, 1 H), 3.53 (d,  $J = 9.6$  Hz, 1 H), 3.49 (br, 1 H), 3.40 (d,  $J = 7.1$  Hz, 1 H), 2.33 (s, 3 H), 1.32 (s, 3 H), 1.09 (s, 3 H).  $^{13}\text{C NMR}$ : ( $\text{CDCl}_3$ , 101 MHz)  $\delta$  ppm 173.6, 136.6, 134.6, 129.5, 119.5, 78.4, 57.8, 38.5, 24.6, 22.9, 20.9, 20.0. **Optical Rotation**  $[\alpha]_D^{25}$ : (c =)  $\text{CHCl}_3$ .

Stereochemical assignment made by analogy to 3-hydroxy-4,4-dimethyl pyrrolidinone. (Table 3, Entry 2) Chiralpak IC Column 10% isopropyl alcohol in hexane, flow rate: 1 mL/min, 25 °C;  $t_R$  36.3 min for (R)-enantiomer (minor) and 41.3 min for (S)-enantiomer (major). (er = 60:40).



Peak #	RetTime [min]	Type	Width [min]	Area [mAU*s]	Height [mAU]	Area %
1	36.544	BB	0.8200	2.68657e4	511.33243	50.0201
2	41.621	BB	0.9388	2.68441e4	438.12311	49.9799



Peak #	RetTime [min]	Type	Width [min]	Area [mAU*s]	Height [mAU]	Area %
1	36.348	BB	0.8104	2.01197e4	385.19290	40.4185
2	41.314	BB	0.9347	2.96587e4	484.80865	59.5815

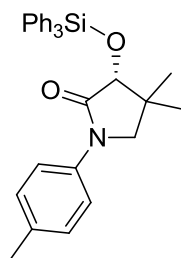
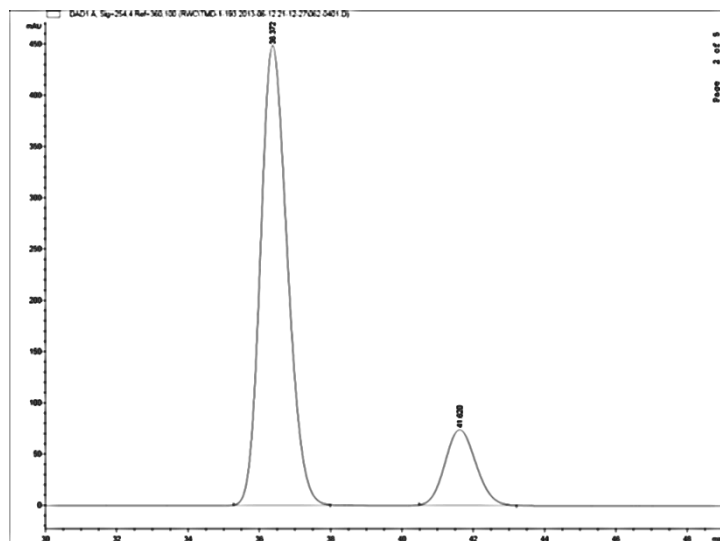


**Table 2.6, Entry 3:** Recovered product: 53 mg, 22%, white solid. **mp range** = 127-130 °C. **<sup>1</sup>H NMR** (400 MHz, CDCl<sub>3</sub>) δ ppm 7.79-7.77 (m, 6 H), 7.47-7.36 (m, 11 H), 7.14 (d, *J* = 8.3 Hz, 2 H), 4.19 (s, 1 H), 3.34 (dd, *J* = 11.5, 9.5 Hz, 2 H), 2.31 (s, 3 H), 1.19 (s, 3 H), 0.95 (s, 3 H). **<sup>13</sup>C NMR** (101 MHz, CDCl<sub>3</sub>) δ ppm 171.7, 137.0, 135.8, 135.3, 134.1, 130.0, 129.3, 127.8, 119.4, 80.3, 57.1, 38.6, 24.3, 20.9, 20.8. **Optical Rotation** [α]<sub>D</sub><sup>25</sup>: = +56.3 (c = 0.76) CHCl<sub>3</sub>. **IR** (neat, cm<sup>-1</sup>) 3047, 2868, 1709, 1513, 1428, 1327, 1142, 1115, 922, 814, 709. **HRMS** (ESI) Calculated for (C<sub>31</sub>H<sub>31</sub>NO<sub>2</sub>Si<sup>+</sup>) (M<sup>+</sup>): 477.2118 Observed: 477.2100.

HPLC data is of the desilylated product. The same conditions as the recovered starting materials were utilized. (er = 84:16).



Peak #	RetTime [min]	Type	Width [min]	Area [mAU*s]	Height [mAU]	Area %
1	36.372	BB	0.8113	2.34163e4	449.07639	83.9933
2	41.620	BB	0.9099	4462.49121	73.85728	16.0067

### Kinetic Resolution Data for Table 2.6, Entry 3

#	er SM	er P	% conv	s	s AVG
1	60:40	84:16	22.0	6.3	<b>7.1</b>
2	58:42	87:13	18.0	7.8	

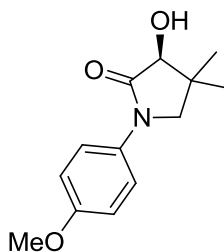
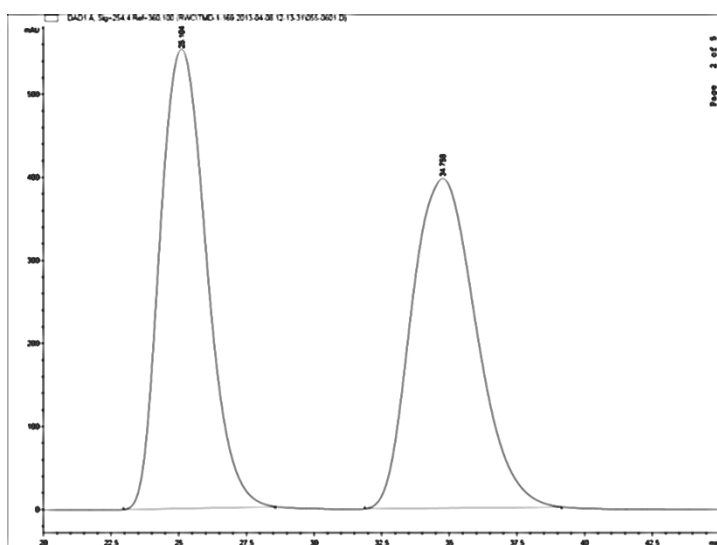


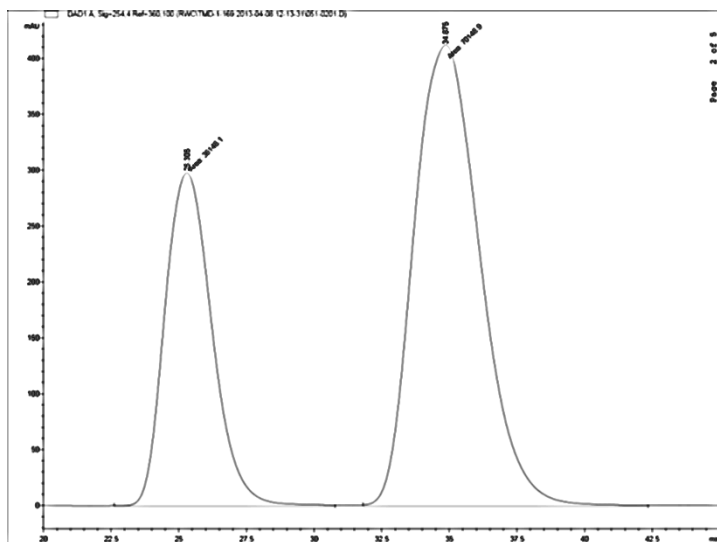
**Table 2.6, Entry 4:** Recovered starting material: 54 mg, 46 % <sup>1</sup>H NMR: (CDCl<sub>3</sub>, 400 MHz) δ ppm 7.52 (d, *J* = 9.2 Hz, 2 H), 6.92 (d, *J* = 9.2 Hz, 2 H), 4.11 (s, 1 H), 3.81 (s, 3

H), 3.54 (d,  $J = 9.6$  Hz, 1 H), 3.40 ( $J = 9.6$  Hz, 1 H), 3.18 (br, 1 H), 1.33 (s, 3 H), 1.10 (s, 3 H).  $^{13}\text{C}$  NMR: ( $\text{CDCl}_3$ , 101 MHz)  $\delta$  ppm 173.4, 157.0, 132.5, 121.4, 114.4, 78.5, 58.3, 55.7, 38.8, 24.8, 20.2. **Optical Rotation**  $[\alpha]_{\text{D}}^{25} = -14.1$  ( $c = 0.87$ )  $\text{CHCl}_3$ .

Stereochemical assignment made by analogy to 3-hydroxy-4,4-dimethyl pyrrolidinone. (Table 3, Entry 2) Chiralpak AD Column 10% isopropyl alcohol in hexane, flow rate: 1 mL/min, 25 °C;  $t_{\text{R}}$  25.3 min for (R)-enantiomer (minor) and 34.8 min for (S)-enantiomer (major). (er = 66:34).



Peak #	RetTime [min]	Type	Width [min]	Area [mAU*s]	Height [mAU]	Area %
1	25.104	BB	1.6664	6.57748e4	553.11914	49.9809
2	34.758	BB	1.9441	6.58250e4	397.06128	50.0191



Peak #	RetTime [min]	Type	Width [min]	Area [mAU*s]	Height [mAU]	Area %
1	25.305	MM	2.0205	3.61481e4	298.17831	34.0067
2	34.875	MM	2.8341	7.01489e4	412.53067	65.9933

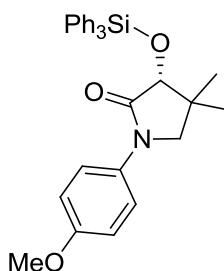
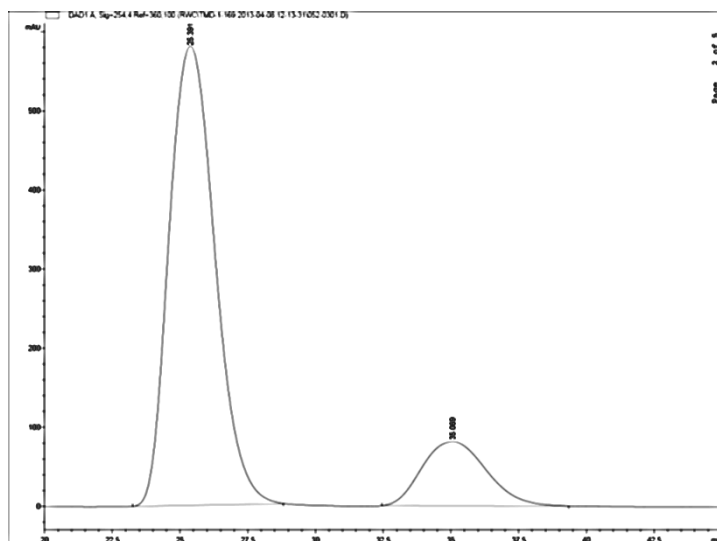


**Table 2.6, Entry 4:** Recovered product: 80 mg, 32 %, white solid. **mp range** = 35-38 °C.

**<sup>1</sup>H NMR** (400 MHz, CDCl<sub>3</sub>) δ ppm 7.79-7.77 (m, 6 H), 7.48-7.36 (m, 11 H), 6.87 (d, *J* = 9.1 Hz, 2 H), 4.19 (s, 1 H), 3.77 (s, 3 H), 3.34 (s, 2 H), 1.19 (s, 3 H), 0.94 (s, 3 H). **<sup>13</sup>C NMR** (101 MHz, CDCl<sub>3</sub>) δ ppm 171.5, 156.4, 135.8, 134.0, 132.8, 130.0, 127.8, 121.1, 114.0, 80.2, 57.4, 55.4, 38.7, 24.3, 20.9. **Optical Rotation** [α]<sub>D</sub><sup>25</sup>: +50.5 (c = 0.78) CHCl<sub>3</sub>. **IR** (neat, cm<sup>-1</sup>) 3397, 2932, 1706, 1510, 1464, 1428, 1246, 1142, 1103, 1032, 828, 709. **HRMS** (ESI) Calculated for (C<sub>31</sub>H<sub>31</sub>NO<sub>3</sub>Si<sup>+</sup>) (M<sup>+</sup>): 493.2067 Observed: 493.2073.

HPLC data is of the desilylated product. The same conditions as the recovered starting materials were utilized. (er = 84:16).





Peak #	RetTime [min]	Type	Width [min]	Area [mAU*s]	Height [mAU]	Area %
1	25.391	BB	1.6183	6.82238e4	580.41565	83.5864
2	35.069	BB	1.9347	1.33968e4	81.12312	16.4136

#### Kinetic Resolution Data for Table 2.6, Entry 4

#	er SM	er P	% conv	s	s AVG
1	66:34	84:16	32.3	6.9	<b>6.8</b>
2	66:34	84:16	31.7	6.8	

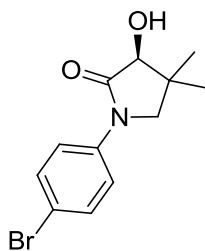
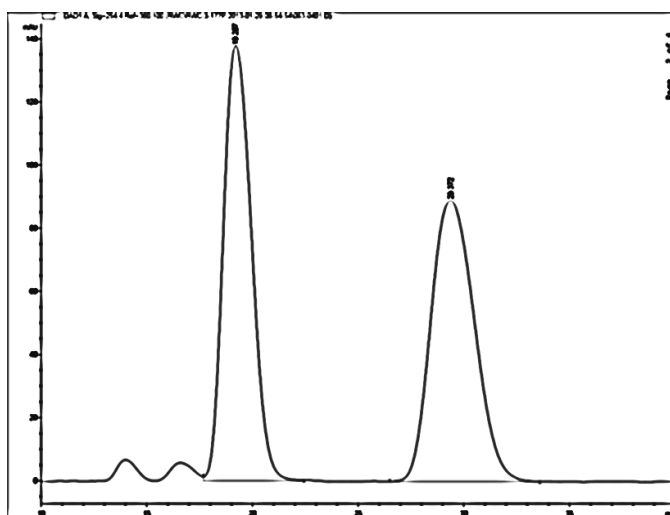


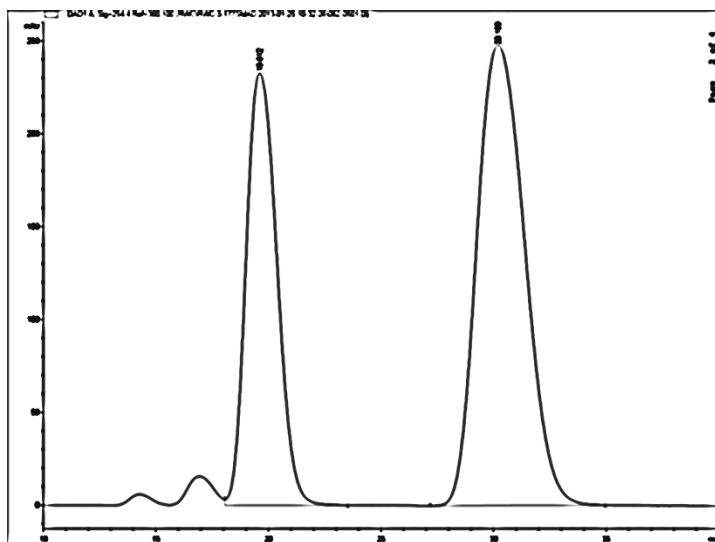
**Table 2.6, Entry 5:** Recovered starting material: 81 mg, 57 %  $^1\text{H NMR}$ : ( $\text{CDCl}_3$ , 400 MHz)  $\delta$  ppm 7.55-7.47 (m, 4 H), 4.11 (s, 1 H), 3.53 (d,  $J = 9.5$  Hz, 1 H), 3.42 (d,  $J = 9.5$  Hz, 1 H), 1.34 (s, 3 H), 1.09 (s, 3 H).  $^{13}\text{C NMR}$ : ( $\text{CDCl}_3$ , 101 MHz)  $\delta$  ppm 173.7, 138.2,

131.9, 120.7, 117.6, 78.3, 57.5, 38.5, 24.5, 19.9. **Optical Rotation**  $[\alpha]_D^{25} = -10.1$  (c = 0.85)  $\text{CHCl}_3$ .

Stereochemical assignment made by analogy to 3-hydroxy-4,4-dimethyl pyrrolidinone. (Table 3, Entry 2) Chiralpak AD Column 10% isopropyl alcohol in hexane, flow rate: 1 mL/min, 25 °C;  $t_R$  19.6 min for (R)-enantiomer (minor) and 30.2 min for (S)-enantiomer (major). (er = 62:38).



Peak #	RetTime [min]	Type	Width [min]	Area [mAU*s]	Height [mAU]	Area %
1	19.207	VB	1.4886	1.26850e4	137.96996	50.0238
2	29.372	BB	2.2948	1.26729e4	88.91835	49.9762



Peak #	RetTime [min]	Type	Width [min]	Area [mAU*s]	Height [mAU]	Area %
1	19.612	VB	1.5259	2.20747e4	232.88571	37.7990
2	30.199	BB	2.3774	3.63255e4	247.92323	62.2010

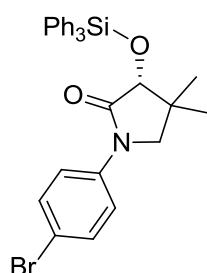
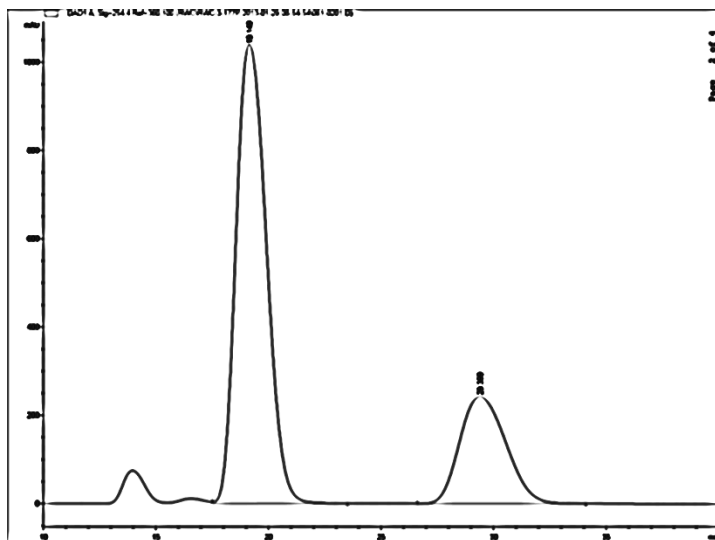


**Table 2.6, Entry 5:** Recovered product: 86 mg, 31 %, white solid. **mp range** = 138-140 °C. **<sup>1</sup>H NMR** (400 MHz, CDCl<sub>3</sub>) δ ppm 7.78-7.75 (m, 6 H), 7.51-7.37 (m, 13 H), 4.19 (s, 1 H), 3.34 (dd, *J* = 15.6, 9.4 Hz, 2 H), 1.19 (s, 3 H), 0.97 (s, 3 H). **<sup>13</sup>C NMR** (101 MHz, CDCl<sub>3</sub>) δ ppm 172.0, 138.6, 135.8, 133.9, 131.7, 130.1, 127.8, 120.7, 117.4, 80.1, 56.8, 38.5, 24.3, 20.9. **Optical Rotation** [ $\alpha$ ]<sub>D</sub><sup>25</sup>: +50.6 (c = 0.93) CHCl<sub>3</sub>. **IR** (neat, cm<sup>-1</sup>) 3067, 2874, 1712, 1589, 1488, 1360, 1328, 1145, 1114, 1003, 825, 709. **HRMS** (ESI) Calculated for (C<sub>24</sub>H<sub>23</sub>BrNO<sub>2</sub>Si<sup>+</sup>) (M-Ph<sup>+</sup>): 464.0675 Observed: 464.0681.

HPLC data is of the desilylated product. The same conditions as the recovered starting materials were utilized. (er = 74:26).



Peak #	RetTime [min]	Type	Width [min]	Area [mAU*s]	Height [mAU]	Area %
1	19.149	VB	1.4899	9.72194e4	1040.65820	73.8774
2	29.399	BB	2.2707	3.43762e4	242.37892	26.1226

#### Kinetic Resolution Data for Table 2.6, Entry 5

#	er SM	er P	% conv	s	s AVG
1	62:38	74:26	34.0	3.6	<b>3.3</b>
2	58:42	72:28	26.0	3.0	

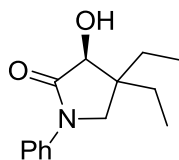
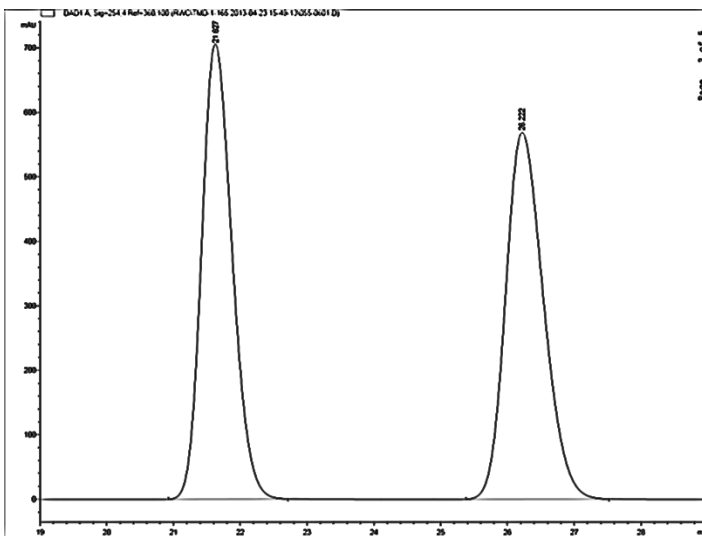


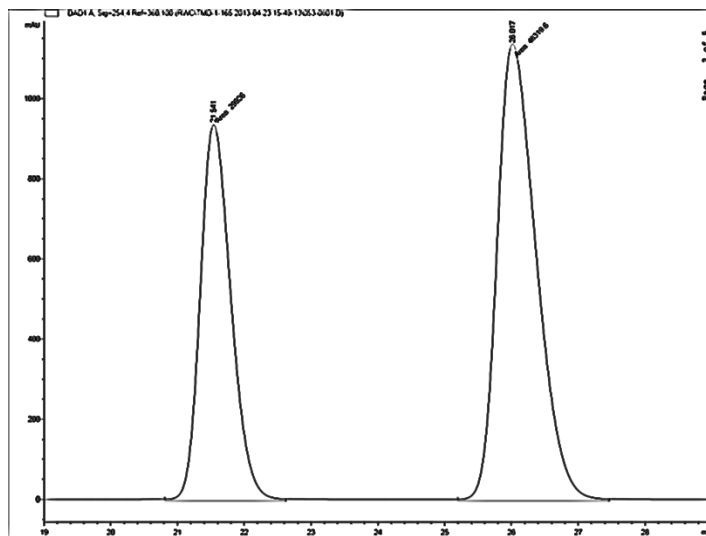
**Table 2.6, Entry 6:** Recovered starting material: 89 mg, 76 %.  $^1\text{H NMR}$  (400 MHz,  $\text{CDCl}_3$ )  $\delta$  ppm 7.63 (d,  $J = 8.1$  Hz, 2 H), 7.37 (t,  $J = 7.7$  Hz, 2 H), 7.16 (t,  $J = 7.5$  Hz, 1 H), 4.24 (s, 1 H), 3.77 (br, 1 H), 3.54 (d,  $J = 9.9$  Hz, 1 H), 3.45 (d,  $J = 9.9$  Hz, 1 H), 1.70-1.50 (m, 4 H), 1.03 (t,  $J = 7.5$  Hz, 3 H), 0.87 (t,  $J = 7.5$  Hz, 3 H).  $^{13}\text{C NMR}$  (101 MHz,  $\text{CDCl}_3$ )  $\delta$  ppm 174.6, 139.0, 128.9, 124.8, 119.6, 77.4, 54.0, 43.9, 29.7, 22.7, 8.9, 8.5.

**Optical Rotation**  $[\alpha]_D^{25}$ : = -5.1 (c = 0.90)  $\text{CHCl}_3$ .

Stereochemical assignment made by analogy to 3-hydroxy-4,4-dimethyl pyrrolidinone.  
 (Table 3, Entry 2) Chiralpak IC Column 10% isopropyl alcohol in hexane, flow rate: 1 mL/min, 25 °C;  $t_R$  21.5 min for (R)-enantiomer (minor) and 26.0 min for (S)-enantiomer (major). (er = 61:39).



Peak #	RetTime [min]	Type	Width [min]	Area [mAU*s]	Height [mAU]	Area %
1	21.627	BB	0.4934	2.23631e4	706.28821	49.9776
2	26.222	BB	0.6130	2.23831e4	568.91089	50.0224



Peak #	RetTime [min]	Type	Width [min]	Area [mAU*s]	Height [mAU]	Area %
1	21.541	MM	0.5314	2.99260e4	938.57977	39.2495
2	26.017	MM	0.6772	4.63196e4	1139.92334	60.7505

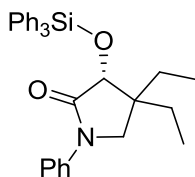
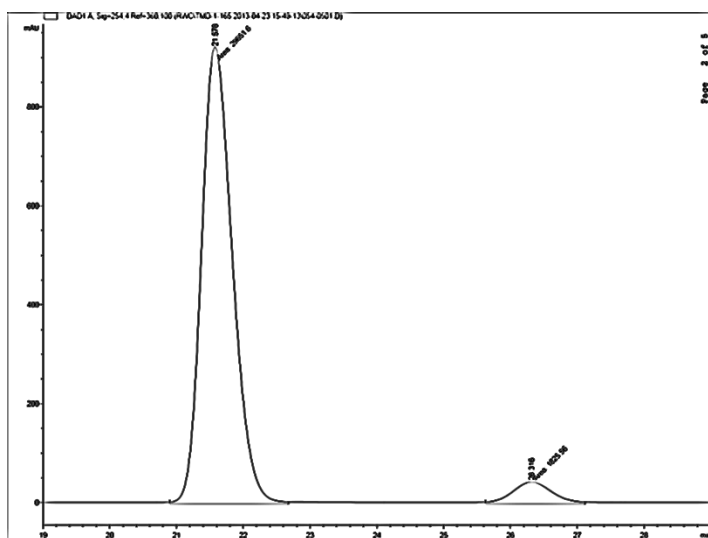


**Table 2.6, Entry 6:** Recovered product: 20 mg, 8 %, white solid. **mp range** = 113-116 °C. **<sup>1</sup>H NMR** (400 MHz, CDCl<sub>3</sub>) δ ppm 7.77-7.74 (m, 6 H), 7.61-7.58 (m, 1 H), 7.44-7.31 (m, 12 H), 7.14-7.09 (m, 1 H), 4.27 (s, 1 H), 3.48 (d, *J* = 9.8 Hz 1 H), 3.40 (d, *J* = 9.8 Hz, 1 H), 1.81-1.63 (m, 2 H), 1.49-1.30 (m, 2 H), 0.95 (t, *J* = 7.5 Hz, 3 H), 0.75 (t, *J* = 7.5 Hz, 3 H). **<sup>13</sup>C NMR** (101 MHz, CDCl<sub>3</sub>) δ ppm 172.3, 139.3, 135.8, 134.3, 129.9, 128.8, 127.7, 124.3, 119.5, 78.4, 52.9, 43.7, 28.8, 25.3, 8.9, 8.6. **Optical Rotation** [α]<sub>D</sub><sup>25</sup> = +69.7 (c = 0.99) CHCl<sub>3</sub>. **IR** (neat, cm<sup>-1</sup>). **HRMS** (CI) Calculated for (C<sub>32</sub>H<sub>34</sub>NO<sub>2</sub>Si) (M+H): 492.2353 Observed: 492.2346.

HPLC data is of the desilylated product. The same conditions as the recovered starting materials were utilized. (er = 94:6).



Peak #	RetTime [min]	Type	Width [min]	Area [mAU*s]	Height [mAU]	Area %
1	21.578	MM	0.5350	2.96516e4	923.72888	94.2004
2	26.316	MM	0.6947	1825.56348	43.79646	5.7996

### Kinetic Resolution Data for Table 2.6 Entry 6

#	er SM	er P	% conv	s	s AVG
1	61:39	94:6	19.6	21	<b>20</b>
2	60:40	95:5	18.0	20	

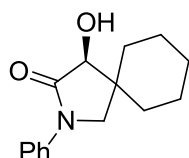
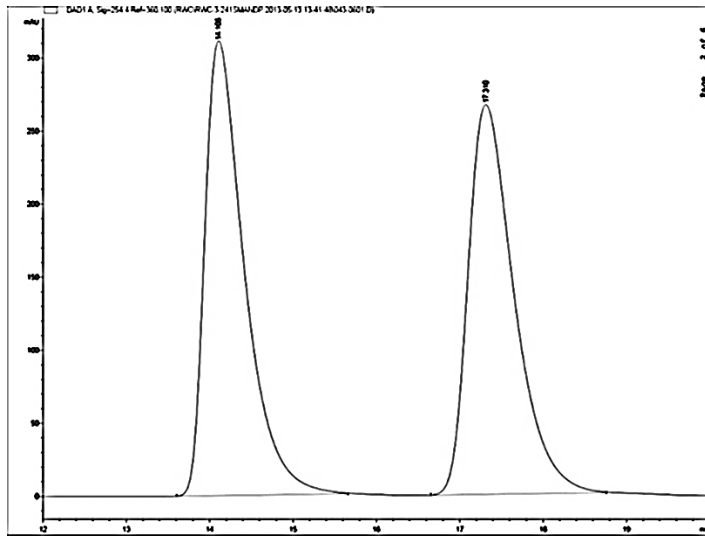
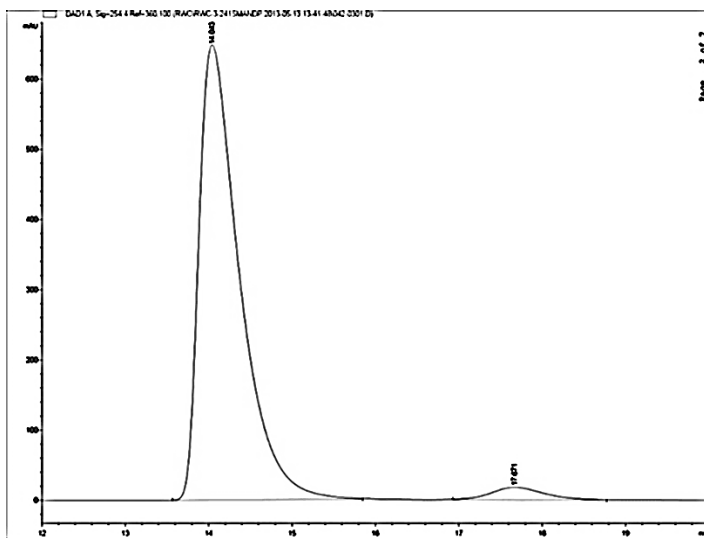


**Table 2.6, Entry 7:** Recovered starting material: 60 mg, 49 %.  $^1\text{H NMR}$  (400 MHz,  $\text{CDCl}_3$ )  $\delta$  ppm 7.64 (d,  $J = 8.2$  Hz, 2 H), 7.39 (t,  $J = 7.7$  Hz, 2 H), 7.18 (t,  $J = 7.3$  Hz, 1 H), 4.09 (s, 1 H), 3.77 (d,  $J = 9.8$  Hz, 1 H), 3.43 (d,  $J = 9.8$  Hz, 1 H), 1.88-1.64 (m, 6 H), 1.39-1.28 (m, 4 H).  $^{13}\text{C NMR}$  (101 MHz,  $\text{CDCl}_3$ )  $\delta$  ppm 173.8, 139.2, 128.9, 124.8, 119.5, 78.5, 54.0, 41.6, 35.0, 26.5, 25.6, 23.1, 22.0. **Optical Rotation**  $[\alpha]_{\text{D}}^{25} = -37.5$  (c = 0.76)  $\text{CHCl}_3$ .

Stereochemical assignment made from X-ray crystallography of the triphenyl silyl-protected product. Chiralpak OD-H Column 6% isopropyl alcohol in hexane, flow rate: 1 mL/min, 25 °C;  $t_{\text{R}}$  14.0 min for (S)-enantiomer (minor) and 17.6 min for (R)-enantiomer (minor). (er = 97:3).



Peak #	RetTime [min]	Type	Width [min]	Area [mAU*s]	Height [mAU]	Area %
1	14.106	BB	0.4964	1.02545e4	311.25766	50.1001
2	17.310	BB	0.5847	1.02135e4	266.74704	49.8999



Peak #	RetTime [min]	Type	Width [min]	Area [mAU*s]	Height [mAU]	Area %
1	14.043	BB	0.5029	2.18370e4	648.45038	96.6104
2	17.671	BB	0.6543	766.14679	17.65303	3.3896



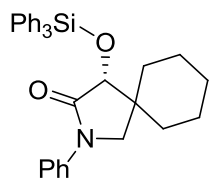
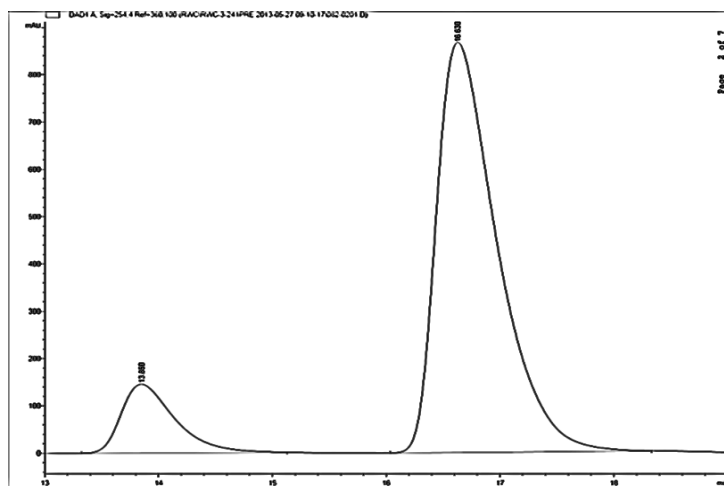


**Table 2.6, Entry 7:** Recovered product: 73 mg, 29 %, white solid. **mp range** = 54-56 °C.

**<sup>1</sup>H NMR** (400 MHz, CDCl<sub>3</sub>) δ ppm 7.77 (d, *J* = 8.7 Hz, 6 H), 7.60 (d, *J* = 6.5 Hz, 3 H), 7.45-7.33 (m, 10 H), 7.13 (t, *J* = 7.0 Hz, 1 H), 4.16 (s, 1 H), 3.74 (d, *J* = 9.7 Hz, 1 H), 3.30 (d, *J* = 9.7 Hz, 1 H), 1.82-1.14 (m, 10 H). **<sup>13</sup>C NMR** (101 MHz, CDCl<sub>3</sub>) δ ppm 171.8, 139.6, 135.8, 134.0, 130.0, 128.7, 127.8, 124.4, 119.5, 80.3, 53.3, 41.8, 34.3, 27.3, 25.7, 22.9, 22.2. **Optical Rotation** [α]<sub>D</sub><sup>25</sup>: = +53.7 (c = 0.83) CHCl<sub>3</sub>. **IR** (neat, cm<sup>-1</sup>) 3068, 2942, 2854, 1712, 1598, 1498, 1428, 1317, 1185, 1106, 904, 860, 755, 708. **HRMS** (CI) Calculated for (C<sub>33</sub>H<sub>34</sub>NO<sub>2</sub>Si<sup>+</sup>) (M+H): 504.2353 Observed: 504.2332.

The compound was further characterized by X-ray crystallography confirming R absolute configuration. HPLC data is of the desilylated product. The same conditions as the recovered starting materials were utilized. (er = 87:13).



Peak #	RetTime [min]	Type	Width [min]	Area [mAU*s]	Height [mAU]	Area %
1	13.850	BB	0.4934	4752.04883	145.35730	12.9192
2	16.630	BB	0.5631	3.20308e4	866.86401	87.0808

### Kinetic Resolution Data for Table 2.6, Entry 7

#	er SM	er P	% conv	s	s AVG
1	80:20	94:6	40.7	26	<b>24</b>
2	97:3	87:13	55.8	22	

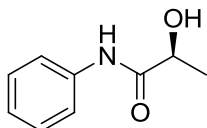
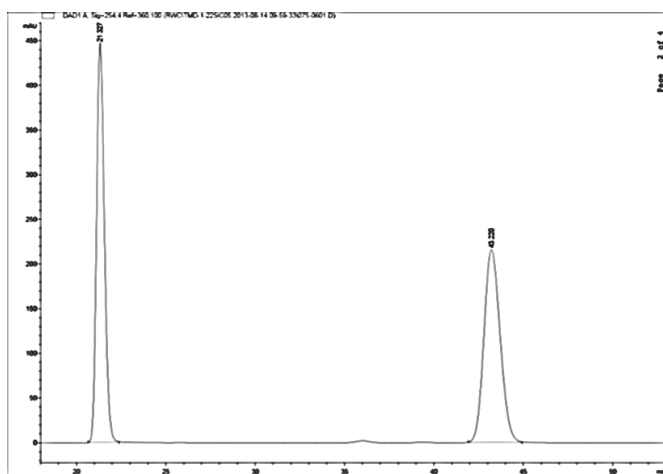
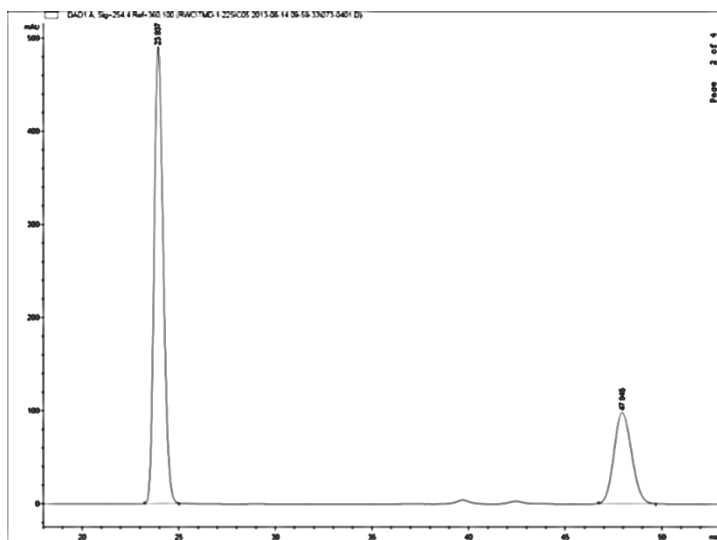


**Table 2.7, Entry 1:** Recovered starting material: 42 mg, 51 %.  $^1\text{H}$  NMR (400 MHz,  $\text{CDCl}_3$ )  $\delta$  ppm 8.53 (br, 1 H), 7.54 (d,  $J = 7.8$  Hz, 2 H), 7.32 (t,  $J = 7.8$  Hz, 2 H), 7.12 (t,  $J = 7.4$  Hz, 1 H), 4.34 (q,  $J = 6.8$  Hz, 1 H), 3.29 (br, 1 H), 1.51 (d,  $J = 6.8$  Hz, 3 H).  $^{13}\text{C}$  NMR (101 MHz,  $\text{CDCl}_3$ )  $\delta$  ppm 172.6, 137.1, 129.0, 124.6, 119.8, 68.8, 21.2. **Optical Rotation**  $[\alpha]_D^{25}$ : -14.2 ( $c = 0.85$ )  $\text{CHCl}_3$ .

Stereochemical assignment made from comparison of optical rotation of the starting material to the literature.<sup>63</sup> Chiralpak IC Column 5% isopropyl alcohol in hexane, flow rate: 1 mL/min, 25 °C;  $t_R$  23.9 min for (S)-enantiomer (major) and 47.9 min for (R)-enantiomer (minor). (er = 72:28).



Peak #	RetTime [min]	Type	Width [min]	Area [mAU*s]	Height [mAU]	Area %
1	21.327	BB	0.4707	1.35362e4	447.70984	49.8879
2	43.220	BB	0.9885	1.35970e4	215.96339	50.1121



Peak #	RetTime [min]	Type	Width [min]	Area [mAU*s]	Height [mAU]	Area %
1	23.937	BB	0.5079	1.60885e4	491.46637	72.0684
2	47.945	BB	1.0005	6235.42627	98.24412	27.9316

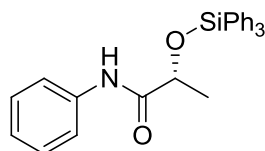
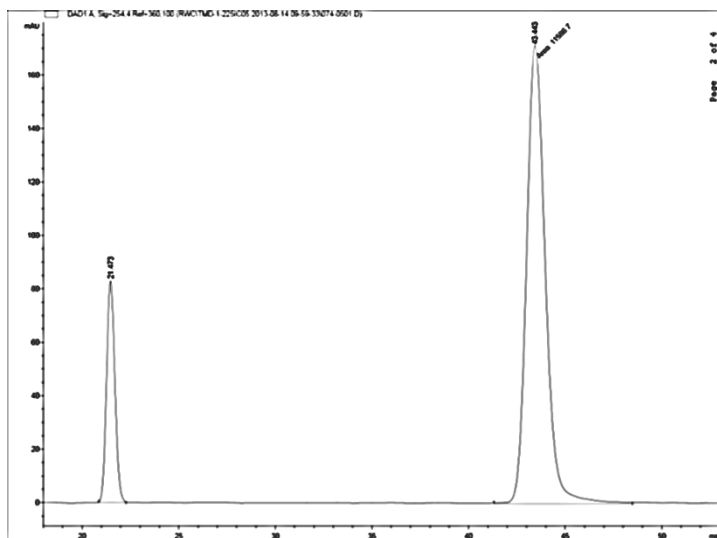


**Table 2.7, Entry 1:** Recovered product: 100 mg, 47% white solid. **mp range** = 94-96 °C.

**<sup>1</sup>H NMR** (400 MHz, CDCl<sub>3</sub>) δ ppm 8.68 (br, 1 H), 7.65-7.63 (m, 6 H), 7.49-7.24 (m, 13 H), 7.10 (t, *J* = 7.4Hz, 1 H), 4.51 (q, *J* = 6.7 Hz, 1 H), 1.46 (d, *J* = 6.7 Hz, 3 H). **<sup>13</sup>C NMR** (101 MHz, CDCl<sub>3</sub>) δ ppm 171.8, 137.3, 135.3, 132.9, 130.6, 129.0, 128.2, 124.3, 119.5, 71.3, 21.7. **Optical Rotation** [ $\alpha$ ]<sub>D</sub><sup>25</sup>: +38.3 (c = 0.95) CHCl<sub>3</sub>. **IR** (neat, cm<sup>-1</sup>) 3381, 3047, 1685, 1599, 1521, 1427, 1114, 911, 757, 712, 692. **HRMS** (ESI) Calculated for (C<sub>27</sub>H<sub>25</sub>NO<sub>2</sub>Si<sup>+</sup>) (M<sup>+</sup>): 423.1649 Observed: 423.1645.

HPLC data is of the desilylated product. The same conditions as the recovered starting materials were utilized. (er = 83:17).



Peak #	RetTime [min]	Type	Width [min]	Area [mAU*s]	Height [mAU]	Area %
1	21.473	BB	0.4645	2480.46484	83.03593	17.6330
2	43.443	MM	1.1247	1.15867e4	171.69344	82.3670

### Kinetic Resolution Data for Table 2.7 Entry 1

#	er SM	er P	% conv	s	s AVG
1	81:19	84:16	47.2	9.9	<b>8.5</b>
2	72:28	82:18	40.5	7.1	

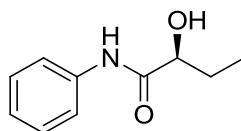
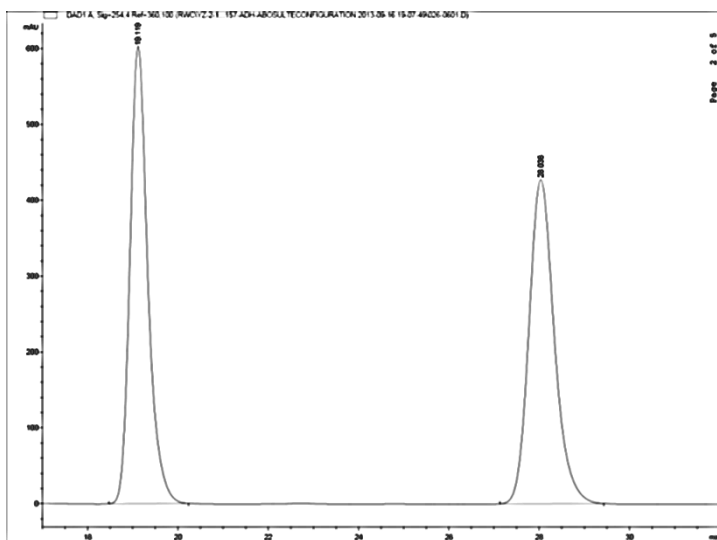


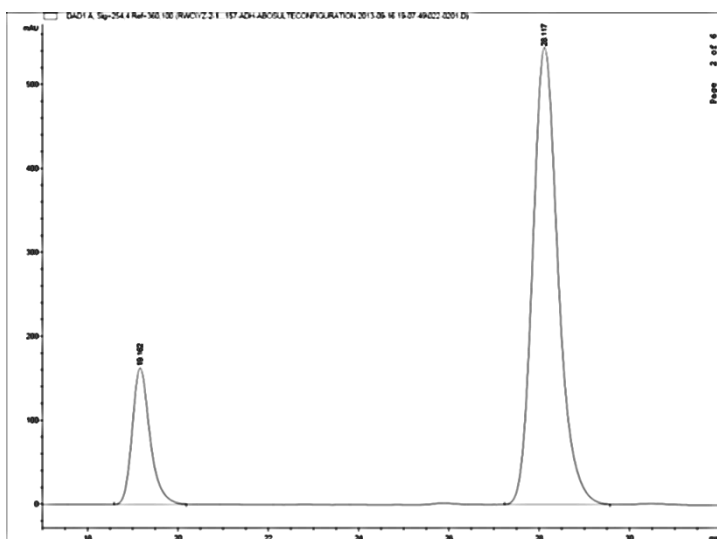
**Table 2.7, Entry 2:** Recovered starting material: 44 mg, 49 %.  $^1\text{H NMR}$  (400 MHz,  $\text{CDCl}_3$ )  $\delta$  ppm 8.37 (br, 1 H), 7.59-7.57 (m, 2 H), 7.36-7.32 (m, 2 H), 7.15-7.11 (m, 1 H), 4.26-4.22 (m, 1 H), 2.49 (br, 1 H), 2.05-1.94 (m, 1 H), 1.81 (dddd,  $J = 14.6, 14.6, 7.3, 7.3$  Hz, 1 H), 1.05 (t,  $J = 7.3$  Hz, 3 H).  $^{13}\text{C NMR}$  (101 MHz,  $\text{CDCl}_3$ )  $\delta$  ppm 171.9, 137.2, 129.0, 124.5, 119.7, 73.6, 27.9, 9.2.

Stereochemical assignment made from comparison of HPLC data in the literature.<sup>64</sup>

Chiralcel AD-H Column 5% isopropyl alcohol in hexane, flow rate: 1 mL/min, 25 °C;  $t_R$  21.5 min for (R)-enantiomer (minor) and 26.0 min for (S)-enantiomer (major). (er = 61:39).



Peak #	RetTime [min]	Type	Width [min]	Area [mAU*s]	Height [mAU]	Area %
1	19.119	BB	0.4168	1.65448e4	603.50372	49.8321
2	28.036	BB	0.5974	1.66563e4	427.66132	50.1679



Peak #	RetTime [min]	Type	Width [min]	Area [mAU*s]	Height [mAU]	Area %
1	19.162	BB	0.4158	4470.45020	163.08342	17.3569
2	28.117	BB	0.5974	2.12856e4	545.36230	82.6431

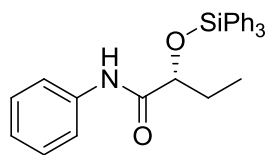
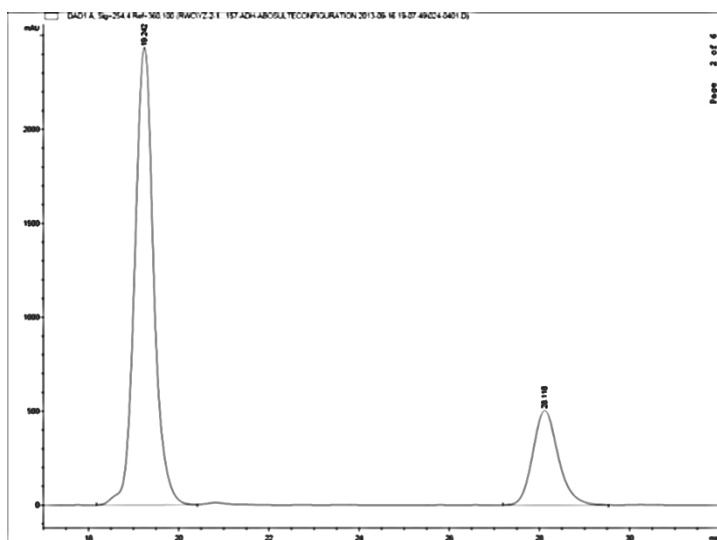


**Table 2.7, Entry 2:** Recovered product: 92 mg, 42 % white solid. **mp range** = 56-59 °C.

**<sup>1</sup>H NMR** (300 MHz, CDCl<sub>3</sub>) δ ppm 8.57 (br, 1 H), 7.65-7.63 (m, 6 H), 7.46-7.25 (m, 13 H), 7.11-7.06 (m, 1 H), 4.49 (m, 1 H), 1.95-1.66 (m, 2 H), 0.95 (t, J = 7.4 Hz, 3 H). **<sup>13</sup>C NMR** (75 MHz, CDCl<sub>3</sub>) δ ppm 171.0, 137.2, 135.4, 132.9, 130.7, 129.0, 128.2, 124.4, 119.6, 75.5, 27.9, 8.3. **Optical Rotation** [α]<sub>D</sub><sup>25</sup>: +40.8 (c = 0.95) CHCl<sub>3</sub>. **IR** (neat, cm<sup>-1</sup>) 3388, 3069, 2969, 1688, 1599, 1520, 1428, 1312, 1115, 1012, 833, 710. **HRMS** (ESI) Calculated for (C<sub>28</sub>H<sub>27</sub>NO<sub>2</sub>Si<sup>+</sup>) (M<sup>+</sup>): 437.1805 Observed: 437.1805.

HPLC data is of the desilylated product. The same conditions as the recovered starting materials were utilized. (er = 78:23).



Peak #	RetTime [min]	Type	Width [min]	Area [mAU*s]	Height [mAU]	Area %
1	19.242	BB	0.4455	7.11708e4	2438.76660	78.2819
2	28.118	BB	0.6003	1.97453e4	503.74457	21.7181

### Kinetic Resolution Data for Table 2.7 Entry 2

#	er SM	er P	% conv	s	s AVG
1	83:17	78:22	53.6	6.9	<b>6.6</b>
2	77:23	79:21	48.5	6.4	

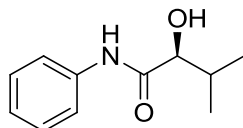
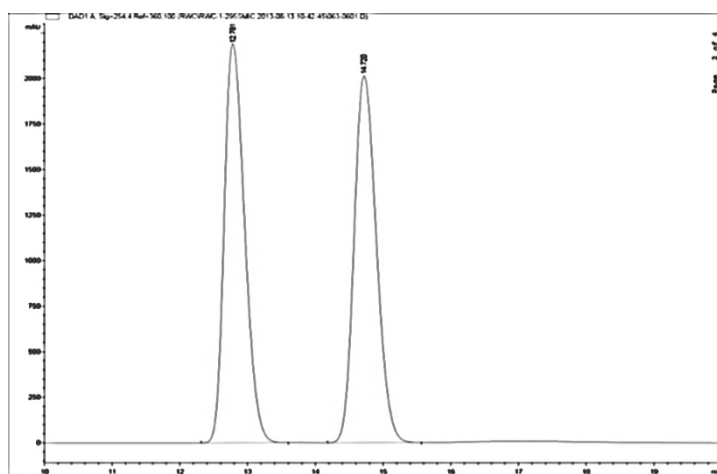
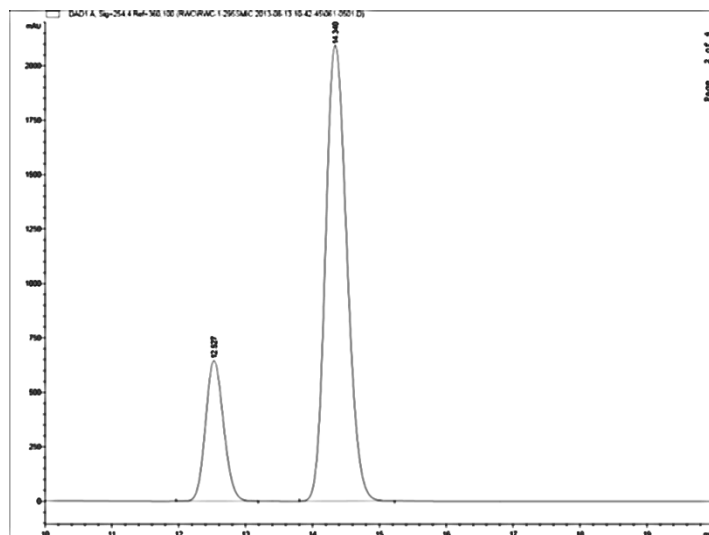


**Table 2.7, Entry 3:** Recovered starting material: 46 mg, 48 %. <sup>1</sup>H NMR (400 MHz, CDCl<sub>3</sub>) δ ppm 8.53 (br, 1 H), 7.55-7.53 (m, 2 H), 7.33-7.31 (m, 2 H), 7.13-7.09 (m, 1 H), 4.08 (d, *J* = 3.2 Hz, 1 H), 3.36 (br, 1 H), 2.27 (dddd, *J* = 20.8, 13.7, 6.9, 3.2 Hz, 1 H), 1.05 (d, *J* = 6.9 Hz, 3 H), 0.90 (d, *J* = 6.9 Hz, 3 H). <sup>13</sup>C NMR (101 MHz, CDCl<sub>3</sub>) δ ppm 171.8, 137.1, 129.0, 124.5, 119.9, 76.6, 31.9, 19.2, 15.5.

Stereochemical assignment made from comparison of optical rotation data for the starting material to the literature.<sup>65</sup> Chiralpak IC Column 5% isopropyl alcohol in hexane, flow rate: 1 mL/min, 25 °C; *t<sub>R</sub>* 12.5 min for (R)-enantiomer (minor) and 14.3 min for (S)-enantiomer (major). (er = 79:21).



Peak #	RetTime [min]	Type	Width [min]	Area [mAU*s]	Height [mAU]	Area %
1	12.781	BB	0.3276	4.57784e4	2192.24414	49.8631
2	14.720	BB	0.3564	4.60297e4	2015.84790	50.1369



Peak #	RetTime [min]	Type	Width [min]	Area [mAU*s]	Height [mAU]	Area %
1	12.527	BB	0.2926	1.21179e4	646.79492	20.6872
2	14.340	BB	0.3467	4.64589e4	2095.53931	79.3128

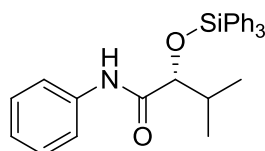
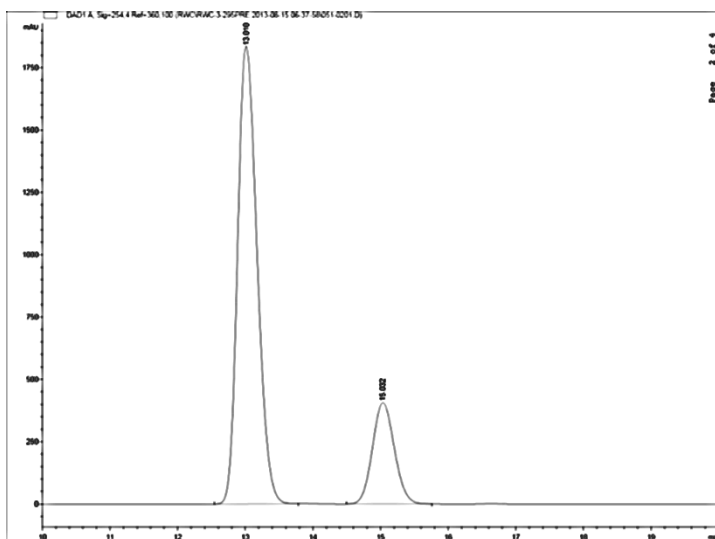


**Table 2.7, Entry 3:** Recovered product: 100 mg, 44 % white solid. **mp range** = 45-48 °C. **<sup>1</sup>H NMR** (400 MHz, CDCl<sub>3</sub>) δ ppm 8.38 (br, 1 H), 7.66-7.62 (m, 6 H), 7.47-7.35 (m, 9 H), 7.28-7.22 (m, 4 H), 7.09-7.05 (m, 1 H), 4.31 (d, *J* = 3.0 Hz, 1 H), 2.19 (dddd, *J* = 13.9, 6.9, 6.9, 3.0 Hz, 1 H), 1.00 (d, *J* = 6.9 Hz, 3 H), 0.94 (d, *J* = 6.9 Hz, 3 H). **<sup>13</sup>C NMR** (101 MHz, CDCl<sub>3</sub>) δ ppm 170.6, 137.0, 135.5, 132.9, 130.6, 128.8, 128.2, 124.3, 119.6, 79.5, 33.3, 18.8, 16.7. **Optical Rotation** [ $\alpha$ ]<sub>D</sub><sup>25</sup>: +67.2 (c = 0.87) CHCl<sub>3</sub>. **IR** (neat, cm<sup>-1</sup>) 3393, 2963, 1670, 1600, 1521, 1440, 1115, 1049, 871, 740, 709, 691. **HRMS** (ESI) Calculated for (C<sub>29</sub>H<sub>29</sub>NO<sub>2</sub>Si<sup>+</sup>) (M<sup>+</sup>): 451.1962 Observed: 451.1963.

HPLC data is of the desilylated product. The same conditions as the recovered starting materials were utilized. (er = 80:20).





Peak #	RetTime [min]	Type	Width [min]	Area [mAU*s]	Height [mAU]	Area %
1	13.010	BB	0.3106	3.66146e4	1836.63074	80.0255
2	15.032	BB	0.3504	9139.08691	406.35092	19.9745

### Kinetic Resolution Data for Table 2.7 Entry 3

#	er SM	er P	% conv	s	s AVG
1	79:21	80:20	49.4	7.1	<b>7.3</b>
2	78:22	81:19	47.2	7.5	

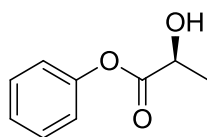
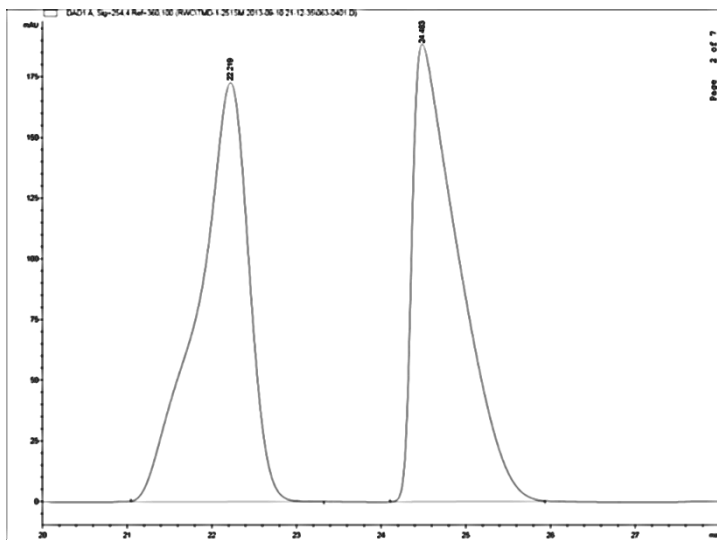
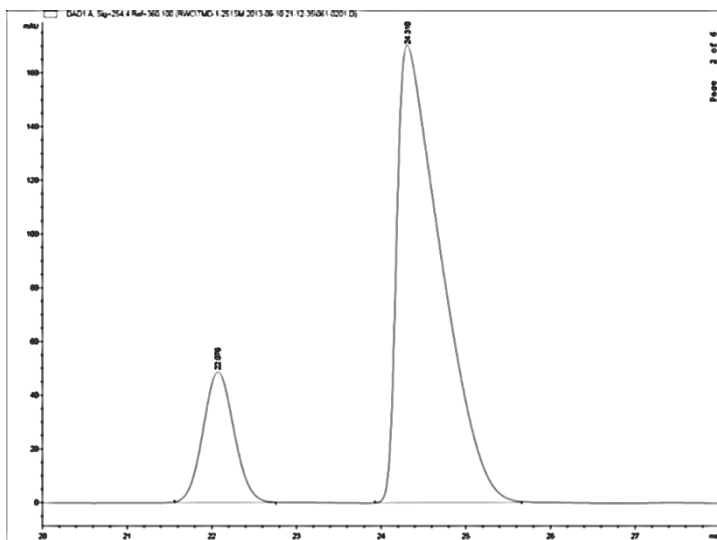


**Table 2.7, Entry 4:** Recovered starting material: 14 mg, 28 %.  $^1\text{H}$  NMR (400 MHz,  $\text{CDCl}_3$ )  $\delta$  ppm 7.42-7.37 (m, 2 H), 7.28-7.24 (m, 1 H), 7.12-7.09 (m, 2 H), 4.54-4.50 (m, 1 H), 2.90 (br, 1 H), 1.60 (d,  $J = 6.9$  Hz, 3 H).  $^{13}\text{C}$  NMR (101 MHz,  $\text{CDCl}_3$ )  $\delta$  ppm 174.3, 150.3, 129.6, 126.3, 121.2, 66.9, 20.4. **Optical Rotation**  $[\alpha]_{\text{D}}^{25}$ : +4.7 (c = 0.90)  $\text{CHCl}_3$ .

Stereochemical assignment of the starting material made by analogy to 2-hydroxy-N-phenylpropanamide. (Table 4, Entry 1) Chiralpak IC Column 7% isopropyl alcohol in hexane, flow rate: 1 mL/min, 25 °C;  $t_R$  22.1 min for (R)-enantiomer (minor) and 24.3 min for (S)-enantiomer (major). (er = 83:17).



Peak #	RetTime [min]	Type	Width [min]	Area [mAU*s]	Height [mAU]	Area %
1	22.219	BB	0.5951	7182.16846	172.74858	49.9955
2	24.483	BB	0.5423	7183.47021	188.62582	50.0045



Peak #	RetTime [min]	Type	Width [min]	Area [mAU*s]	Height [mAU]	Area %
1	22.076	BB	0.3953	1241.80798	48.73894	16.7663
2	24.310	BB	0.5320	6164.78467	170.44815	83.2337

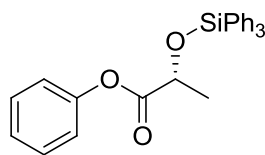
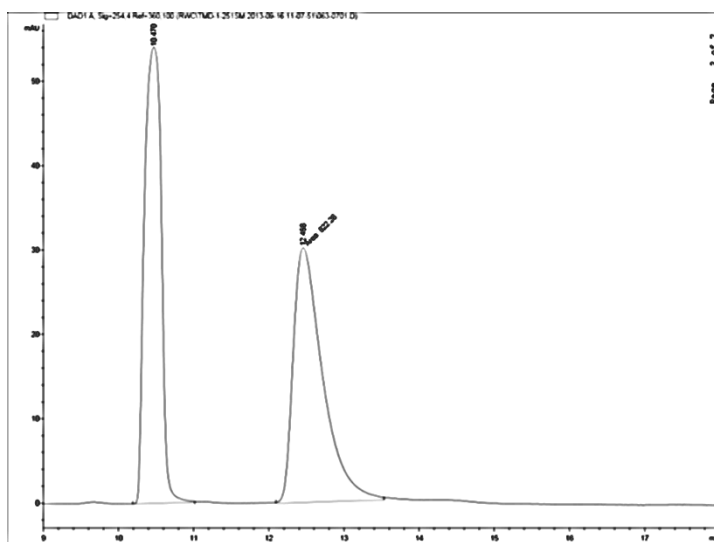
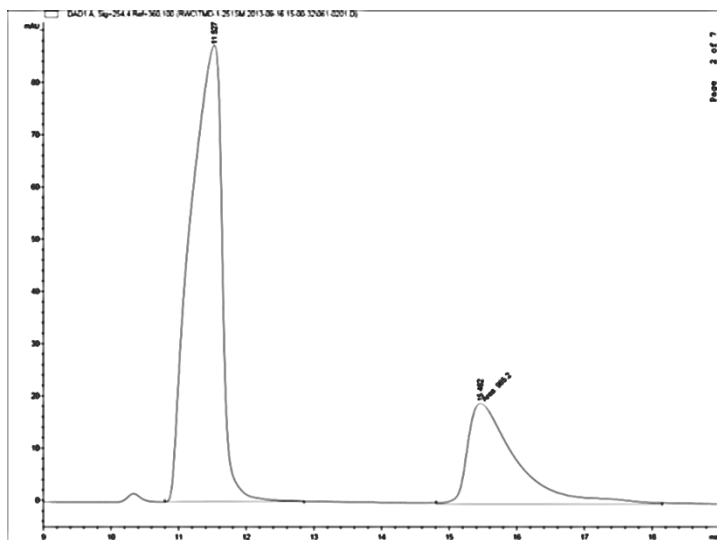


**Table 2.7, Entry 4:** Recovered product: 45 mg, 35 % colorless oil.  $^1\text{H NMR}$  (400 MHz,  $\text{CDCl}_3$ )  $\delta$  ppm 7.71-7.69 (m, 6 H), 7.48-7.38 (m, 9 H), 7.33-7.29 (m, 2 H), 7.21-7.17 (m, 1 H), 6.8 (d,  $J = 7.7$  Hz, 2 H), 4.69 (q,  $J = 6.8$  Hz, 1 H), 1.63 (d,  $J = 6.8$  Hz, 3 H).  $^{13}\text{C NMR}$  (101 MHz,  $\text{CDCl}_3$ )  $\delta$  ppm 172.1, 150.4, 135.6, 133.6, 130.2, 129.3, 127.9, 125.8, 121.3, 68.9, 21.3. **Optical Rotation**  $[\alpha]_{\text{D}}^{25}$ : +13.7 ( $c = 0.80$ )  $\text{CHCl}_3$ . **IR** (neat,  $\text{cm}^{-1}$ ) 3069, 3000, 1774, 1590, 1492, 1428, 1194, 1114, 974, 738, 710. **HRMS** (ESI) Calculated for  $(\text{C}_{21}\text{H}_{19}\text{O}_3\text{Si}^+)$  (M-Ph $^+$ ): 347.1097 Observed: 347.1091.

HPLC data is of the triphenylsilyl-protected products. Chialcel OD-H column 1% isopropyl alcohol in hexane, flow rate: 1 mL/min, 25 °C;  $t_{\text{R}}$  11.5 min for (R)-enantiomer (major) and 15 min for (S)-enantiomer (minor). (er = 75:25).



Peak #	RetTime [min]	Type	Width [min]	Area [mAU*s]	Height [mAU]	Area %
1	10.470	BB	0.2629	838.59637	54.08620	50.4912
2	12.458	MM	0.4536	822.28033	30.21317	49.5088



Peak #	RetTime [min]	Type	Width [min]	Area [mAU*s]	Height [mAU]	Area %
1	11.527	BB	0.5757	2821.60254	87.39584	74.5115
2	15.462	MM	0.8331	965.20007	19.31045	25.4885

#### Kinetic Resolution Data for Table 2.7 Entry 4

#	er SM	er P	% conv	s	s AVG
1	83:17	75:25	57.5	5.6	<b>3.9</b>
2	69:31	61:39	63.9	2.2	

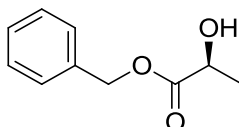
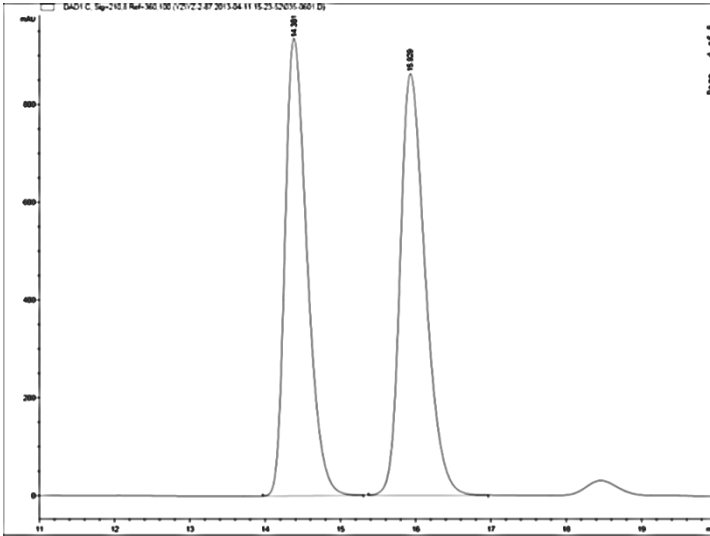


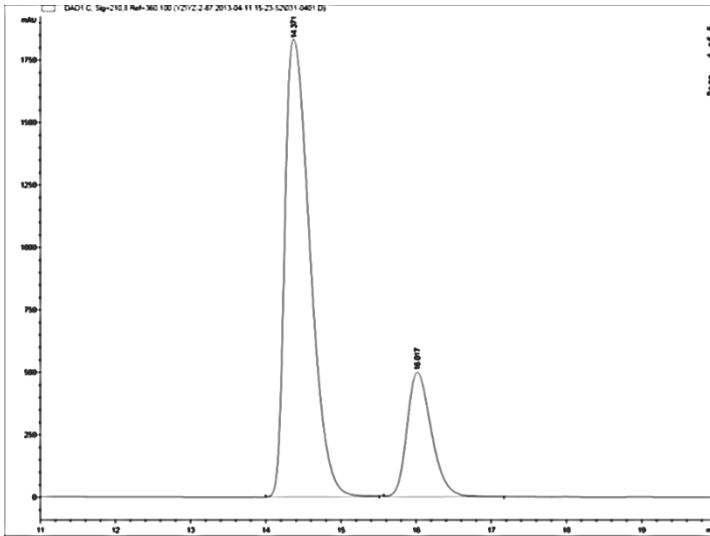
**Table 2.7, Entry 5:** Recovered starting material: 28 mg, 32 %.  $^1\text{H NMR}$  (400 MHz,  $\text{CDCl}_3$ )  $\delta$  ppm 7.40-7.33 (m, 5 H), 5.22 (s, 2 H), 4.32 (q,  $J = 6.8$  Hz, 1 H), 2.89 (br, 1 H), 1.43 (d,  $J = 6.8$  Hz, 3 H).  $^{13}\text{C NMR}$  (101 MHz,  $\text{CDCl}_3$ )  $\delta$  ppm 175.5, 135.2, 128.6, 128.2, 128.1, 67.3, 66.7, 20.4. **Optical Rotation**  $[\alpha]_D^{25}$ : +4.7 (c = 0.90)  $\text{CHCl}_3$ .

Stereochemical assignment made by analogy to 2-hydroxy-N-phenylpropanamide. (Table 4, Entry 1) Chiralcel OD-H Column 4% isopropyl alcohol in hexane, flow rate: 1

mL/min, 25 °C;  $t_R$  14.4 min for (S)-enantiomer (major) and 16.0 min for (S)-enantiomer (minor). (er = 79:21).



Peak #	RetTime [min]	Type	Width [min]	Area [mAU*s]	Height [mAU]	Area %
1	14.381	BB	0.3136	1.90670e4	936.06421	48.7755
2	15.929	BB	0.3547	2.00243e4	862.98395	51.2245



Peak #	RetTime [min]	Type	Width [min]	Area [mAU*s]	Height [mAU]	Area %
1	14.371	BB	0.3646	4.25237e4	1833.64392	79.0408
2	16.017	BB	0.3473	1.12760e4	499.70148	20.9592

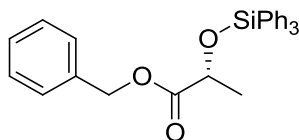
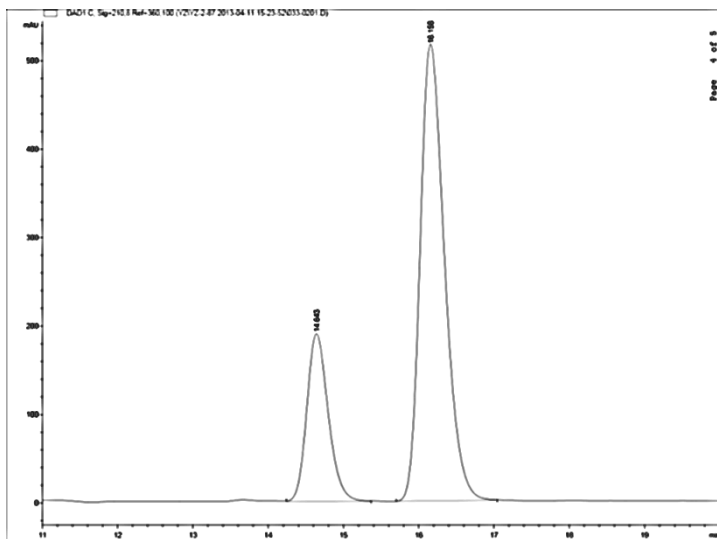


**Table 2.7, Entry 5:** Recovered product: 51 mg, 23 % colorless oil.  $^1\text{H NMR}$  (300 MHz,  $\text{CDCl}_3$ )  $\delta$  ppm 7.64-7.62 (m, 6 H), 7.42-7.23 (m, 14 H), 4.97 (s, 2 H), 4.49 (q,  $J = 6.7$  Hz, 1 H), 1.46 (d,  $J = 6.7$  Hz, 3 H).  $^{13}\text{C NMR}$  (75 MHz,  $\text{CDCl}_3$ )  $\delta$  ppm 173.3, 135.5, 133.7, 130.1, 128.5, 128.3, 128.2, 128.2, 127.9, 69.0, 66.5, 21.2. **Optical Rotation**  $[\alpha]_{\text{D}}^{25}$ : +15.0 ( $c = 0.85$ )  $\text{CHCl}_3$ . **IR** (neat,  $\text{cm}^{-1}$ ) 3429, 2956, 1721, 1443, 1429, 1178, 1033, 988, 918, 853, 710. **HRMS** (ESI) Calculated for  $(\text{C}_{22}\text{H}_{21}\text{O}_3\text{Si}^+)$  (M-Ph $^+$ ): 361.1254 Observed: 361.1248.

HPLC data is of the desilylated product. The same conditions as the recovered starting materials were utilized. (er = 76:24).



Peak #	RetTime [min]	Type	Width [min]	Area [mAU*s]	Height [mAU]	Area %
1	14.643	BB	0.3047	3751.95410	189.70892	24.4029
2	16.158	BB	0.3464	1.16231e4	516.72723	75.5971

### Kinetic Resolution Data for Table 2.7 Entry 5

#	er SM	er P	% conv	<i>s</i>	<i>s</i> AVG
1	79:21	76:24	53.1	5.4	<b>5.6</b>
2	73:27	78:22	45.2	5.7	

## 2.11. References

1. Sheppard, C. I.; Taylor, J. L.; Wiskur, S. L. Silylation-Based Kinetic Resolution of Monofunctional Secondary Alcohols. *Org. Lett.* **2011**, *13*, 3794.
2. Nishiyama, H. In *Comp. Asymm. Catal.* **1999**, *1*, 267.
3. Riant, O.; Mostefaï, N.; Courmarcel, J. Recent Advances in the Asymmetric Hydrosilylation of Ketones, Imines and Electrophilic Double Bonds. *Synthesis* **2004**, *2004*, 2943.
4. Arena, C. G. Recent Progress in the Asymmetric Hydrosilylation of Ketones and Imines. *Mini Rev. Org. Chem.* **2009**, *6*, 159.
5. Kagan, H. B.; Fiaud, J. C., In *Topics in Stereochemistry*, L., E.; Wilen, S. H., Eds. John Wiley and Sons: 1988; pp 249.
6. Keith, J. M.; Larrow, J. F.; Jacobsen, E. N. Practical Considerations in Kinetic Resolution Reactions. *Adv. Synth. Catal.* **2001**, *343*, 5.
7. Vedejs, E.; Jure, M. Efficiency in Nonenzymatic Kinetic Resolution. *Angew. Chem., Int. Ed.* **2005**, *44*, 3974.
8. Rendler, S.; Oestreich, M. Kinetic Resolution and Desymmetrization by Stereoselective Silylation of Alcohols. *Angew. Chem. Int. Ed.* **2008**, *47*, 248.
9. Weickgenannt, A.; Mewald, M.; Oestreich, M. Asymmetric Si-O Coupling of Alcohols. *Org. Biomol. Chem.* **2010**, *8*, 1497.
10. Greene, T. W.; Wuts, P. G. M., *Protective Groups in Organic Synthesis*. 3 ed.; John Wiley and Sons: New York, USA, 1999.
11. Zhao, Y.; Rodrigo, J.; Hoveyda, A. H.; Snapper, M. L. Enantioselective Silyl Protection of Alcohols Catalysed by an Amino-Acid-Based Small Molecule. *Nature* **2006**, *443*, 67.



12. Zhao, Y.; Mitra, A. W.; Hoveyda, A. H.; Snapper, M. L. Kinetic Resolution of 1,2-Diols Through Highly Site and Enantioselective Catalytic Silylation. *Angew. Chem., Int. Ed.* **2007**, *46*, 8471.
13. Sun, X.; Worthy, A. D.; Tan, K. L. Scaffolding Catalysts: Highly Enantioselective Desymmetrization Reactions. *Angew. Chem., Int. Ed.* **2011**, *50*, 8167.
14. You, Z.; Hoveyda, A. H.; Snapper, M. L. Catalytic Enantioselective Silylation of Acyclic and Cyclic Triols: Application to Total Syntheses of Cleroindicans D, F, and C. *Angew. Chem., Int. Ed.* **2009**, *48*, 547.
15. Rendler, S.; Auer, G.; Oestreich, M. Kinetic Resolution of Chiral Secondary Alcohols by Dehydrogenative Coupling with Recyclable Silicon-Stereogenic Silanes. *Angew. Chem., Int. Ed.* **2005**, *44*, 7620.
16. Klare, H. F. T.; Oestreich, M. Chiral Recognition with Silicon-Stereogenic Silanes: Remarkable Selectivity Factors in the Kinetic Resolution of Donor-Functionalized Alcohols. *Angew. Chem., Int. Ed.* **2007**, *46*, 9335.
17. Rendler, S.; Fröhlich, R.; Keller, M.; Oestreich, M. Enantio- and Diastereotopos Differentiation in the Palladium(II)-Catalyzed Hydrosilylation of Bicyclo[2.2.1]alkene Scaffolds with Silicon-Stereogenic Silanes. *Eur. J. Org. Chem.* **2008**, *2008*, 2582.
18. Weickgenannt, A.; Mewald, M.; Muesmann, T. W. T.; Oestreich, M. Catalytic Asymmetric Si-O Coupling of Simple Achiral Silanes and Chiral Donor-Functionalized Alcohols. *Angew. Chem., Int. Ed.* **2010**, *49*, 2223.
19. Isobe, T.; Fukuda, K.; Araki, Y.; Ishikawa, T. Modified Guanidines as Chiral Superbases: the First Example of Asymmetric Silylation of Secondary Alcohols. *Chem. Commun.* **2001**, 243.
20. Patel, S. G.; Wiskur, S. L. Mechanistic Investigations of the Mukaiyama Aldol Reaction as a Two Part Enantioselective Reaction. *Tetrahedron Lett.* **2009**, *50*, 1164.
21. Denmark, S. E.; Beutner, G. L. Lewis Base Catalysis in Organic Synthesis. *Angew. Chem., Int. Ed.* **2008**, *47*, 1560.

22. Winterbottom, R.; Clapp, J. W.; Miller, W. H.; English, J. P.; Roblin, R. O. Studies in Chemotherapy; Amides of Pantoyltaurine. *J. Am. Chem. Soc.* **1947**, *69*, 1393.
23. King, T. E.; Stewart, C. J.; Cheldelin, V. H.  $\beta$ -Aletheine and Pantetheine. *J. Am. Chem. Soc.* **1953**, *75*, 1290.
24. Dolle, R. E.; Nicolaou, K. C. Total Synthesis of Elfamycins: Aurodox and Efrotomycin. 1. Strategy and Construction of Key Intermediates. *J. Am. Chem. Soc.* **1985**, *107*, 1691.
25. Fischer, G. C.; Turakhia, R. H.; Morrow, C. J. Irreducible Analogs of Mevaldic Acid Coenzyme A Hemithioacetal as Potential Inhibitors of HMG-CoA Reductase. Synthesis of a Carbon-Sulfur Interchanged Analog of Mevaldic Acid Pantetheine Hemithioacetal. *J. Org. Chem.* **1985**, *50*, 2011.
26. Grieco, P. A.; Henry, K. J.; Nunes, J. J.; Matt, J. E. Total Synthesis of Sesbanimide A and B. *Chem. Commun.* **1992**, 368.
27. Camps, P.; Munoz-Terrero, D. Synthesis and Applications of (R)- and (S)-Pantolactone as Chiral Auxiliaries. *Curr. Org. Chem.* **2004**, *8*, 1339.
28. Ojima, I.; Kogure, T.; Terasaki, T.; Achiwa, K. Effective Biomimetic Route to D-(+)-Pantothenate Using Asymmetric Hydrogenation Catalyzed by a Chiral Rhodium Complex in the Key Step. *J. Org. Chem.* **1978**, *43*, 3444.
29. Pansare, S. V.; Jain, R. P. Enantioselective Synthesis of (S)-(+)-Pantolactone. *Org. Lett.* **2000**, *2*, 175.
30. Ptzl, M.; Pritz, S.; Liebscher, J. In *The Science of Synthesis* **2005**, *21*, 487.
31. Camps, P.; Giménez, S.; Font-Bardia, M.; Solans, X. (R)- and (S)-3-Hydroxy-4,4-Dimethyl-1-Phenyl-2-Pyrrolidinone by Lipase-Catalyzed Resolution of the Racemic Mixture: New Chiral Auxiliaries Related to Pantolactone. *Tetrahedron: Asymmetry* **1995**, *6*, 985.
32. Baumann, M.; Hauer, B. H.; Bornscheuer, U. T. Rapid Screening of Hydrolases for the Enantioselective Conversion of 'Difficult-to-Resolve' Substrates. *Tetrahedron: Asymmetry* **2000**, *11*, 4781.

33. Kurono, N.; Kondo, T.; Wakabayashi, M.; Ooka, H.; Inoue, T.; Tachikawa, H.; Ohkuma, T. Enantiomer-Selective Carbamoylation of Racemic Alpha-Hydroxy Gamma-Lactones with Chiral Cu(II) Catalysts: an Example of a Highly Active Lewis Acid Catalyzed Reaction. *Chem. Asian J.* **2008**, *3*, 1289.
34. Nakata, K.; Gotoh, K.; Ono, K.; Futami, K.; Shiina, I. Kinetic Resolution of Racemic 2-Hydroxy-Gamma-Butyrolactones by Asymmetric Esterification Using Diphenylacetic Acid with Pivalic Anhydride and a Chiral Acyl-Transfer Catalyst. *Org. Lett.* **2013**, *15*, 1170.
35. Birman, V. B.; Li, X. Benzotetramisole: a Remarkably Enantioselective Acyl Transfer Catalyst. *Org. Lett.* **2006**, *8*, 1351.
36. Birman, V. B.; Guo, L. Kinetic Resolution of Propargylic Alcohols Catalyzed by Benzotetramisole. *Org. Lett.* **2006**, *8*, 4859.
37. Yang, X.; Lu, G.; Birman, V. B. Benzotetramisole-Catalyzed Dynamic Kinetic Resolution of Azlactones. *Org. Lett.* **2010**, *12*, 892.
38. Clark, R. W.; Deaton, T. M.; Zhang, Y.; Moore, M. I.; Wiskur, S. L. Silylation-Based Kinetic Resolution of  $\alpha$ -Hydroxy Lactones and Lactams. *Org. Lett.* **2013**, *15*, 6132.
39. Selectivity factor ( $s$ ) = (rate of the fast reacting enantiomer)/(rate of slow reacting enantiomer).
40. Birman, V. B.; Li, X. Homobenzotetramisole: an Effective Catalyst for Kinetic Resolution of Aryl-Cycloalkanols. *Org. Lett.* **2008**, *10*, 1115.
41. (a) Conversions and selectivity factors are based on the ee of the recovered starting materials and products. (b) Selectivity factors are an average of two runs. Conversions are from a single run.
42. Hata, H.; Morishita, T.; Akutsu, S.; Kawamura, M. Synthesis of Dihydro-2,3-Furandiones from Diethyl Oxalate and Aldehydes Through the Action of Sodium Methoxide. *Synthesis* **1991**, *1991*, 289.

43. Davis, F. A.; Sheppard, A. C. Applications of Oxaziridines in Organic Synthesis. *Tetrahedron* **1989**, *45*, 5703.
44. Hassner, A.; Reuss, R. H.; Pinnick, H. W. Synthetic Methods. VIII. Hydroxylation of Carbonyl Compounds via Silyl Enol Ethers. *J. Org. Chem.* **1975**, *40*, 3427.
45. Savostianoff, D. Preparation of ( $\pm$ )-Hydroxy Lactones by the Action of Glyoxalic Acid on Olefins. *Comptes Rendus* **1966**, *263*, 605.
46. Wang, L.; Akhani, R. K.; Wiskur, S. L. Diastereoselective and Enantioselective Silylation of 2-Arylcyclohexanols. *Org. Lett.* **2015**, *17*, 2408.
47. Barrios, I.; Camps, P.; Comes-Franchini, M.; Muñoz-Torrero, D.; Ricci, A.; Sánchez, L. One-Pot Synthesis of N-Substituted Pantolactams from Pantolactone. *Tetrahedron* **2003**, *59*, 1971.
48. Vedejs, E.; Engler, D. A.; Telschow, J. E. Transition-Metal Peroxide Reactions. Synthesis of Alpha-Hydroxycarbonyl Compounds from Enolates. *J. Org. Chem.* **1978**, *43*, 188.
49. Manhas, M. S.; Jeng, S.; Bose, A. K. Studies on Lactams—VIII. *Tetrahedron* **1968**, *24*, 1237.
50. Gautrot, J. E.; Hodge, P.; Cupertino, D.; Helliwell, M. Experimental Evidence for Carbonyl-Electron Cloud Interactions. *New J. Chem.* **2006**, *30*, 1801.
51. Anslyn, E. V.; Dougherty, D. A., *Modern Physical Organic Chemistry*. University Science Books: Sausalito, Ca, 2006.
52. Akhani, R. K.; Moore, M. I.; Pribyl, J. G.; Wiskur, S. L. Linear Free-Energy Relationship and Rate Study on a Silylation-Based Kinetic Resolution: Mechanistic Insights. *J. Org. Chem.* **2014**, *79*, 2384.
53. Denny, G. H.; Zambito, A. J.; Babson, R. D. Phenyl Ester of Lactic Acid. *J. Med. Chem.* **1968**, *11*, 403.
54. Lubineau, A.; Augé, J.; Grand, E.; Lubin, N. Aqueous Hetero Diels-Alder Reactions: The Carbonyl Case. *Tetrahedron* **1994**, *50*, 10265.

55. Szabo, A.; Künzle, N.; Mallat, T.; Baiker, A. Enantioselective Hydrogenation of Pyrrolidine-2,3,5-Triones Over the Pt–Cinchonidine System. *Tetrahedron: Asymmetry* **1999**, *10*, 61.
56. Little, R. D.; Muller, G. W.; Venegas, M. G.; Carroll, G. L.; Bukhari, A.; Patton, L.; Stone, K. *Tetrahedron* **1981**, *37*, 4371.
57. García Ruano, J. L.; Alemán, J.; Fajardo, C.; Parra, A. A New General Method for the Preparation of N-Sulfonyloxaziridines. *Org. Lett.* **2005**, *7*, 5493.
58. Gharpure, S. J.; Shukla, M. K.; Vijayasree, U. Stereoselective Synthesis of Donor-Acceptor Substituted Cyclopropafuranones by Intramolecular Cyclopropanation of Vinylogous Carbonates: Divergent Synthesis of Tetrahydrofuran-3-one, Tetrahydropyran-3-one, and Lactones. *Org. Lett.* **2009**, *11*, 5466.
59. Shiina, I.; Shibata, J.; Ibuka, R.; Imai, Y.; Mukaiyama, T. An Effective Method for the Preparation of Chiral Polyoxy 8-Membered Ring Enone Corresponding to the B Ring of Taxol. *Bull. Chem. Soc. Jpn.* **2001**, *74*, 113.
60. White, J. D.; Hrcniar, P. Synthesis of Polyhydroxylated Pyrrolizidine Alkaloids of the Alexine Family by Tandem Ring-Closing Metathesis–Transannular Cyclization. (+)-Australine. *J. Org. Chem.* **2000**, *65*, 9129.
61. Shinkre, B. A.; Deshmukh, A. R. A. S. The Synthesis of (*S*)-(+)-Pantolactone and its Analogues from an Ephedrine-Derived Morpholinone. *Tetrahedron: Asymmetry* **2004**, *15*, 1081.
62. Pansare, S. V.; Bhattacharyya, A. Enantioselective Synthesis of Pantolactone Analogues from an Ephedrine-Derived Morpholine-Dione. *Tetrahedron* **2003**, *59*, 3275.
63. Westerbeek, A.; Szymański, W.; Wijma, H. J.; Marrink, S. J.; Feringa, B. L.; Janssen, D. B. Kinetic Resolution of  $\alpha$ -Bromoamides: Experimental and Theoretical Investigation of Highly Enantioselective Reactions Catalyzed by Haloalkane Dehalogenases. *Adv. Synth. Catal.* **2011**, *353*, 931.

64. Westerbeek, A.; Szymański, W.; Feringa, B. L.; Janssen, D. B. Dynamic Kinetic Resolution Process Employing Haloalkane Dehalogenase. *ACS Catalysis* **2011**, *1*, 1654.
65. Girreser, U.; Noe, C. R. Synthesis of Enantiopure (*S*)- $\alpha$ -Hydroxy Carboxanilides from (*S*)- $\alpha$ -Amino Acids. *Synthesis* **1995**, *1995*, 1223.

## Chapter 3 Polymer-Bound Triphenylsilyl Chloride for the Kinetic Resolution of Secondary Alcohols

### 3.1 Introduction and Scope

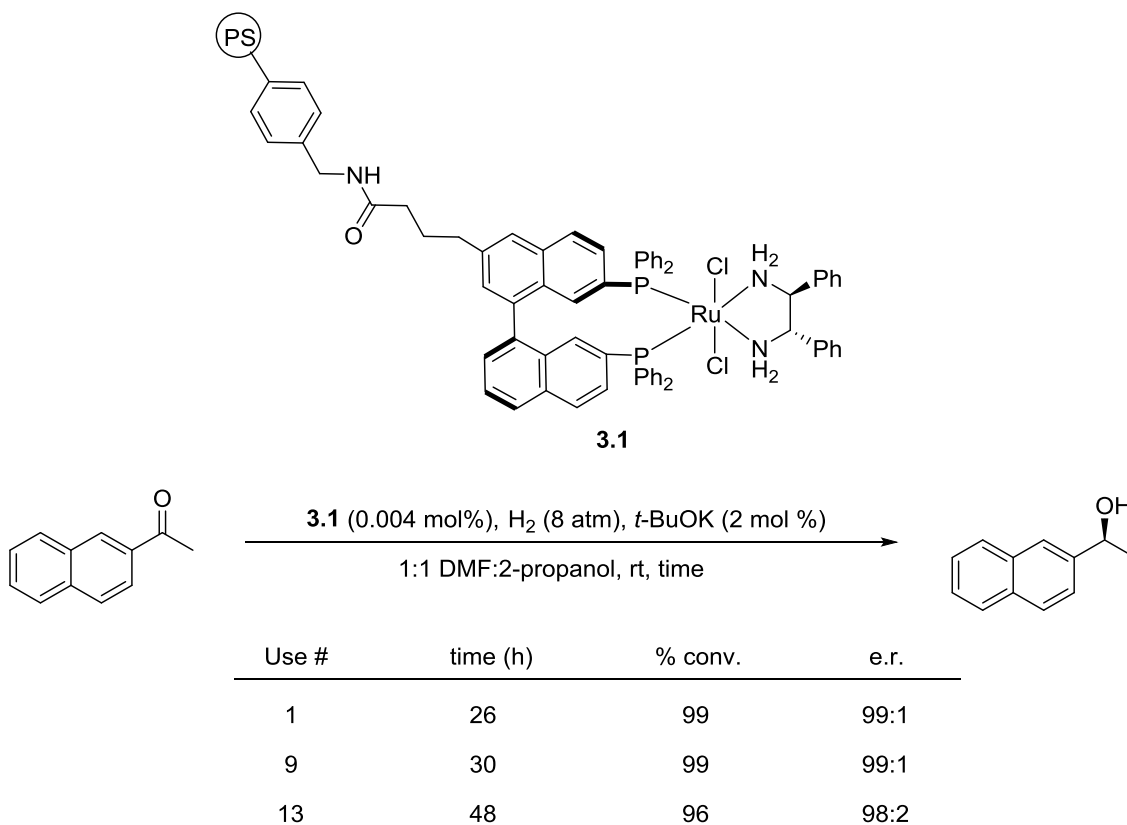
In Chapter 1, the advantages of kinetic resolutions were highlighted. However, a major drawback to kinetic resolutions is the ultimate separation process of the derivatized enantiomer from the unreacted starting material. This is usually accomplished through laborious column chromatography. This problem is a major hurdle to the use of kinetic resolutions in industrial applications. As a result, chemists have devised several methods to avoid chromatography separations aimed for the separation of unreacted starting materials from the products. Most of these approaches depend upon the ability to recover enantioenriched starting materials or products via precipitation. In this chapter, the employment of polymer-supported silyl chlorides in the silylation-based resolution of secondary alcohols and subsequent avoidance of chromatography will be discussed.

A variety of polymeric supports have been utilized to facilitate purification in several organic transformations in addition to kinetic resolutions and other asymmetric reactions.<sup>1</sup> These approaches depend upon polymer-supported catalysts, reagents, or substrates depending upon the reaction targeted. For asymmetric catalysis from prochiral compounds, a polymer support containing the chiral catalyst is particularly advantageous since these reactions are usually driven to completion. Asymmetric reactions with polymer-bound catalysts can be employed in continuous flow reactions, and<sup>2</sup> assuming

no loss to catalytic activity, the polymer can be recycled indefinitely to produce enantioenriched compounds. Many polymer-supported organocatalysts and metal-organic catalysts are known.<sup>3</sup> The process of affixing a catalyst onto a support is particularly vital when costly transition metal catalysts are needed. These expensive catalysts can be more efficiently reused and are not extracted into an aqueous or organic phases upon work up. For example, a Ruthenium-BINAP complex **3.1** bound to polystyrene produces highly enriched secondary alcohols from ketones via transfer hydrogenation (Table 3.1).<sup>4</sup> The support could be utilized multiple times with only minor loss of catalytic activity, which can be compensated for by extended reaction times. In contrast to many other examples, the enantioselectivity of the reaction was also nearly the same as that reported for the homogeneous reaction conditions. The benzylic alcohol, (*S*)-1-naphthylethanol, was obtained in excellent yield and e.r. (up to 99% conversions and 99:1 e.r.) after up to 13 uses. Note portions of this chapter are published in the following journal article and adapted here with permission from the publisher: Akhani, R.K.; Clark, R.W.; Yuan, L.; Wang, L.; Tang, C.; Wiskur, S.L. *ChemCatChem* **2015**, 7, 1527.

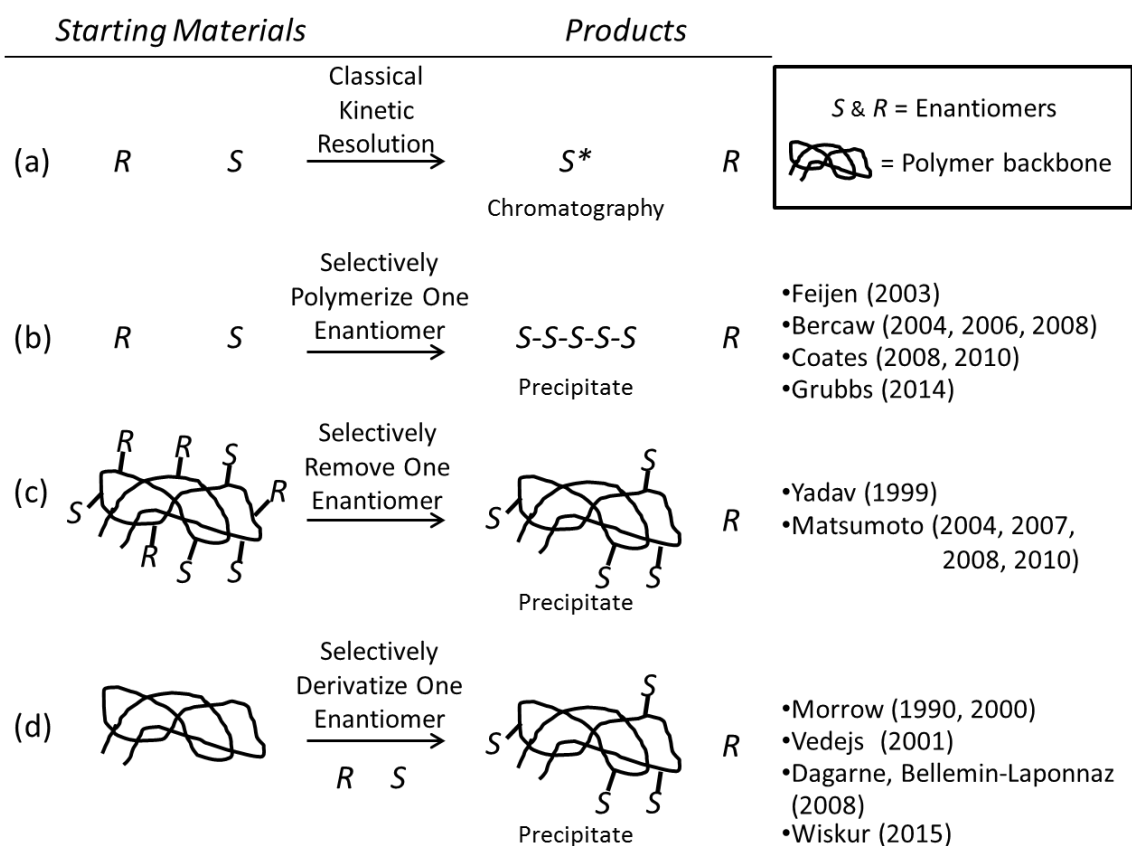


**Table 3.1 Noyori's Polystyrene-Supported Asymmetric Hydrogenation**



Classical kinetic resolutions (Scheme 3.1a) have also been carried out employing polymer supports. As opposed to polymer-bound catalysts discussed above, a kinetic resolution would be more advantageous when the product becomes attached to the polymer. The principle chromatographic step is not the recovery of alcohols but the separation of starting material from product. The polymer-bound products can potentially be easily removed from the solution through precipitation and filtration versus employment of expensive chromatography. Despite research surrounding solid-supported catalysts for asymmetric reactions (Scheme 3.1)<sup>1, 3, 5</sup> relatively little work has been done with polymer supported reagents for the purpose of facilitating purification in kinetic resolutions.

Generally, there are three different approaches for the employment of polymer supports in resolutions. A single enantiomer can be selectively polymerized in presence of a chiral catalyst (Scheme 3.1b).<sup>6-11</sup> An alternate method involves a polymer derivatized with a racemic mixture of substrate.<sup>12-15</sup> In this resolution an enantiomer is selectively removed thus yielding an enantioenriched polymer and a free enantioenriched small molecule in solution (Scheme 3.1c). Finally, a polymer-bound reagent can be utilized to selectively bind an enantiomer to the support.<sup>16-19</sup> In this case precipitation yields the unreacted, enantioenriched starting material without the need for chromatography (Scheme 3.1d). Specific examples of each of these methods will be discussed below.



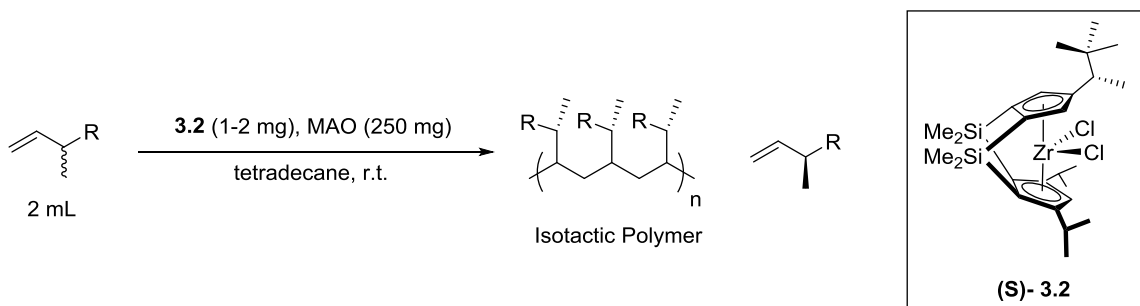
**Scheme 3.1 Approaches to Kinetic Resolutions on Polymer Supports**

### 3.2 Polymerization-Based Kinetic Resolutions

Recently, several polymerization induced kinetic resolutions have been reported providing a method to isolate one enantiomer free in solution. These asymmetric enantiomer-differentiating polymerizations<sup>20</sup> require the use of an enantioenriched initiator and are particularly interesting as they produce enantioenriched, isotactic polymers with substituents on the same side of the polymer backbone. Optically active macromolecules offer several intriguing and useful properties over ordinary polymers such as semi-crystallinity<sup>21</sup> or helical arrangements<sup>6</sup>. Indeed, polypeptides are stereoenriched polymers formed from chiral amino acids. Thus, these approaches may offer the means to synthesize polymers with secondary structures commonly found in proteins.

Generally the viable polymerization-based resolutions are limited to monomers that possess a stereocenter very near to or adjacent to the catalyst during polymerization. One of the earliest successful examples is the Ziegler-Natta polymerization of chiral olefins in the presence of chiral zirconium catalyst **3.2** (Table 3.2).<sup>7-8</sup> The reaction utilized methylaluminoxane (MAO) as the co-catalyst to produce isotactic polymers and enantioenriched olefins. Selectivity factors up to 2.4 were obtained with several racemic alkenes. A pair of diastereomeric olefins was also resolved to an e.e. of 59% and an *s*-factor of 16. Recall from chapter 1 that selectivity factor is the ratio of rates of the fast reacting enantiomer vs the slow reacting enantiomer. This polymerization is notable due to the challenges associated with stereoenrichment of simple alkenes.<sup>22</sup>

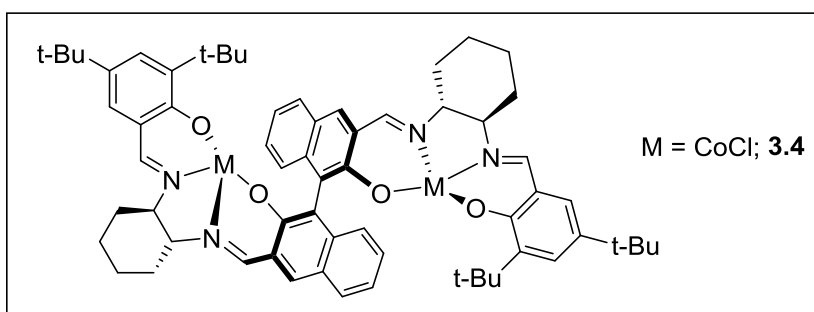
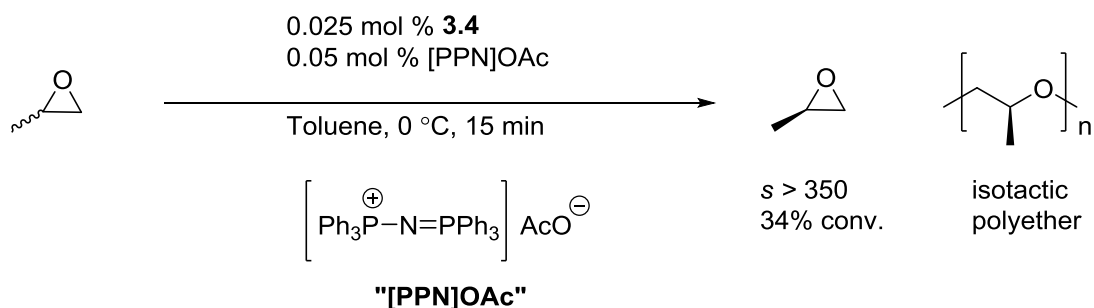
**Table 3.2 Enantioselective Ziegler-Natta Polymerization of Olefins**



Olefin	t (h)	% conv.	% ee	s
	47	38.3	20.3	2.4
	13.5	75	40.0	1.8
	43	56.1	30.3	2.0
	69	42.4	58.6	16

A variety of ring opening polymerizations have also been employed to resolve racemic compounds and generate chiral polymers. Examples of stereoselective ring opening polymerizations of lactones,<sup>23-24</sup> cycloalkenes,<sup>6</sup> and epoxides<sup>25</sup> have been reported. The most well studied of these is the ring-opening polymerization of epoxides. One of the most stereoselective of these reactions is the stereoselective epoxide ring opening utilizing bimetallic cobalt catalyst **3.4** (Scheme 3.2).<sup>9-10, 26</sup> This asymmetric polymerization is similar the asymmetric epoxide hydrolysis developed by Jacobsen.<sup>27</sup> Isotactic polyethers (up to 98.8% isotacticity) are obtained at ambient temperature in minutes using a bis(triphenylphosphine)iminium (PPN) co-catalyst. In addition to the

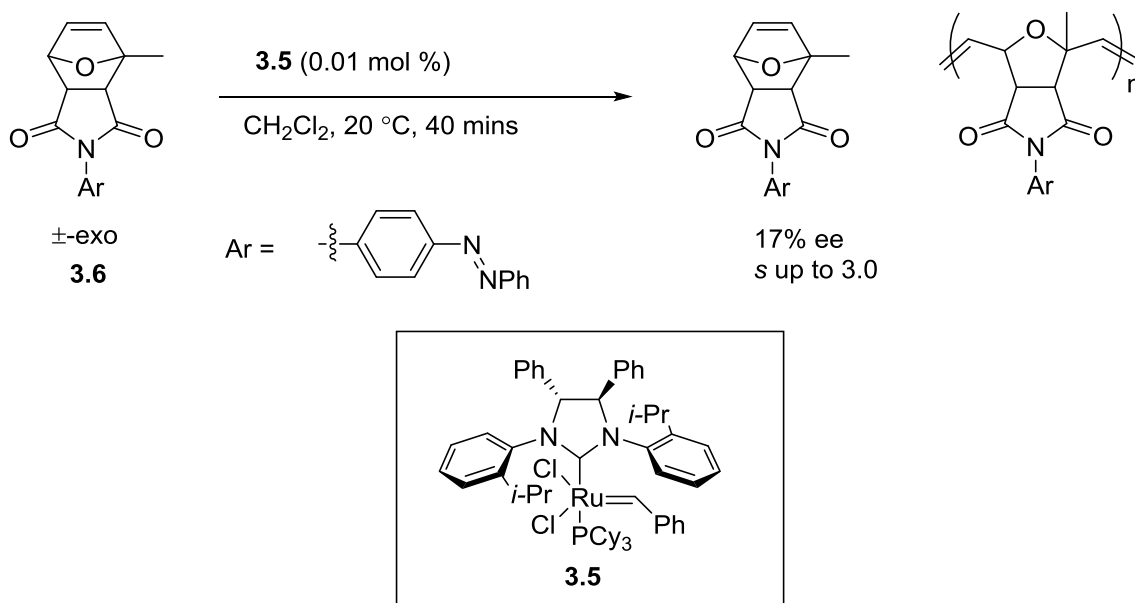
polymer, the unreacted propene oxide is obtained with an ee of 51% and selectivity factor greater than 350.



### Scheme 3.2 Enantioselective Ring-Opening Polymerization of Propene Oxide

These polymerization-based kinetic resolutions have direct application to the production of chiral macromolecules which possess interesting chiroptical properties.<sup>28</sup> Until recently, synthetic approaches to chiral secondary structures common in proteins, for example helices, beta barrels, beta sheets, etc., have been limited. Such chiroptical properties have been observed in polymer products of polymerization-based resolutions. A partial kinetic resolution via ring-opening metathesis polymerization utilizing chiral ruthenium carbene **3.6** was recently reported by Grubbs (Scheme 3.3).<sup>6</sup> The resolution was most selective with a 1-methyloxanorbornene monomer. Selectivity-factors up to 3.0 were obtained and unreacted monomer was obtained with an ee of up to 17%. Interestingly, the polymerization's selectivity was found to be highly solvent dependent.

The *s*-factor also changed with increasing molecular weight which was attributed to induced secondary structure in the growing polymer chain. Monomer **3.6** possessing a visible light absorbing azobenzene functionality was polymerized in order to probe these secondary structures. Interestingly, circular dichroism spectra suggested that a helical arrangement of the polymer forms and can be modified somewhat by varying solvents in the polymerization. This is presumably a result of modifying the selectivity factor by changing the solvent conditions.

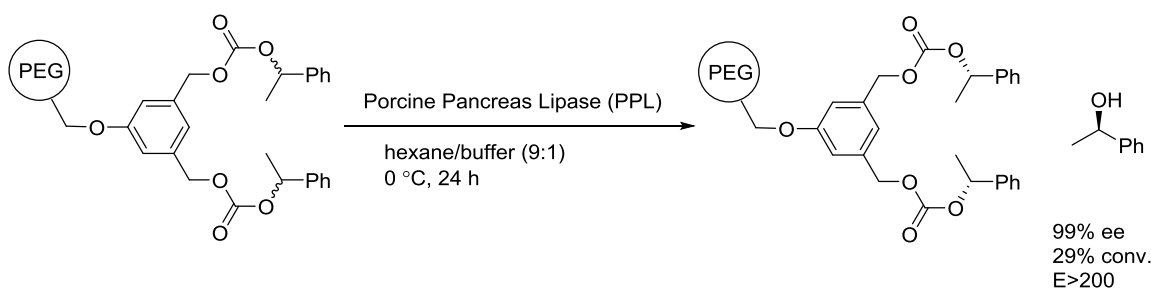


**Scheme 3.3 Kinetic Resolution via Ring Opening Metathesis**

### 3.3 Enzymatic Kinetic Resolutions on Polymer Supports

The direct polymerization routes described above continue to be a significant challenge to future researchers. The major disadvantages include expanding substrates beyond those possessing stereocenters adjacent to the growing polymer chain and the resolution of functional groups incompatible with polymerization. Fortunately, other

approaches to polymer-based resolutions have been reported that also lead to the simplified separation of racemates. For example, Scheme 3.4 shows the selective removal of one alcohol enantiomer from a polyethylene glycol (PEG) polymer derivatized with the racemic alcohol.<sup>13-14, 29</sup> This system required a carbonate linker that is hydrolyzed enantioselectively by Porcine Pancreas Lipase (PPL) at 0 °C in a hexane-phosphate buffer solution. After the resolution, the polymer is isolated by precipitation from ether. The unreacted starting material, for instance 1-phenylethanol, was isolated with 99% ee with only 29% conversion of the carbonate to alcohol. For an enzyme, the selectivity factor is termed an E-value and is calculated using the same equations for selectivity factor shown in chapter 1. The efficiency of this reaction is therefore quite selective obtaining an E-value<sup>30</sup> over 200 for this substrate.

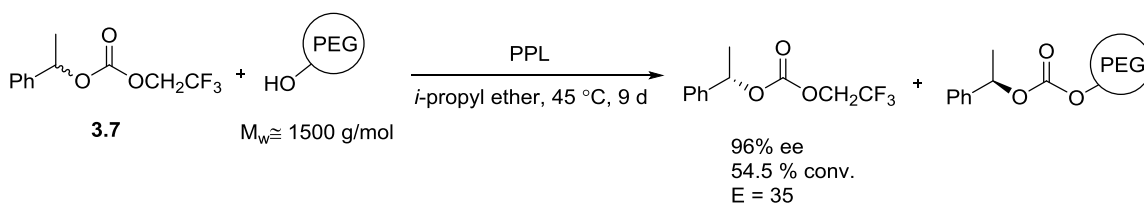


### Scheme 3.4 Enzyme Induced Deprotection of Polymer-Bound Alcohols

Alternatively, the PPL enzyme has also been utilized to selectively acylate alcohols onto macromolecule supports. Polyethylene glycol (PEG) was again used as the polymer support (Scheme 3.5). However, in this case, the PPL enzyme catalyzed the transesterification of one enantiomer of the carbonate **3.7** onto the polymer from a racemic mixture.<sup>17-18</sup> The reaction was carried out in *iso*-propyl ether at 45 °C and

required very long reaction times (9 days). Despite the sluggish reactivity, the unreacted, enantioenriched carbonate was obtained after cooling to 0 °C and filtration. The recovered starting material carbonate, containing the (*S*)-1-phenylethanol moiety, was isolated with an ee of 96% and an E-value of 35.

It is noteworthy that a non-enzymatic resolution using polymeric supports as a means of separating enantioenriched starting material from products has yet to be realized. This knowledge has provided the driving force to expand the silylation-based resolutions developed by Wiskur<sup>31-32</sup> to include the polymer-supported methodology.



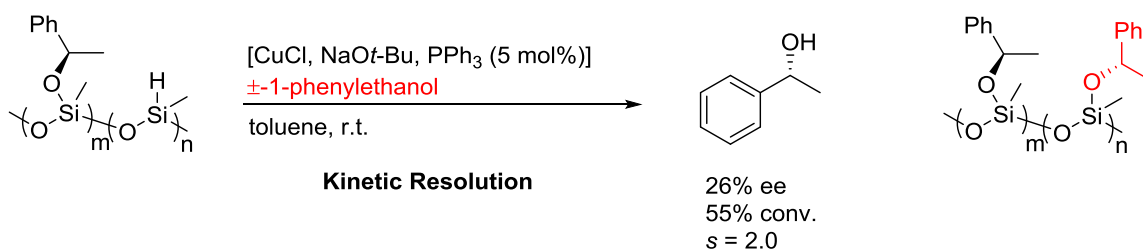
### Scheme 3.5 Enzymatic Acylation of Alcohols Utilizing a Polymer Support

#### 3.4 Silylation-Based Kinetic Resolutions on Polymer Supports

As previously reviewed in Chapter 1 section 1.5, silylation-based kinetic resolutions offer several advantages over other derivatizing reagents in kinetic resolutions. Despite these advantages, relatively few examples of silylation-based resolutions exist in comparison to acylation based methods. Resultantly, before our work only one example of silylation-based kinetic resolution exists utilizing a polymer support.<sup>16</sup> This method utilized an asymmetric, dehydrogenative silicon-oxygen coupling similar to those developed by Oestreich<sup>33</sup> and others.<sup>34-35</sup> These reactions utilize a copper chloride catalyst with chiral ligands in the presence of *tert*-butoxide to achieve the



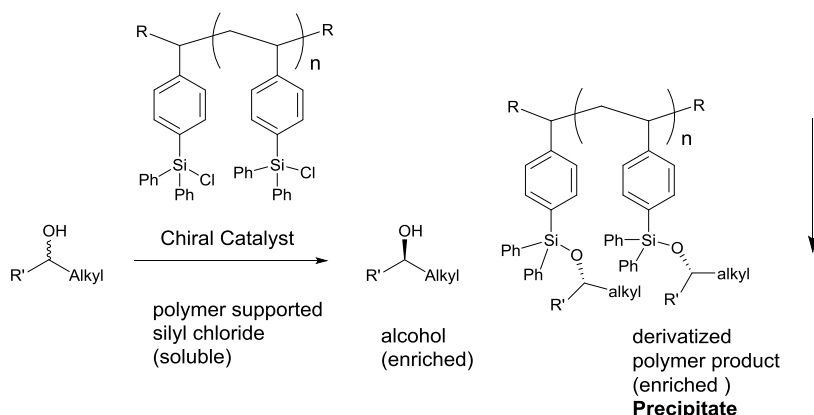
silylation-based resolution of secondary alcohols. However, it was discovered that a stereoenriched silyl ether modified polymethylhydrosiloxane PMHS performed better in the resolution than employing chiral ligands. The environment around the silicon was the source of stereoiduction, and chiral ligands such as (*R*)-BINAP had little effect on the enantioselectivity. Therefore, the reaction could be run with achiral triphenylphosphine as the ligand. The reaction achieved a conversion of 55% and a very modest *s*-factor of 2.0 with 1-phenylethanol as the substrate (Scheme 3.6). The reaction in essence required a polymer-bound chiral derivatizing agent to achieve a resolution. In order for this silylation-based approach to be synthetically viable, more efficient resolutions that function catalytically in chiral materials must be realized.



### Scheme 3.6 Kinetic Resolution via Silicon-Oxygen Coupling on a Polymeric Support

To the best of our knowledge, the work described in this chapter is one of the few successful examples of the selective attachment of one enantiomer to a polymer through a small-molecule catalyzed kinetic resolution (Sections 3.5 and 3.6 were carried out by Ravish Akhiani and the polymerization of the monomer described in Section 3.5 was carried out by Liang Zhang in Dr Chuanbing Tang's group). In one of our previous studies, substitution of triphenylsilyl chloride with sterically large alkyl groups<sup>36</sup> in the

para-position actually enhanced selectivity<sup>37</sup>; therefore, we hypothesized that our methodology could retain selectivity if a polymeric version of triphenylsilyl chloride was employed. We envisioned a resolution employing a relatively low molecular weight polystyrene silyl chloride such that the polymer should be homogeneous during the reaction and presumably exhibit similar kinetics and reactivity when compared to previous solution-based studies<sup>38-39</sup> (Scheme 3.7). After completion of the reaction, the polymer derivatized product would be precipitated from solution by methanol affording the enriched starting material without the need for chromatography.

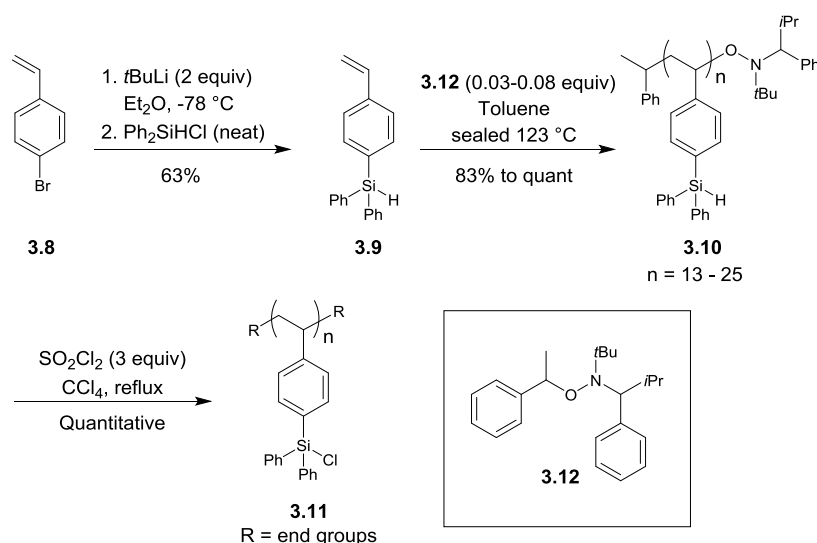


**Scheme 3.7 Design of the Polymer-Supported Silylation-Based Resolution**

### 3.5 Synthesis of Polystyrene Supported Triphenylsilyl Chloride

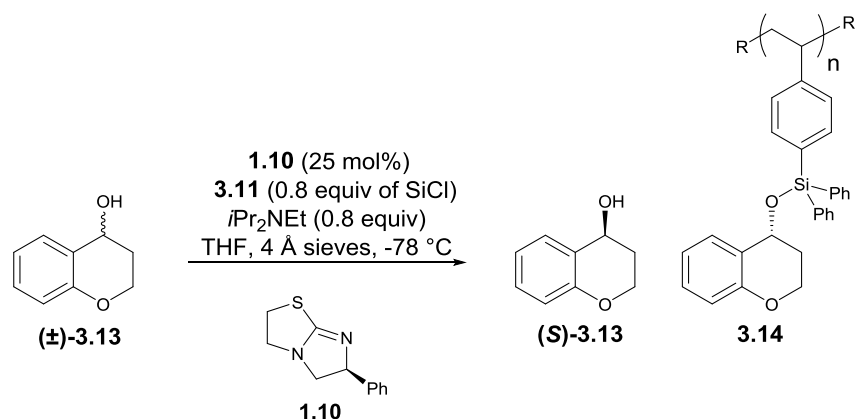
A polystyrene-supported triphenylsilyl chloride was synthesized in three different lengths to test the effect of polymer molecular weight on selectivity in the silylation-based kinetic resolution. The polymer synthesis started with a lithium-halogen exchange on commercially available para-bromo styrene **3.8** that was reacted with diphenylchlorosilane to generate the silane monomer **3.9** (Scheme 3.8).<sup>36</sup> Three different molecular weight polymers **3.10** were generated through a nitroxide-mediated radical polymerization (NMP) with the universal initiator **3.12**.<sup>40</sup> The number-average molecular

weight ( $M_n$ ) of the silane polymers **3.10** were calculated from the crude reaction conversions ( $^1\text{H NMR}$ ), ranging from 4000 to 7500 g/mol (Table 3.3) depending on the amount of initiator employed. This equated to 13 to 25 repeating units of monomer **3.9**, respectively. These relatively low molecular weights were designed to facilitate solubility of the polymers in the reaction mixture. The dispersity ( $\mathcal{D}$ ) of the polymers was around 1.2-1.3 for all three polymers (See experimental for table of all polymers prepared). Other methods of polymerization generated much higher dispersities, presumably due to poor reactivity of the bulky monomer. Finally, these polymers were chlorinated through a radical chlorination with sulfuryl chloride<sup>41-42</sup> to generate **3.11**.



**Scheme 3.8 Synthesis of Polystyrene-Supported Triphenylsilylchloride**

**Table 3.3 Optimization of the Polystyrene-Supported Kinetic Resolution**



Entry	$M_n$ of <b>3.11</b>	n	$D$ (GPC)	er of <b>(S)</b> - <b>3.13</b>	conv (%) <sup>a</sup>	$s^a$
1	3950	13	1.2	72:28	40	8
2	6130	20	1.2	73:27	44	6
3	7580	25	1.3	79:21	46	9
4 <sup>b</sup>	--	--	--	85:15	49	15

<sup>a</sup>See ref.<sup>43</sup> <sup>b</sup>Data taken from previous study.<sup>37</sup>

### 3.6 Optimization of the Polymer-Bound Silyl Source

The kinetic resolution of racemic 4-chromanol ((±)-**3.13**) was performed with the three different molecular weight silyl chloride polymers (**3.11**, n = 13, 20, & 25), using standard reaction conditions developed for our previous work on kinetic resolutions with triphenylsilyl chloride and catalyst **1.10** (Table 3.3, entries 1-3).<sup>31</sup> These polymers are soluble at -78 °C in THF at the reaction concentration, fulfilling our requirement for a homogeneous silyl chloride source. After reaction completion, the polymer product, enantioenriched silyl ether **3.14**, was isolated by removal of the reaction solvent, followed by the addition of methanol, centrifugation, and filtration for the easy recovery of the solid polymer product. Ultimately, the polymer length had little effect on the selectivity of the kinetic resolution, generating selectivity factors ranging between 6 to 9 for the three polymers. The higher molecular weight polymer ( $M_n = 7580$  g/mol, n = 25)

was ultimately chosen for further studies, due to the increased efficiency of polymer precipitation over the shorter polymers. Ultimately, the polymer supported reactions showed a decrease in selectivity compared to triphenylsilyl chloride (Table 3.3, Entry 4). This is presumably due to the changes in polar environments in the polymer-bound silyl chloride versus  $\text{Ph}_3\text{SiCl}$ .<sup>44</sup> This hypothesis is supported by the dramatic effect solvent polarity has on selectivity observed in previous studies<sup>31-32</sup> (See Table 2.4, Chapter 2). The slower diffusion of starting materials into the polymer also affected the conversion. Therefore, additional equivalents of silyl chloride were needed when the polymer was employed to obtain the same conversion as when triphenylsilyl chloride was employed (0.8 equiv vs. 0.6 equiv, respectively).

### 3.7 Substrate Scope of the Resolution Utilizing Polymer-Bound Silyl-Chloride

Substrates that have been successfully employed in previous silylation-based kinetic resolutions were resolved utilizing the silyl chloride polymer **3.11**. Two cyclic secondary alcohols (Table 3.4, entry 1 and 2) and two  $\alpha$ -hydroxy lactones (Table 3.4, entry 3 and 4) were resolved employing **1.10** and **1.5** as the catalysts, respectively. Overall, the substrates resulted in synthetically useful selectivities, ranging from 8 to 16. While these selectivities are lower than those obtained with triphenylsilyl chloride (Table 3.4, far right column),<sup>31-32</sup> as discussed above, the results show that efficient resolution is possible with this polymer-bound reagent.

**Table 3.4 Substrate Scope of the Polymer-Bound Silylchloride Method**

Entry	recovered alcohol	catalyst	er of recovered alcohol	er of desilylated alcohol	conv (%) <sup>a</sup>	s <sup>a</sup> ( <b>3.11</b> )	s <sup>a</sup> (Ph <sub>3</sub> SiCl) <sup>b</sup>
<div style="border: 1px solid black; padding: 5px; display: inline-block;"> <p><b>1.10</b></p> </div>		<b>1.9</b>	65:35	14:86	30	8	15
		<b>1.9</b>	72:28	11:89	36	12	25
<div style="border: 1px solid black; padding: 5px; display: inline-block;"> <p><b>1.5</b></p> </div>		<b>1.5</b>	63:37	9:91	25	11	36
		<b>1.5</b>	63:37	7:93	24	16	100

<sup>a</sup>See ref.43 <sup>b</sup>Data taken from previous studies for lactones (Entries 3 and 4)<sup>32</sup> and simple secondary alcohols (Entries 1 and 2).<sup>31</sup> Entries 1 and 2 employed *i*PrNCH<sub>2</sub>Et<sub>2</sub> instead of *i*Pr<sub>2</sub>NEt <sup>c</sup>Reactions used 1.0 equiv. of **3.11** and *i*Pr<sub>2</sub>NEt with 94 h reaction time.

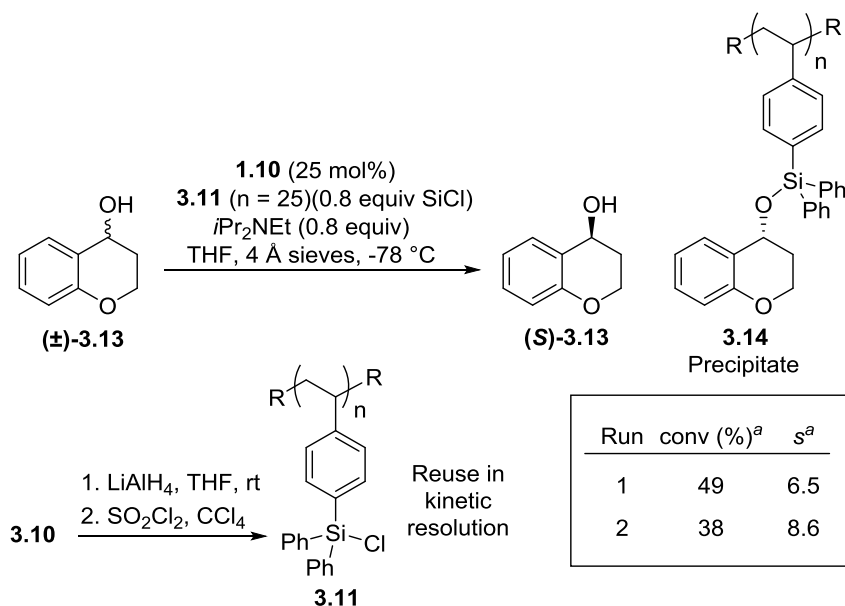
To the best of our knowledge, this is the most efficient polymer-supported kinetic resolution employing a small molecule catalyst. Additionally the need for chromatography was eliminated by use of the silyl chloride polymer. After performing an acid wash to remove the catalyst and amine base, the enantiomers were effectively separated by dissolving the reaction mixture in methanol and filtering off the insoluble polymer-bound silyl ether product. The recovered, unreacted alcohol in the filtrate was

generally pure enough to use in further syntheses if desired. The other enantiomer was cleanly obtained after the silyl ether polymer was reacted with tetrabutylammonium fluoride (TBAF) and removal of the silane polymer by precipitation. Even though multiple cycles of precipitation were needed to effectively recover the relatively short polymer ( $n = 25$ ). On large scale, this could be more advantageous than the non-polymer supported methodology employing  $\text{Ph}_3\text{SiCl}$  which required two columns. Employing  $\text{Ph}_3\text{SiCl}$  in the kinetic resolution necessitates one column to separate starting material from product and another to isolate the deprotected product.

### **3.8 Recycling and Subsequent Reuse of Polymer-Bound Silyl Chlorides in Kinetic Resolution**

To show the recyclability of the silyl chloride polymer **3.11**, it was employed in a preparative scale run with the intention of recovering the polymer and employing it in a second kinetic resolution (Scheme 3.9). The reaction was run under standard reaction conditions using 0.6 g of racemic **3.13** and 1 g of **3.11**. The selectivity factor of the first run was 6.5, which is only a minor reduction in selectivity compared to previous smaller scale runs. The polymer product was isolated, and the derivatized alcohol was desilylated by reduction with lithium aluminium hydride at room temperature to obtain the silane and the alcohol. Lithium aluminium hydride was employed over TBAF for the removal of the alcohol in order to generate the silane polymer instead of the fluorinated silicon. Attempts to reduce the silyl ether with diisobutylaluminum hydride (DIBAL-H) were lower yielding and required longer reaction times. The silane was again chlorinated and subjected to a second kinetic resolution which resulted in a comparable selectivity factor as compared to the first run ( $s = 8.6$ ). The dispersity of the recovered silanes after each

kinetic resolution was identical to the original silane **3.10** showing that the polymer does not degrade during the kinetic resolution or reduction (See experimental for table of dispersity data). This highlights the ability of the polymer to be recycled without degradation while maintaining the selectivity of the reaction, which is an important aspect towards reducing waste and cost.



**Scheme 3.9 Recycling procedure and Large Scale Resolution using Polystyrene-Bound Triphenylsilyl Chloride**

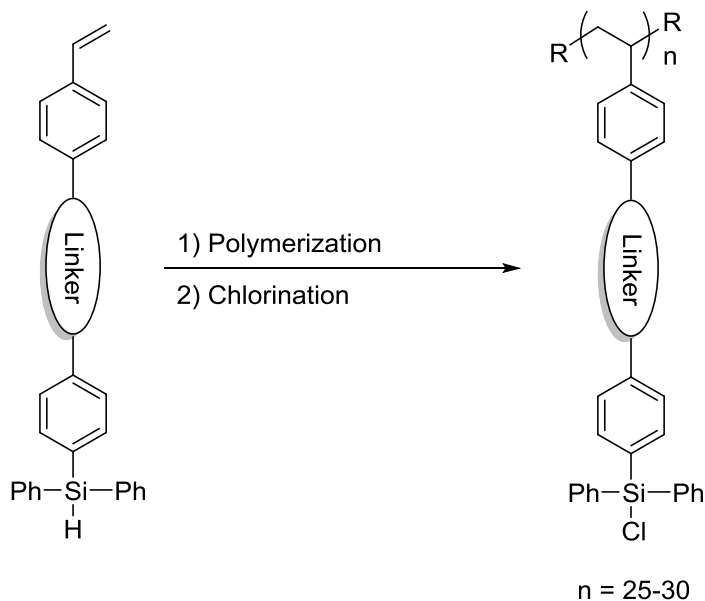
<sup>a</sup>See ref.<sup>43</sup>

### 3.9 Conclusion and Outlook

Future work will be focused on optimization of the polymer-support for the silyl chloride to improve conversion, enantioselectivity, and polymer recoverability. Higher molecular weight polymers will invariably be required to assist in polymer recovery. The conversion and selectivity can most likely be improved by implementing a linker or spacer between polymer backbone and silyl chloride (Scheme 3.10). This connection moves the reactive site away from the relatively non-polar polymer backbone. This



would presumably modify the microenvironment at the polymer reactive site to more polar, solvent-like conditions. As proof of concept, these spacers have been demonstrated to increase reactivity of polymer supported catalysts and increase in selectivity for asymmetric catalysis reactions.<sup>45</sup> A variety of structures have been utilized for this purpose including alkyl, polyether, and amide linkages. This polystyrene-supported triphenylsilylchloride with an additional linker could be more reactive than **3.11** requiring less polymer to achieve the desired conversion. Synthesis of these polymeric silyl chlorides could follow the procedure generally demonstrated previously in this chapter. A monomer prepared with an ideal spacer could be polymerized followed by post-polymerization chlorination yielding a suitable polymer-supported silyl chloride for testing in the kinetic resolution.



**Scheme 3.10 Employing a Linker on the Polymer Support**

In conclusion, a polystyrene-supported triphenylsilyl chloride was employed in a silylation-based kinetic resolution for the facile separation of alcohol enantiomers. While

this technique has been applied to enzyme catalyzed kinetic resolutions, to the best of our knowledge this is one of the first selective small molecule catalyzed versions. Cyclic secondary alcohols and  $\alpha$ -hydroxy lactones were resolved with selectivity factors ranging from 8-16, showing the viability of this approach. The enantiomers were separated by simple filtration of the derivatized polymers, and the polymers can be recycled by reducing the silyl ether and re-chlorinating the silicon without loss of selectivity or polymer degradation.

### 3.10 Experimental

#### General Information

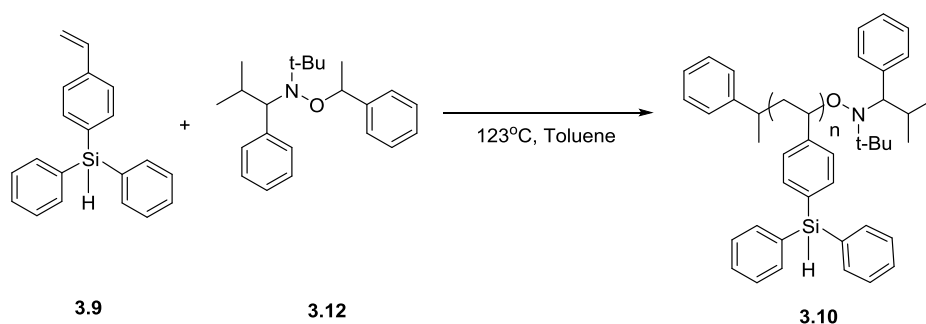
All reactions were carried out under a N<sub>2</sub> atmosphere using oven dried glassware. Molecular sieves were activated for 48 h at 130 °C in an oven. Tetrahydrofuran (THF) and diethyl ether were dried by passing through a column of activated alumina before use and stored over molecular sieves. Carbon tetrachloride was distilled, degassed and stored over molecular sieves under argon. Sulfuryl chloride was distilled prior to use. The monomer **3.9** 1-diphenylsilyl-4-ethenylbenzene<sup>36</sup> and 4,4-diethyl-3-hydroxydihydrofuran-2 (3H)-one<sup>32</sup> were prepared according to a known procedure All other chemicals were obtained commercially and used without further purification. Flash column chromatography was performed on silica gel (32-63 microns). <sup>1</sup>H NMR was taken on a Bruker Avance III (400 or 300 MHz). Chemical shifts are reported in ppm with TMS or chloroform as an internal standard (TMS 0.00 ppm for <sup>1</sup>H and <sup>13</sup>C or CHCl<sub>3</sub> 7.26 ppm and 77.16 for <sup>1</sup>H and <sup>13</sup>C respectively). <sup>13</sup>C NMR spectra were taken on a Bruker Avance III (101 or 75 MHz) with complete proton decoupling. Data reported in

$^1\text{H}$  NMR are as follows: Chemical shift, multiplicity (s = singlet, d = doublet, t = triplet, q = quartet, dd = doublet of doublet, dt = doublet of triplet, sept = septet, m = multiplet). Enantiomeric ratios were determined via **HPLC** using an Agilent 1200 series using chiral stationary phases Daicel Chiralcel OD-H or Daicel Chiralpak IC (4.6 x 250 mm x 5  $\mu\text{m}$ ) columns, monitored by a diode array detector in comparison to racemic materials. **Molecular weights and dispersity ( $\bar{M}_w/\bar{M}_n$ )** were determined by GPC conducted on a Varian 390-LC system. Refractive index detector and 3 $\times$ PLgel 10 $\mu\text{m}$  mixed-BLS columns (300 $\times$ 7.5mm) were installed using THF as eluent at 30  $^\circ\text{C}$ . The flowing rate of THF is set at 1.0 mL/min. The GPC system was calibrated with poly(styrene) (PS) from Polymer Laboratories.

### **Nitroxide-Mediated Polymerization of 3.9**

The monomer, 1-diphenylsilyl-4-ethenylbenzene, **3.9**, (2.0 g, 7 mmol) and the calculated amount of initiator **3.12** (For example polymer with repeat units of  $n = 13$  a 12.5:1 monomer: initiator ratio was used; for repeat units of  $n = 20$  a 20:1 monomer: initiator ratio was used) were dissolved in 6.0 ml of dry toluene and charged into a 25 ml Schlenk flask (Scheme 3.12). The sealed system was degassed with three freeze-pump-thaw cycles and refilled with  $\text{N}_2$ . The flask was warmed in an oil bath to 123  $^\circ\text{C}$ . The reaction was stopped by quenching into liquid nitrogen when the conversion of the monomer was higher than 90% as confirmed by  $^1\text{H}$  NMR of the crude product. The product was recovered by precipitating from cold methanol twice followed by filtration. The material was then dried under vacuum overnight.

Polymers with different molecular weight were prepared by adjusting the molar ratio between the monomer and the initiator. The repeating unit ( $n$ ) of each polymer was calculated from the conversion of monomer as characterized from the crude product. Four polymers with  $n = 13, 20, 25, 40$  were prepared. The GPC traces shows symmetric curves (Figure 3.1) for each polymer, with the dispersity ( $\mathcal{D}$ ) between 1.2-1.3 (Table 3.4), indicated controlled polymerization.  $^1\text{H}$  NMR spectrum of the polymer product is given in Figure 3.2.



**Scheme 3.11 Nitroxide Mediated Polymerization to Generate Polymer-Bound Silane**

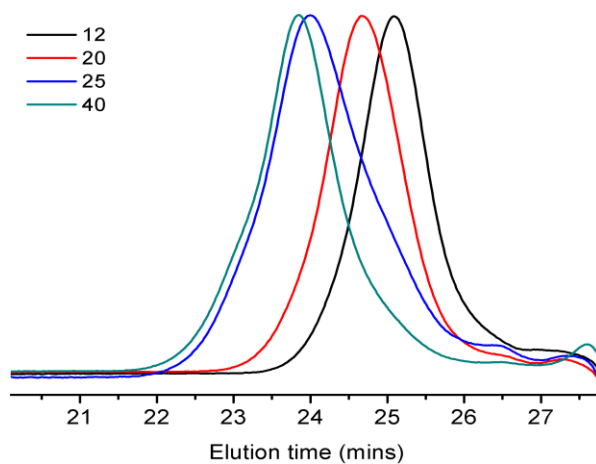


**Figure 3.1 GPC trace of polymers of varying  $M_n$**

**Table 3.5 Molecular weight parameters of polymers characterized from GPC and  $^1\text{H}$  NMR**

Polymer	$M_n$ ( $^1\text{H}$ NMR)	$M_n$ (GPC)	$\bar{D}$
P13	3950	2620	1.2
P20	6130	4330	1.2
P25	7580	5590	1.3
P40	11930	6990	1.3

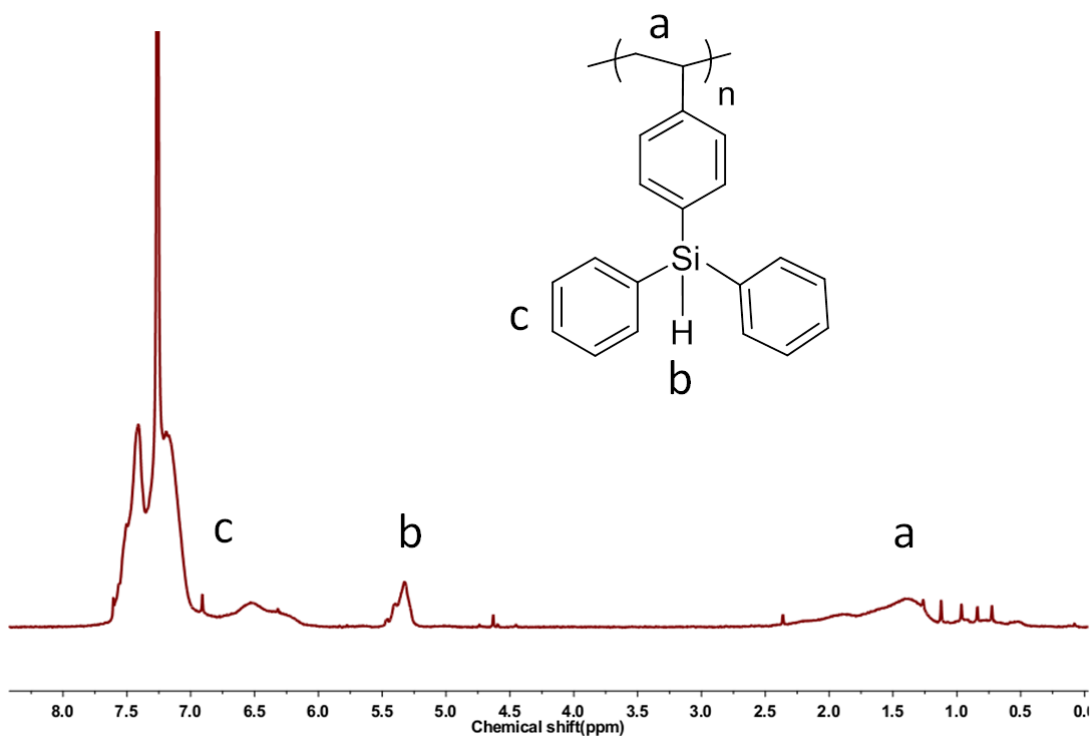


**Figure 3.2  $^1\text{H}$  NMR spectrum of the polymer synthesized**

### **Example Procedure for the Chlorination of Polymer-Bound Triphenyl Silane**

A 50 mL round bottomed flask was equipped with stir bar. Next, 3.7 mmol of polymer **3.10** was weighed into the vessel. The flask was then equipped with a reflux condenser and purged with argon. The polymer was dissolved in 15 mL of  $\text{CCl}_4$  with

stirring. The solution was warmed to reflux then 11.1 mmol of  $\text{SO}_2\text{Cl}_2$  was added via syringe dropwise. The mixture was allowed to reflux for 3 h at which point complete conversion was achieved as determined by  $^1\text{H}$  NMR. The solvent was removed in vacuo to yield the chlorinated polymer **3.11** ready for use in kinetic resolution, 1.19 g, pale yellow solid, quantitative yield.

### **General Procedure for the Polymer Supported Silylation-Based Kinetic Resolution of Secondary Alcohols (GP1)**

Into a 1-dram vial equipped with a stir bar and activated 4Å molecular sieves, racemic substrate (0.4 mmol) and catalyst (0.1 mmol) was added. The vial was then purged with argon and sealed with a septum. The starting materials were then dissolved in 1.4 mL of THF. Base,  $i\text{Pr}_2\text{NEt}$  (0.32 mmol), was added via syringe and the vial was cooled to  $-78\text{ }^\circ\text{C}$  in a cryocool for 30 mins. The cooled mixture was then treated with 0.64 mL of a freshly prepared 0.5 M polymer-bound silyl chloride solution in THF. The reaction was left to stir a set amount of time at  $-78\text{ }^\circ\text{C}$  then quenched with 0.3 mL of methanol. The solution was left to warm to room temperature then the contents of the vial were extracted into a 4-dram vial with ethyl acetate. Concentration gave an oil which was diluted with 20 mL of ethyl acetate. The resulting solution was washed with 5% HCl followed by saturated aqueous  $\text{NaHCO}_3$ . The organic layer was then dried over sodium sulfate, filtered and concentrated. The starting material was precipitated from the product by addition of methanol (5-10 mL). The polymer was filtered away and the supernatant concentrated. The precipitation process was repeated three times. Removal of the methanol afforded the starting material. Further purification on column chromatography

(ethyl acetate hexanes mixtures) was required to provide the starting material suitable for conversion to the benzoate ester or separation on chiral stationary phase HPLC.

### **General Procedure for the Deprotection of Polymer-Bound Products**

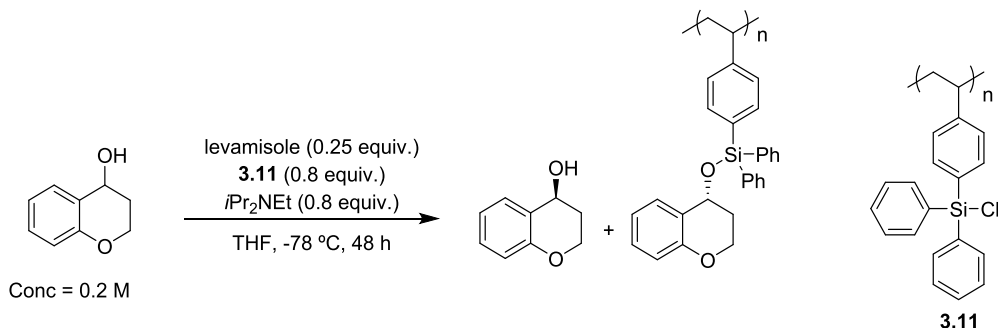
The polymer-bound product obtained by vacuum filtration was weighed into a 4-dram vial equipped with stir bar and septum. The polymer was then dissolved in 1 mL of THF with stirring and treated with 1 mL of TBAF (1 M in THF). The reaction was monitored via TLC. (1:3 EtOAc: hexanes). The reactions were generally complete in less than 2 h. The reaction was then quenched with brine, extracted with diethyl ether three times and dried over a sodium sulfate silica gel mixture and filtered. Concentration via rotovap afforded an oil. Subsequent purification on silica gel column chromatography (ethyl acetate hexanes mixtures) afforded the deprotected products suitable for conversion to the benzoate ester or separation on chiral stationary phase HPLC.

### **General Procedure for the Benzoylation of Secondary Alcohols<sup>32</sup>**

A 4-dram vial containing the lactone was fitted with a stir bar and a septum. DMAP (0.1 equiv.) was weighed and added to the vial. The mixture was then dissolved in 2 mL of dichloromethane with stirring. Triethyl amine (2.0 equivalents) was added via syringe and the vessel was cooled to 0 °C in an ice bath. Benzoyl chloride (1.4 equivalents) was then added drop wise via syringe and the reaction was left to stir for 30 mins at which point TLC of the crude indicated reaction was complete. The reaction was quenched with saturated sodium bicarbonate and extracted three times with dichloromethane. The combined organic layers were then dried over sodium sulfate. After concentration the crude was then purified via silica gel column chromatography

(1:9 EtOAc: hexanes) to obtain the desired benzoylated lactone. The benzoate esters were then analyzed by HPLC using chiral stationary phases.

**Table 3.6 Silylation-based Kinetic Resolution of 4-Chromanol Varying the Molecular Weight of Polymer Supported Silyl Source**



Entry	n	er SM	er P	% conv.	s	Avg
1	13	72:28	16:84	39.8	7.9	<b>7.5</b>
		73:27	18:82	42.4	7.1	
2	20	73:27	21:79	44.2	5.9	<b>5.5</b>
		71:29	23:77	44.0	5.0	
3	25	78:22	15:85	44.9	9.7	<b>9.4</b>
		79:21	16:84	46.0	9.0	
4	40	70:30	14:86	35.5	8.8	<b>8.1</b>
		71:29	17:83	39.2	7.4	

#### Analytical Data and HPLC Data for Kinetic Resolutions

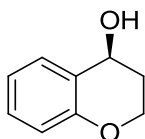
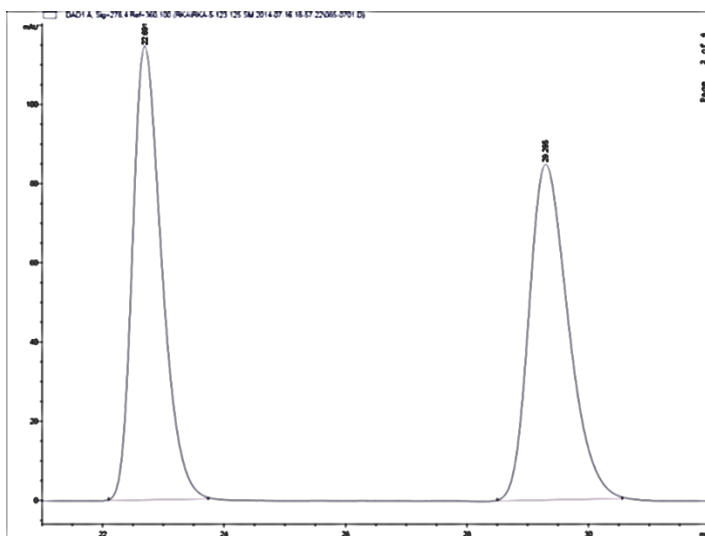


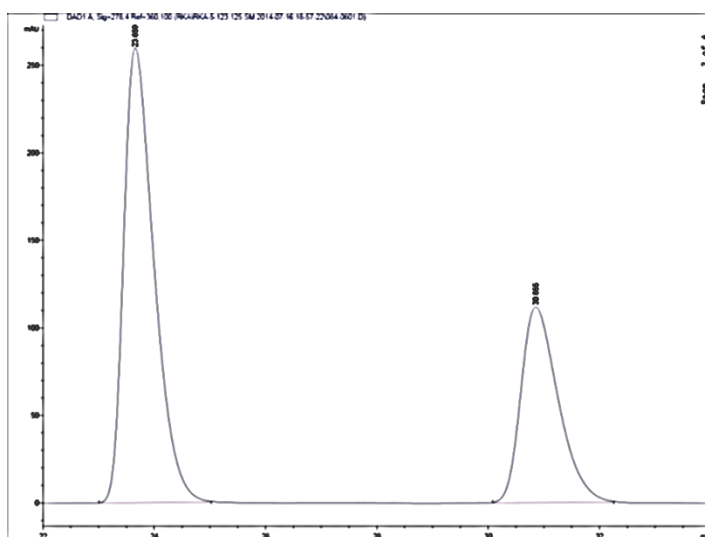
**Table 3.4, Entry 1:** 34 mg, 54 % recovered.  $^1\text{H NMR}$  (400 MHz,  $\text{CDCl}_3$ )  $\delta$  ppm 7.31 (d,  $J = 8.2$  Hz, 1 H), 7.23-7.19 (m, 1 H), 6.95-6.90 (m, 1 H), 6.84 (d,  $J = 8.2$  Hz, 1 H), 4.78, (t,  $J = 3.9$  Hz, 1 H), 4.32-4.24 (m, 2 H), 2.15-1.86 (m, 3 H).  $^{13}\text{C NMR}$ : (101



MHz, CDCl<sub>3</sub>) δ ppm 154.6, 129.7, 129.6, 124.3, 120.6, 117.0, 63.2, 61.9, 30.8. HPLC separation<sup>31</sup> was achieved on Chiralpak OD-H Column 2% isopropyl alcohol in hexane, flow rate: 1.3 mL/min, 25 °C; t<sub>R</sub> 23.3 min for (S)-enantiomer (major) and 30.3 min for (R)-enantiomer (minor). (er = 63:37).



Peak #	RetTime [min]	Type	Width [min]	Area [mAU*s]	Height [mAU]	Area %
1	22.691	BB	0.5041	3814.17749	114.67128	50.0790
2	29.295	BB	0.6761	3802.14673	84.79882	49.9210



Peak #	RetTime [min]	Type	Width [min]	Area [mAU*s]	Height [mAU]	Area %
1	23.347	BB	0.5524	7291.22510	201.36371	63.2946
2	30.297	BB	0.6708	4228.28906	96.00488	36.7054

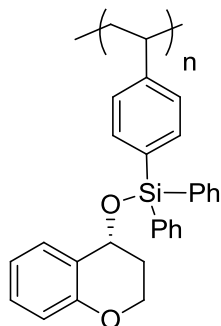
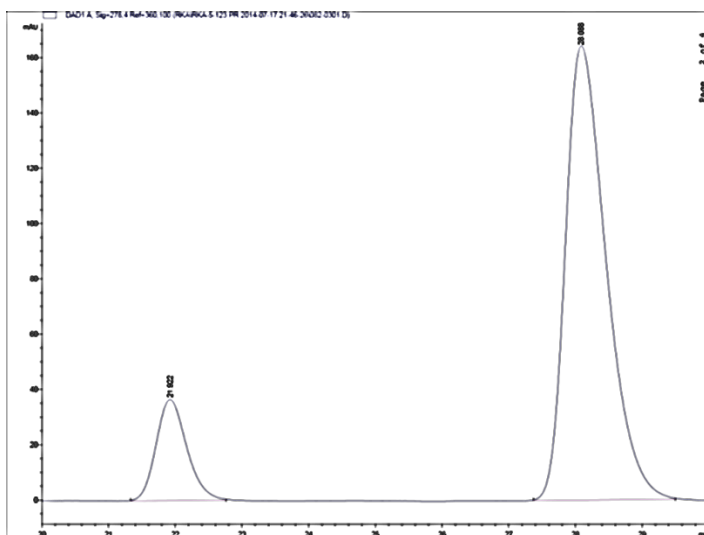


**Table 3.4, Entry 1:** 51 mg. HPLC data is of the desilylated product following GP2, 13 mg, 20 % yield. The same conditions as the recovered starting materials were utilized. (er = 87:13).



Peak #	RetTime [min]	Type	Width [min]	Area [mAU*s]	Height [mAU]	Area %
1	21.085	BB	0.4515	431.42133	14.23988	13.3698
2	27.015	BB	0.6041	2795.40527	69.97284	86.6302

Entry	er SM	er P	% conv.	s	Avg
1	63:37	13:87	26.7	8.3	<b>8.2</b>
2	65:35	14:86	30.1	8.1	

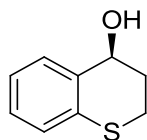
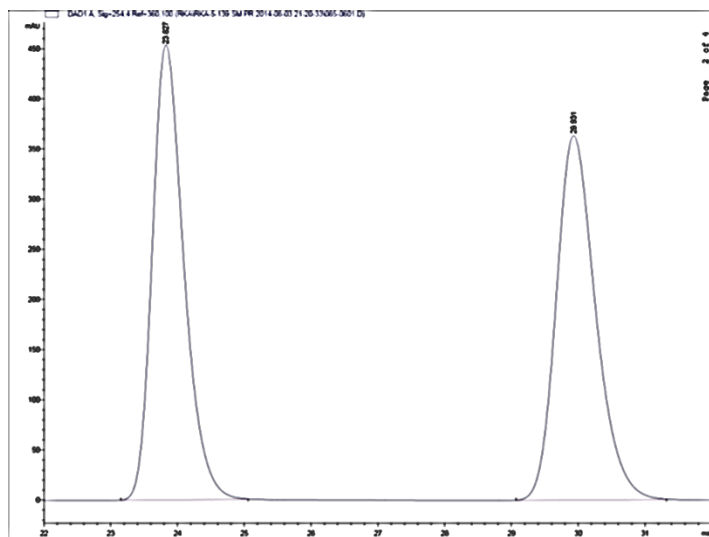
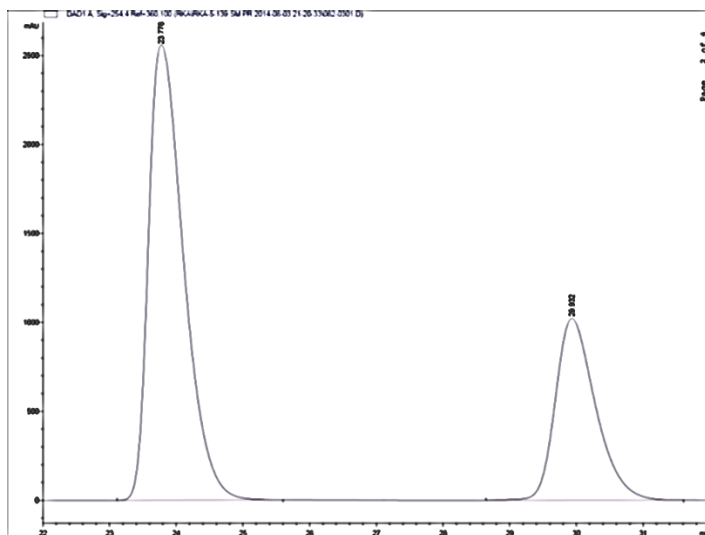


**Table 3.4, Entry 2:** 39 mg, 58 % recovered.  $^1\text{H NMR}$ : (300 MHz,  $\text{CDCl}_3$ )  $\delta$  ppm 7.33 (d,  $J = \text{Hz}$ , 1 H), 7.19-7.15 (m, 2 H), 7.10-7.04 (m, 1 H), 4.83 (dd,  $J = 4.7, 3.2$  Hz, 1 H), 3.33 (dt,  $J = 24.5, 12.3, 3.0$  Hz 1 H), 2.91-2.84 (m, 1 H), 2.41-2.32 (m, 1 H), 2.12-2.01 (m, 1 H), 1.74 (d,  $J = 4.7$  Hz, 1 H).  $^{13}\text{C NMR}$ : (75 MHz,  $\text{CDCl}_3$ )  $\delta$  ppm 134.5, 133.1, 130.3, 128.4, 126.7, 124.3, 66.6, 30.0, 21.5. HPLC separation<sup>31</sup> was achieved on Chiralpak OD-H Column 5 % isopropyl alcohol in hexane, flow rate: 0.6 mL/min, 25 °C;  $t_R$  23.4 min for (S)-enantiomer (major) and 29.7 min for (R)-enantiomer (minor). (er = 72:28).



Peak #	RetTime [min]	Type	Width [min]	Area [mAU*s]	Height [mAU]	Area %
1	23.827	BB	0.5014	1.48722e4	453.75287	50.0342
2	29.931	BB	0.6228	1.48519e4	363.37177	49.9658



Peak #	RetTime [min]	Type	Width [min]	Area [mAU*s]	Height [mAU]	Area %
1	23.448	BB	0.5560	1.89428e4	510.35437	72.0590
2	29.749	BB	0.6591	7345.09375	169.31036	27.9410

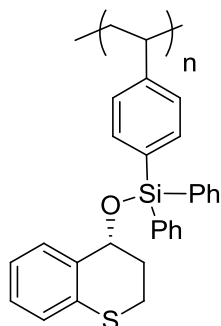
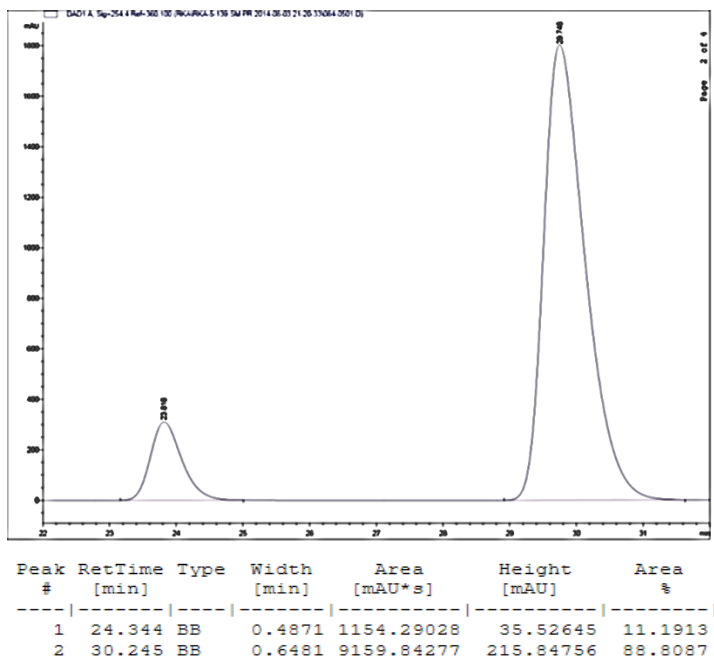


**Table 3.4, Entry 2:** 69 mg. HPLC data is of the desilylated product following GP2, 19 mg, 28 % yield. The same conditions as the recovered starting materials were utilized. (er = 89:11).



Entry	er SM	er P	% conv.	s	Avg
1	72:28	11:89	36.3	12.1	<b>11.9</b>
2	70:30	11:89	33.8	11.6	

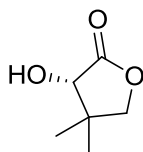
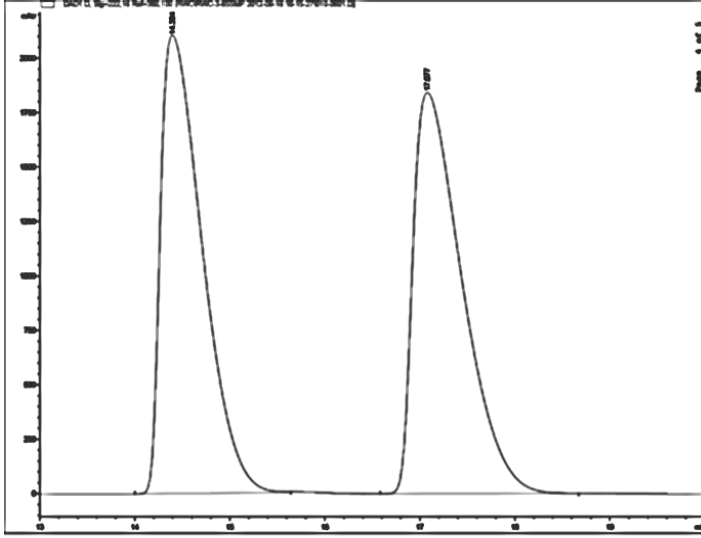
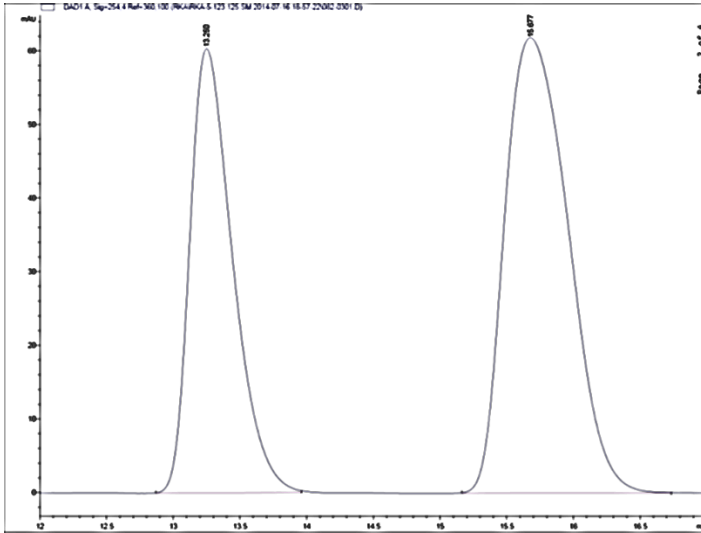


**Table 3.4, Entry 3:** 16 mg, 31 % recovered.  $^1\text{H NMR}$  (400 MHz,  $\text{CDCl}_3$ )  $\delta$  ppm 4.13 (s, 1H), 4.00 (d,  $J = 8.9$  Hz 1H), 3.95 (d,  $J = 8.9$  Hz 1H), 2.93 (br, 1H), 1.24 (s, 3H), 1.09 (s, 3H).  $^{13}\text{C NMR}$  (101 MHz,  $\text{CDCl}_3$ )  $\delta$  ppm 177.7, 76.4, 75.8, 40.9, 22.9, 18.8. The recovered starting material was converted to the benzoylated ester according to GP3 for HPLC analysis. HPLC separation was achieved on Chiralpak OD-H Column 6 %

isopropyl alcohol in hexane, flow rate: 1 mL/min, 25 °C;  $t_R$  13.2 min for (R)-enantiomer (minor) and 15.7 min for (S)-enantiomer (major). (er = 60:40)



Peak #	RetTime [min]	Type	Width [min]	Area [mAU*s]	Height [mAU]	Area %
1	14.394	BB	0.4725	6.40074e4	2106.32520	49.3149
2	17.077	BB	0.5504	6.57859e4	1843.21606	50.6851



Peak #	RetTime [min]	Type	Width [min]	Area [mAU*s]	Height [mAU]	Area %
1	13.250	BB	0.3421	1345.11450	60.34479	39.7052
2	15.677	BB	0.5433	2042.64099	61.84784	60.2948

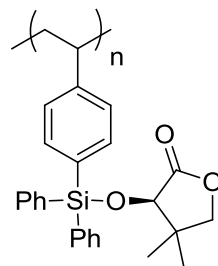
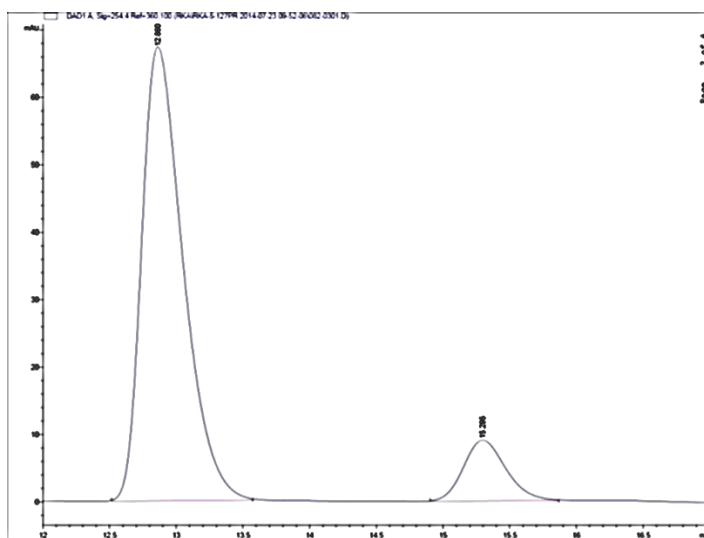


**Table 3.4, Entry 3:** 67 mg. HPLC data is of the desilylated product following GP2, 10 mg, 19% yield. The desilylated alcohol was then benzoylated according to GP3 for HPLC analysis. The same conditions as the benzoylated starting materials were utilized. (er = 88:12)



Peak #	RetTime [min]	Type	Width [min]	Area [mAU*s]	Height [mAU]	Area %
1	12.860	BB	0.3312	1449.31287	67.32273	87.9448
2	15.295	BB	0.3392	198.66721	9.01183	12.0552

Entry	er SM	er P	% conv.	s	Avg
1	37:63	91:9	24.9	12.2	<b>10.8</b>
2	40:60	88:12	21.1	9.4	

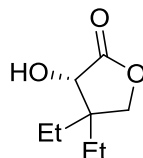
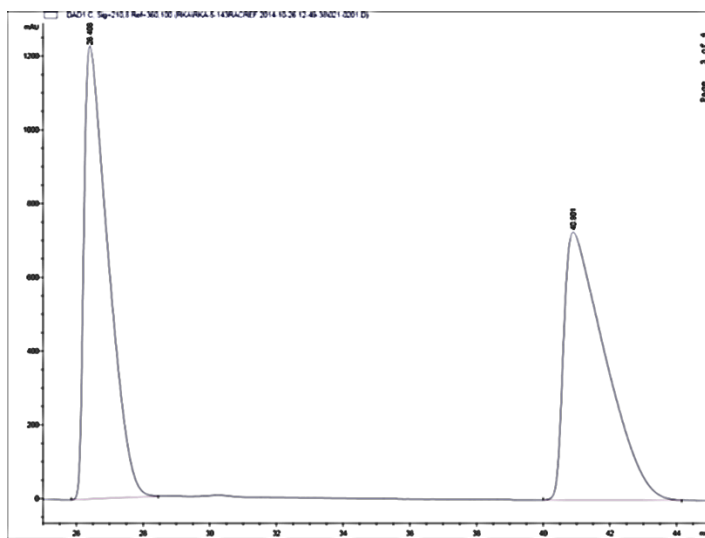
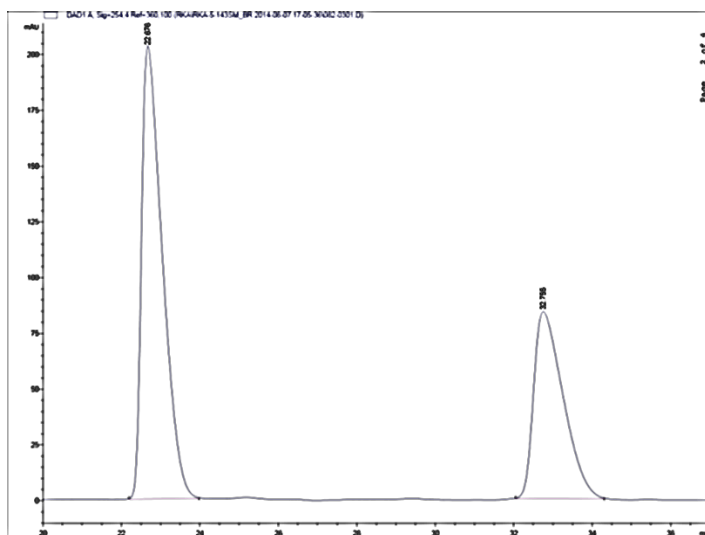


**Table 3.4, Entry 4:** 29 mg, 46 % recovered.  $^1\text{H NMR}$ : (400 MHz,  $\text{CDCl}_3$ )  $\delta$  ppm 4.22 (s, 1 H), 4.00 (d,  $J = 9.3$  Hz, 1 H), 2.73 (br, 1 H), 1.69-1.38 (m, 4 H), 0.99 (t,  $J = 7.4$  Hz, 3 H), 0.91 (t,  $J = 7.4$ , 3 H).  $^{13}\text{C NMR}$ : (101 MHz,  $\text{CDCl}_3$ )  $\delta$  ppm 178.3, 74.7, 73.1, 46.7, 28.1, 21.5, 8.5, 8.1. The recovered starting material was converted to the benzoylated ester according to GP3 for HPLC analysis. HPLC separation was achieved on Chiralpak IC column 15 % isopropyl alcohol in hexane, flow rate: 1 mL/min, 25 °C;  $t_{\text{R}}$  22.6 min for (S)-enantiomer (major) and 32.7 min for (R)-enantiomer (minor). (er = 63:37).



Peak #	RetTime [min]	Type	Width [min]	Area [mAU*s]	Height [mAU]	Area %
1	26.408	BB	0.7201	6.17392e4	1228.98547	49.6939
2	40.901	BB	1.1813	6.24999e4	726.76227	50.3061





Peak #	RetTime [min]	Type	Width [min]	Area [mAU*s]	Height [mAU]	Area %
1	22.676	BB	0.5590	7472.81396	203.23041	63.0036
2	32.755	BB	0.7956	4388.12158	83.97570	36.9964

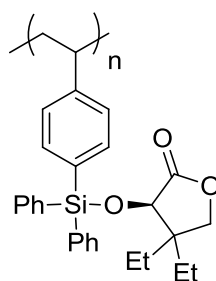
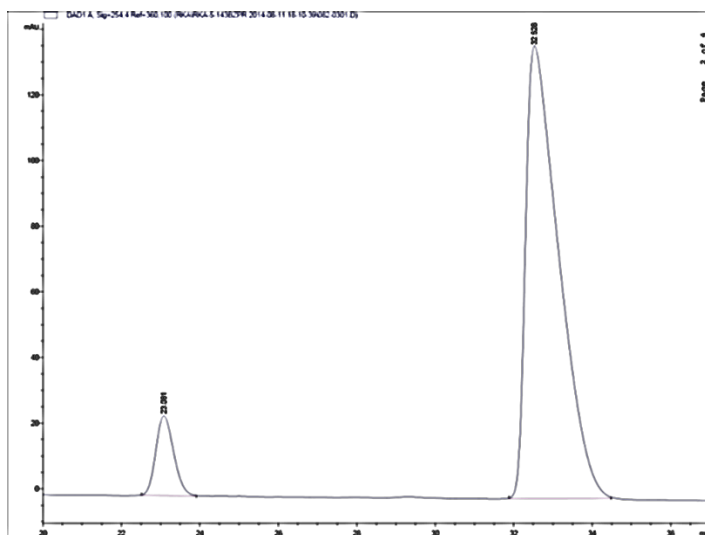


**Table 3.4, Entry 4:** 111 mg. HPLC data is of the desilylated product following GP2, 10 g, 16% yield. The desilylated alcohol was then benzyolated according to GP3 for HPLC analysis. The same conditions as the benzyolated starting materials were utilized. (er = 91:9).



Peak #	RetTime [min]	Type	Width [min]	Area [mAU*s]	Height [mAU]	Area %
1	23.081	BB	0.4931	4235.45410	133.14027	8.7196
2	32.528	BB	0.8576	4.43385e4	752.29413	91.2804

Entry	er SM	er P	%conv.	s	Avg
1	63:37	7:93	23.6	18.3	<b>16</b>
2	63:37	9:91	23.9	13.6	

### Procedure for Large Scale Kinetic Resolution

A 15 mL round bottomed flask was equipped with stir bar, 4Å molecular sieves and septum. Next, 600 mg (4.0 mmol) of **3.13** 4-chromanol and 204 mg of **1.9** levamisole (0.1 mmol) was added under argon and the vessel sealed. The alcohol was dissolved in 22 mL of THF with stirring. Next, 0.56 mL of *i*Pr<sub>2</sub>NEt was added via syringe. The mixture was cooled to -78 °C in a cryocool for 15 mins. The polymer-bound silyl chloride **3.11** was added as a solution (0.74 M, 4.3 mmol) via syringe dropwise. The mixture was left to react at -78 °C for 48 h then quenched with 1 mL of methanol. The solution was left to warm to room temperature then the contents of the vessel were extracted with ethyl

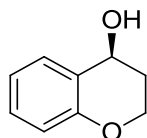
acetate. Concentration gave an oil which was diluted with 100 mL of ethyl acetate. The resulting solution was washed with 5% HCl followed by saturated aqueous NaHCO<sub>3</sub>. The organic layer was then dried over sodium sulfate, filtered and concentrated. The starting material was precipitated from the product by addition of methanol (20 mL). The heterogeneous polymer solution was centrifuged for 30 mins. The supernatant was concentrated and the precipitation process followed by centrifugation was repeated a total of three times. Removal of the methanol afforded the starting material. Further purification on column chromatography (ethyl acetate hexanes mixtures) was required to provide the starting material suitable for separation on chiral stationary phase HPLC. (0.21 g, 35% recovered alcohol) The combined pellets from the centrifugation process were dried under vacuum to provide the polymer-bound silyl ether free of alcohol and other impurities. (0.91 g)

#### **Recycling Procedure: Reduction of the Polymer-Bound Silyl Ether**

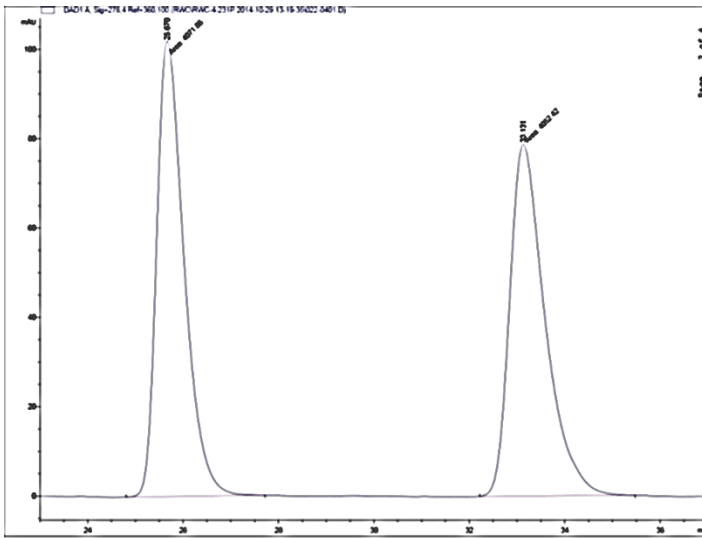
A 50 mL round bottomed flask was equipped with stir bar and septum. The polymer-bound silyl ether **3.14** from the above large scale reaction was then weighed into the flask (455 mg, 1.1 mmol). The vessel was purged with argon and the solid was dissolved in 6.5 mL of THF. The solution was cooled to 0 °C and lithium aluminum hydride (4.4 mL, 1.0 M in THF) was added drop wise via syringe. The reaction was left to stir for 15 mins at 0 °C then allowed to warm to ambient temperature. The mixture was allowed to stir for 24 h at which point <sup>1</sup>H NMR indicated complete conversion. The solution was again cooled to 0 °C and quenched with a few drops of acetone. The mixture was then diluted with 50 mL of ethyl acetate. The aluminum byproducts were decomposed by treatment with 75

mL of 5% HCl. The organic layer was then separated and the aqueous layer extracted with ethyl acetate (3x 50 mL). The combined organic layers were washed with saturated aqueous NaHCO<sub>3</sub>, dried of sodium sulfate and filtered. The product was precipitated from the polysilane by addition of methanol (20 mL). The heterogeneous polymer solution was centrifuged for 30 mins. The supernatant was concentrated and the precipitation process followed by centrifugation was repeated again for a total of three times. Removal of the methanol afforded the free product. Further purification on column chromatography (ethyl acetate hexanes mixtures) was required to provide the starting material suitable for separation on chiral stationary phase HPLC. (95 mg, 16% yield) The combined pellets from the centrifugation process were dried under vacuum to provide the polymer-bound silyl ether free of alcohol and other impurities. (224 mg, 42% yield over two steps)

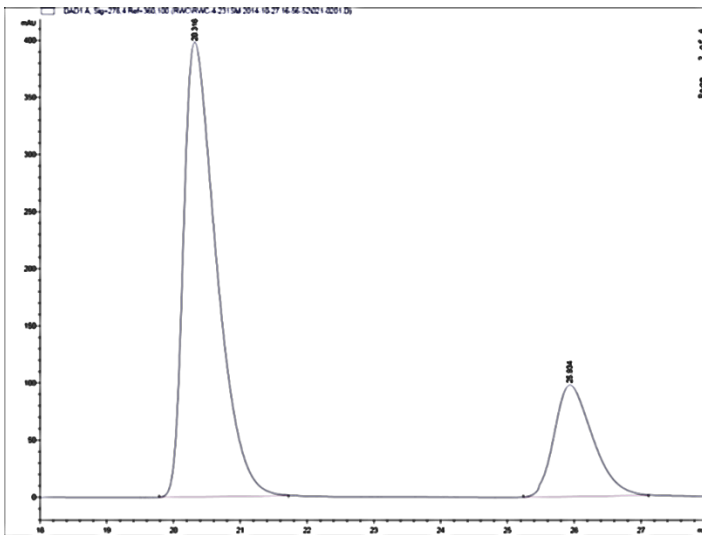
#### Analytical Data: Large Scale Kinetic Resolution



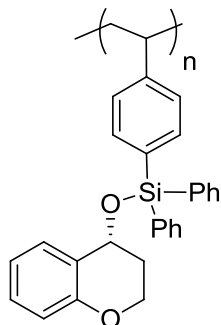
**Scheme 3.10, Run 1:** 212 mg, 35 % recovered. HPLC separation was achieved on Chiralpak OD-H Column 2% isopropyl alcohol in hexane, flow rate: 1.3 mL/min, 25 °C;  $t_R$  20.3 min for (S)-enantiomer (major) and 25.3 min for (R)-enantiomer (minor). (er = 78:22).



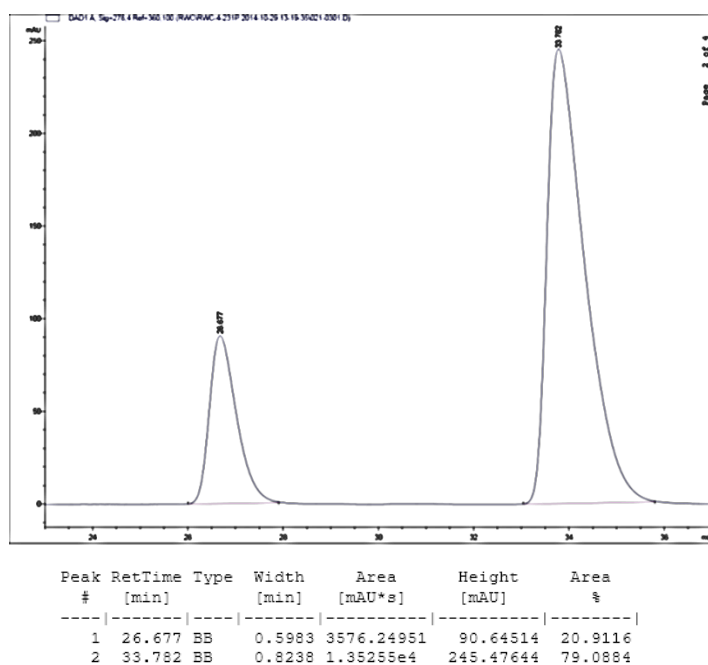
Peak #	RetTime [min]	Type	Width [min]	Area [mAU*s]	Height [mAU]	Area %
1	25.670	MM	0.6651	4071.86206	102.04146	50.1197
2	33.131	MM	0.8576	4052.41846	78.75686	49.8803



Peak #	RetTime [min]	Type	Width [min]	Area [mAU*s]	Height [mAU]	Area %
1	20.316	BB	0.5155	1.36071e4	398.39514	77.6926
2	25.934	BB	0.6017	3906.91333	97.67393	22.3074



**Scheme 3.10, Run 1:** 911 mg. HPLC data is of the desilylated product following reduction with  $\text{LiAlH}_4$ , 95 mg, 32 % yield. The same conditions as the recovered starting materials were utilized. (er = 79:21)



Entry	er SM	er P	% conv.	s
1	78:22	21:79	48.8	<b>6.5</b>

### **Recycling Procedure: Chlorination of Polymer-Supported Triphenyl Silane**

A 15 mL round bottomed flask was equipped with stir bar. Next, 0.71 mmol of polymer isolated from the above reduction was weighed into the vessel. The flask was then equipped with a reflux condenser and purged with argon. The polymer was dissolved in 2.9 mL of CCl<sub>4</sub> with stirring. The solution was warmed to reflux then 2.1 mmol of SO<sub>2</sub>Cl<sub>2</sub> was added via syringe dropwise. The mixture was allowed to reflux for 3 h at which point complete conversion was achieved as determined by <sup>1</sup>H NMR. The solvent was removed in vacuo to yield the chlorinated polymer ready for use in kinetic resolution, 227 mg, quantitative yield. The chlorosilane was used again in the kinetic resolution.

### **Kinetic Resolution Utilizing Recycled Polymer-Supported Silyl Chloride**

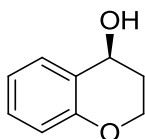
The same procedure as the large scale reaction was followed with 0.8 mmol of 4-chromanol **3.13**, 0.2 mmol of **1.9** levamisole, 0.64 mmol of *i*Pr<sub>2</sub>NEt. The recycled polymer-bound chlorosilane was added as a solution (0.9 mL, 0.71M in THF). The centrifugation procedure yielded the polymer-bound silyl ether free of impurities. (181 mg) The alcohol was purified further via column chromatography (ethyl acetate hexanes mixtures) for HPLC analysis. (56 mg, 47 % recovered alcohol)

### **Reduction of the Recycled Polymer-Bound Silyl Ether**

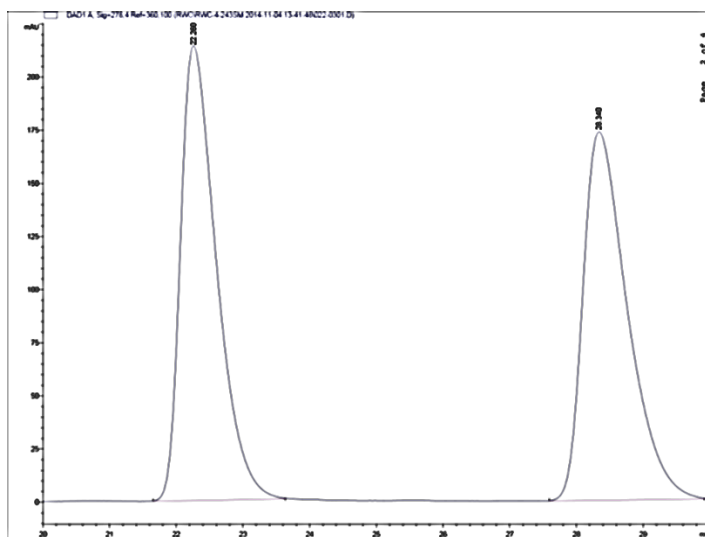
The recycled polymer-bound silyl ether was reduced following the same procedure as above using 0.42 mmol of polymer and 1.7 mmol of lithium aluminum hydride (1.0 M in THF) in 2.6 mL of THF. Centrifugation yielded the polymer free of alcohol and ready for

further recycling. ( 103 mg, 56 % over two steps) The desilylated alcohol was further purified via column chromatography (ethyl acetate hexanes mixtures) to yield the product suitable for HPLC analysis. (34 mg, 28% yield)

### Analytical Data: Kinetic Resolution Utilizing Recycled Polymer-Bound Silyl Chloride

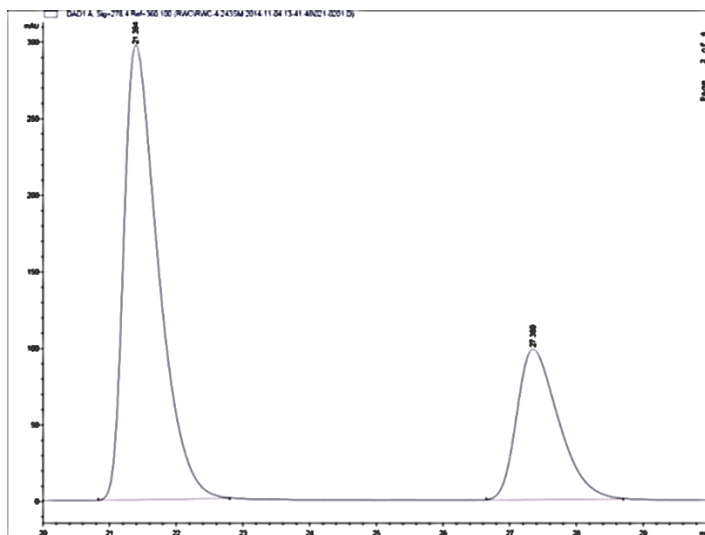


**Scheme 3.10, Run 2:** 56 mg, 47 % recovered. HPLC separation was achieved on Chiralpak OD-H Column 2% isopropyl alcohol in hexane, flow rate: 1 mL/min, 25 °C;  $t_R$  23.3 min for (R)-enantiomer (minor) and 30.3 min for (S)-enantiomer (major). (er = 71:29).

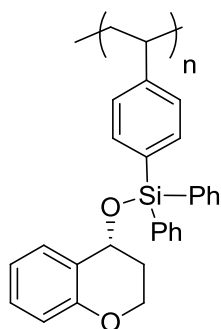


Peak #	RetTime [min]	Type	Width [min]	Area [mAU*s]	Height [mAU]	Area %
1	22.260	BB	0.5610	7993.14551	213.88905	49.9750
2	28.340	BB	0.6955	8001.13770	173.35023	50.0250

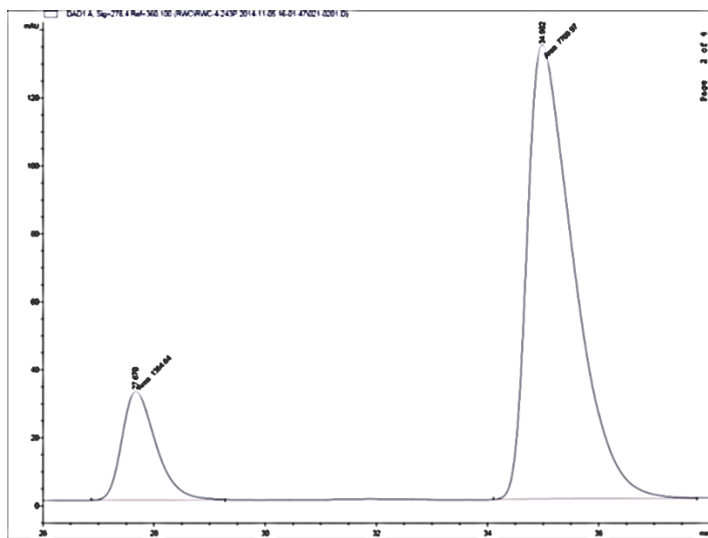




Peak #	RetTime [min]	Type	Width [min]	Area [mAU*s]	Height [mAU]	Area %
1	21.394	BB	0.5339	1.06448e4	297.15524	71.3699
2	27.350	BB	0.6448	4270.15625	98.30170	28.6301



**Scheme 3.10, Run 2:** 181 mg. HPLC data is of the desilylated product following reduction with  $\text{LiAlH}_4$ , 34 mg, 28 % yield. The same conditions as the recovered starting materials were utilized. (er = 85:15)



Peak #	RetTime [min]	Type	Width [min]	Area [mAU*s]	Height [mAU]	Area %
1	27.670	MM	0.7114	1364.64063	31.97292	14.9392
2	34.982	MM	0.9693	7769.97070	133.60175	85.0608

Entry	er SM	er P	% conv.	s
1	71:29	15:85	37.8	<b>8.6</b>

### 3.11 References

1. McNamara, C. A.; Dixon, M. J.; Bradley, M., Recoverable Catalysts and Reagents Using Recyclable Polystyrene-Based Supports. *Chem. Rev.* **2002**, *102*, 3275.
2. Webb, D.; Jamison, T. F., Continuous Flow Multi-Step Organic Synthesis. *Chem. Sci.* **2010**, *1*, 675.
3. Benaglia, M.; Puglisi, A.; Cozzi, F., Polymer-Supported Organic Catalysts. *Chem. Rev.* **2003**, *103*, 3401.
4. Ohkuma, T.; Takeno, H.; Honda, Y.; Noyori, R., Asymmetric Hydrogenation of Ketones with Polymer-Bound BINAP/Diamine Ruthenium Catalysts. *Adv. Synth. Catal.* **2001**, *343*, 369.
5. Clapham, B.; Reger, T. S.; Janda, K. D., Polymer-Supported Catalysis in Synthetic Organic Chemistry. *Tetrahedron* **2001**, *57*, 4637.
6. Daeffler, C. S.; Miyake, G. M.; Li, J.; Grubbs, R. H., Partial Kinetic Resolution of Oxanorbornenes by Ring-Opening Metathesis Polymerization with a Chiral Ruthenium Initiator. *ACS Macro Lett.* **2014**, *3*, 102.
7. Baar, C. R.; Levy, C. J.; Min, E. Y.; Henling, L. M.; Day, M. W.; Bercaw, J. E., Kinetic Resolution of Chiral Alpha-Olefins Using Optically Active Ansa-Zirconocene Polymerization Catalysts. *J. Am. Chem. Soc.* **2004**, *126*, 8216.
8. Min, E. Y. J.; Byers, J. A.; Bercaw, J. E., Catalyst Site Epimerization during the Kinetic Resolution of Chiral  $\alpha$ -Olefins by Polymerization. *Organometallics* **2008**, *27*, 2179.
9. Hirahata, W.; Thomas, R. M.; Lobkovsky, E. B.; Coates, G. W., Enantioselective Polymerization of Epoxides: a Highly Active and Selective Catalyst for the Preparation of Stereoregular Polyethers and Enantiopure Epoxides. *J. Am. Chem. Soc.* **2008**, *130*, 17658.
10. Thomas, R. M.; Widger, P. C.; Ahmed, S. M.; Jeske, R. C.; Hirahata, W.; Lobkovsky, E. B.; Coates, G. W., Enantioselective Epoxide Polymerization Using a Bimetallic Cobalt Catalyst. *J. Am. Chem. Soc.* **2010**, *132*, 16520.

11. Zhong, Z.; Dijkstra, P. J.; Feijen, J., Controlled and Stereoselective Polymerization of Lactide: Kinetics, Selectivity, and Microstructures. *J. Am. Chem. Soc.* **2003**, *125*, 11291.
12. Nanda, S.; Rao, A. B.; Yadav, J. S., Enzyme Catalysed Kinetic Resolution of Racemic 2,2-dimethyl-3-(2,2-disubstituted vinyl)cyclopropane Carboxylic Acids Anchored on Polymer Supports. *Tetrahedron Lett.* **1999**, *40*, 5905.
13. Okudomi, M.; Nogawa, M.; Chihara, N.; Kaneko, M.; Matsumoto, K., Enzyme-Mediated Enantioselective Hydrolysis of Soluble Polymer-Supported Dendritic Carbonates. *Tetrahedron Lett.* **2008**, *49*, 6642.
14. Okudomi, M.; Shimojo, M.; Nogawa, M.; Hamanaka, A.; Taketa, N.; Matsumoto, K., Easy Separation of Optically Active Products by Enzymatic Hydrolysis of Soluble Polymer-Supported Substrates. *Tetrahedron Lett.* **2007**, *48*, 8540.
15. Okudomi, M.; Shimojo, M.; Nogawa, M.; Hamanaka, A.; Taketa, N.; Nakagawa, T.; Matsumoto, K., Easy Separation of Optically Active Secondary Alcohols by Enzymatic Hydrolysis of Soluble Polymer-Supported Carbonates. *Bull. Chem. Soc. Jpn.* **2010**, *83*, 182.
16. Issenhuth, J. T.; Dagonne, S.; Bellemin-Lapponnaz, S., A Practical Concept for the Kinetic Resolution of a Chiral Secondary Alcohol Based on a Polymeric Silane. *J. Mol. Cat. A* **2008**, *286*, 6.
17. Wallace, J. S.; Reda, K. B.; Williams, M. E.; Morrow, C. J., Resolution of a Chiral Ester by Lipase-Catalyzed Transesterification with Polyethylene Glycol in Organic Media. *J. Org. Chem.* **1990**, *55*, 3544.
18. Whalen, L. J.; Morrow, C. J., Resolution of a Chiral Alcohol Through Lipase-Catalyzed Transesterification of its Mixed Carbonate by Poly(Ethylene Glycol) in Organic Media. *Tetrahedron: Asymmetry* **2000**, *11*, 1279.
19. Vedejs, E.; Rozners, E., Parallel Kinetic Resolution Under Catalytic Conditions: A Three-Phase System Allows Selective Reagent Activation Using Two Catalysts. *J. Am. Chem. Soc.* **2001**, *123*, 2428.

20. Odian, G., *Principles of Polymerization*. 4th ed.; John Wiley and Sons: Hoboken, N.J., 2004; p 705.
21. Mandelkern, L., The Structure of Crystalline Polymers. *Acc. Chem. Res.* **1990**, *23*, 380.
22. Keith, J. M.; Larrow, J. F.; Jacobsen, E. N., Practical Considerations in Kinetic Resolution Reactions. *Adv. Synth. Catal.* **2001**, *343*, 5.
23. Le Borgne, A.; Spassky, N., Stereoselective Polymerization of  $\beta$ -Butyrolactone. *Polymer* **1989**, *30*, 2312.
24. Carpentier, J.-F., Discrete Metal Catalysts for Stereoselective Ring-Opening Polymerization of Chiral Racemic  $\beta$ -Lactones. *Macromol. Rapid Commun.* **2010**, *31*, 1696.
25. Childers, M. I.; Longo, J. M.; Van Zee, N. J.; LaPointe, A. M.; Coates, G. W., Stereoselective Epoxide Polymerization and Copolymerization. *Chem. Rev.* **2014**, *114*, 8129.
26. Widger, P. C. B.; Ahmed, S. M.; Hirahata, W.; Thomas, R. M.; Lobkovsky, E. B.; Coates, G. W., Isospecific Polymerization of Racemic Epoxides: a Catalyst System for the Synthesis of Highly Isotactic Polyethers. *Chem. Commun.* **2010**, *46*, 2935.
27. Tokunaga, M.; Larrow, J. F.; Kakiuchi, F.; Jacobsen, E. N., Asymmetric Catalysis with Water: Efficient Kinetic Resolution of Terminal Epoxides by Means of Catalytic Hydrolysis. *Science* **1997**, *277*, 936.
28. Miyake, G. M.; Chen, E. Y. X., Metallocene-Mediated Asymmetric Coordination Polymerization of Polar Vinyl Monomers to Optically Active, Stereoregular Polymers. *Macromolecules* **2008**, *41*, 3405.
29. Shimojo, M.; Matsumoto, K.; Nogawa, M.; Nemoto, Y.; Ohta, H., Enzyme-Mediated Enantioselective Hydrolysis of Poly(Ethylene Glycol)-Supported Carbonates. *Tetrahedron Lett.* **2004**, *45*, 6769.
30. Chen, C. S.; Fujimoto, Y.; Girdaukas, G.; Sih, C. J., Quantitative Analyses of Biochemical Kinetic Resolutions of Enantiomers. *J. Am. Chem. Soc.* **1982**, *104*, 7294.

31. Sheppard, C. I.; Taylor, J. L.; Wiskur, S. L., Silylation-Based Kinetic Resolution of Monofunctional Secondary Alcohols. *Org. Lett.* **2011**, *13*, 3794.
32. Clark, R. W.; Deaton, T. M.; Zhang, Y.; Moore, M. I.; Wiskur, S. L., Silylation-Based Kinetic Resolution of  $\alpha$ -Hydroxy Lactones and Lactams. *Org. Lett.* **2013**, *15*, 6132.
33. Rendler, S.; Auer, G.; Oestreich, M., Kinetic Resolution of Chiral Secondary Alcohols by Dehydrogenative Coupling with Recyclable Silicon-Stereogenic Silanes. *Angew. Chem., Int. Ed.* **2005**, *44*, 7620.
34. Moritani, Y.; Appella, D. H.; Jurkauskas, V.; Buchwald, S. L., Synthesis of  $\beta$ -Alkyl Cyclopentanones in High Enantiomeric Excess via Copper-Catalyzed Asymmetric Conjugate Reduction. *J. Am. Chem. Soc.* **2000**, *122*, 6797.
35. Lorenz, C.; Schubert, U., An Efficient Catalyst for the Conversion of Hydrosilanes to Alkoxysilanes. *Chem. Ber.* **1995**, *128*, 1267.
36. Lindsley, C. W.; Hodges, J. C.; Filzen, G. F.; Watson, B. M.; Geyer, A. G., Rasta Silanes: New Silyl Resins with Novel Macromolecular Architecture via Living Free Radical Polymerization. *J. Combin. Chem.* **2000**, *2*, 550.
37. Akhani, R. K.; Moore, M. I.; Pribyl, J. G.; Wiskur, S. L., Linear free-energy relationship and rate study on a silylation-based kinetic resolution: mechanistic insights. *J. Org. Chem.* **2014**, *79*, 2384.
38. Toy, P. H.; Janda, K. D., Soluble Polymer-Supported Organic Synthesis. *Acc. Chem. Res.* **2000**, *33*, 546.
39. Dickerson, T. J.; Reed, N. N.; Janda, K. D., Soluble Polymers as Scaffolds for Recoverable Catalysts and Reagents. *Chem. Rev.* **2002**, *102*, 3325.
40. Benoit, D.; Chaplinski, V.; Braslau, R.; Hawker, C. J., Development of a Universal Alkoxyamine for "Living" Free Radical Polymerizations. *J. Am. Chem. Soc.* **1999**, *121*, 3904.
41. Arai, M., Chlorination by Sulfuryl Chloride. III. The Reactivities of the C-H Bond to Sulfuryl Chloride. *Bull. Chem. Soc. Jpn.* **1964**, *37*, 1280.

42. Lee, K. H., Directive Effects in Benzylic Hydrogen Atom Abstraction—II : Radical Chlorination by Sulphuryl Chloride. *Tetrahedron* **1969**, 25, 4363.
43. (a) Conversions and selectivity factors are based on the ee of the recovered starting materials and products. (b) Selectivity factors are an average of two runs. Conversions are from a single run.
44. Alexandratos, S. D.; Miller, D. H. J., Microenvironmental Effect in Polymer-Supported Reagents. 1. Influence of Copolymer Architecture on the Mitsunobu Reaction. *Macromolecules* **1996**, 29, 8025.
45. Anyanwu, U. K.; Venkataraman, D., Effect of Spacers on the Activity of Soluble Polymer Supported Catalysts for the Asymmetric Addition of Diethylzinc to Aldehydes. *Tetrahedron Lett.* **2003**, 44, 6445.

## Chapter 4 Mechanistic Investigations of a Silylation-Based Kinetic Resolution: Reaction Progress Kinetic Analysis

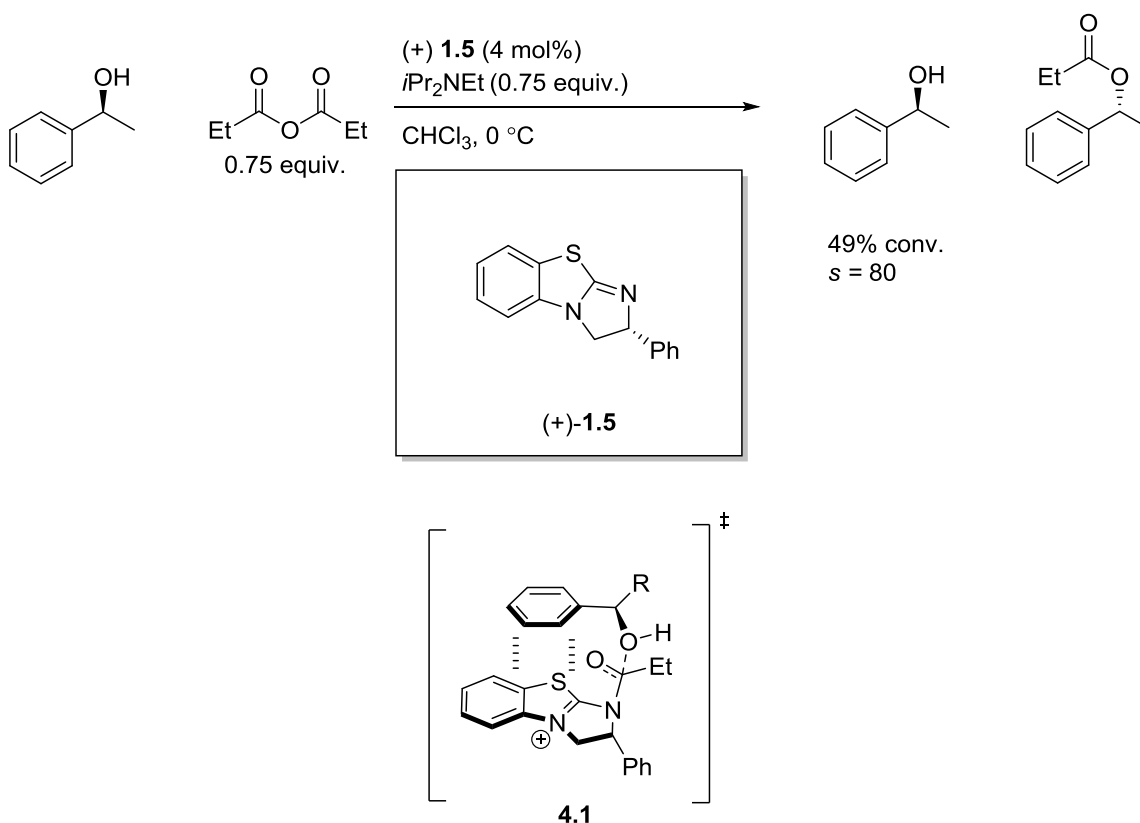
### 4.1. Introduction and Scope

In this chapter, the endeavors to understand the mechanism of the triphenylsilyl chloride-based resolution of secondary alcohols will be discussed. Despite similarities to the asymmetric acyl transfer kinetic resolutions developed by Birman, relatively little is known about the intermediate or overall mechanism involved specifically in the silylation-based resolution. Herein, the effort to develop a kinetic model for the reaction employing reaction progress kinetic analysis (RPKA) is highlighted.

The isothiourea catalyzed acylation-based resolution discovered by Birman<sup>1-3</sup> has been thoroughly studied and is relatively well understood. As mentioned in chapter 1, this resolution and related reactions are capable of enriching a variety of alcohols to include secondary benzylic alcohols with excellent selectivities (Scheme 4.1) utilizing benzotetramisole **1.5** and related catalysts. The proposed diastereomeric transition state **4.1** is thought to be facilitated by favorable  $\pi$ - $\pi$  stacking interaction between the alcohol and the isothiourea catalyst (Scheme 4.1). This hypothesis was supported by computational analysis of related acylations of secondary alcohols catalyzed by related isothiourea catalysts.<sup>4</sup> Birman has also found that these non-bonding interactions at the transition state are important in the resolution of other substrates including the resolution of azlactones<sup>3</sup> and lactones.<sup>5</sup> Additionally, a decrease in enantioselectivity between



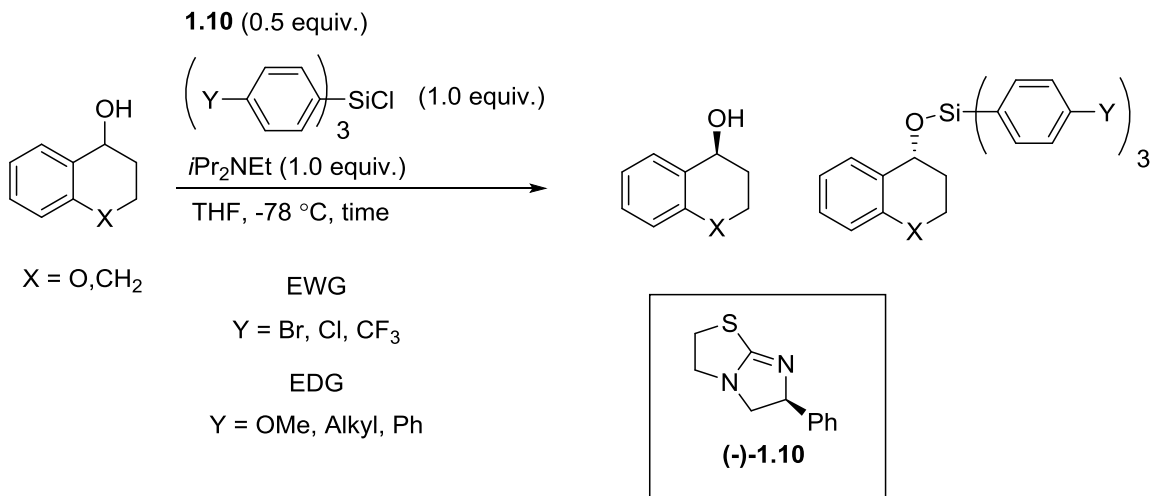
catalysts **1.5** and levamisole **1.10** has been attributed to this favorable intramolecular interaction.<sup>1</sup> Levamisole **1.10** lacks the extended  $\pi$ -system that the benzo moiety affords to benzotetramisole **1.5**. The experimental result of a lower selectivity with levamisole vs benzotetramisole further corroborates the computational findings in regards to the transition state structure **4.1**.



**Scheme 4.1 Acylation-Based Kinetic Resolution Developed by Birman including Proposed Transition State**

Previously, a linear-free energy relationship study<sup>6</sup> was employed to probe the silylation-based resolution developed by Wiskur.<sup>7</sup> This investigation utilized two different benzylic alcohols, 4-chromanol and  $\alpha$ -tetralol, and a variety of synthetically

prepared<sup>8</sup> triarylsilyl chlorides bearing *para*-electron-withdrawing or *para*-electron-donating groups (EWG or EDG; Scheme 4.2). The alkyl EDG were found to significantly slow the rate of reaction as well as increase the selectivity factors for the kinetic resolution for both of the aforementioned alcohols. Conversely, the rate increased and the selectivity factor degraded when *para*-EWGs were employed. The sterics of the substituents were also found to have a small effect on enantioselectivity through evaluation of the Charton parameters,<sup>9-11</sup> but the electronic effects<sup>12</sup> of the substituents were found to be far more important to enantioselectivity. The results were consistent with increase in negative charge or decrease in positive charge at the transition state<sup>13</sup> consistent with structures proposed by Bassindale<sup>14-15</sup> (See section 4.7 for a discussion of plausible intermediate structures). The enantioselective step was proposed to proceed through a tetravalent intermediate with an S<sub>N</sub>2-like alcohol attack on the catalyst-activated silyl chloride. This is based upon the selectivity increasing effect of sterically demanding substituents in the *para*-position of several triarylsilyl chlorides. The knowledge gained from this linear free energy mechanistic investigation has led to the use of more enantioselective silyl sources bearing EDG alkyl groups in the *para*-position. Use of these triaryl silyl sources has expanded the substrate scope to include 2-arylcyclohexanols<sup>16</sup> and inspired a polymer-supported methodology.<sup>17</sup>



### Scheme 4.2 General Approach to Linear-Free Energy Relationship Studies

With the data from the LFER study in hand, we next turned our attention to other methods of determining a viable, complete mechanistic picture. A collaborative computational study has to date not been successful. However, the kinetic evaluation of 2-arylcycloalcohols in the homobenzotetramisole<sup>2</sup> (**2.4**) catalyzed acylation-based resolution sparked our interest towards this route of investigation. In this recent investigation, a thorough kinetic model for the acylation based kinetic resolution was realized.<sup>18</sup> After kinetic investigations, the mechanistic cycle was determined to most likely proceed via the mechanistic cycle shown in Figure 4.1. A pre-equilibrium was found to exist between free catalyst and acylated catalyst (**2.4**) and (**4.2**) which favored the free catalyst. This equilibration step was supported by <sup>1</sup>H NMR analysis of various mixtures of catalyst and propanoic anhydride. The rate determining step was demonstrated to be the acylation of the alcohol. Overall, the order was found to be third order with alcohol, catalyst and anhydride demonstrated to each be first order.

This study was able to gather kinetic data by employing the RPKA method of analyzing kinetic data pioneered by Blackmond.<sup>19</sup> The RPKA method has been successfully utilized to investigate a variety of complex, catalytic reactions.<sup>20-25</sup>

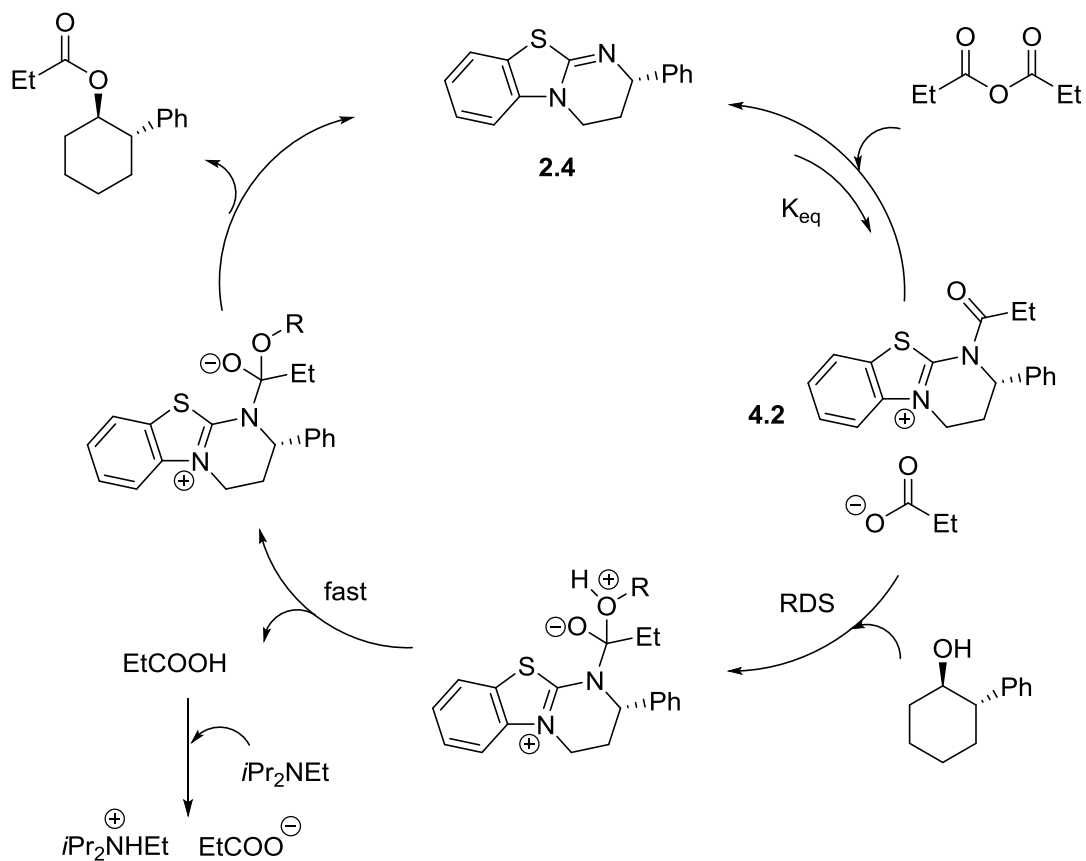


**Figure 4.1 Mechanistic Cycle for the Asymmetric Acylation of 2-Arylcyclohexanols**

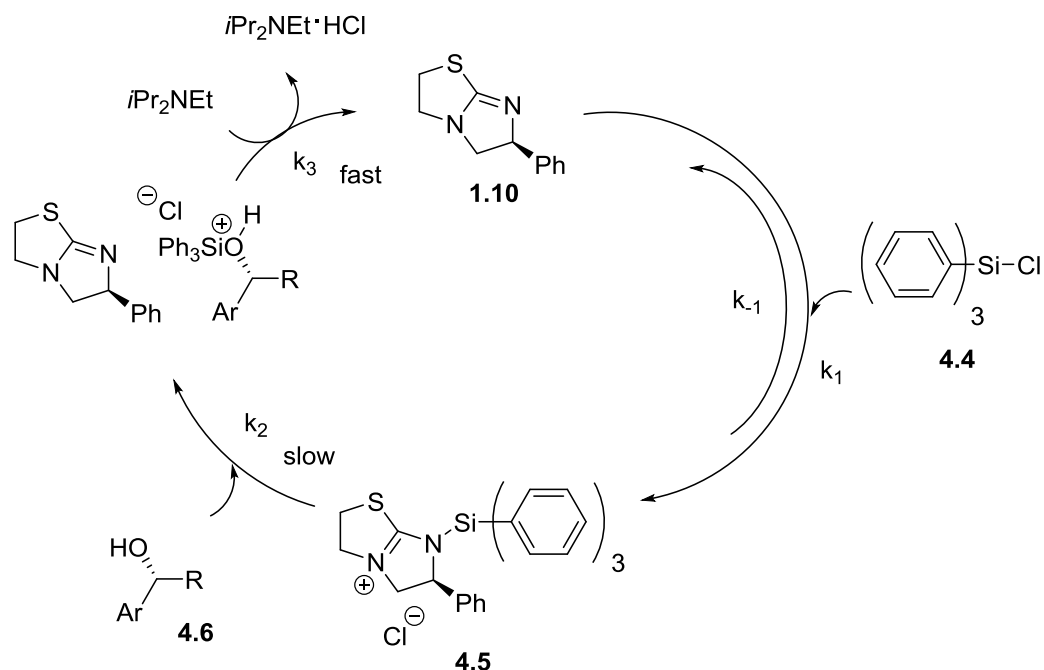


**Figure 4.2 Proposed Mechanistic Cycle for the Silylation Reaction**

#### 4.2. Reaction Progress Kinetic Analysis: an Overview

The kinetic analysis techniques developed by Blackmond<sup>19</sup> allows the investigator to gather kinetic data in fewer experiments than classical approaches and run the kinetic experiments under conditions similar to actual reaction conditions. This avoids the use of reagents in ten-fold excess common to classic approaches.<sup>26-27</sup> Instead, the reaction progress is monitored at experimental reaction conditions from approximately 15-80% conversion via an in situ analytical technique, commonly NMR or IR spectroscopy. Since the kinetic experiments are designed under similar conditions from optimized conditions, these reactions can be more accurate to the true catalytic cycle by avoiding the large excesses of different reagents.

Since all mechanistic investigations are based upon hypothesis, we first sought to propose a catalytic cycle for the silylation-based kinetic resolution (Figure 4.2). Based

upon the knowledge gained from kinetic analysis of the Briman's acylation, we too proposed the reaction proceeds through a pre-equilibrium step between free catalyst and silylated catalyst (**1.10** and **4.5**, Figure 4.2). The presumed rate determining step is thought to be the enantioselective step, the silylation of the alcohol (**4.6**) to form product ( $k_2$ , Figure 4.2). It is unknown what affect base has on rate. It had been demonstrated in previous studies<sup>7</sup> that changes in base structure had a measurable effect on enantioselectivity. Despite this, we hypothesized the base would act as an HCl scavenger after the rate determining step and therefore have no effect on rate ( $k_3$ , Figure 4.2).

With a proposed catalytic cycle in hand, focus was next placed on determining a kinetic equation which matches our proposed mechanism. If an equilibration step occurs prior to a second rate determining step, the rate for the silylation reaction can be characterized by the diagram shown in Figure 4.3. Because  $k_2$  is much smaller than  $k_1$ , or  $k_2 \ll k_1$ , we can invoke the pre-equilibrium approximation<sup>28</sup> which assumes that the reactants, silyl chloride and catalyst, are in equilibrium with the active species **4.5**. If this is the case, the rates of formation of intermediate (A, equation 4.1) and destruction of intermediate (B and C, equation 4.2) eventually equal one another. The intermediate can either be destroyed by reaction to form product or disassociation to form free catalysts and silyl chloride. As a result of the stability of silyl ethers,<sup>29</sup> we also assume the formation of product (pathway C) is irreversible; therefore,  $k_{-2}$  is considered negligible.

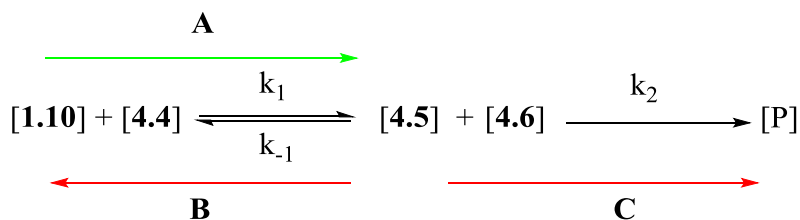


**Figure 4.3 Employing the Pre-Equilibrium Approximation**

We can now write the rate law for each of these individual steps (equations 4.1 and 4.2) in terms of formation of intermediate (rate<sub>A</sub>) or destruction of intermediate (rate<sub>B</sub> + rate<sub>C</sub>).

$$\text{rate}_A = \frac{d [4.5]}{dt} = k_1 [1.10] [4.4]$$

**Equation 4.1**

$$\text{rate}_{B+C} = - \frac{d [4.5]}{dt} = k_2 [4.5] [4.6] + k_{-1} [4.5]$$

**Equation 4.2**

Invoking the equilibrium approximation as discussed above indicates rate<sub>A</sub> and rate<sub>B+C</sub> are equal during a reaction at steady state. This yields equation 4.3 which contains two concentration values that are unknown: concentration of intermediate **4.5** and concentration of free catalyst **1.10**.

$$k_2 [4.5] [4.6] + k_{-1} [4.5] = k_1 [1.10] [4.4]$$

**Equation 4.3**

We can use a simple equation that describes the equilibrium between free and silylated catalyst to remove the unknown concentration of free catalyst [1.10]. The initial concentration of catalyst must equal the sum of the concentrations of the free and bound catalyst. This gives us equation 4.4 which we can rearrange to equation 4.5 to yield an equation that equals the concentration of free catalyst in terms of a known concentration: initial catalyst concentration.

$$[1.10]_o = [1.10] + [4.5]$$

**Equation 4.4**

$$[1.10] = [1.10]_o - [4.5]$$

**Equation 4.5**

Recall from equation 4.3 we had the conundrum of having two unknown concentrations: free catalyst [1.10] and intermediate [4.5]. We can insert equation 4.5 in for [1.10] to yield equation 4.6 that contains only species 4.5 as the unknown concentration. We can then solve for the unknown species 4.5 by following the algebraic steps outlined in equations 4.6-4.10.

$$k_2 [4.5] [4.6] + k_{-1} [4.5] = k_1 \{ [1.10]_o - [4.5] \} [4.4]$$

**Equation 4.6**

$$k_2 [4.5] [4.6] + k_{-1} [4.5] = k_1 [1.10]_o [4.4] - k_1 [4.5] [4.4]$$

**Equation 4.7**

$$k_2 [4.5] [4.6] + k_{-1} [4.5] + k_1 [4.5] [4.4] = k_1 [1.10]_o [4.4]$$

**Equation 4.8**

$$[4.5] \{ k_2 [4.6] + k_{-1} + k_1 [4.4] \} = k_1 [1.10]_o [4.4]$$

**Equation 4.9**

$$[4.5] = \frac{k_1 [1.10]_o [4.4]}{k_2 [4.6] + k_{-1} + k_1 [4.4]}$$

**Equation 4.10**



Finally, we must look at the catalytic cycle to determine our proposed rate determining step. If pathway C from Figure 4.3 is the rate determining step, the rate is dependent upon  $k_2$ , alcohol concentration [4.6], and intermediate concentration [4.5] (equation 4.11). Since we have used the equilibrium approximation demonstrated above to find [4.5], we can substitute equation 4.10 in for the unknown intermediate concentration to yield the overall rate equation 4.12.

$$\text{rate} = \frac{d [P]}{dt} = k_2 [4.6] [4.5]$$

**Equation 4.11**

$$\text{rate} = \frac{k_1 k_2 [4.6] [4.4] [1.10]_o}{k_{-1} + k_1 [4.4] + k_2 [4.6]}$$

**Equation 4.12**

The overall rate equation depicted above is no simple equation. The alcohol and silyl chloride appear in both the numerator and the denominator meaning simple integer orders with respect to these substrates may not be possible. Moreover, the equation is complicated by an unknown rate constant  $k_{-1}$  that is additive in the denominator without an associated concentration. We can remove this rate constant by dividing the numerator and denominator by  $k_{-1}$  to yield the rate equation in the one-plus form where rate constants are given as a, b and c (Equation 4.13).

$$\text{rate} = \frac{a [4.6] [4.4] [1.10]_o}{1 + b [4.4] + c [4.6]}$$

$$a = \frac{k_1}{k_{-1}} k_2 \quad b = \frac{k_1}{k_{-1}} \quad c = \frac{k_2}{k_{-1}}$$

**Equation 4.13**

Even after this simplification the concentrations of alcohol and silyl chloride appear in the rate equation in the numerator and denominator. This is further complicated by the fact that they are both changing since they are consumed as the reaction progresses. This major difficulty is solved by using a new term “excess” which is defined as the difference in initial concentration of alcohol **4.6** and silyl chloride **4.4**. We can use the stoichiometry of the silylation reaction shown in Figure 4.2 to assume that for every molecule of product that is formed, a molecule of alcohol and silyl chloride must be consumed. In this way we can monitor only one species, alcohol or silyl chloride, and know by default the concentration of the other species. We must only know the difference in initial concentrations. Another implication of this stoichiometry is the fact that the excess must remain constant throughout the reaction. This principle gives us equation 4.14 which we can rearrange to show the silyl chloride concentration in terms of [“excess”] which is a constant and alcohol which we can monitor via in situ analytical techniques.

$$[\text{“excess”}]_0 = [4.4]_0 - [4.6]_0$$

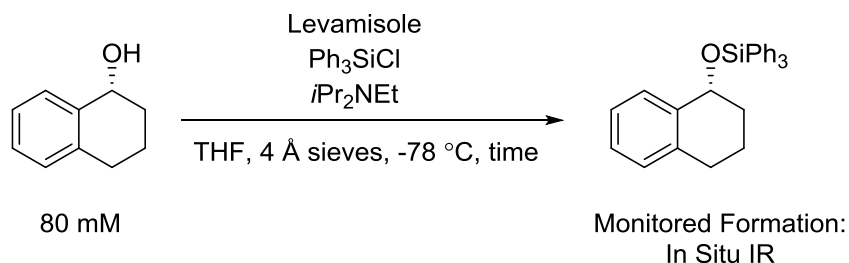
**Equation 4.14**

$$[4.4] = [\text{“excess”}]_0 + [4.6]$$

**Equation 4.15**

With the hypothetical kinetics of the reaction understood, we sought an analytical technique to measure the alcohol concentration throughout the reaction. In situ IR was selected as the analytical technique for this investigation since the kinetic resolution is

carried out at  $-78\text{ }^{\circ}\text{C}$ , a costly temperature to analyze a reaction employing NMR. Rate data from previous LFER studies<sup>6</sup> using in situ IR spectra were found to be accurate and reproducible; therefore, this method of analysis was applied to the kinetic analysis of a silylation-based reaction. An alcohol from this previous study, (*R*)-tetralol was also selected for analysis. We have selected the (*R*)-enantiomer since it is the fast reacting enantiomer when silylated with triphenylsilyl chloride by levamisole **1.10** as catalyst (Scheme 4.3).<sup>7</sup> By using a single enantiomer we make the rate data less complicated since the rate of the slow reacting enantiomer proceeds at a different rate. A resolution of a racemic mixture is a reaction with two competing rates of reaction. Subsequent kinetic studies will vary the quantities of reagents to determine each substrates effect on rate with respect to the fast reacting enantiomer.



**Scheme 4.3 General Reaction for Kinetic Experiments**

Regardless of the analytical method employed, the data for an RPKA study is generally processed as shown for one of our kinetic experiments below. The primary data obtained from monitoring a reaction in all studies discussed in this chapter is absorbance (A). The absorbance is directly related to the concentration of product according to Beer's Law (Equation 4.16) with path length and molar absorptivity as constants. Aliquots are removed during the reaction and analyzed via  $^1\text{H}$  NMR in order to determine

the fraction conversion (See experimental section for details). This conversion data is then used to determine the remaining alcohol starting material concentration [ROH] by using the fraction conversion (x) and initial alcohol concentration (Equation 4.18 and 4.19). With the alcohol concentration and associated absorbance known at each aliquot point, a plot can be prepared where absorbance is the y-axis and concentration of alcohol [ROH] is the x-axis. The slope of this line when the y-intercept is set to the absorbance at  $t_0$  corresponds to the molar attenuation coefficient for the product multiplied times path length both of which are constants ( $\epsilon$  and  $l$ , respectively, Figure 4.4). Note that all data have been smoothed with an adjacent three points averaging. The purpose of subtracting the initial absorbance from the observed absorbance is to force the data to start at an absorbance of zero to give a zero start point for concentration (Equation 4.17).

$$A = \epsilon c l$$

**Equation 4.16**

$$\frac{(A - A_0)}{\epsilon l} = c = [P]$$

**Equation 4.17**

$$x = \frac{[P]}{[ROH]_0}$$

**Equation 4.18**

$$[ROH] = [ROH]_0(1-x)$$

**Equation 4.19**

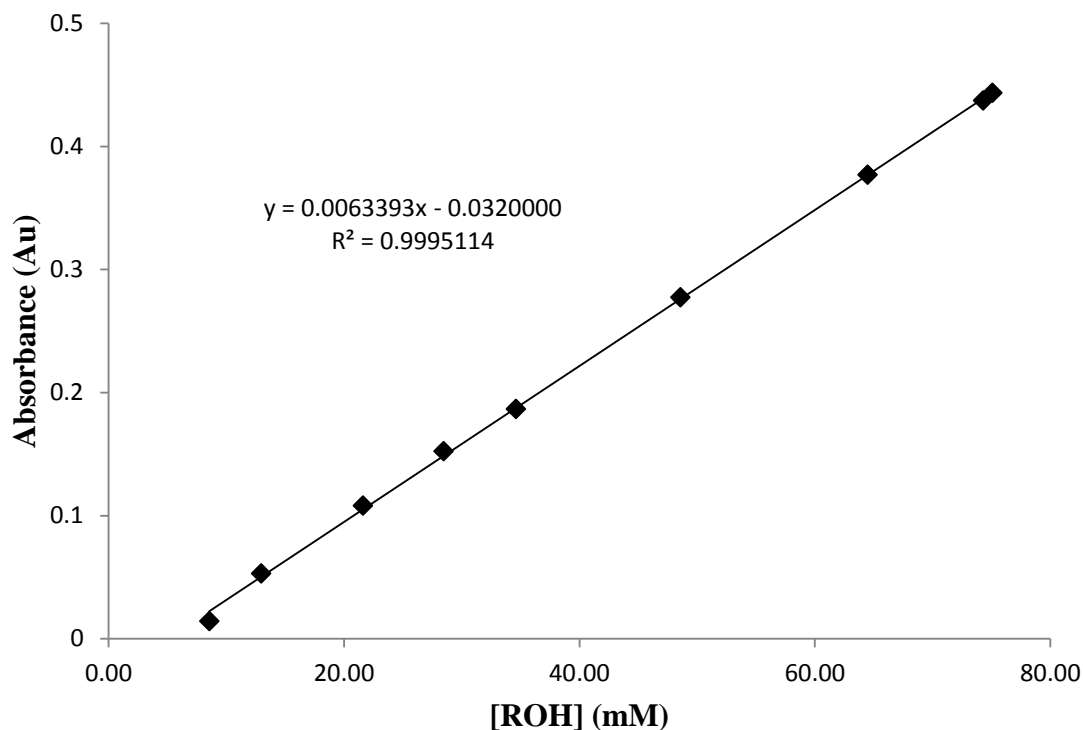


**Figure 4.4 Employing NMR Analysis to Determine IR Concentration Data**

Reaction was run with 0.25 equiv. of catalysts, 1.2 equiv. of silyl chloride and 1.2 equiv. of  $i\text{Pr}_2\text{NEt}$  according to Scheme 4.3. Alcohol concentration data was determined by  $^1\text{H}$  NMR of aliquots taken during the reaction.

With the product of path length and molar absorptivity obtained as described above, the concentration of alcohol can be calculated for each absorbance data point by employing the Beer's Law equation. Furthermore the percent conversion or product conversion can also be obtained by subtracting the alcohol concentration at each time from the starting alcohol concentration. This data is plotted together with time on the x-axis and the percent conversion on the y-axis the NMR data obtained above to confirm both methods give the same conversion data (Figure 4.5, green curve). This ensures the data obtained from the in situ IR is accurate throughout the experiment.

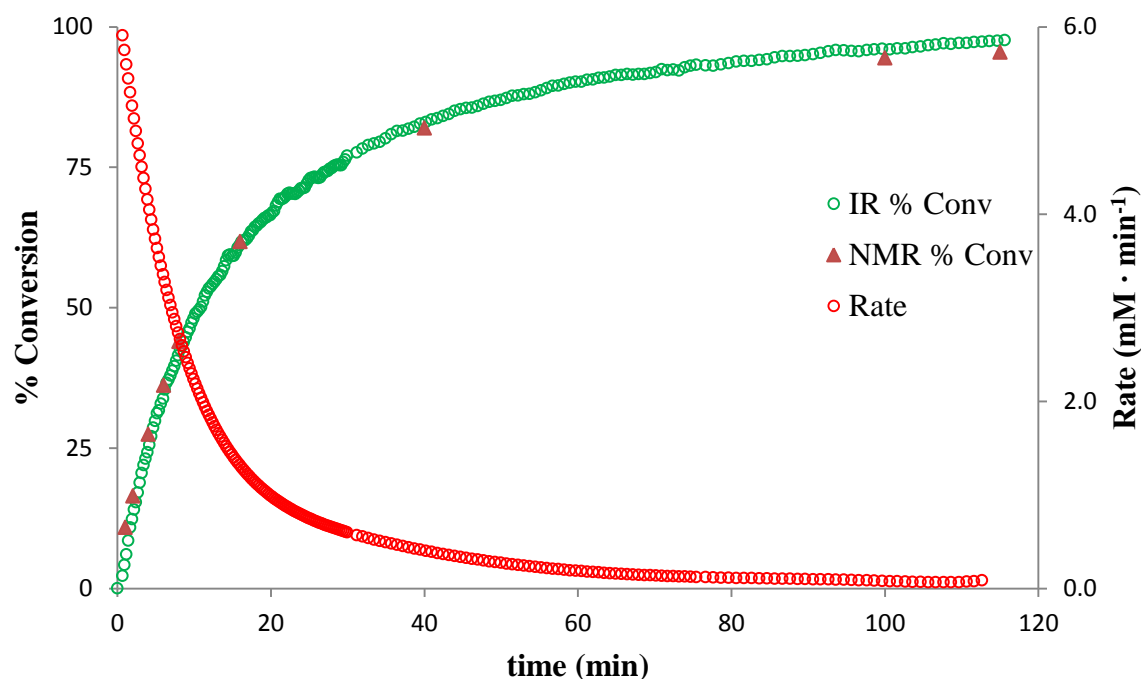


**Figure 4.5 Verifying the Conversion from IR Data with NMR Analysis**

Reaction was run with 0.25 equiv. of catalysts, 1.2 equiv. of silyl chloride and 1.2 equiv. of  $i\text{Pr}_2\text{NEt}$  according to Scheme 4.3. Alcohol concentration data was determined by  $^1\text{H}$  NMR.

With concentration of product [P] obtained at every point of reaction time from in situ IR measurements, the rate of the reaction can now be determined. In fact, the rate of the entire reaction can be observed at each measured point by taking the derivative of an equation that fits the concentration over time data. This is one of the advantages of the RPKA approach, a large quantity of rate data is produced from a single run. To accomplish this conversion versus time data was fit to a 9<sup>th</sup> -11<sup>th</sup> order polynomial equation employing a mathematical program (Origin version 6.6 or PolySolve version

3.7). The derivative of this polynomial equation through the use of the power rule yields  $d[P]/dt$ , or rate. Recall that prior to polynomial fit all data was smoothed through simple adjacent three points averaging. This smoothing step facilitates the non-linear curve fitting process. For our example reaction, the derivative of the polynomial fit is shown; therefore, a plot is produced containing rate vs time data (Figure 4.5, red curve). Note that fraction conversion and not percent conversion are used for the data that is fitted to the polynomial in order to conform to equation 4.19.

The rate data obtained from this method can then be plotted in various ways to form graphical rate equations. These graphical approaches are advantageous as they offer the ability to quickly analyze and understand kinetic data. A classic approach to analyze the kinetics of reactions primarily deals with a large excess of a reagent and the first 10 to 15% of reaction progress. For the graphical rate data discussed in this chapter, the rate data corresponding to 15% to 80% conversion is utilized. This conversion range corresponds to the first turnovers of catalyst to the last turnover of catalyst and represents steady state conditions for the reaction. The steady state refers to a reaction state in a constant rate of conversion; therefore, the graphical rate approaches discussed here become inaccurate for induction periods or at high conversions. This is not to be confused with the steady state approximation which is an approximation based upon a different catalytic cycle from our proposed mechanism. Again, we propose a slow second step which would conform to pre-equilibrium conditions.

For our silylation reaction, we have demonstrated the method for the determination of alcohol concentration  $[ROH]$  at each time-point. A graphical rate equation of rate on the y-axis and  $[ROH]$  on the x-axis produces a simple graphical rate

equation which can provide valuable information. The reaction proceeds from right to left on these graphs as the concentration of the starting material is consumed (Figure 4.6). Elementary first order reactions, reactions that only have one substrate that is first order, would demonstrate a straight line plot with respect to substrate. However, for our proposed pre-equilibrium like mechanism further evaluation of the data is required to determine orders with respect to each reagent, catalyst, and substrate. This is because of the complex nature of the equation derived previously (Equation 4.13).<sup>19</sup> These simple graphical rate equations are useful to discriminate between zeroth and positive order with respect to substrates and catalysts for complex reactions. For example, a demonstration of zeroth order in a reactant can be obtained relatively simply. If a reactant is varied while holding the other reagents' concentration constant, overlay of data from the two runs when plotted as rate versus substrate concentration would suggest zeroth order in the varied substrate. An example of this will be demonstrated for the base concentration in the silylation-based resolution (Figure 4.13). Otherwise, determining the order more accurately (1<sup>st</sup>, 2<sup>nd</sup>, 3<sup>rd</sup>, fractional) with respect to substrate or reagent requires further interrogation of the data. In each of the following sections methods to interrogate the data will be discussed in further detail.



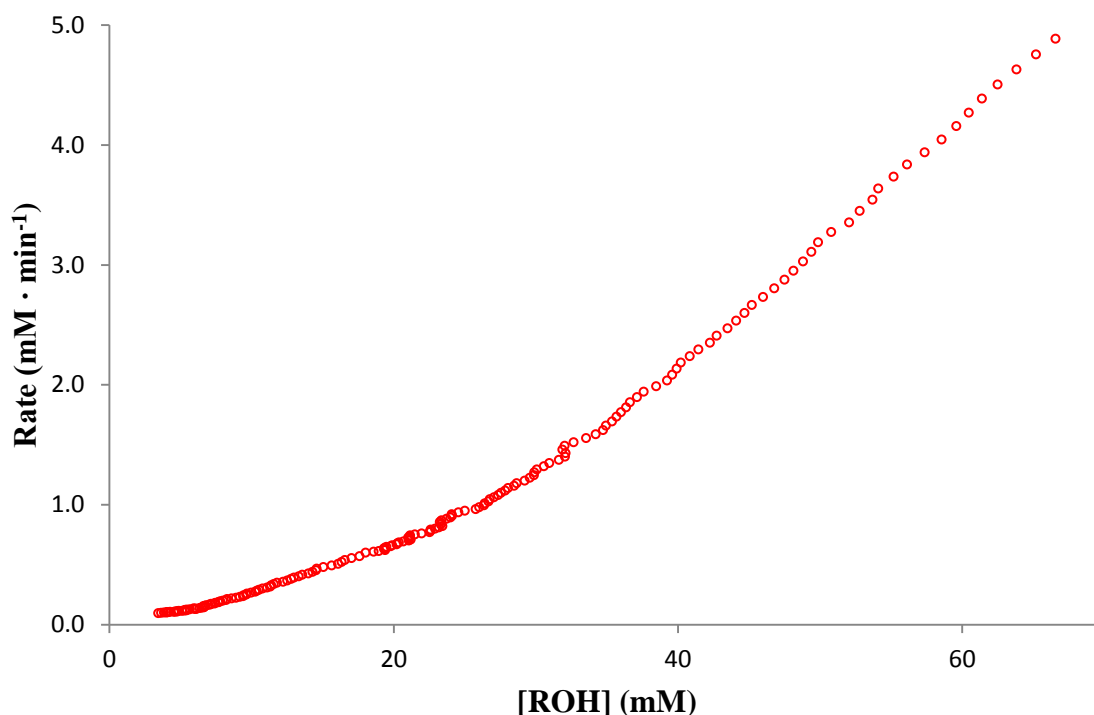


**Figure 4.6 Simple Graphical Rate of the Silylation-Based Reaction**

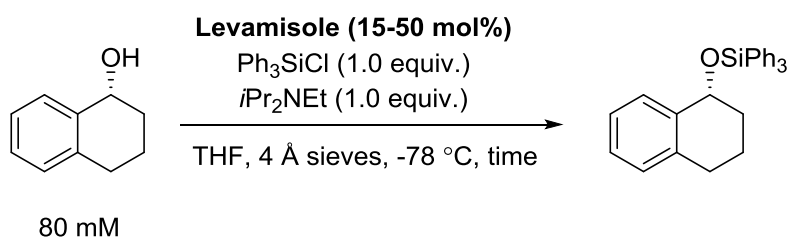
Reaction was run with 0.25 equiv. of catalysts, 1.2 equiv. of silyl chloride and 1.2 equiv. of *i*Pr<sub>2</sub>NEt according to Scheme 4.3. Alcohol concentration data was determined by <sup>1</sup>H NMR.

In the following sections a variety of these graphical rate equations are explored to determine the order with respect to the alcohol **4.6**, silyl chloride **4.4**, base and catalyst **1.10**. These graphical equations will also be utilized to refute catalyst degradation and product inhibition.

#### **4.3. Turnover Frequency Study: Determination of Catalyst Reaction Order**

We first turned our attention to the catalyst, and the effect on overall rate of catalyst concentration. According to our presumed catalytic cycle the reaction should be overall first order with respect to catalyst. It is common for silyl species to form

pentavalent<sup>30-31</sup> and even hexavalent species in the presence of Lewis base.<sup>32</sup> In order to demonstrate the reaction is proceeding with only one catalyst molecule bound to the silicon, a series of four experiments were designed. These reactions were carried out keeping the concentration of silyl chloride and alcohol constant while changing the catalyst concentration from 15-50 mol % with respect to alcohol (Scheme 4.6). These reactions are analyzed under the same “excess” i.e. the difference between alcohol and silyl chloride concentrations are the same for all experiments. This is possible because the concentration of the catalyst appears only once in the numerator of equation 4.13.



**Scheme 4.4 General Reaction for Turnover Frequency Experiments**

We first plot a simple graphical rate equation of rate on the y-axis and alcohol concentration on the x-axis. From the data of the simple graphical rate equation (Figure 4.7) the catalyst has an expected positive effect on rate, such that the rate increases with each increase in initial catalyst. Also notable from these plots is the failure to reach full conversion despite an equimolar concentration of silyl chloride to alcohol. The data from these runs was further evaluated by dividing the rate by initial catalyst concentration  $[1.10]_0$ , a constant, to yield the turnover frequency (TOF). This normalizes the data, eliminating initial catalyst concentration from the numerator of equation 4.13 to yield a new equation 4.20.

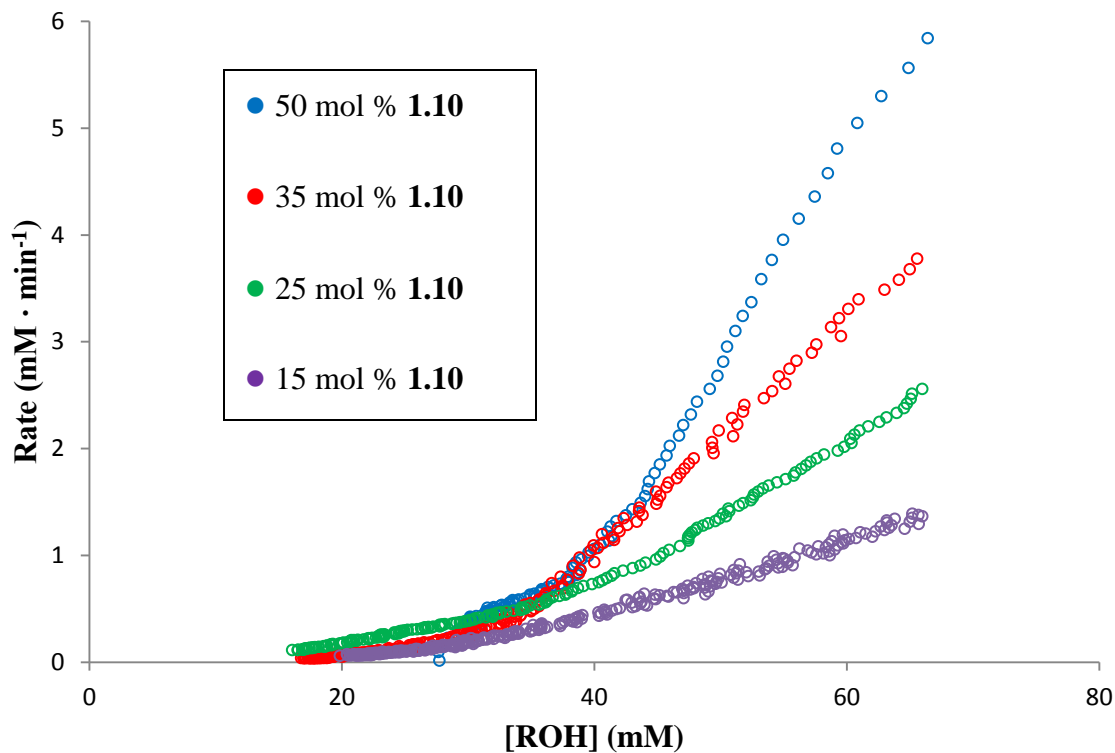


**Figure 4.7 Demonstration of Positive Order in Catalyst**

Reaction was run with the shown mol% of catalyst, 1.0 equiv. of silyl chloride and 1.0 equiv. of *i*Pr<sub>2</sub>NEt according to Scheme 4.3.

$$\frac{\text{rate}}{[\mathbf{1.10}]_0} = \frac{a[\mathbf{4.6}][\mathbf{4.4}]}{1 + b[\mathbf{4.4}] + c[\mathbf{4.6}]}$$

**Equation 4.20**

By removing the catalyst from the numerator the rate should now no longer be dependent upon catalysts concentration, assuming the correct order with respect to catalyst is chosen. In this case we have chosen an order of one in catalyst to plot. When TOF is plotted on the y-axis and substrate concentration [ROH] is plotted on the x-axis, the different runs overlay. This suggests the reaction is first order in catalyst (Figure 4.8).

The shape of these plots is irrelevant. The goal of these plots is overlay of the data. The non-linear shape of the reaction (Figure 4.6) is retained in these plots due to the fact that the rate is normalized to a constant as opposed to the other approaches to be discussed later (Section 4.4).

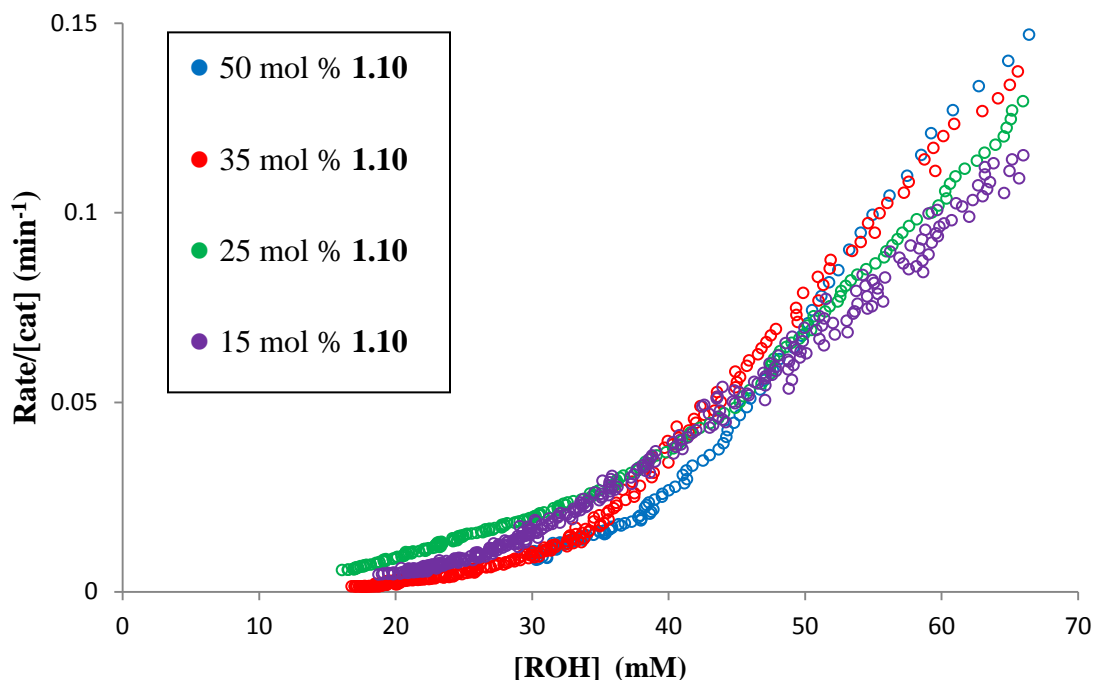


**Figure 4.8 Overlay of Turnover Frequency versus Alcohol Concentration**

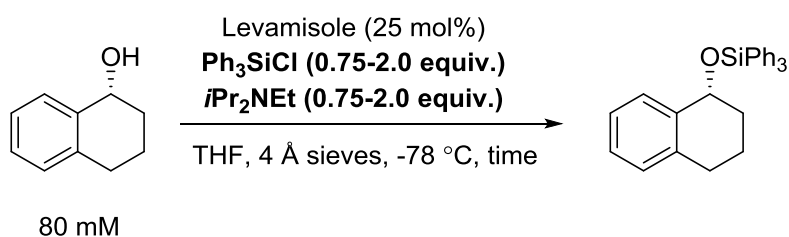
Reaction was run with the shown mol% of catalyst, 1.0 equiv. of silyl chloride and 1.0 equiv. of *i*Pr<sub>2</sub>NEt according to Scheme 4.3.

#### 4.4. Different Excess Studies of Alcohol and Silyl Chloride

A series of experiments were then carried out to determine the order of two substrates, silyl chloride and alcohol, in the overall kinetic scheme. Based upon our hypothetical catalytic cycle the kinetic resolution should demonstrate it is first order in alcohol (Figure 4.2). The order in silyl chloride may be either first order or zeroth order

depending upon the magnitudes of  $k_1$  and  $k_{-1}$  that exists between free catalyst and complexed catalyst **1.10** and **4.5**, respectively. If for instance  $k_1$  is large and  $k_2$  is small, a build-up of active species **4.5** occurs. Thus the resting state of the catalyst would be the catalyst-silylchloride complex and the b-term from equation 4.13 would become large. This would cause the silyl chloride order to become fractional even to a point where the reaction becomes “saturated” with silyl chloride and thus has no significant effect on rate. This is termed pseudo-zeroth order. An order of one with respect to silyl chloride could occur if  $k_2$  is large, such that the rate determining step is  $k_1$  over  $k_{-1}$ , which is the  $K_{eq}$  for the catalyst complexation. Therefore, the reaction would become zeroth order in alcohol as the  $K_{eq}$  becomes dominant and rate determining.

With this general knowledge, we designed a series of experiments with different “excess” concentrations. We ran four trials with varying silyl chloride concentration from 0.75 to 2.0 equivalents while holding the alcohol concentration constant. The base concentration was also varied to match the silyl chloride concentration (Scheme 4.7).



**Scheme 4.5 General Reaction for “Different Excess” Experiments**

The selected reagent or substrate to vary is of no consequence, since the term excess is the constant difference between silyl chloride and alcohol (Equation 4.15). As long as the difference between initial concentrations of alcohol and silyl chloride are

known, graphical rate equations can be produced that monitor both species at once. When the order of alcohol is first order, a plot of rate normalized to alcohol concentration versus the silyl chloride concentration should yield a straight line with overlay of the different data even though they were obtained with different excess. Again, dividing the rate equation 4.13 by alcohol concentration removes it from the numerator of the rate equation to produce a new equation shown below as equation 4.21. If the correct power is chosen for alcohol concentration [4.6] (i.e. first order) and the c term is negligible the data is should theoretically form a straight line with overlay of data. Note here that both alcohol concentration and silyl chloride concentration are both changing as the reaction progresses. This is in stark contrast to the TOF data in section 4.3.

$$\frac{\text{rate}}{[4.6]} = \frac{a[4.4][1.10]_o}{1 + b[4.4] + c[4.6]}$$

**Equation 4.21**

When all four reactions from scheme 4.5 are plotted as rate normalized to alcohol concentration a straight line forms. Additionally, excellent overlay of data makes it abundantly clear that the alcohol is first order employing the range of conditions shown (Figure 4.9). The c-term in equation 4.21 is negligible.

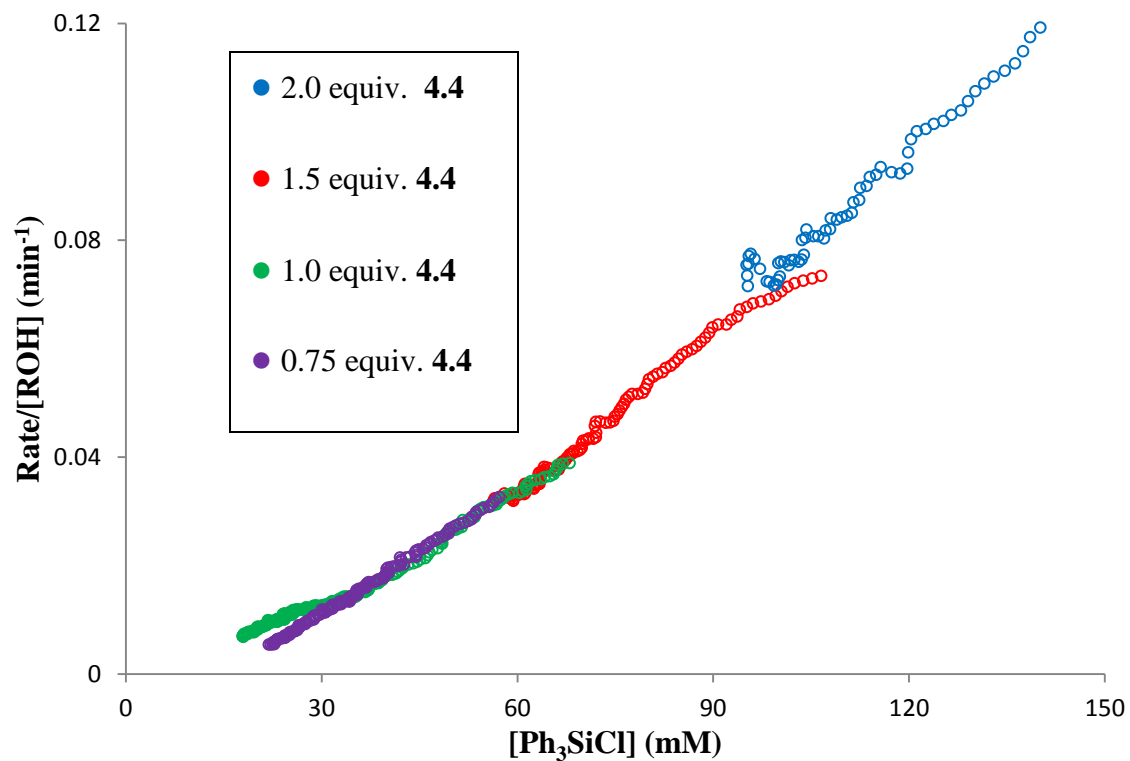


**Figure 4.9 Determining the Order with Respect to Alcohol with “Different Excess” Protocol**

Reaction was run with the shown 25 mol% of catalyst, the shown equivalents of silyl chloride with an equivalent of *i*Pr<sub>2</sub>NEt to match the silyl chloride concentration. See Scheme 4.3.

We next plotted same data from the four runs in scheme 4.5 in a different manner in order to determine the silyl chloride order. A simple graphical rate equation demonstrates a positive effect of silyl chloride concentration on rate (Figure 4.10). Each increase in silyl chloride concentration results in an overall increase in rate.

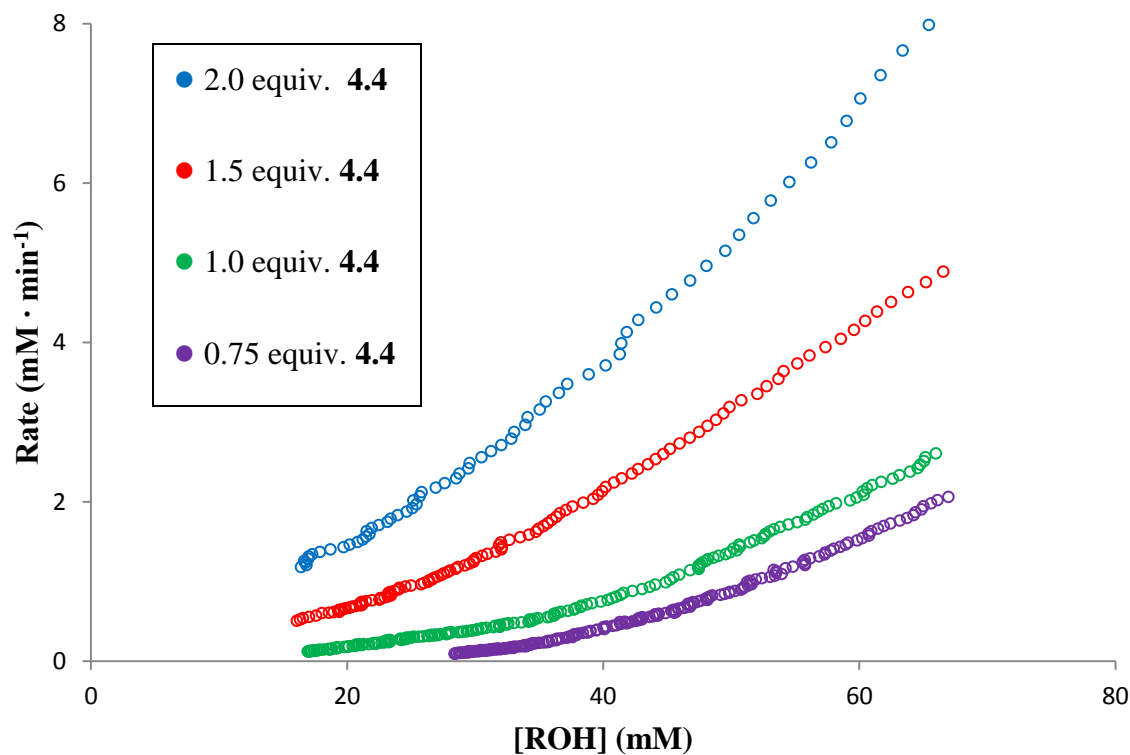


**Figure 4.10 Demonstrated Positive Order in Silyl Chloride**

Reaction was run with the shown 25 mol% of catalyst, the shown equivalents of silyl chloride with an equivalent of *i*Pr<sub>2</sub>NEt to match the silyl chloride concentration. See Scheme 4.3.

As previously described for the alcohol data, a plot of rate normalized to silyl chloride concentration versus the alcohol concentration should also yield a straight line of data. Good overlay would be observed if the catalytic system is first order in silyl source. When the rate equation 4.13 is divided by silyl chloride concentration, equation 4.22 is produced. In this case an integer order would suggest the b-term is negligible when data plotted versus alcohol on the x-axis results in overlay. A fractional order less than one would suggest the b-term dominates, which would signal Michaelis-Menton kinetics are likely.



$$\frac{\text{rate}}{[\mathbf{4.4}]} = \frac{a[\mathbf{4.6}][\mathbf{1.10}]_o}{1 + b[\mathbf{4.4}] + c[\mathbf{4.6}]}$$

Equation 4.22

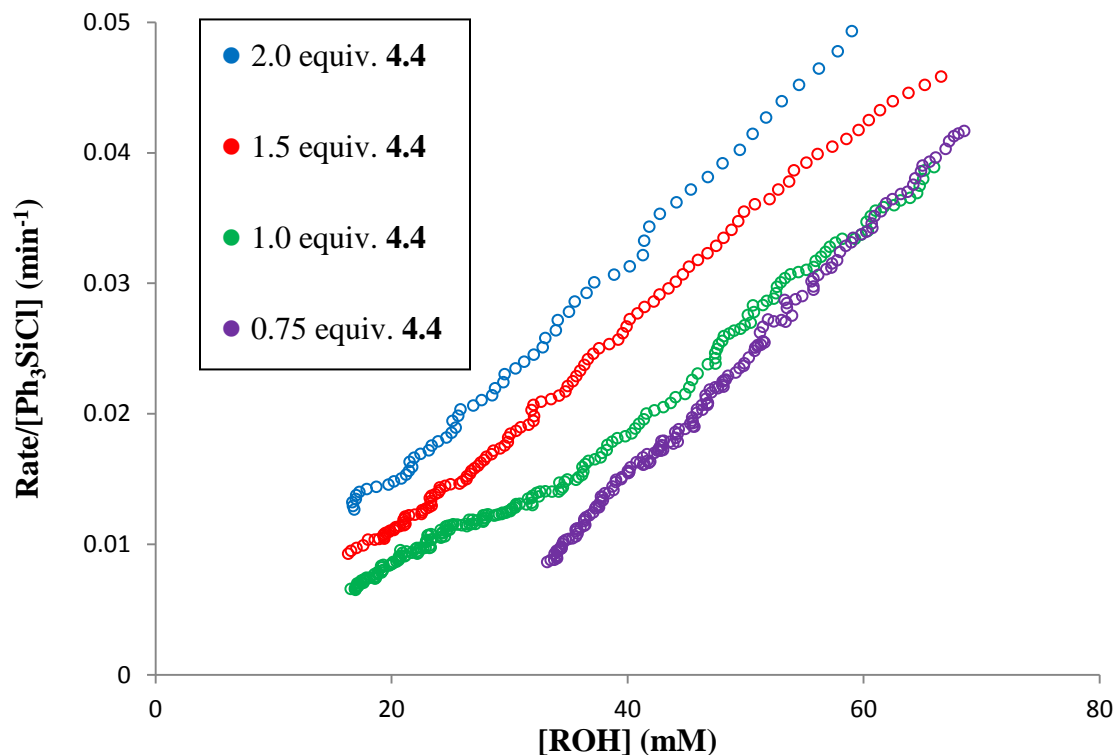


**Figure 4.11 Determining the Order with Respect to Silyl Chloride with “Different Excess” Protocol**

Reaction was run with the shown 25 mol% of catalyst, the shown equivalents of silyl chloride with an equivalent of *i*Pr<sub>2</sub>NEt to match the silyl chloride concentration. See Scheme 4.3.

When these data are plotted, the data does not overlay suggesting a non-integer order with respect to triphenylsilyl chloride (Figure 4.11). With this knowledge in hand, we next modified the order with respect to silyl chloride until an order of 1.5 produced the ideal straight line plots with overlay (Figure 4.12). Similar scenarios have been discovered in a copper catalyzed oxidative coupling reaction.<sup>25</sup> Based upon this study our

result of 1.5 order in silyl chloride suggests an alternate pathway involving two molecules of silyl source occurs on the catalytic cycle. Obviously, our proposed mechanistic cycle is inaccurate with respect to silyl chloride. A proposed alternate catalytic cycle is needed; equation 4.13 does not accurately describe the kinetics of the silylation. An alternate proposed cycle is discussed further in section 4.8.

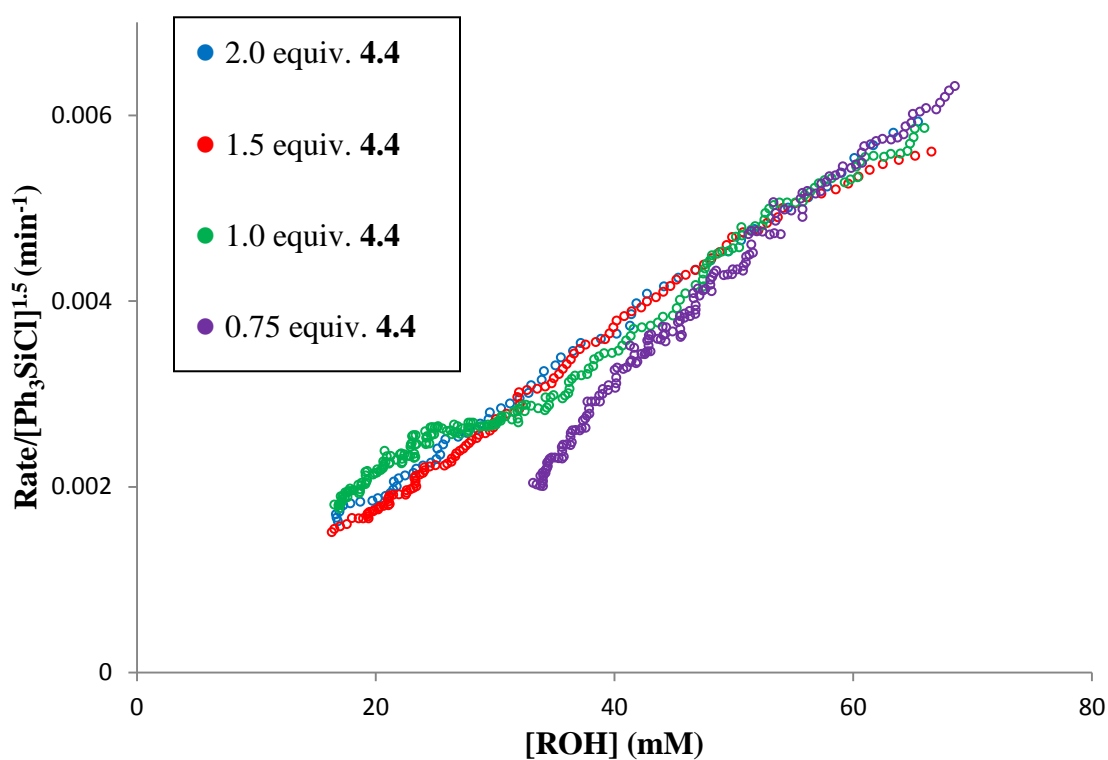
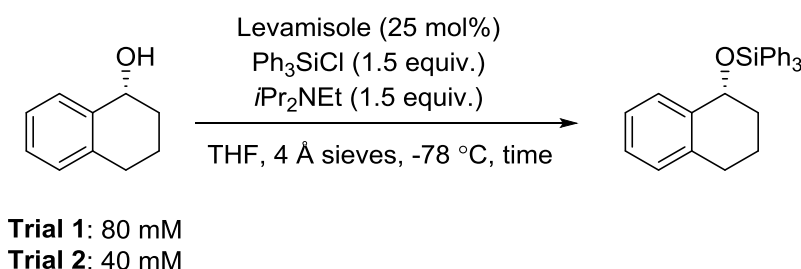


**Figure 4.12 Overlay of Data with Higher Order in Silyl Chloride**

Reaction was run with the shown 25 mol% of catalyst, the shown equivalents of silyl chloride with an equivalent of *i*Pr<sub>2</sub>NEt to match the silyl chloride concentration. See Scheme 4.3.

#### 4.5. Same Excess Study: Implications for Catalyst Degradation

Next, two experiments were analyzed which possessed a “same excess” of silyl chloride with respect to alcohol while varying the alcohol concentration. This reaction determines whether the reaction suffers from catalyst deactivation or product inhibition. Two experiments were designed with two different alcohol concentrations to begin the reaction. One run had 80 mM (from our standard reactions discussed above) whereas the other had an alcohol concentration of 40 mM. Both reactions were reacted with 1.5 equivalents of silyl chloride and base relative to the starting alcohol concentration (Scheme 4.8). This produces an “excess” of 40 mM of silyl chloride to alcohol for both runs.



#### Scheme 4.6 General Reaction Conditions for the “Same Excess” Studies

The same excess experiment seeks to compare the last few turnovers of a reaction to another reaction that has just begun to convert alcohol to product. This is equivalent to setting up the reaction half way through the reaction. The same excess allows the two reactions to be compared directly and graphically in order to implicate catalyst degradation or deactivation. Adjusting the time<sup>33</sup> of the second, lower 40 mM concentration to match the 40 mM concentration point in the 80 mM allows the two reactions to be directly compared. If they overlay, then the catalyst is not degrading or the

product formed does not inhibit the reaction products. The overlay of the two sets of data in Figure 4.13 suggests that the catalytic cycle of the kinetic resolution is not affected from either of the aforementioned problems. In the silylation reaction, the catalyst proceeds at the same rate whether it has just begun to convert silyl chloride or has converted half of the initial substrate.

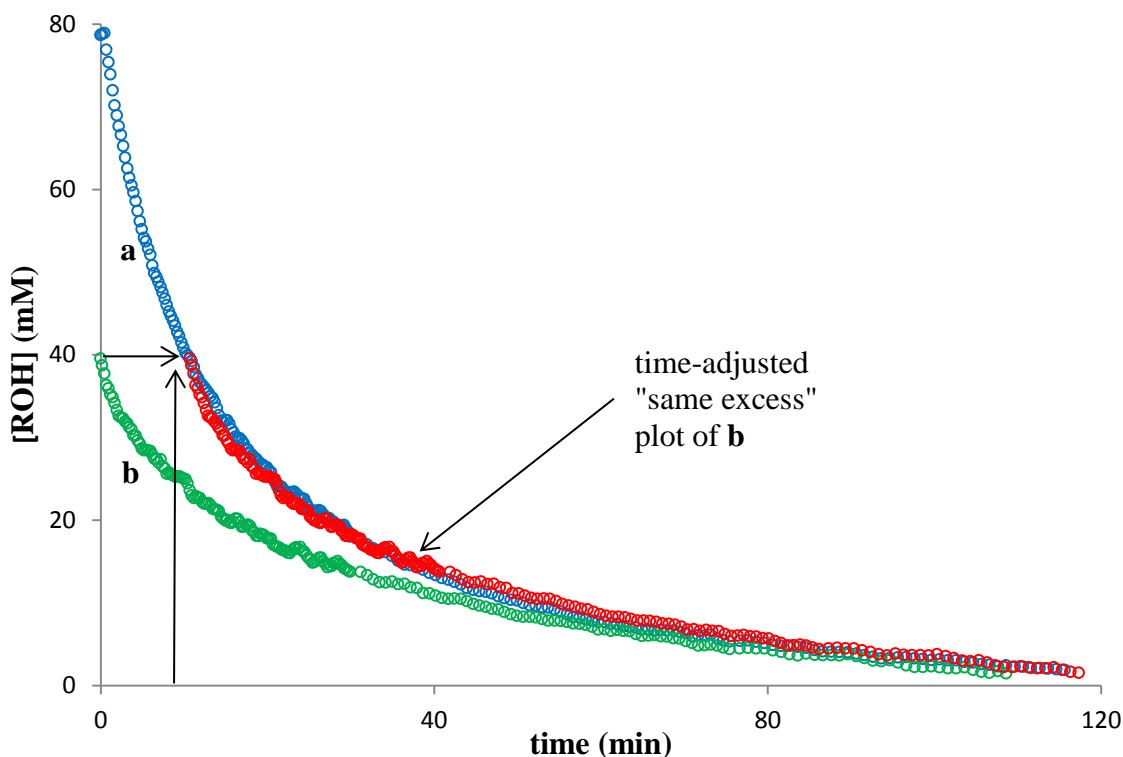


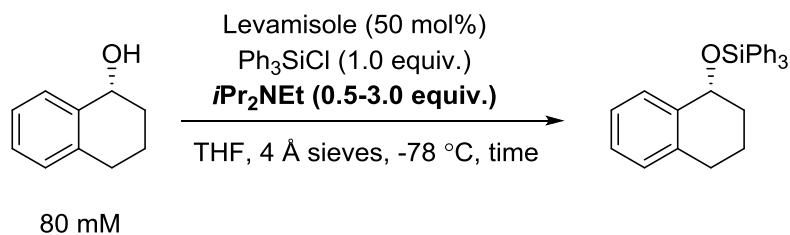
**Figure 4.13 Time-Adjusted “Same Excess” Experiment**

Reaction A and B were run with 25 mol% of catalyst and 1.5 equivalent each of silyl chloride with and  $i\text{Pr}_2\text{NEt}$ . Reaction A used 80 mM of alcohol; Reaction B used 40 mM of alcohol. See Scheme 4.6.

#### 4.6. A Case of Zeroth Order with Respect to Base: Initial Rate Investigations

The investigations to explore the hypothesized mechanistic scheme also determined the effect of base concentration on initial rate. Initial rate data was simpler

to analyze for the base. Since we were primarily interested in the first 10-15% conversion for these reactions, all reactions were analyzed with a rapid collection (1 scan per 5 seconds) using in situ IR spectroscopy and the aforementioned processing techniques.



#### Scheme 4.7 General Reaction for Rate Determination with Respect to Base

Since we were interested in initial rate, we utilized reaction conditions similar to our LFER study<sup>6</sup> which utilized 50 mol% of catalyst and one equivalent of silyl chloride with respect to the alcohol. This series of duplicate experiments with ranging base concentrations from 40-240 mM base (0.5 to 3.0 equivalents of base, Scheme 4.9) indicated there was no appreciable effect on rate when the initial base concentration was changed (Figure 4.14).

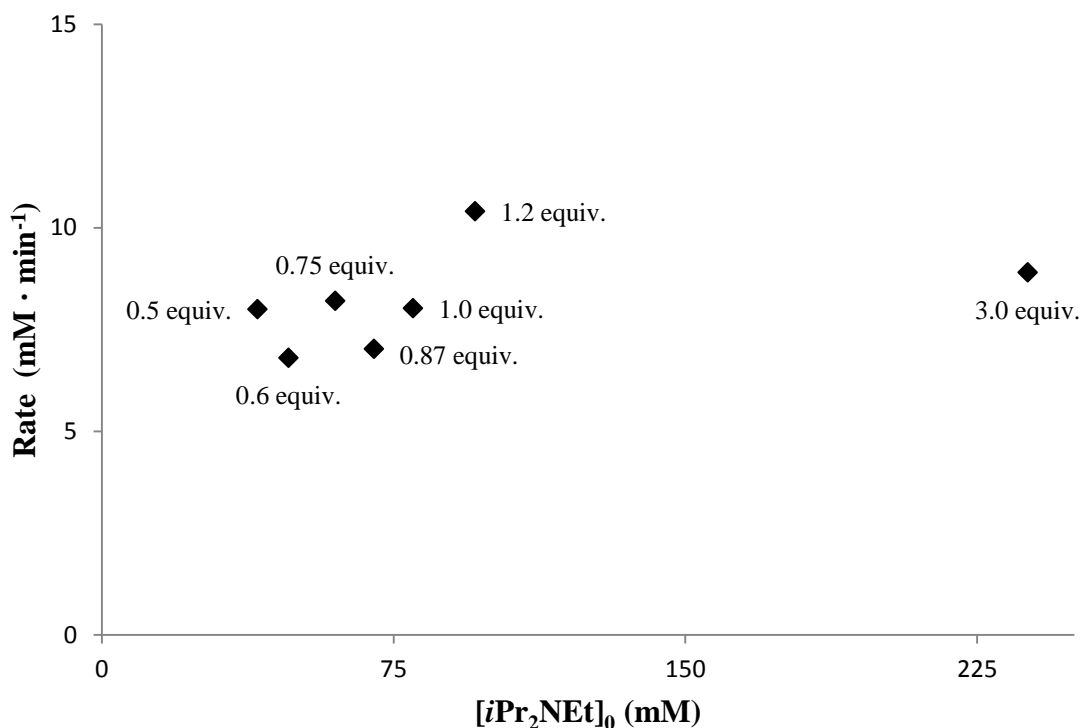


**Figure 4.14 Initial Rate Investigations with Various Base Concentrations**

Reaction was run with 50 mol% of catalyst and 1 equivalent of silyl chloride. The equivalents of *iPr*<sub>2</sub>NEt are shown. Each point is an average of two runs. See experimental for data on each experiment. The 3.0 equivalents of *iPr*<sub>2</sub>NEt experiment was a single run. See Scheme 4.7.

To insure the base has no effect on rate late in the reaction a simple graphical rate equation was constructed like those used previously for catalyst and silyl chloride. Two runs were compared when plotted as rate on the y-axis and alcohol concentration on the x-axis (Figure 4.15). These plots produced excellent overlay despite a three equivalents excess base in one run. This overlay of data strongly supports a fast deprotonation step ( $k_3$ , Figure 4.2) in the mechanistic cycle. If the base was indeed having a positive effect

on reaction rate poor overlay would be expected like those shown previously for catalyst and silyl chloride as evident in Figures 4.7 and 4.10, respectively.

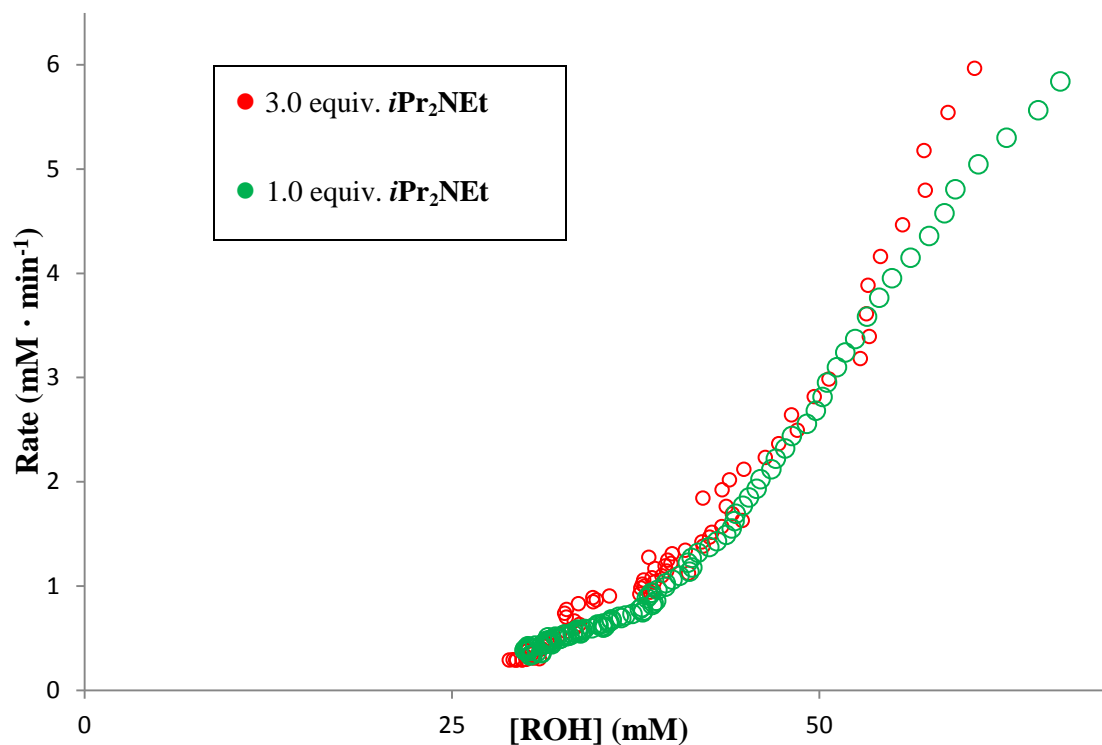
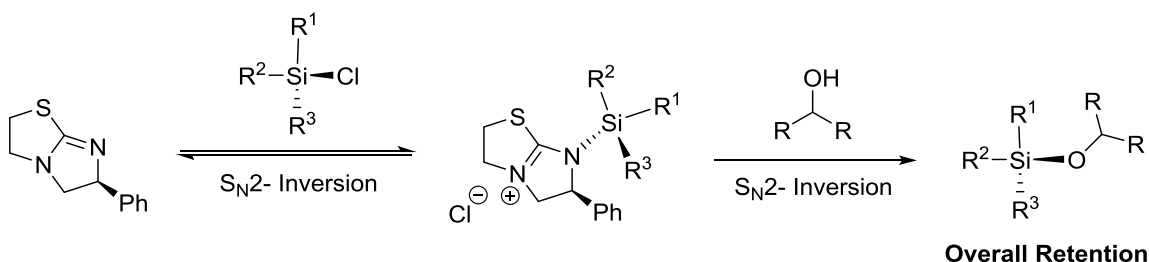


**Figure 4.15 Graphical Rate Equation with Varied Base Concentration**

Reaction was run with 50 mol% of catalyst and 1 equivalent of silyl chloride. The equivalents of *iPr*<sub>2</sub>NEt are shown. See Scheme 4.7.

#### 4.7. Stereogenic at Silicon Silyl Chlorides as Chiral Probes

With this kinetic data in hand, we next turned our attention to the proposed transition state and intermediate structure. The transfer of chirality should proceed with retention of stereochemistry at silicon if a true double S<sub>N</sub>2 type transformation<sup>15</sup> occurs (Scheme 4.8).



**Scheme 4.8 Proposed Double Inversion Pathway at Silicon**

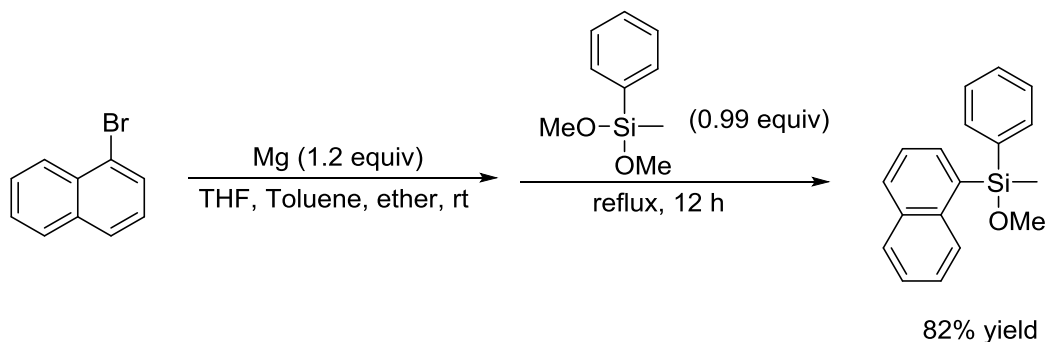
Stereochemical outcomes for a variety of reactions employing stereogenic at silicon compounds are well studied.<sup>30-31, 34-35</sup> Based upon previous investigations, it is known that both pentavalency and tetravalency at silicon is common. The formation of pentavalent silyl species has been implicated in the racemization of chiral silanes.<sup>31</sup> Thus, the structure of the intermediate **4.5** may be either tetravalent or pentavalent. Several attempts to isolate or analyze this intermediate via low temperature and ambient temperature NMR have been unsuccessful. An experiment-based approach to explore this species was therefore designed whereby a stereoenriched silyl chloride could be used as a chiral probe in the kinetic resolution.

The most well studied chiral silane is the methylphenylnaphthylsilane and its derivatives.<sup>36</sup> This silane has routinely been utilized as a chiral probe in complex mechanisms. The stereochemical outcomes of this particular chiral silane in a variety of reactions including reductions<sup>37</sup>, hydrolysis<sup>38</sup>, or other substitutions<sup>39-40</sup> are known.

The enantioenriched silane was prepared in a four-step synthesis according to a reported procedure.<sup>41-42</sup> The racemic methoxymethylnaphthylphenyl silane was prepared in excellent yield by displacing a methoxy group from dimethoxymethylphenyl silane

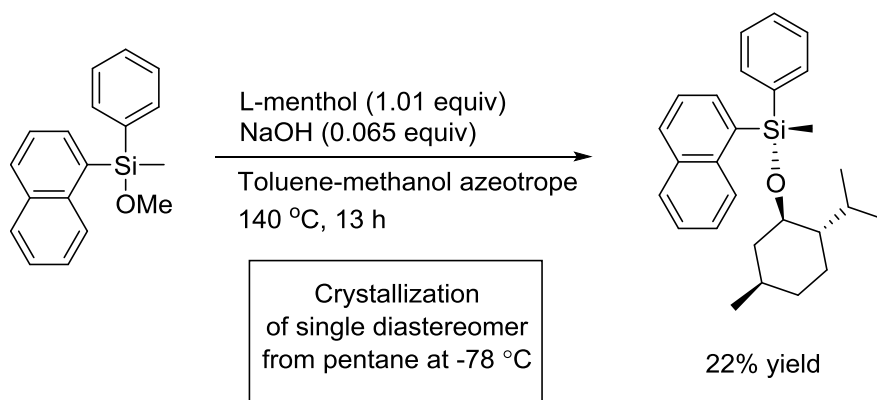


with 1-naphthylmagnesium bromide in a ternary mixture of ether, toluene and THF (Scheme 4.9).



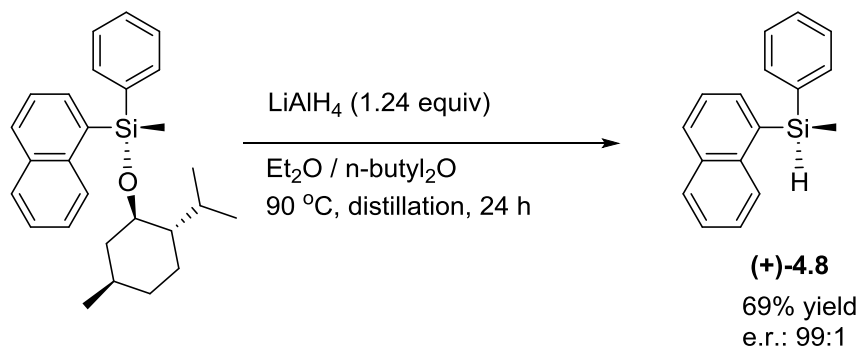
**Scheme 4.9 Synthesis of Enantioenriched Silane Precursor**

The methoxy group is then exchanged with an L-menthoxy group under base catalyzed conditions. Toluene is used as the solvent to remove methanol in an azeotrope, thereby facilitating reaction completion. The mixture of diastereomers is enriched in a classical resolution using pentane at  $-78\text{ }^{\circ}\text{C}$  to crystallize a single diastereomer (Scheme 4.10). The yields for this reaction were quite moderate, 22% based on the single diastereomer.



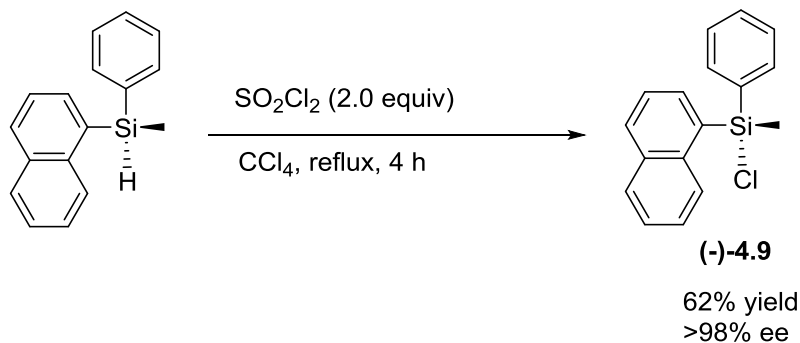
**Scheme 4.10 Classical Resolution of Stereogenic Silanes**

Next, the chiral auxiliary is removed with a stereoretentive lithium aluminum hydride reduction in refluxing dibutylether. This provides the stereoenriched (98% ee) silane after chromatographic purification in good yield (Scheme 4.11).



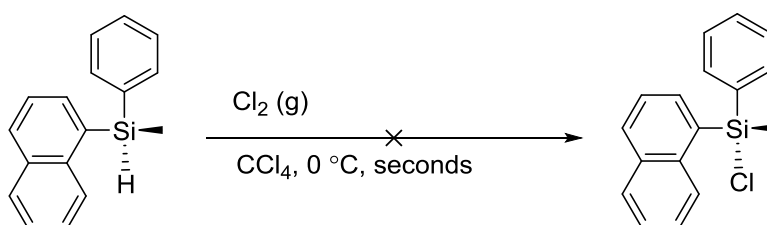
**Scheme 4.11 Stereoretentive Reduction of Silyl Ether with  $\text{LiAlH}_4$**

The final step to prepare the stereoenriched silylchloride has presented a significant challenge. Attempts to chlorinate the silane utilizing sulfuryl chloride<sup>6, 17</sup> in  $\text{CCl}_4$  have been inconsistent. The desired chlorosilane has only been obtained in stereoenriched form on two occasions utilizing this method (Scheme 4.12). Loss of the naphthyl group was frequently observed as well as racemization of the silyl chloride utilizing this approach.



**Scheme 4.12 Stereoretentive Chlorination with Sulfuryl Chloride**

In order to solve this problem, the previously reported methods were attempted.<sup>40,</sup>  
<sup>42</sup> The originally reported synthesis of enriched chlorosilane (-)-**4.9** employed chlorine gas in CCl<sub>4</sub> chilled to 0 °C (Scheme 4.13). Due to the high cost of chlorine, a small quantity of dry chlorine was generated from HCl and KMNO<sub>4</sub> for this transformation.<sup>43</sup> Unfortunately, this reaction led to complete decomposition of the silane via loss of the naphthyl group as observed in previous sulfonylchloride induced chlorinations.

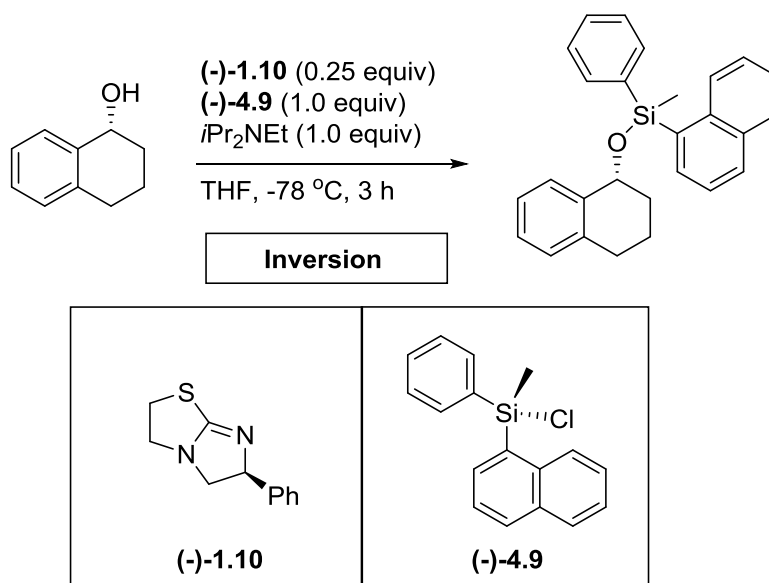


**Scheme 4.13 Attempted Chlorination with Chlorine Gas**

The chlorination of this silane has also been reported using benzoyl peroxide as a radical initiator in CCl<sub>4</sub>.<sup>40, 44</sup> In these reactions the radical initiator facilitates chlorine abstraction from the solvent. Attempts to chlorinate the silane from this benzoylperoxide-CCl<sub>4</sub> method were very sluggish using both pressure vessels and refluxing CCl<sub>4</sub>. Full conversions were never achieved. This problem was further complicated since the silane starting material and initiator impurities could not be removed from the desired product using recrystallization or trituration.

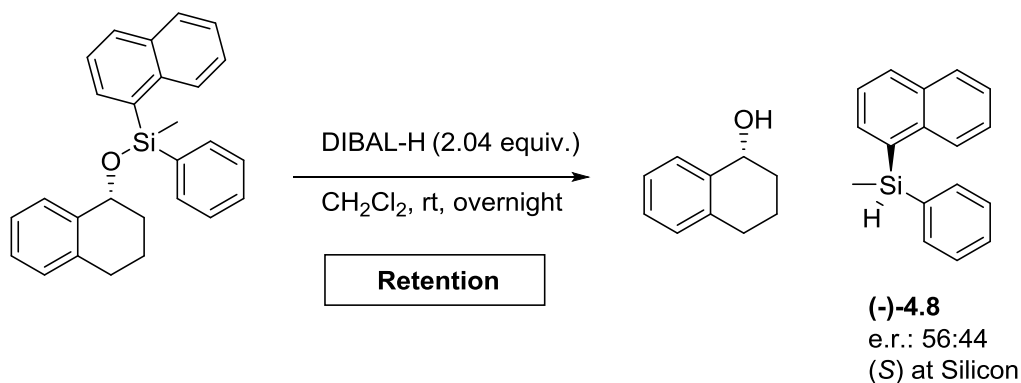
Enough of the enantioenriched chlorosilane was prepared according to Scheme 4.12 for several preliminary studies. Recall, we initially hypothesized retention of configuration via a double inversion type mechanism of substitution would be observed (See Scheme 4.8). The first of these experiments utilized (*R*)-tetralol and 0.25 equivalents

of catalyst **1.10** and 1 equivalent of the enantioenriched chlorosilane **4.9** since similar conditions utilized for all kinetic investigations (Scheme 4.14).



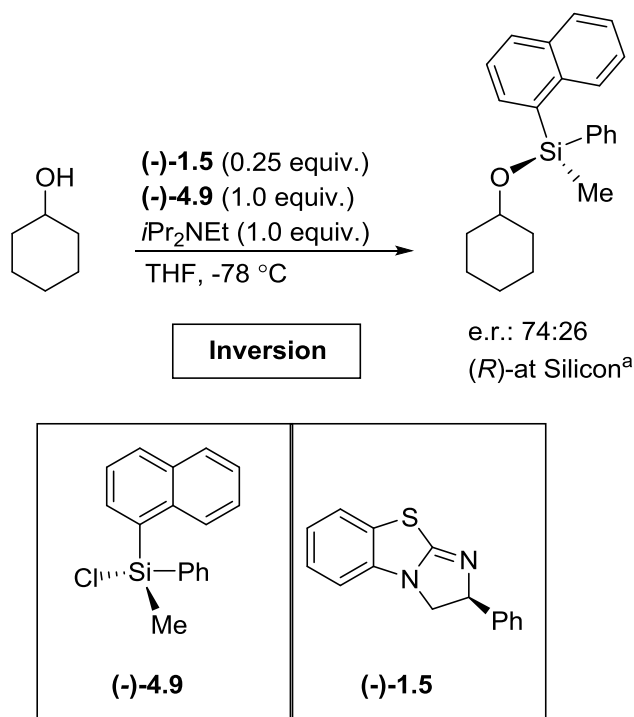
**Scheme 4.14** Stereoenriched Chlorosilanes for the Silylation of (*R*)-Tetralol

The product of this reaction was isolated and analyzed. Unfortunately, the diastereomeric ratio was difficult to determine from HPLC and GC-MS. It was estimated to possess a d.r. of 59:41 from deconvolution of <sup>1</sup>H NMR spectra. The silyl ether was reduced in a stereoretentive<sup>45</sup> fashion with DIBAL-H at ambient temperature (Scheme 4.15). Analysis of the silane on HPLC indicated an e.r. of 56:44 enriched in the (*S*)-enantiomer by comparison to the authentic (*R*)-enantiomer. Overall, these results indicate significant racemization accompanied by inversion of stereochemistry at silicon. This result is in contrast to the double inversion mechanism proposed earlier (Scheme 4.8).<sup>6</sup>



#### Scheme 4.15 Stereoretentive Reduction of a Diastereomeric Silyl Ether

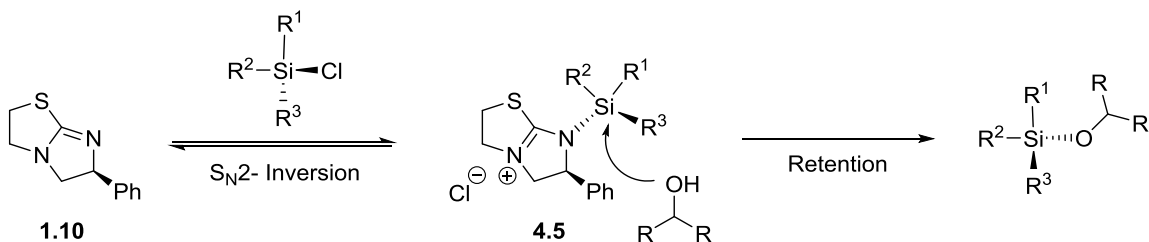
With the intriguing results of the silylation of (*R*)-tetralol with chiral silane **4.9** in hand, we next focused on a control experiment. We hypothesized that the enantioenriched alcohol could be responsible for the observed significant racemization at silicon since a pair of diastereomers were formed in these reactions. The active species is thought to be in equilibrium with catalyst and free silyl chloride. Thus the diastereomeric mixture of intermediates may have led to the observed racemization. In order to control this, the reaction was thus reattempted with an achiral alcohol, cyclohexanol. Additionally, the catalyst **1.5** was utilized as the catalyst since both enantiomers are commercially available, and it had been demonstrated to be significantly more enantioselective in the silylation-based resolution of lactones<sup>16, 46</sup>(Scheme 4.16).



**Scheme 4.16 Stereoenriched Chlorosilanes for the Silylation of Cyclohexanol**

When cyclohexanol was employed as the alcohol and **1.5** as catalyst a similar overall inversion of stereochemistry was again observed. The level of enantioenrichment in the silyl ether was significantly higher with an e.r. of 74:26 in the (*R*)-enantiomer as determined from HPLC and comparison to reported optical rotation data (Scheme 4.16).<sup>47</sup> In this experiment, aliquots were removed throughout the reaction to determine the relationship of reaction time and e.r. of the product. All aliquots had similar levels of enantioenrichment (See experimental section). Unfortunately, the conversion of these aliquots was difficult to determine from <sup>1</sup>H NMR of the crude samples. The volatility of cyclohexanol further eroded the confidence in conversion data as determined by GC-MS. Further investigations should seek to employ a less volatile achiral alcohol. One candidate is 2-indanol which possesses the similar topologies to the benzylic alcohol

substrate class.<sup>7</sup> Unfortunately, further important investigations using stereoenriched silyl chlorides as probes in the reaction have yet to be realized.



#### Scheme 4.17 Plausible Explanation for Inversion of Configuration at Silicon

One possible explanation for the observed racemization is by substitution of the silyl chloride with chloride ion. Alternatively, pentavalent intermediate structures have been implicated in racemization pathways; therefore, these structures cannot yet be ruled out entirely. Interestingly the reaction inverts the stereochemistry at silicon. One possibility is the alcohol may approach the silylated catalyst from the catalyst side (Scheme 4.17). We presume that the catalyst inverts the stereochemistry based upon the wealth of examples that demonstrate the chloride leaving group prefers inversion of stereochemistry.<sup>48</sup> The limited quantity of data gained thus far suggests the backside attack proposed in our previous studies may not be valid. More experimentation than the few experiments discussed previously are needed to further solidify or refute this hypothesis. Interestingly, this type of approach would be consistent with the transition states invoked by Birman<sup>1, 4</sup> such as transition state **4.1**. In our silylation-based kinetic resolution, the catalyst may play an important role in stabilizing and directing the approaching alcohol more so than was previously thought.

#### 4.8. Overall Mechanistic Picture Based on Kinetic Investigations and Other Mechanistic Studies

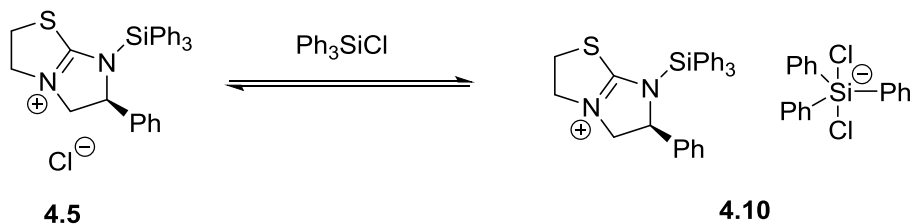
With the variety of mechanistic investigations completed to date including chiral probe reaction, kinetic and linear-free investigations allow us to propose a more accurate mechanistic picture. From kinetic evaluations the rate equation can be written in power law form as demonstrated by equation 4.23.

$$\text{rate} = k_{\text{obs}} [\mathbf{1.10}]^1 [\mathbf{4.6}]^1 [\mathbf{4.4}]^{1.5} [\text{Base}]^0$$

##### Equation 4.23

The rate of reaction is independent of base concentration. Also as predicted in our presumed mechanistic cycle (Figure 4.2) the reaction is first order in alcohol and catalyst. Interestingly, the reaction is highly dependent upon silyl chloride concentration. The cause for this phenomenon is intriguing. In order for a greater than one order in silyl chloride to occur, more than one molecule of silyl chloride must be required on the mechanistic cycle. Since the order is not quite second order, this suggests a more complex reaction occurs only part of the time. Initially, it was hypothesized that the chloride ion in the intermediate structure may be responsible for the 1.5 order in silyl source. It is known from other mechanistic studies involving chlorosilanes that the chloride ion leaving group forms various complex silyl species in situ. For instance, this ligation of silyl chlorides with free chloride formed upon catalyst complexation has been implicated in the non-stereoselective allylation background pathways investigated by Denmark.<sup>32, 49</sup> In our system, the chloride ion formed upon catalyst complexation could conceivably coordinate with another triphenyl silyl chloride according to the equilibrium shown in Scheme 4.18.

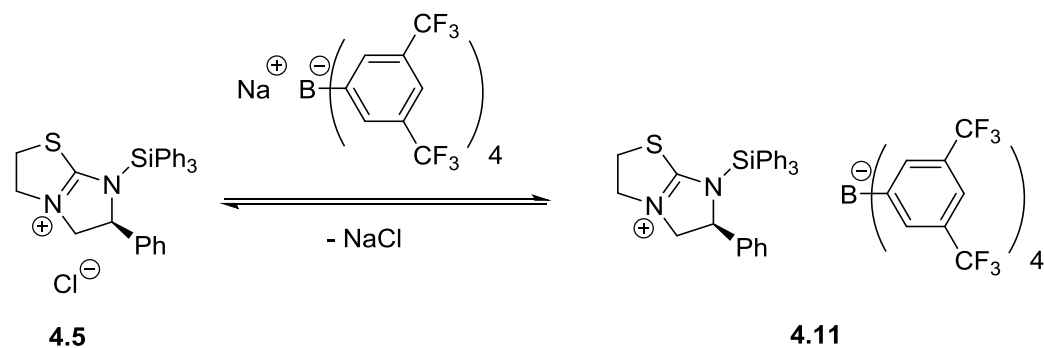




**Scheme 4.18 Hypothetical Intermediates to Explain Order in Silyl Chloride**

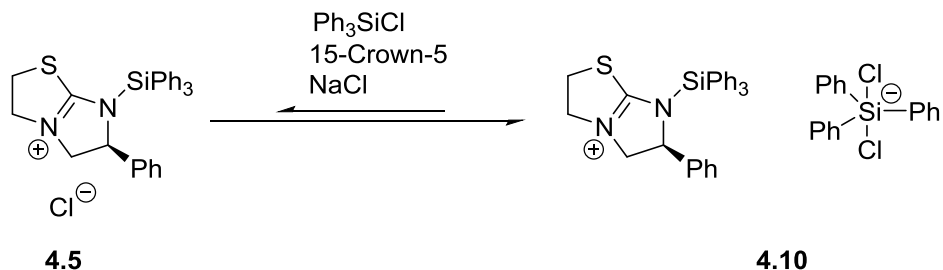
This pathway is supported by the stability of relative pentavalent silanes such as  $\text{Ph}_3\text{SiF}_2$ <sup>50</sup> which is isolatable and usable for the silylation of alcohols without the need for catalysts. The pentavalent silane complex **4.10** would thus be considerably more reactive than the presumed triphenylsilyl chloride catalyst complex **4.5**. This alternative pathway could offer a less stereoselective pathway to product. The formation of **4.10** may also explain the partial racemization observed in reaction employing stereo-enriched silyl chloride (Scheme 4.14 and 4.16). Fully understanding these possible pathways are paramount to increasing the efficiency of the silylation-based methodology.

In order to test this hypothesis, a series of reactions have been designed. These studies will employ an additive to attempt to control the fate of the free chloride ion. Non-coordination ions have been demonstrated to remove chloride via precipitation of NaCl in metal catalyst activations.<sup>51-52</sup> Presumably the addition of an equivalent of sodium tetrakis (3,5-trifluoromethylphenyl)borate (NaBARF) would remove the chloride from solution (Scheme 4.19).



**Scheme 4.19 Removal of Chloride with a Non-Coordinating Anion**

In order to determine the effect on order with respect to silyl chloride, two different excess studies with an equivalent of the non-coordinating anion to silyl source (Scheme 4.19) producing overlay would implicate the pathway described in Scheme 4.18. Alternatively, the addition of a soluble chloride source such as tetrabutylammonium chloride or crown ether sodium chloride complex could further exacerbate and contribute to a background reaction involving pentavalent silyl chloride complex **4.10** (Scheme 4.20). Failure to overlay kinetic data in two separate different excess experiments would support a complex formation like **4.10**. Additionally, the pentavalent  $\text{Ph}_3\text{SiCl}_2$  may even be reactive enough to silylate an alcohol without the presence of catalyst; therefore, supporting the presumption of a pentavalent triphenylsilyl chloride with similar reactivity to the catalyst activated species **4.5**. A highly reactive pentavalent silyl chloride would undoubtable result in an undesired background reaction.



**Scheme 4.20 Chloride Containing Additive in the Silylation Reaction**

#### 4.9. Conclusions and Outlook

To date, additional mechanistic investigations have been carried out to determine the complete mechanism of a triphenylsilylchloride based kinetic resolution catalyzed by chiral isothioureas. Kinetic evaluations determined that the reaction was first order in catalyst and alcohol. The sterically hindered base, *i*Pr<sub>2</sub>NEt, had no effect on reaction rate suggesting a fast deprotonation step occurring after the rate determining step. Interestingly, the reaction was found to be highly sensitive to chlorosilane concentration. A 1.5 overall order in triphenylchlorosilane suggests that a variety of unknown activated species form during the reaction. Experiments employing a chiral silylchloride as the silicon source provided stereochemical information for the reaction. Both reactions tested demonstrated inversion of stereochemistry with significant amounts of racemization occurring during silylation of the alcohol. This result does not support the backside attack hypothesis developed from linear free energy relationship studies.<sup>6</sup> The racemization discovered in these reactions combined with the sensitivity observed to silyl chloride in kinetic data point to a more complicated mechanism than that represented in Figure 4.2. Further investigations are clearly needed and several approaches have been described in this chapter.

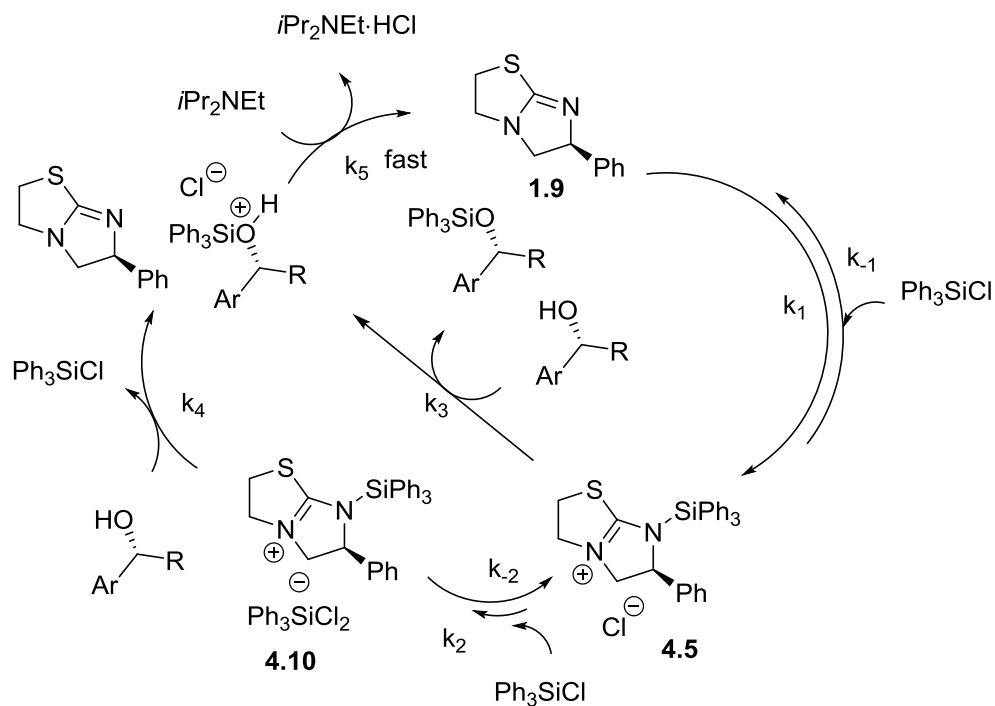


**Figure 4.16 Overall Mechanistic Picture after Mechanistic Investigations**

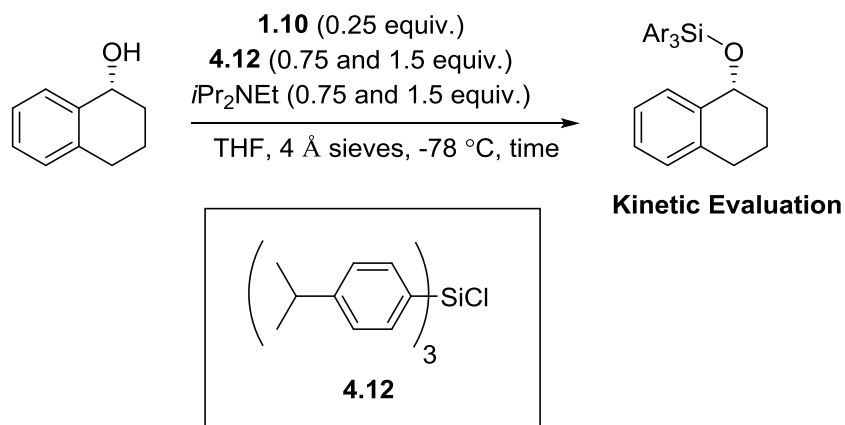
Nevertheless, a new and improved mechanistic cycle can be proposed from the wealth of knowledge gained from these direct mechanistic investigations performed herein (Figure 4.16). A pre-equilibrium most likely occurs between the catalyst **1.10** and silyl chloride. This equilibrium presumably lies towards free catalyst due to our previous inability to observe the active complex; however, a significant quantity of active species is formed as evidenced by the positive order in silyl chloride and alcohol. If only a trace quantity of active species is formed, pseudo-zeroth order in alcohol would be expected.<sup>18,</sup>  
<sup>53</sup> The active species formed in the pre-equilibrium then reacts with alcohol in the rate determining step  $k_3$  or reacts with additional silyl chloride to form more complex structures like **4.10**. These more activated complexes would be highly reactive and contribute significantly to the overall rate as evidenced in our different excess studies

with varied silyl chloride. Once the silicon-oxygen bond is formed the base scavenges HCl to regenerate the active catalyst. The catalyst in this reaction is not affected by catalyst degradation or product inhibition.

In order to test this proposed mechanism more fully, computational studies similar to those done for the acylation-based reactions should be pursued. Particularly, the transition state structure of the active species **4.5** alcohol bond formation would be particularly vital to a thorough understanding of the mechanism. Next steps also include generation of a new rate law for this new cycle and subsequent testing against the data already obtained. Additionally the additive control experiments should produce meaningful data to confirm or deny the existence of the active complex species proposed here.

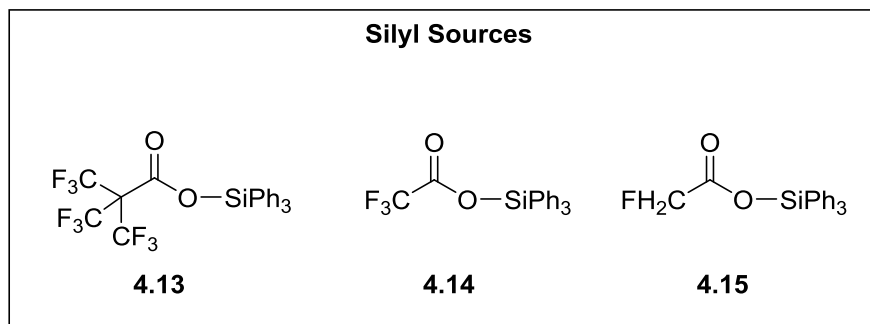
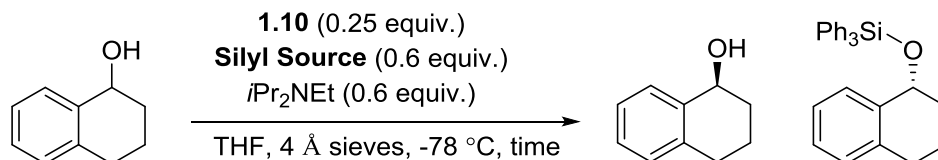
In addition to the additive control experiments discussed previously (Schemes 4.19 and 4.20) other kinetic experiments could produce meaningful and vital results. For example, the 2-arylcylcohexanol substrate class has been optimized to utilize a tris(*para*-isopropylsilyl) chloride as the silyl source (Li Wang).<sup>16</sup> This silyl source is significantly more selective than triphenylsilyl chloride when utilized with benzylic alcohols as well. This increase in selectivity was attributed to electron-donating stabilization of a late transition state in the silylation reaction.<sup>6</sup> However, the kinetic investigations discussed here suggest a significant side reaction occurs when utilizing triphenylsilyl chloride. It is conceivable that electron donating groups on the chlorosilane could limit complexation by free chloride anion (See Scheme 4.18). Additional kinetic experiments can be used to dispel or corroborate this possibility. Using the reaction progress approach, only two experiments at different excess of the triarylsilylchloride **4.12** would be required. If the

data of the two runs of 0.75 and 1.5 equivalents of silylchloride overlay when plotted in the same fashion as Figure 4.11, this would support this hypothesis and suggest the side reaction ( $k_2$ , Figure 4.16) is responsible for a non-enantioselective background reaction.



**Scheme 4.21 Evaluating the Kinetics of Alternate Silyl Sources**

In addition to the addition kinetic experiments and mechanistic experiments discussed above, the knowledge we have gained from the kinetic investigations should be utilized to improve the existing silylation-based kinetic resolution. Efforts should be made to make the reaction more selective. It would be important to test additional silyl sources in the resolution of alcohols. We know from previous investigations<sup>46</sup> that the triaryl moiety is vital to obtaining enantio-discrimination; however, very little work has been done with variations to the leaving group on the silyl source. Electronic effects at silicon are important to selectivity with electron-donating groups being most beneficial. Altering the leaving group to be less electronegative and less nucleophilic could also hinder the side reaction proposed in Figure 4.16.



**Scheme 4.22 Alternate Triphenylsilyl Sources in the Kinetic Resolution**

Unfortunately, triarylsilyl sources bearing leaving groups other than chlorine, bromine or triflate are not commercially available. Many other potential silyl sources have simply not been tested in Lewis base catalyzed silylation reactions.<sup>29</sup> In Scheme 4.22, several silyl sources are proposed that could possibly be utilized for silyl transfer. Silylated carboxylates, **4.13** and **4.14**, can be prepared via several methods.<sup>29, 54</sup> Moreover, the silyl sources containing the trifluoroacetate leaving group have been utilized successfully for the protection of alcohols.<sup>55</sup> These carboxylate leaving groups provide the advantage of simple tunability of the electronics to yield structures like **4.15**. Electron-withdrawing groups like those shown would yield a reactive silyl source bearing a less nucleophilic leaving group as compared to chloride. These properties may limit more competitive side reaction pathways from occurring and improve the selectivity of the reaction.

In conclusion, the experiments described above represent an overview of possible future study. The silylation-based kinetic resolution developed and studied herein has

relatively unlimited potential. The next principle concern should be to understand more clearly the complex side reaction and ultimately control this undesired pathway. Efforts to make the reaction more economically feasible should be attempted to include increased reaction temperature. Unfortunately, Lewis base catalyzed silylation reactions are known to be highly entropically driven<sup>31, 56</sup> and thus highly ordered at the transition state. This property would make the selectivity of the reaction highly temperature dependent. Despite this, the reaction should be attempted at higher temperatures, especially for substrates exhibiting high selectivities ( $s > 30$ ) at  $-78\text{ }^{\circ}\text{C}$ , to demonstrate the applicability of the reaction on industrial scale. Continued study into substrate scope expansion is also necessary and will be benefited by the mechanistic investigations detailed in this chapter. Truly, the scope of study encompassing the silylation-based kinetic resolution appears restricted only by the imagination of the researchers.

#### 4.10. Experimental

##### General Information

Infrared spectra were obtained with a Mettler Toledo iCIR 10 in situ IR bearing a silicon probe. The data was processed using iC IR version 4.3.27 and spectra from  $\sim 900\text{-}1200\text{ cm}^{-1}$ . Each kinetic study employed flame dried glassware under argon atmosphere. Flame dried volumetric flasks were used for the preparation of all stock solutions. Dry THF was obtained via passage through a column of activated alumina and stored over four angstrom sieves. Carbon tetrachloride was distilled, degassed, and stored over  $4\text{ \AA}$  sieves. Sulfuryl chloride was distilled prior to use. Chlorine gas was generated from HCl and  $\text{KMnO}_4$  and dried according to a known method.<sup>43</sup> (*R*)-tetralol (>97 % ee) was obtained



from TCI and used without further purification. (*R*)-methyl-naphthylphenylsilane (+)-**4.8** (98 % ee) was prepared according to a previously reported method.<sup>41</sup> Cyclohexanol was distilled and stored over molecular sieves prior to use. All <sup>1</sup>H NMR <sup>13</sup>C NMR spectra were obtained using a Bruker AVANCE III 400 MHz or 101 MHz in CDCl<sub>3</sub> with TMS as the internal standard.

### **General Procedure for Kinetic Analysis Experiments**

A three necked conical reaction vessel was flame dried, equipped with flea and 4 Å sieves, and sealed with septum. The vessel was then purged with argon and the ReactIR probe was inserted. The air background was taken then the IR was set to record spectra. The sieves were suspended in the specified amount of dry THF listed for each experiment. The solvent was then cooled to -78 °C in a dry ice/ acetone bath and allowed to equilibrate for 10 minutes. A stock solution of starting materials (alcohol, catalyst, and base) was prepared in a volumetric flask and added via syringe. A stock solution of Ph<sub>3</sub>SiCl was prepared in a volumetric flask and addition was made to the starting material mixture with a syringe. The *t*<sub>0</sub> was typically 30 minutes. Data was recorded throughout the experiment at 1 spectrum every 15 seconds. Initial rate data was obtained at a rate of 1 spectrum every 5 seconds. Aliquots (~80 μL) were removed with a syringe and quenched immediately with methanol. Data from the IR was processed according to the procedure described in section 4.2. Actual amounts of starting materials and reagents utilized per each run are listed below.

### **Determining Reaction Progress- <sup>1</sup>H NMR**

Integration of the proton geminal to the oxygen in the product and starting material yields accurate conversion data from crude aliquots (~80 μL). The product proton is observed as

a triplet at 4.96 ppm, and the starting material is observed as a triplet at 4.79 ppm. The integrals for both peaks are normalized to a sum of 100 to determine the percent conversion. The below spectra (Figure 4.17) indicates 44.3% conversion. This NMR data corresponds to aliquot number five at eight minutes reaction time corresponding to the data point in Figure 4.3.

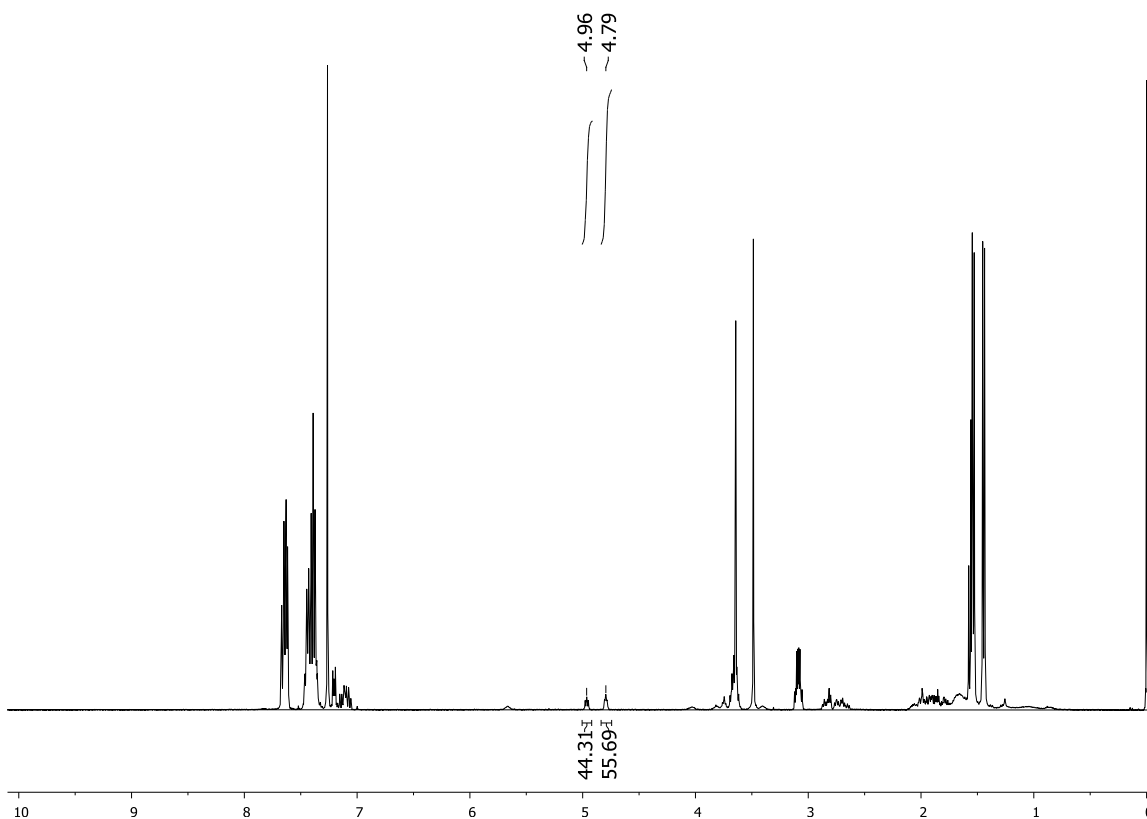


**Figure 4.17 Determination of Conversion from Aliquots and NMR Analysis**

### Experiments with Varied Catalyst Loading

#### 50 mol % [Cat]

A stock solution of starting materials was prepared under argon in a 1 mL volumetric flask using THF as the solvent. The following amounts were utilized: 54.2 mg, 0.366

mmol of (*R*)-tetralol, 37.5 mg, 0.183 mmol of levamisole **1.10**, 64  $\mu\text{L}$ , 0.367 mmol of *iPr*<sub>2</sub>NEt. The solution was thoroughly mixed under argon by taking the solution into the dry syringe followed by returning the solution to the volumetric flask under argon. Prior to addition of starting materials, the reaction vessel was filled with 2.1 mL of THF using a syringe. Once the THF had cooled to -78 °C, 810  $\mu\text{L}$  of the starting material solution was added. Finally, the reaction was initiated with 840  $\mu\text{L}$  of a stock solution of silyl chloride which was prepared in a 2 mL volumetric flask using 210.4 mg, 0.715 mmol of silyl chloride. Overall, the initial concentrations in mM of alcohol, silyl chloride and catalyst were: [ROH]: 78.99 [Ph<sub>3</sub>SiCl]: 80.05 [Cat]: 39.73.

### **35 mol % [Cat]**

A stock solution of starting materials was prepared under argon in a 1 mL volumetric flask using THF as the solvent. The following amounts were utilized: 54.3 mg, 0.366 mmol of (*R*)-tetralol, 26.0 mg, 0.127 mmol of levamisole **1.10**, 64  $\mu\text{L}$ , 0.367 mmol of *iPr*<sub>2</sub>NEt. The solution was thoroughly mixed under argon by taking the solution into the dry syringe followed by returning the solution to the volumetric flask under argon. Prior to addition of starting materials, the reaction vessel was filled with 2.1 mL of THF using a syringe. Once the THF had cooled to -78 °C, 810  $\mu\text{L}$  of the starting material solution was added. Finally, the reaction was initiated with 840  $\mu\text{L}$  of a stock solution of silyl chloride which was prepared in a 2 mL volumetric flask using 210.4 mg, 0.715 mmol of silyl chloride. Overall, the concentrations in mM of alcohol, silyl chloride and catalyst were: [ROH]: 79.15 [Ph<sub>3</sub>SiCl]: 80.05 [Cat]: 27.50.

### 25 mol % [Cat]

A stock solution of starting materials was prepared under argon in a 1 mL volumetric flask using THF as the solvent. The following amounts were utilized: 54.2 mg, 0.366 mmol of (*R*)-tetralol, 18.7 mg, 0.0915 mmol of levamisole **1.10**, 64  $\mu$ L, 0.367 mmol of *i*Pr<sub>2</sub>NEt. The solution was thoroughly mixed under argon by taking the solution into the dry syringe followed by returning the solution to the volumetric flask under argon. Prior to addition of starting materials, the reaction vessel was filled with 2.1 mL of THF using a syringe. Once the THF had cooled to -78 °C, 810  $\mu$ L of the starting material solution was added. Finally, the reaction was initiated with 840  $\mu$ L of a stock solution of silyl chloride which was prepared in a 2 mL volumetric flask using 210.3 mg, 0.715 mmol of silyl chloride. Overall, the concentrations in mM of alcohol, silyl chloride and catalyst were: [ROH]: 78.99 [Ph<sub>3</sub>SiCl]: 80.03 [Cat]: 19.77.

### 15 mol % [Cat]

A stock solution of starting materials was prepared under argon in a 1 mL volumetric flask using THF as the solvent. The following amounts were utilized: 54.2 mg, 0.366 mmol of (*R*)-tetralol, 11.2 mg, 0.0548 mmol of levamisole **1.10**, 64  $\mu$ L, 0.367 mmol of *i*Pr<sub>2</sub>NEt. The solution was thoroughly mixed under argon by taking the solution into the dry syringe followed by returning the solution to the volumetric flask under argon. Prior to addition of starting materials, the reaction vessel was filled with 2.1 mL of THF using a syringe. Once the THF had cooled to -78 °C, 810  $\mu$ L of the starting material solution was added. Finally, the reaction was initiated with 840  $\mu$ L of a stock solution of silyl chloride which was prepared in a 2 mL volumetric flask using 210.3 mg, 0.715 mmol of

silyl chloride. Overall, the concentrations in mM of alcohol, silyl chloride and catalyst were: [ROH]: 78.99 [Ph<sub>3</sub>SiCl]: 80.03 [Cat]: 11.84.

### Experiments with “Different Excess” of Silyl Chloride to Alcohol

#### Trial 1

A stock solution of starting materials was prepared under argon in a 1 mL volumetric flask using THF as the solvent. The following amounts were utilized: 54.2 mg, 0.366 mmol of (*R*)-tetralol, 18.7 mg, 0.0915 mmol of levamisole **1.10**, 64  $\mu$ L, 0.367 mmol of *i*Pr<sub>2</sub>NEt. The solution was thoroughly mixed under argon by taking the solution into the dry syringe followed by returning the solution to the volumetric flask under argon. Prior to addition of starting materials, the reaction vessel was filled with 2.1 mL of THF using a syringe. Once the THF had cooled to -78 °C, 810  $\mu$ L of the starting material solution was added. Finally, the reaction was initiated with 840  $\mu$ L of a stock solution of silyl chloride which was prepared in a 2 mL volumetric flask using 210.3 mg, 0.715 mmol of silyl chloride. Overall, the concentrations in mM of alcohol, silyl chloride and catalyst were: [ROH]: 78.99 [Ph<sub>3</sub>SiCl]: 80.03 [Cat]: 19.77. The value of excess is the difference between the concentration of alcohol and silyl chloride, thus [“Excess”]: 1.04 mM.

#### Trial 2

A stock solution of starting materials was prepared under argon in a 1 mL volumetric flask using THF as the solvent. The following amounts were utilized: 54.1 mg, 0.365 mmol of (*R*)-tetralol, 18.7 mg, 0.0915 mmol of levamisole **1.10**, 96  $\mu$ L, 0.551 mmol of *i*Pr<sub>2</sub>NEt. The solution was thoroughly mixed under argon by taking the solution into the dry syringe followed by returning the solution to the volumetric flask under argon. Prior to addition of starting materials, the reaction vessel was filled with 1.7 mL of THF using

a syringe. Once the THF had cooled to  $-78\text{ }^{\circ}\text{C}$ ,  $810\text{ }\mu\text{L}$  of the starting material solution was added. Finally, the reaction was initiated with  $1.25\text{ mL}$  of a stock solution of silyl chloride which was prepared in a  $2\text{ mL}$  volumetric flask using  $210.3\text{ mg}$ ,  $0.715\text{ mmol}$  of silyl chloride. Overall, the concentrations in mM of alcohol, silyl chloride and catalyst were:  $[\text{ROH}]$ :  $78.64$   $[\text{Ph}_3\text{SiCl}]$ :  $118.8$   $[\text{Cat}]$ :  $19.72$ . The value of excess is the difference between the concentration of alcohol and silyl chloride, thus [ $\text{Excess}$ ]:  $40.13\text{ mM}$ .

### **Trial 3**

A stock solution of starting materials was prepared under argon in a  $1\text{ mL}$  volumetric flask using THF as the solvent. The following amounts were utilized:  $54.1\text{ mg}$ ,  $0.365\text{ mmol}$  of (*R*)-tetralol,  $18.7\text{ mg}$ ,  $0.0915\text{ mmol}$  of levamisole **1.10**,  $128\text{ }\mu\text{L}$ ,  $0.735\text{ mmol}$  of *iPr*<sub>2</sub>NEt. The solution was thoroughly mixed under argon by taking the solution into the dry syringe followed by returning the solution to the volumetric flask under argon. Prior to addition of starting materials, the reaction vessel was filled with  $2.35\text{ mL}$  of THF using a syringe. Once the THF had cooled to  $-78\text{ }^{\circ}\text{C}$ ,  $810\text{ }\mu\text{L}$  of the starting material solution was added. Finally, the reaction was initiated with  $590\text{ }\mu\text{L}$  of a stock solution of silyl chloride which was prepared in a  $2\text{ mL}$  volumetric flask using  $588.6\text{ mg}$ ,  $2.0\text{ mmol}$  of silyl chloride. Overall, the concentrations in mM of alcohol, silyl chloride and catalyst were:  $[\text{ROH}]$ :  $78.85$   $[\text{Ph}_3\text{SiCl}]$ :  $157.3$   $[\text{Cat}]$ :  $19.77$ . The value of excess is the difference between the concentration of alcohol and silyl chloride, thus [ $\text{Excess}$ ]:  $78.48\text{ mM}$ .

### **Trial 4**

A stock solution of starting materials was prepared under argon in a  $1\text{ mL}$  volumetric flask using THF as the solvent. The following amounts were utilized:  $54.2\text{ mg}$ ,  $0.366\text{ mmol}$  of (*R*)-tetralol,  $18.7\text{ mg}$ ,  $0.0915\text{ mmol}$  of levamisole **1.10**,  $48\text{ }\mu\text{L}$ ,  $0.275\text{ mmol}$  of

*iPr*<sub>2</sub>NEt. The solution was thoroughly mixed under argon by taking the solution into the dry syringe followed by returning the solution to the volumetric flask under argon. Prior to addition of starting materials, the reaction vessel was filled with 2.2 mL of THF using a syringe. Once the THF had cooled to -78 °C, 810 μL of the starting material solution was added. Finally, the reaction was initiated with 770 μL of a stock solution of silyl chloride which was prepared in a 2 mL volumetric flask using 588.6 mg, 2.0 mmol of silyl chloride. Overall, the concentrations in mM of alcohol, silyl chloride and catalyst were: [ROH]: 78.49 [Ph<sub>3</sub>SiCl]: 58.98 [Cat]: 19.61. The value of excess is the difference between the concentration of alcohol and silyl chloride, thus [“Excess”]: -19.51 mM.

### **Experiment “Same Excess” of Silyl Chloride to Alcohol in Comparison to Trial 2**

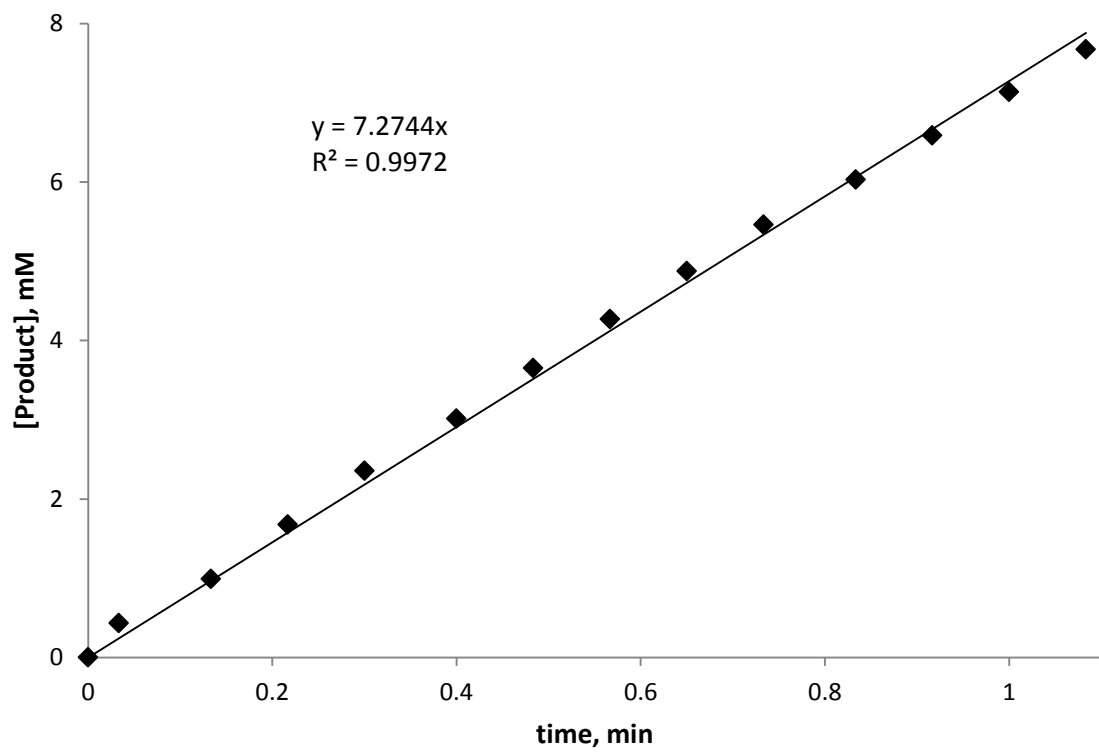
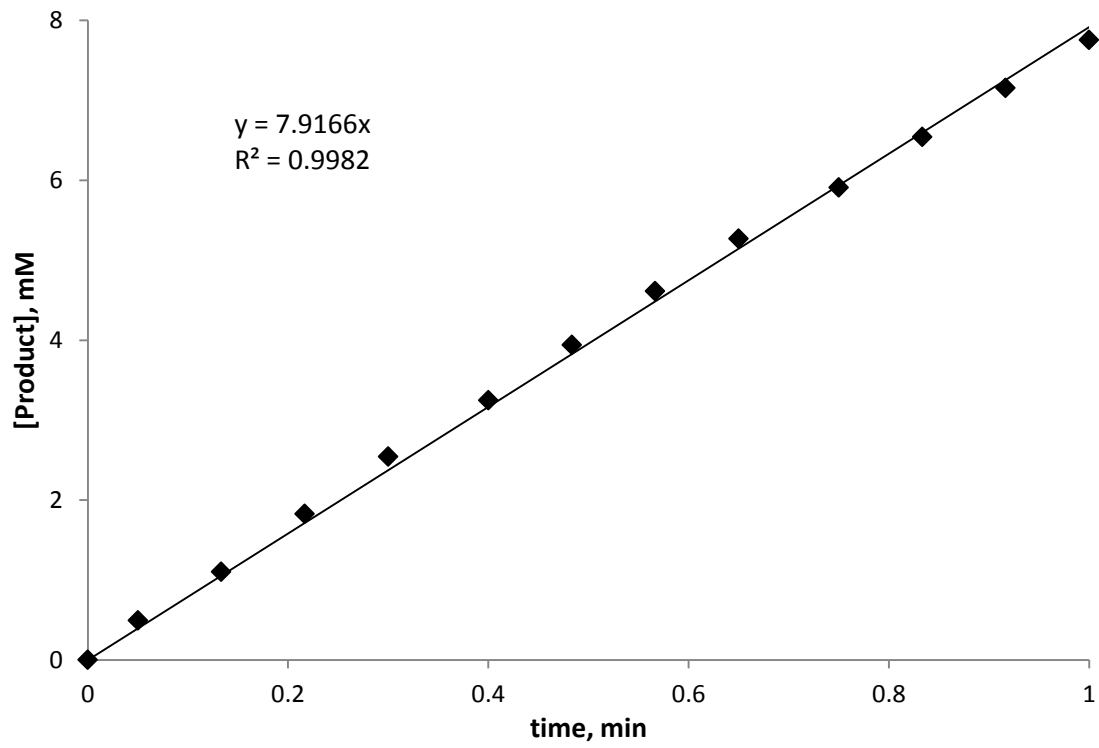
A stock solution of starting materials was prepared under argon in a 1 mL volumetric flask using THF as the solvent. The following amounts were utilized: 27.1 mg, 0.183 mmol of (*R*)-tetralol, 18.7 mg, 0.0915 mmol of levamisole **1.10**, 52 μL, 0.299 mmol of *iPr*<sub>2</sub>NEt. The solution was thoroughly mixed under argon by taking the solution into the dry syringe followed by returning the solution to the volumetric flask under argon. Prior to addition of starting materials, the reaction vessel was filled with 2.1 mL of THF using a syringe. Once the THF had cooled to -78 °C, 810 μL of the starting material solution was added. Finally, the reaction was initiated with 835 μL of a stock solution of silyl chloride which was prepared in a 2 mL volumetric flask using 210.3 mg, 0.715 mmol of silyl chloride. Overall, the concentrations in mM of alcohol, silyl chloride and catalyst were: [ROH]: 39.54 [Ph<sub>3</sub>SiCl]: 79.68 [Cat]: 19.80. The value of excess is the difference between the concentration of alcohol and silyl chloride, thus [“Excess”]: 40.13 mM.

## Initial Rate Studies: Variation of Base Concentration

### 1.0 equiv. of Base

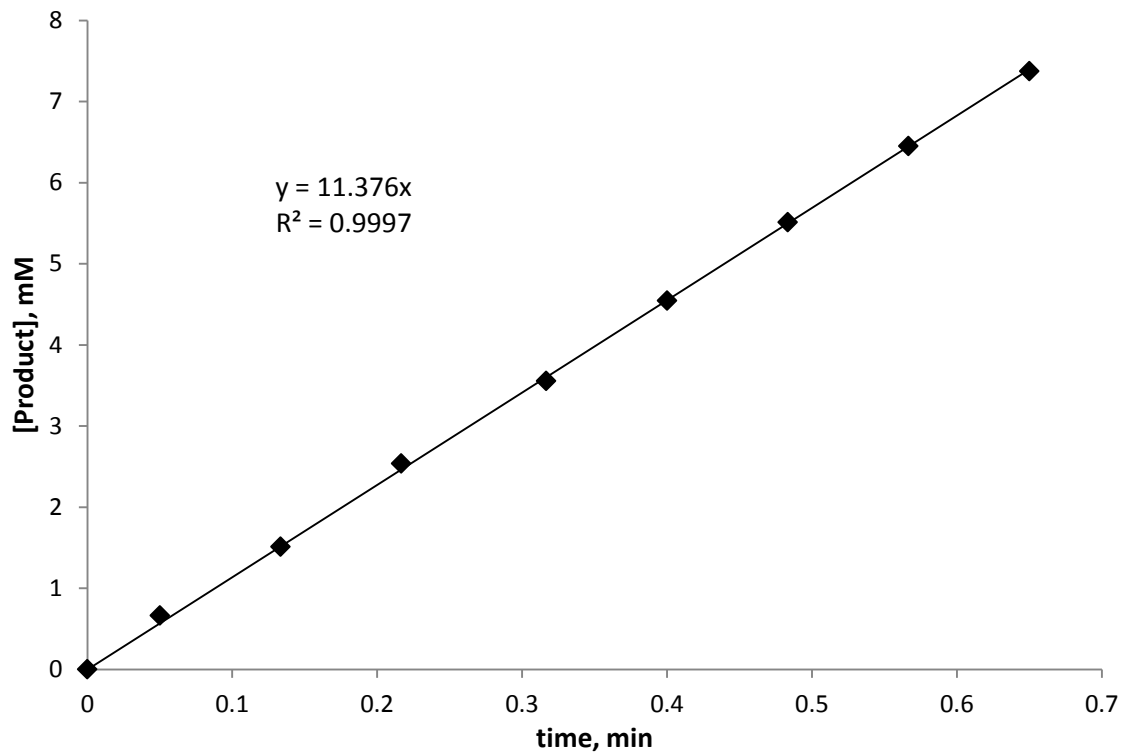
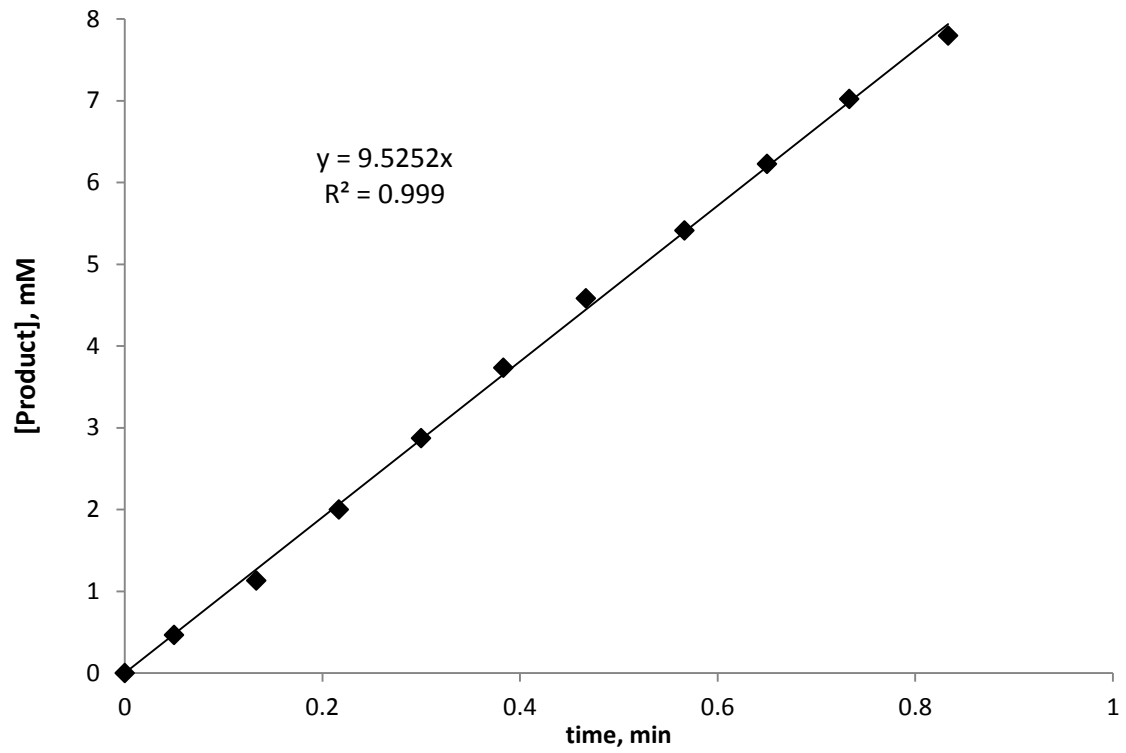
A stock solution of starting materials was prepared under argon in a 2 mL volumetric flask using THF as the solvent. The following amounts were utilized: 108.6 mg, 0.733 mmol of (*R*)-tetralol, 76.0 mg, 0.372 mmol of levamisole **1.10**, 128  $\mu$ L, 0.735 mmol of *i*Pr<sub>2</sub>NEt. The solution was thoroughly mixed under argon by taking the solution into the dry syringe followed by returning the solution to the volumetric flask under argon. Prior to addition of starting materials, the reaction vessel was filled with 2.1 mL of THF using a syringe. Once the THF had cooled to -78 °C, 810  $\mu$ L of the starting material solution was added. Finally, the reaction was initiated with 840  $\mu$ L of a stock solution of silyl chloride which was prepared in a 2 mL volumetric flask using 210.4 mg, 0.715 mmol of silyl chloride. Overall, the concentrations in mM of alcohol, silyl chloride and catalyst and base were: [ROH]: 78.14, [Ph<sub>3</sub>SiCl]: 79.92, [Cat]: 40.2, [Base]: 79.36. The experiment was immediately run in duplicate using the same stock solution. IR data was processed to yield product concentrations according to Beer's Law. The initial rate was determined by measuring the slope employing least squares fit to the first 10 % of reaction conversion (~8 mM) The data was smoothed with a simple 3 pts adjacent average. Data shown in Figure 4.12 is an average of the two runs. The initial rate for the two trials was 7.9 and 7.3 mM/min.





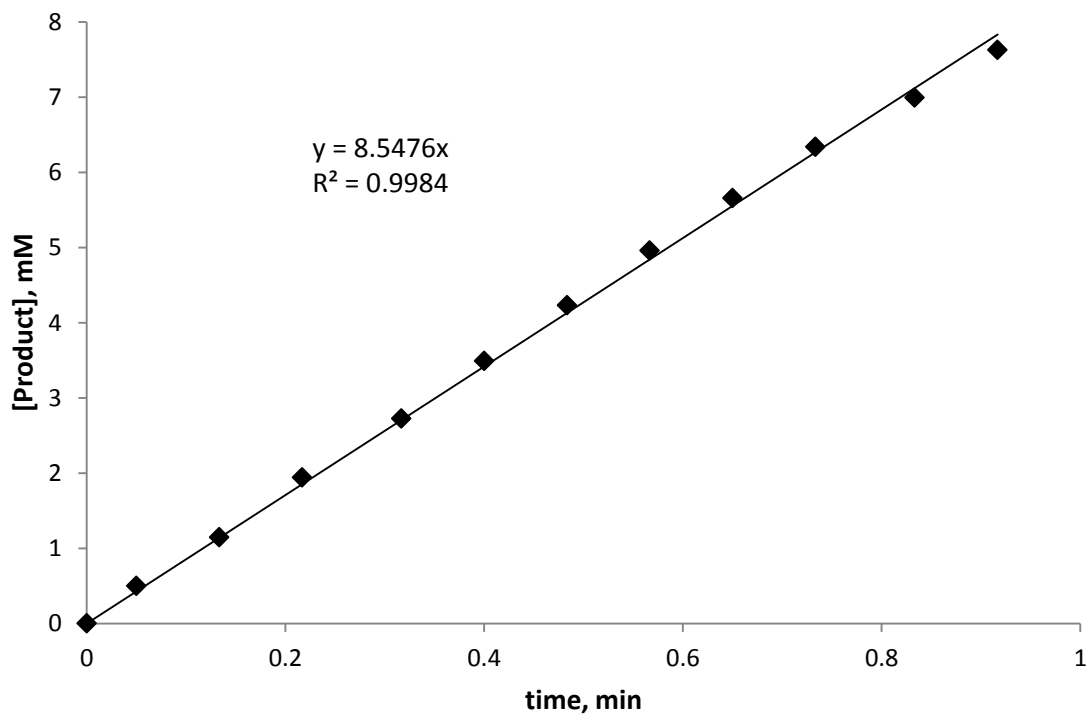
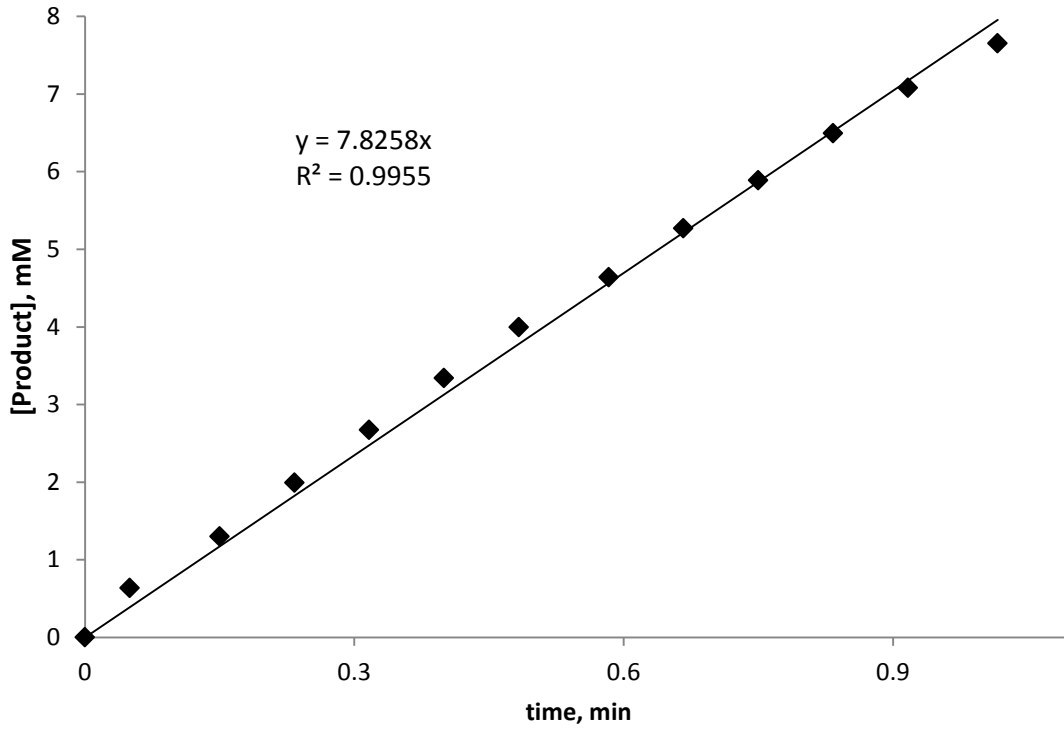
## 1.2 equiv. of base

A stock solution of starting materials was prepared under argon in a 2 mL volumetric flask using THF as the solvent. The following amounts were utilized: 108.6 mg, 0.733 mmol of (*R*)-tetralol, 76.0 mg, 0.372 mmol of levamisole **1.10**, 155  $\mu$ L, 0.89 mmol of *i*Pr<sub>2</sub>NEt. The solution was thoroughly mixed under argon by taking the solution into the dry syringe followed by returning the solution to the volumetric flask under argon. Prior to addition of starting materials, the reaction vessel was filled with 2.1 mL of THF using a syringe. Once the THF had cooled to -78 °C, 810  $\mu$ L of the starting material solution was added. Finally, the reaction was initiated with 840  $\mu$ L of a stock solution of silyl chloride which was prepared in a 2 mL volumetric flask using 210.4 mg, 0.715 mmol of silyl chloride. Overall, the concentrations in mM of alcohol, silyl chloride and catalyst and base were: [ROH]: 78.14, [Ph<sub>3</sub>SiCl]: 79.92, [Cat]: 40.2, [Base]: 96.10. The experiment was immediately run in duplicate using the same stock solution. IR data was processed to yield product concentrations according to Beer's Law. The initial rate was determined by measuring the slope employing least squares fit to the first 10 % of reaction conversion (~8 mM) The data was smoothed with a simple 3 pts adjacent average. Data shown in Figure 4.12 is an average of the two runs. The initial rate for the two trials was 9.5 and 11.4 mM/min.



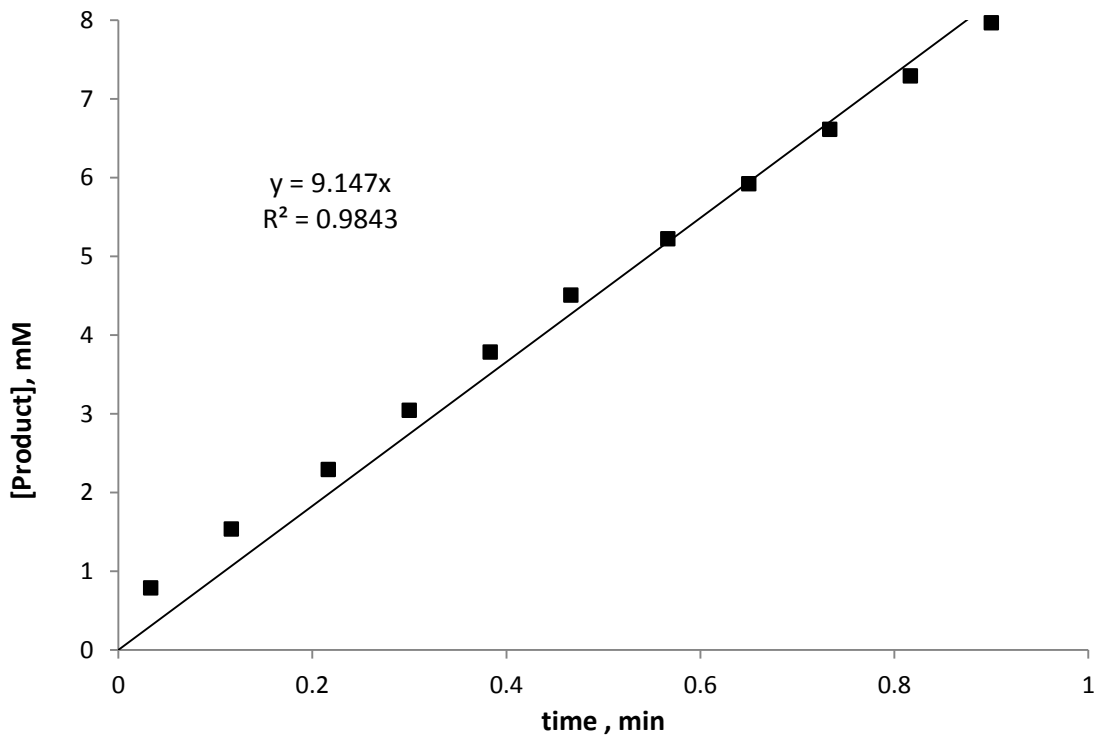
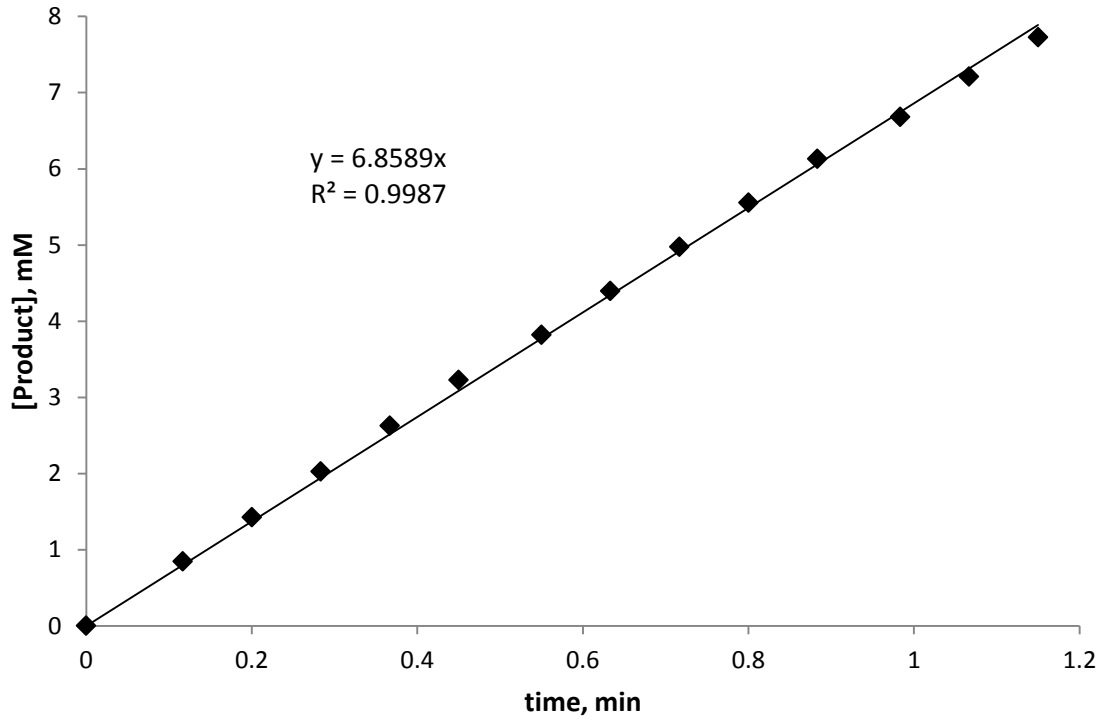
### 0.75 equiv. of base

A stock solution of starting materials was prepared under argon in a 2 mL volumetric flask using THF as the solvent. The following amounts were utilized: 108.6 mg, 0.733 mmol of (*R*)-tetralol, 76.0 mg, 0.372 mmol of levamisole **1.10**, 97  $\mu$ L, 0.551 mmol of *i*Pr<sub>2</sub>NEt. The solution was thoroughly mixed under argon by taking the solution into the dry syringe followed by returning the solution to the volumetric flask under argon. Prior to addition of starting materials, the reaction vessel was filled with 2.1 mL of THF using a syringe. Once the THF had cooled to -78 °C, 810  $\mu$ L of the starting material solution was added. Finally, the reaction was initiated with 840  $\mu$ L of a stock solution of silyl chloride which was prepared in a 2 mL volumetric flask using 210.5 mg, 0.715 mmol of silyl chloride. Overall, the concentrations in mM of alcohol, silyl chloride and catalyst and base were: [ROH]: 78.14, [Ph<sub>3</sub>SiCl]: 80.0, [Cat]: 40.2, [Base]: 60.14. The experiment was immediately run in duplicate using the same stock solution. IR data was processed to yield product concentrations according to Beer's Law. The initial rate was determined by measuring the slope employing least squares fit to the first 10 % of reaction conversion (~8 mM) The data was smoothed with a simple 3 pts adjacent average. Data shown in Figure 4.12 is an average of the two runs. The initial rate for the two trials was 7.8 and 8.5 mM/min.



### 0.5 equiv. of base

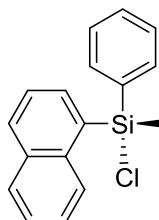
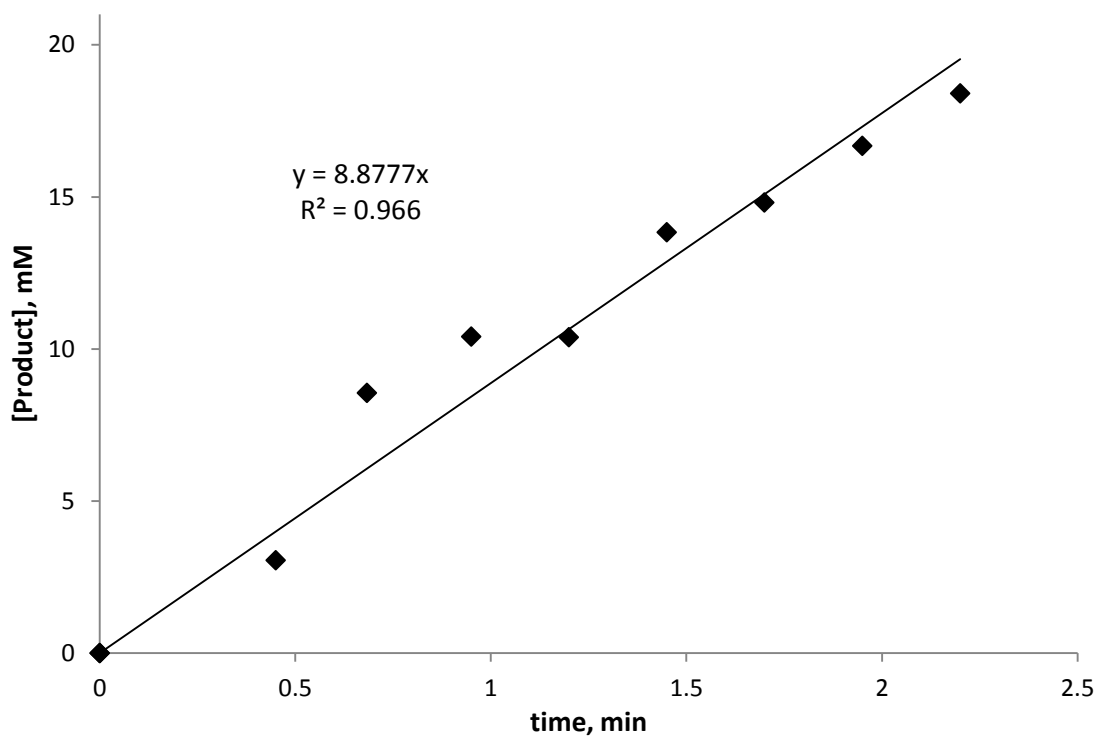
A stock solution of starting materials was prepared under argon in a two, 1 mL volumetric flasks using THF as the solvent. The following amounts were utilized: 54.3 mg, 0.366 mmol of (*R*)-tetralol, 38.0 mg, 0.186 mmol of levamisole **1.10**, 32  $\mu$ L, 0.116 mmol of *i*Pr<sub>2</sub>NEt. The solution was thoroughly mixed under argon by taking the solution into the dry syringe followed by returning the solution to the volumetric flask under argon. Prior to addition of starting materials, the reaction vessel was filled with 2.1 mL of THF using a syringe. Once the THF had cooled to -78 °C, 810  $\mu$ L of the starting material solution was added. Finally, the reaction was initiated with 840  $\mu$ L of a stock solution of silyl chloride which was prepared in a 1 mL volumetric flask using 105.1 mg, 0.357 mmol of silyl chloride. Overall, the concentrations in mM of alcohol, silyl chloride and catalyst and base were: [ROH]: 78.14, [Ph<sub>3</sub>SiCl]: 79.8, [Cat]: 40.2, [Base]: 39.68. The experiment was run in duplicate using the aforementioned quantities of reagents. IR data was processed to yield product concentrations according to Beer's Law. The initial rate was determined by measuring the slope employing least squares fit to the first 10 % of reaction conversion (~8 mM). The data was smoothed with a simple 3 pts adjacent average. Data shown in Figure 4.12 is an average of the two runs. The initial rate for the two trials was 6.9 and 9.1 mM/min.



### 3.0 equiv of Base

A stock solution of starting materials was prepared under argon in a 1 mL volumetric flask using THF as the solvent. The following amounts were utilized: 54.3 mg, 0.366 mmol of (*R*)-tetralol, 37.5 mg, 0.183 mmol of levamisole **1.10**, 192  $\mu$ L, 1.1 mmol of *i*Pr<sub>2</sub>NEt. The solution was thoroughly mixed under argon by taking the solution into the dry syringe followed by returning the solution to the volumetric flask under argon. Prior to addition of starting materials, the reaction vessel was filled with 2.1 mL of THF using a syringe. Once the THF had cooled to -78 °C, 810  $\mu$ L of the starting material solution was added. Finally, the reaction was initiated with 840  $\mu$ L of a stock solution of silyl chloride which was prepared in a 2 mL volumetric flask using 210.4 mg, 0.715 mmol of silyl chloride. Overall, the concentrations in mM of alcohol, silyl chloride and catalyst and base were: [ROH]: 79.14, [Ph<sub>3</sub>SiCl]: 80.08, [Cat]: 39.65, [Base]: 238.1. The experiment was a single run. IR data was processed to yield product concentrations according to Beer's Law. The initial rate was determined by measuring the slope employing least squares fit to the first 25 % of reaction conversion (~20 mM) as the rate of data collection was one spectra per 15 seconds. The data was smoothed with a simple 3 pts adjacent average. Data shown in Figure 4.12 is the initial rate for the trial: 8.9 mM/min.

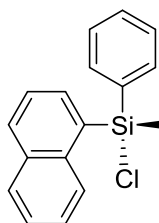




(*S*)-methyl-naphthylphenylsilyl chloride, (-)-**4.9**

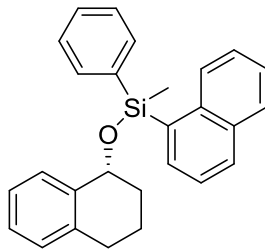
A 25 mL three necked round bottomed flask was equipped with stir bar, condenser, and septum. Next, 250 mg, 1.0 mmol of (*R*)-methyl-naphthylphenylsilane (+)-**4.8** was added to the flask, and the vessel was purged with argon. The silane was dissolved in 4 mL of  $\text{CCl}_4$  with stirring. After the silane had dissolved completely, 162  $\mu\text{L}$ , 2.0 mmol of sulfonyl chloride was added via syringe. The solution was brought to reflux for 5 h. Partial conversion was determined by NMR; therefore, a second addition of 162  $\mu\text{L}$ , 2.0 mmol of sulfonyl chloride was added and the mixture was allowed to reflux 2 additional hours. NMR analysis indicated complete conversion. The solvent was removed in vacuo

yielding a pale yellow oil. Trituration from pentane at  $-78\text{ }^{\circ}\text{C}$  yielded two crops of desired product as a white solid, 111 mg and 65 mg, 62% yield total. The level of enantioenrichment and configuration was determined from comparison of optical rotation to the literature,  $[\alpha]_{\text{D}}^{25}$ :  $-6.4$   $c = 0.94$  pentane,  $[\alpha]_{\text{D}}^{25}$ :  $-6.3$   $c = 4.0$  pentane (97% ee, (*S*)-configuration)<sup>40</sup>. **<sup>1</sup>H NMR** (400 MHz, CDCl<sub>3</sub>)  $\delta$  ppm 8.05 (d,  $J = 8.3$  Hz, 1 H), 7.98 (d,  $J = 8.3$  Hz, 1 H), 7.90-7.86 (m, 2 H), 7.67-7.64 (m, 2 H), 7.53-7.37 (m, 6 H), 1.09 (s, 3 H). **<sup>13</sup>C NMR** (101 MHz, CDCl<sub>3</sub>)  $\delta$  ppm 136.1, 135.5, 135.2, 134.0, 133.4, 131.8, 131.4, 130.5, 129.0, 128.2, 128.1, 126.3, 125.8, 125.0, 2.44. **HRMS** (EI) Calculated for ( $\text{M}^+$ ) ( $\text{C}_{17}\text{H}_{15}\text{ClSi}^+$ ): 282.0626 Observed: 282.0631. **IR** (neat,  $\text{cm}^{-1}$ ) 1589, 1459, 1428, 1257, 1111, 997.



(*S*)-methylnaphthylphenylsilyl chloride, (-)-**4.9**

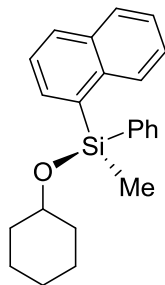
A 25 mL three necked round bottomed flask was equipped with stir bar, condenser, and septum. Next, 250 mg, 1.0 mmol of (*R*)-methylnaphthylphenylsilane (+)-**4.8** was added to the flask, and the vessel was purged with argon. The silane was dissolved in 4 mL of CCl<sub>4</sub> with stirring. After the silane had dissolved completely, the mixture was cooled to 0 °C in an ice bath. A slow stream of dry chlorine was added to the solution producing a yellow-green solution in seconds. The solvent and excess chlorine gas was immediately removed in vacuo. NMR analysis indicated complete degradation of the silane to dichloromethylphenylsilane via loss of a naphthyl group.



A 4 dram vial was equipped with stir bar and septum. In the the vial under a stream of argon, 74.1 mg, 0.50 mmol of (*R*)-tetralol, and 25.5 mg, 0.125 mmol of levamisole **1.10** were weighed into the vial. The starting materials were dissolved in 2.1 mL of dry THF. Base, *i*Pr<sub>2</sub>NEt, 87  $\mu$ L was added via syringe and the mixture cooled to -78  $^{\circ}$ C in a dry ice/acetone bath. The reaction was started by addition of 141 mg, 0.50 mmol of (*S*)-methylnaphthylphenylsilyl chloride (-)-**4.9** dissolved in 600  $\mu$ L of THF. The reaction was monitored by TLC and <sup>1</sup>H NMR At 3 h reaction time; both indicated conversion of <85%. The reaction was quenched with 0.5 mL of methanol and concentrated. The product was isolated as a colorless oil after purification on column hexanes gradient to 5% EtOAc in hexanes, 173 mg, 88 % yield. The product was obtained as a pair of diastereomers according to the analytical data; reduction of the silyl group indicated the major diastereomer was the (*R*),(*R*<sub>Si</sub>) diastereomer. Major Diastereomer: <sup>1</sup>H NMR (400 MHz, CDCl<sub>3</sub>)  $\delta$  ppm 8.19 (t, *J* = 9.0 Hz, 1 H), 7.99-7.96 (m, 2 H), 7.90 (d, *J* = 8.1 Hz, 1 H), 7.70 (m, 2 H), 7.57-7.08 (m, 10 H), 4.94 (dd, *J* = 12.4, 6.5, Hz 1 H), 2.86-2.77 (m, 1 H), 2.69-2.62 (m, 1 H), 2.08-1.58 (m, 4 H), 0.84 (s, 3 H). Minor Diastereomer: <sup>1</sup>H NMR (400 MHz, CDCl<sub>3</sub>)  $\delta$  ppm 8.19 (t, *J* = 9.0 Hz, 1 H), 7.99-7.96 (m, 2 H), 7.90 (d, *J* = 8.1 Hz, 1 H), 7.70 (m, 2 H), 7.57-7.08 (m, 10 H), 4.94 (dd, *J* = 12.4, 6.5, Hz 1 H), 2.86-2.77 (m, 1 H), 2.69-2.62 (m, 1 H), 2.08-1.58 (m, 4 H), 0.83 (s, 3 H). Deconvolution of the proton NMR spectra singlets at 0.83 and 0.84 indicated the d.r. was 59:41. The carbon spectrum of all peaks from the mixture of diastereomers is given here. <sup>13</sup>C NMR (101

MHz, CDCl<sub>3</sub>) δ ppm 139.1, 139.0, 137.5, 137.1, 137.0, 137.0, 135.3, 135.1, 134.6, 134.4, 134.3, 134.3, 133.4, 130.8, 129.7, 129.1, 128.8, 128.7, 128.4, 127.9, 127.9, 127.2, 125.8, 125.8, 125.7, 125.7, 125.5, 125.5, 125.0. HRMS (EI) Calculated for (M<sup>+</sup>) (C<sub>27</sub>H<sub>26</sub>OSi<sup>+</sup>): 394.1747 Observed: 394.1742. IR (neat, cm<sup>-1</sup>) 2936, 1505, 1428, 1113, 1070.

In order to determine the configuration at silicon for the major diastereomer the silylether was reduced using a known procedure.<sup>45</sup> A 4 dram vial was fitted with stir bar and septum. The silyl ether was added, 91 mg, 0.23 mmol and the vessel purged with nitrogen. The starting material was dissolved in 4 mL of dry CH<sub>2</sub>Cl<sub>2</sub> with stirring and cooled to -78 °C in a dry ice/ acetone bath. DIBAL-H, 240 μL, 0.24 mmol was added via syringe and the mixture was allowed to stir for 1.5 h. the vial was then allowed to warm to ambient temperature. A second addition of DIBAL-H, 240 μL, 0.24 mmol was made and the reaction was allowed to proceed overnight since TLC analysis indicated incomplete conversion. The vial was again cooled to -78 °C and quenched with 1 mL of acetone. The was agan warmed to room temperature and aluminum byproduct was decomposed by addition of 1 mL of concentrated HCl followed by 10 mL of water. The organic layer was then separated and the aqueous layer extracted (3 x 5 mL) with CH<sub>2</sub>Cl<sub>2</sub>. The combined organic layers were washed with sat. aqueous NaHCO<sub>3</sub>, sat. aqueous NaCl, then dried over sodium sulfate. Filtration and concentration gave an oil which was purified on column using hexanes and eluent. The silane was isolated as a colorless oil, 31.2 mg, 55 % yield. Analysis of the silane on HPLC using OD-H column 1 mL/min flow rate at 254 nm indicated an e.r. of 56:44 enriched in the (*R*)-enantiomer.



A 100 mL flame dried round bottomed flask was fitted with stir bar and septum. Under argon, 113 mg, 0.45 mmol of (-)-benzotetramisole **1.5** was added to the flask. The vessel was sealed and the catalyst dissolved in 20.6 mL of dry THF. Base, *i*Pr<sub>2</sub>NEt, 313  $\mu$ L, 1.8 mmol and cyclohexanol, 187  $\mu$ L, 1.8 mmol were added via syringe. The mixture was cooled to -78 °C with stirring. The reaction was started by adding 1.9 mL of a 0.94 M solution of (*S*)-methylnaphthylphenylsilyl chloride (-)-**4.9**. Aliquots were removed (2 mL each) at intervals according to Table 4.1 and analyzed employing NMR and GC-MS. Conversion could not be determined from these samples. The enantiomers of the product were thus purified on column employing hexanes gradient to 3% EtOAc in hexanes. Purified samples possessed the following properties: <sup>1</sup>H NMR (400 MHz, CDCl<sub>3</sub>)  $\delta$  ppm 8.21 (d, *J* = 8.2 Hz, 1 H), 7.89 (d, *J* = 8.2 Hz, 1 H), 7.83-7.80 (m, 2 H), 7.62-7.60 (m, 2 H), 7.47-7.37 (m, 7 H), 3.82-2.75 (m, 1 H), 1.82-1.86 (m, 4 H), 1.50-1.13 (m, 6 H), 0.78 (s, 3 H). <sup>13</sup>C NMR (101 MHz, CDCl<sub>3</sub>)  $\delta$  ppm .137.6, 137.0, 134.9, 134.8, 134.2, 133.3, 130.5, 129.5, 129.0, 128.6, 127.8, 125.7, 125.4, 124.9, 71.7, 35.7, 25.6, 24.0, -1.1. Optical rotation:  $[\alpha]_D^{25}$ : +3.4 c = 2.6 CHCl<sub>3</sub>;  $[\alpha]_D^{25lit}$ : +6.7 c = 1.2 CHCl<sub>3</sub>.<sup>47</sup> Configuration is (*R*) at silicon. This conforms to the e.r. as determined by HPLC on OD-H column, 0.4 mL flow rate,  $\lambda$  = 254 nm.

**Table 4.1 Monitoring the Enantioenrichment throughout the Reaction**

Aliquot	time, mins	e.r.	R/S
1	2	74:26	R
2	4	72:28	R
3	6	72:28	R
4	8	72:28	R
5	17	73:27	R
6	32	72:28	R
7	64	72:28	R
8	128	72:28	R
9	158	72:28	R

#### 4.11. References

1. Birman, V. B.; Li, X. Benzotetramisole: a Remarkably Enantioselective Acyl Transfer Catalyst. *Org. Lett.* **2006**, *8*, 1351.
2. Birman, V. B.; Li, X. Homobenzotetramisole: an Effective Catalyst for Kinetic Resolution of Aryl-Cycloalkanols. *Org. Lett.* **2008**, *10*, 1115.
3. Yang, X.; Lu, G.; Birman, V. B. Benzotetramisole-Catalyzed Dynamic Kinetic Resolution of Azlactones. *Org. Lett.* **2010**, *12*, 892.
4. Li, X.; Liu, P.; Houk, K. N.; Birman, V. B. Origin of Enantioselectivity in CF<sub>3</sub>-PIP-Catalyzed Kinetic Resolution of Secondary Benzylic Alcohols. *J. Am. Chem. Soc.* **2008**, *130*, 13836.
5. Nakata, K.; Gotoh, K.; Ono, K.; Futami, K.; Shiina, I. Kinetic Resolution of Racemic 2-Hydroxy-Gamma-Butyrolactones by Asymmetric Esterification Using Diphenylacetic Acid with Pivalic Anhydride and a Chiral Acyl-Transfer Catalyst. *Org. Lett.* **2013**, *15*, 1170.
6. Akhani, R. K.; Moore, M. I.; Pribyl, J. G.; Wiskur, S. L. Linear Free-Energy Relationship and Rate Study on a Silylation-Based Kinetic Resolution: Mechanistic Insights. *J. Org. Chem.* **2014**, *79*, 2384.
7. Sheppard, C. I.; Taylor, J. L.; Wiskur, S. L. Silylation-Based Kinetic Resolution of Monofunctional Secondary Alcohols. *Org. Lett.* **2011**, *13*, 3794.
8. Wander, M.; Hausoul, P. J. C.; Sliedregt, L. A. J. M.; van Steen, B. J.; van Koten, G.; Klein Gebbink, R. J. M. Synthesis of Polyaryl Rigid-Core Carbosilane Dendrimers for Supported Organic Synthesis. *Organometallics* **2009**, *28*, 4406.

9. Charton, M. Steric Effects. III. Bimolecular Nucleophilic Substitution. *J. Am. Chem. Soc.* **1975**, *97*, 3694.
10. Charton, M. Steric Effects. II. Base-Catalyzed Ester Hydrolysis. *J. Am. Chem. Soc.* **1975**, *97*, 3691.
11. Charton, M. Steric Effects. I. Esterification and Acid-Catalyzed Hydrolysis of Esters. *J. Am. Chem. Soc.* **1975**, *97*, 1552.
12. Hansch, C.; Leo, A.; Taft, R. W. A Survey of Hammett Substituent Constants and Resonance and Field Parameters. *Chem. Rev.* **1991**, *91*, 165.
13. Anslyn, E. V.; Dougherty, D. A., *Modern Physical Organic Chemistry*. University Science Books: Sausalito, Ca, 2006.
14. Bassindale, A. R.; Stout, T. A  $^{29}\text{Si}$ ,  $^{13}\text{C}$  and  $^1\text{H}$  NMR Study of the Interaction of Various Halotrimethylsilanes and Trimethylsilyl Triflate with Dimethyl Formamide and Acetonitrile, a Comment on the Nucleophile Induced Racemisation of Halosilanes. *J. Organomet. Chem.* **1982**, *238*, C41.
15. Bassindale, A. R.; Lau, J. C. Y.; Taylor, P. G. Nucleophile-assisted Racemisation of Halosilanes; an Alternative Pathway Involving Halide Exchange. *J. Organomet. Chem.* **1988**, *341*, 213.
16. Wang, L.; Akhani, R. K.; Wiskur, S. L. Diastereoselective and Enantioselective Silylation of 2-Arylcyclohexanols. *Org. Lett.* **2015**, *17*, 2408.
17. Akhani, R. K.; Clark, R. W.; Yuan, L.; Wang, L.; Tang, C.; Wiskur, S. L. Polystyrene-Supported Triphenylsilyl Chloride for the Silylation-Based Kinetic Resolution of Secondary Alcohols. *ChemCatChem* **2015**, *7*, 1527.



18. Wagner, A. J.; Rychnovsky, S. D. Kinetic Analysis of the HBTM-Catalyzed Esterification of an Enantiopure Secondary Alcohol. *Org. Lett.* **2013**, *15*, 5504.
19. Blackmond, D. G. Reaction Progress Kinetic Analysis: A Powerful Methodology for Mechanistic Studies of Complex Catalytic Reactions. *Angew. Chem., Int. Ed.* **2005**, *44*, 4302.
20. Shekhar, S.; Ryberg, P.; Hartwig, J. F.; Mathew, J. S.; Blackmond, D. G.; Strieter, E. R.; Buchwald, S. L. Reevaluation of the Mechanism of the Amination of Aryl Halides Catalyzed by BINAP-Ligated Palladium Complexes. *J. Am. Chem. Soc.* **2006**, *128*, 3584.
21. Mathew, J. S.; Klussmann, M.; Iwamura, H.; Valera, F.; Futran, A.; Emanuelsson, E. A. C.; Blackmond, D. G. Investigations of Pd-Catalyzed ArX Coupling Reactions Informed by Reaction Progress Kinetic Analysis. *J. Org. Chem.* **2006**, *71*, 4711.
22. Blackmond, D. G.; Ropic, M.; Stefinovic, M. Kinetic Studies of the Asymmetric Transfer Hydrogenation of Imines with Formic Acid Catalyzed by Rh–Diamine Catalysts. *Org. Process Res. Dev.* **2006**, *10*, 457.
23. Ruiz-Castillo, P.; Blackmond, D. G.; Buchwald, S. L. Rational Ligand Design for the Arylation of Hindered Primary Amines Guided by Reaction Progress Kinetic Analysis. *J. Am. Chem. Soc.* **2015**, *137*, 3085.
24. Gulzar, N.; Jones, K. M.; Konnerth, H.; Breugst, M.; Klussmann, M. Experimental and Computational Studies on the C-H Amination Mechanism of Tetrahydrocarbazoles via Hydroperoxides. *Chem. – Eur. J.* **2015**, *21*, 3367.
25. Scott, M.; Sud, A.; Boess, E.; Klussmann, M. Reaction Progress Kinetic Analysis of a Copper-Catalyzed Aerobic Oxidative Coupling Reaction with N-Phenyl Tetrahydroisoquinoline. *J. Org. Chem.* **2014**, *79*, 12033.

26. Lineweaver, H.; Burk, D. The Determination of Enzyme Dissociation Constants. *J. Am. Chem. Soc.* **1934**, *56*, 658.
27. Cornish-Bowden, A., *Fundamentals of Enzyme Kinetics*. 4th Edition ed.; Wiley-VCH: Singapore, 2012.
28. House, J. E., *Principles of Chemical Kinetics*. 2nd ed.; Academic Press. : Amsterdam, 2007; p 70.
29. Greene, T. W.; Wuts, P. G. M., *Protective Groups in Organic Synthesis*. 3 ed.; John Wiley and Sons: New York, USA, 1999.
30. Corriu, R. J. P.; Dabosi, G.; Martineau, M. The Nature of the Interaction of Nucleophiles such as HMPT, DMSO, DMF and Ph<sub>3</sub>PO with Triorganohalo-Silanes, -Germanes, and -Stannanes and Organophosphorus Compounds. Mechanism of Nucleophile Induced Racemization and Substitution at Metal. *J. Organomet. Chem.* **1980**, *186*, 25.
31. Corriu, R. J. P.; Guérin, C.; Moreau, J. J. E., Stereochemistry at Silicon. In *Topics in Stereochemistry*, John Wiley & Sons, Inc.: 1984; Vol. 15, pp 43.
32. Denmark, S. E.; Su, X.; Nishigaichi, Y. The Chemistry of Trichlorosilyl Enolates. 6. Mechanistic Duality in the Lewis Base-Catalyzed Aldol Addition Reaction. *J. Am. Chem. Soc.* **1998**, *120*, 12990.
33. Baxter, R. D.; Sale, D.; Engle, K. M.; Yu, J.-Q.; Blackmond, D. G. Mechanistic Rationalization of Unusual Kinetics in Pd-Catalyzed C–H Olefination. *J. Am. Chem. Soc.* **2012**, *134*, 4600.

34. Corriu, R. J. P.; Dabosi, G.; Martineau, M. Mécanisme de L'hydrolyse des Chlorosilanes, Catalysée par un Nucléophile: Étude Cinétique et Mise en Evidence d'un Intermediaire Hexacoordonné. *J. Organomet. Chem.* **1978**, *150*, 27.
35. Corriu, R. J. P.; Dabosi, G.; Martineau, M. A New Method for the Determination of Water in Organic Solvents, and Some Comments on an Electrochemical Method of synthesizing Si-Si bonds. *J. Organomet. Chem.* **1981**, *222*, 195.
36. Sommer, L. H.; Frye, C. L. Optically Active Organosilicon Compounds Having Reactive Groups Bonded to Asymmetric Silicon. Displacement Reactions at Silicon with Pure Retention and Pure Inversion of Configuration. *J. Am. Chem. Soc.* **1959**, *81*, 1013.
37. Sommer, L. H.; Blankman, H. D.; Miller, P. C. Non-Rearrangement Reactions of the Neopentyl-Oxygen Bond. New Syntheses of Neopentyl Halides. *J. Am. Chem. Soc.* **1951**, *73*, 3542.
38. Sommer, L. H.; Frye, C. L. Stereochemistry of Chloride Ion Displacement from Silicon. Hydrolysis and Methanolysis of an Optically Active Organochlorosilane. *J. Am. Chem. Soc.* **1960**, *82*, 4118.
39. Sommer, L. H.; Lyons, J. E.; Fujimoto, H.; Michael, K. W. Stereospecific exchange reactions of optically active  $R_3Si^*H(D)$  catalyzed by Group VIII metals. *J. Am. Chem. Soc.* **1967**, *89*, 5483.
40. Sommer, L. H.; Ulland, L. A. Chirality and Structure of Organosilicon Radicals. *J. Org. Chem.* **1972**, *37*, 3878.
41. Ojima, Y.; Yamaguchi, K.; Mizuno, N. An Efficient Solvent-Free Route to Silyl Esters and Silyl Ethers. *Adv. Synth. Catal.* **2009**, *351*, 1405.

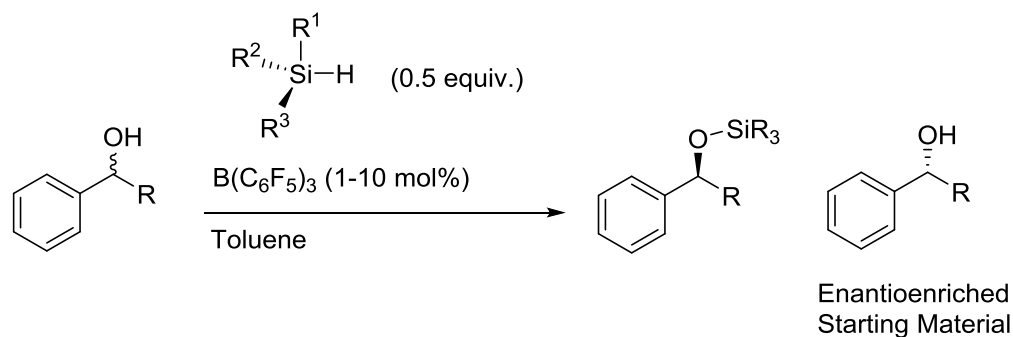
42. Sommer, L. H.; Frye, C. L.; Parker, G. A.; Michael, K. W. Stereochemistry of Asymmetric Silicon. I. Relative and Absolute Configurations of Optically Active  $\alpha$ -Naphthylphenylmethylsilanes. *J. Am. Chem. Soc.* **1964**, *86*, 3271.
43. *Encyclopedia of Reagents for Organic Synthesis*. 1st ed.; John Wiley and Sons: West Sussex, England, Vol. 2, p 1057.
44. Sakurai, H.; Murakami, M.; Kumada, M. Silyl Radicals. II. Stereochemical Course of the Reaction of an Optically Active Hydrosilane with Carbon Tetrachloride by a Free-Radical Mechanism. Retention of Configuration. *J. Am. Chem. Soc.* **1969**, *91*, 519.
45. Oestreich, M.; Schmid, U. K.; Auer, G.; Keller, M. A Convergent Method for the Synthesis of Highly Enantiomerically Enriched Cyclic Silanes with Silicon-Centered Chirality. *Synthesis* **2003**, 2725.
46. Clark, R. W.; Deaton, T. M.; Zhang, Y.; Moore, M. I.; Wiskur, S. L. Silylation-Based Kinetic Resolution of  $\alpha$ -Hydroxy Lactones and Lactams. *Org. Lett.* **2013**, *15*, 6132.
47. Shinke, S.; Tsuchimoto, T.; Kawakami, Y. Stereochemistry in Lewis Acid-Catalyzed Silylation of Alcohols, Silanols, and Methoxysilanes with Optically Active Methyl(1-naphthyl)phenylsilane. *Silicon Chem.* **2007**, *3*, 243.
48. Corriu, R. J. P.; Guerin, C.; Moreau, J. J. E., *Topics in Stereochemistry*. John Wiley and Sons: 1984; Vol. 15, p 55.
49. Denmark, S. E.; Wong, K.-T.; Stavenger, R. A. The Chemistry of Trichlorosilyl Enolates. 2. Highly-Selective Asymmetric Aldol Additions of Ketone Enolates. *J. Am. Chem. Soc.* **1997**, *119*, 2333.

50. Brefort, J. L.; Corriu, R. J. P.; Guerin, C.; Henner, B. J. L.; Wong Chi Man, W. W. C. Pentacoordinated Silicon Anions: Synthesis and Reactivity. *Organometallics* **1990**, *9*, 2080.
51. Yakelis, N. A.; Bergman, R. G. Safe Preparation and Purification of Sodium Tetrakis[(3,5-trifluoromethyl)phenyl]borate (NaBARF): Reliable and Sensitive Analysis of Water in Solutions of Fluorinated Tetraarylborates. *Organometallics* **2005**, *24*, 3579.
52. Erker, G. Tris(pentafluorophenyl)borane: a Special Bboron Lewis Acid for Special Reactions. *Dalton Trans.* **2005**, 1883.
53. Johnson, K. A.; Goody, R. S. The Original Michaelis Constant: Translation of the 1913 Michaelis–Menten Paper. *Biochemistry* **2011**, *50*, 8264.
54. Dietze, P. E. The Reaction of Carboxylate Nucleophiles with Tert-Butyldimethylphenoxysilanes in Dimethylformamide. *J. Org. Chem.* **1992**, *57*, 1042.
55. Stöver, D. H.; Lü, P.; Fréchet, J. D. Polymeric Reagents: Preparation and Characterization of Novel Solid-Phase, Silylating Agents Derived from Copolymers Containing 4-[3'-(dimethyl phenyl silyl)-propyl]-styrene. *Polym. Bull.* **1991**, *25*, 575.
56. Patschinski, P.; Zhang, C.; Zipse, H. The Lewis Base-Catalyzed Silylation of Alcohols—A Mechanistic Analysis. *J. Org. Chem.* **2014**, *79*, 8348.

## Chapter 5 Kinetic Resolution of Secondary Alcohols via Borane Lewis Acid Catalyzed Silylation

### 5.1 Introduction and Scope

The goal of the research described in this chapter is to develop a novel enantioselective methodology based upon kinetic resolution of alcohols.<sup>1</sup> The approach of the resolution is distinctly different from the Lewis base catalyzed<sup>2</sup> reactions discussed in previous chapters. Specifically the work herein describes the use of Lewis acids to facilitate silylation of alcohols, thiols, and amines with silanes via a Lewis acid catalyzed dehydrogenative silicon-oxygen coupling reaction.<sup>3-5</sup> These couplings are advantageous as they eliminate the need for extraneous reagents and the only side product formed is dihydrogen. In order to develop a kinetic resolution based on borane catalyzed silylation (Scheme 5.1) various stereogenic silanes were synthesized and the stereochemical result was determined for the reaction. Attempts to determine and expand on a substrate scope for the resolution are also demonstrated.



Scheme 5.1 Proposed Lewis Acid Catalyzed Kinetic Resolution

Silylation via chlorosilanes as a protecting group for alcohols is synthetically ubiquitous in organic chemistry.<sup>6</sup> However, this method of protection demonstrates poor atom economy with the loss of chlorine, utilizes moisture sensitive chlorosilanes, and results in formation of HCl, a potentially unwanted side product that must be controlled with a stoichiometric quantity of base. An alternate method of silylation has been well developed based upon commercially available and stable silanes. In these reactions, Lewis acids have been shown to produce an electrophilic organosilane via activation of the silicon hydrogen bond. This activated species has been successfully utilized in the hydrosilylation of a variety of functional groups: alcohols and thiols are silylated cleanly via this method. Appealingly, gaseous dihydrogen is the only side product.<sup>3</sup>

Appealingly, a commercially available Lewis acid,  $B(C_6F_5)_3$  has been employed to activate a silicon hydrogen bond via activation of the hydrogen-silicon bond. The activated silane is electrophilic enough to prompt immediate silylation of alcohols with simultaneous reduction to yield dihydrogen. The mechanism (Figure 5.1) for alcohol protection is well understood<sup>7</sup> and begins with free  $B(C_6F_5)_3$  entry into the catalytic cycle. The observed reaction rate has been demonstrated to be dependent upon the  $K_{eq}$  between Lewis acid-substrate complexation and free  $B(C_6F_5)_3$ . The species **5.1** of the borane catalyst complexed with the alcohol is readily isolatable owing to the Lewis acidity of the catalyst.

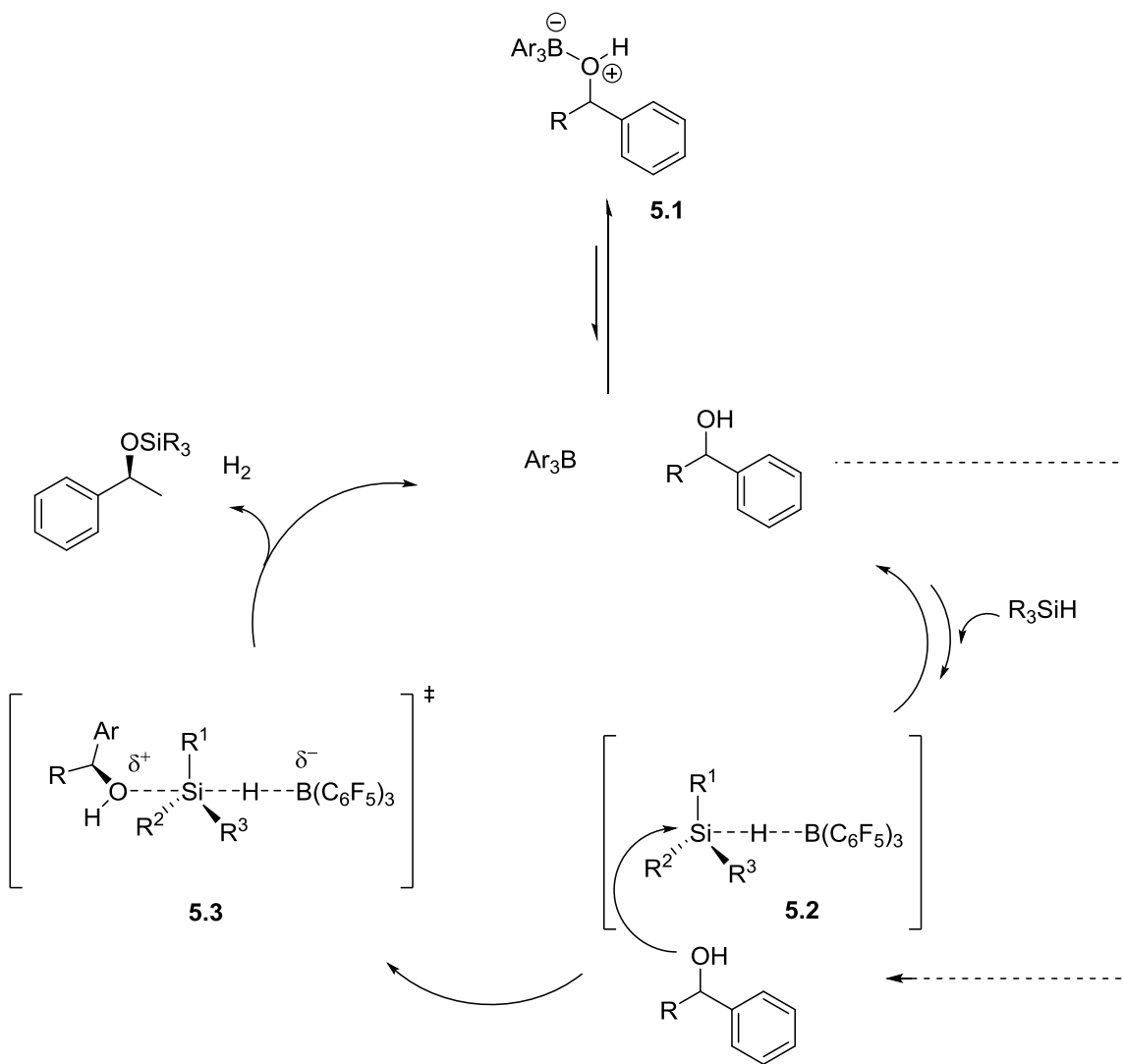


**Figure 5.1 Detailed Mechanism for Borane Catalyzed Silicon-Oxygen Couplings**

Once free,  $\text{B}(\text{C}_6\text{F}_5)_3$  complexes to the hydride from the silane to yield a highly electrophilic silyl species **5.2**. The alcohol is then silylated via an  $\text{S}_{\text{N}}2$  reaction at silicon depicted as species **5.3**. Species **5.2** and **5.3** are not only unrecoverable, but they are also unobservable via  $^1\text{H}$ ,  $^{19}\text{F}$ , or  $^{29}\text{Si}$  NMR. This is indicative of the high reactivity of the electrophilic silane **5.2**. Experimental support for the active species **5.2** includes near perfect inversion of stereochemistry at silicon due to the apparent  $\text{S}_{\text{N}}2$  reaction with the



alcohol substrate. This result has been further corroborated by DFT studies that place the LUMO along the silicon-hydrogen bond.<sup>3,7</sup> A recent study utilizing stereogenic silanes in hydrosilylations of prochiral ketones demonstrated the reaction proceeds with 97% inversion of stereochemistry.<sup>8</sup> Additionally, an experiment in the presence of half an equivalent of a deuterium labeled achiral silane resulted in scrambling yet maintained stereochemistry at silicon.<sup>7</sup> Likewise, no racemization at silicon would be expected for the borane catalyzed silylation of alcohols. Indeed, a recent study has indicated near perfect inversion of stereochemistry at silicon in a reaction utilizing a stereoenriched silane.<sup>9</sup>

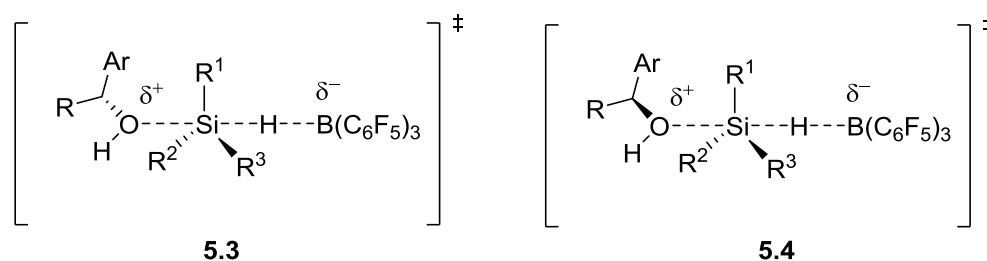


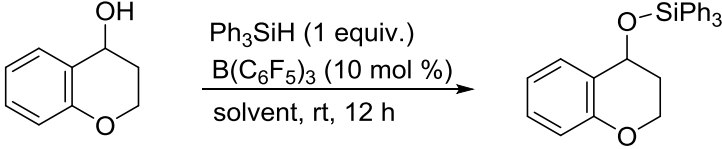
**Figure 5.2 Diastereomeric Transition States in the Borane Catalyzed Silylation**

With the mechanism firmly established for borane catalyzed dehydrogenative silicon oxygen coupling the method of kinetically resolving a racemic alcohol was envisioned (Scheme 5.1). Since the silylation proceeds through an  $S_N2$  transition state after activation of the silane by the borane catalyst<sup>7</sup>, a chiral silane is hypothesized to produce the energy differences required for an efficient kinetic resolution. A silicon-stereogenic silane<sup>10-11</sup> is presumed to affect selectivity for these transformations due to the proximity of the silicon to the approaching alcohol.<sup>8</sup> Since the approaching alcohol and silane both contain stereocenters, the products and transition state to product are both inherently diastereomeric. Significant differences in energy between the two

diastereomeric transition states, **5.3** and **5.4**, (Figure 5.2) would correlate directly to the selectivity factor (Equation 1.2).<sup>12</sup>

## 5.2 Preliminary Data

First, the reaction conditions were probed to include the silyl source, solvent and substrates. Chromanol was selected as a suitable substrate for the initial reactions, because of its high selectivity in our previously reported silylation-based kinetic resolution.<sup>13</sup> Achiral triphenylsilane was used as the silane source for these initial studies since it was commercially available. The protection of alcohols via silylation is inherently moisture sensitive. A simple experiment using toluene dried via passage through activated alumina columns was compared against the same solvent dried over  $\text{CaH}_2$  followed by fractional distillation. As evident in Table 5.1, Entries 1 and 2 an additional drying step is clearly required for solvents utilized in the reaction. Reactions occurring with significant moisture content result in formation of unwanted hexaphenyldisiloxane presumably via reaction with the silanol formed from the water present. Additionally attempts to prepare the silyl ether with another dried solvent,  $\text{CH}_2\text{Cl}_2$ , previously utilized in an alternate procedure for these silicon-oxygen coupling was unsuccessful (Table 5.1 Entry 3). With the reaction successfully reproduced in our laboratory (Entry 2), we next focused our attention on asymmetric silane sources for use in the silylation reaction.

**Table 5.1 Initial Conditions for the Lewis Acid Catalyzed Silylation**

Entry	solvent	% conv <sup>a</sup>
1	toluene	<5
2 <sup>b</sup>	toluene	50
3 <sup>b</sup>	CH <sub>2</sub> Cl <sub>2</sub>	<5

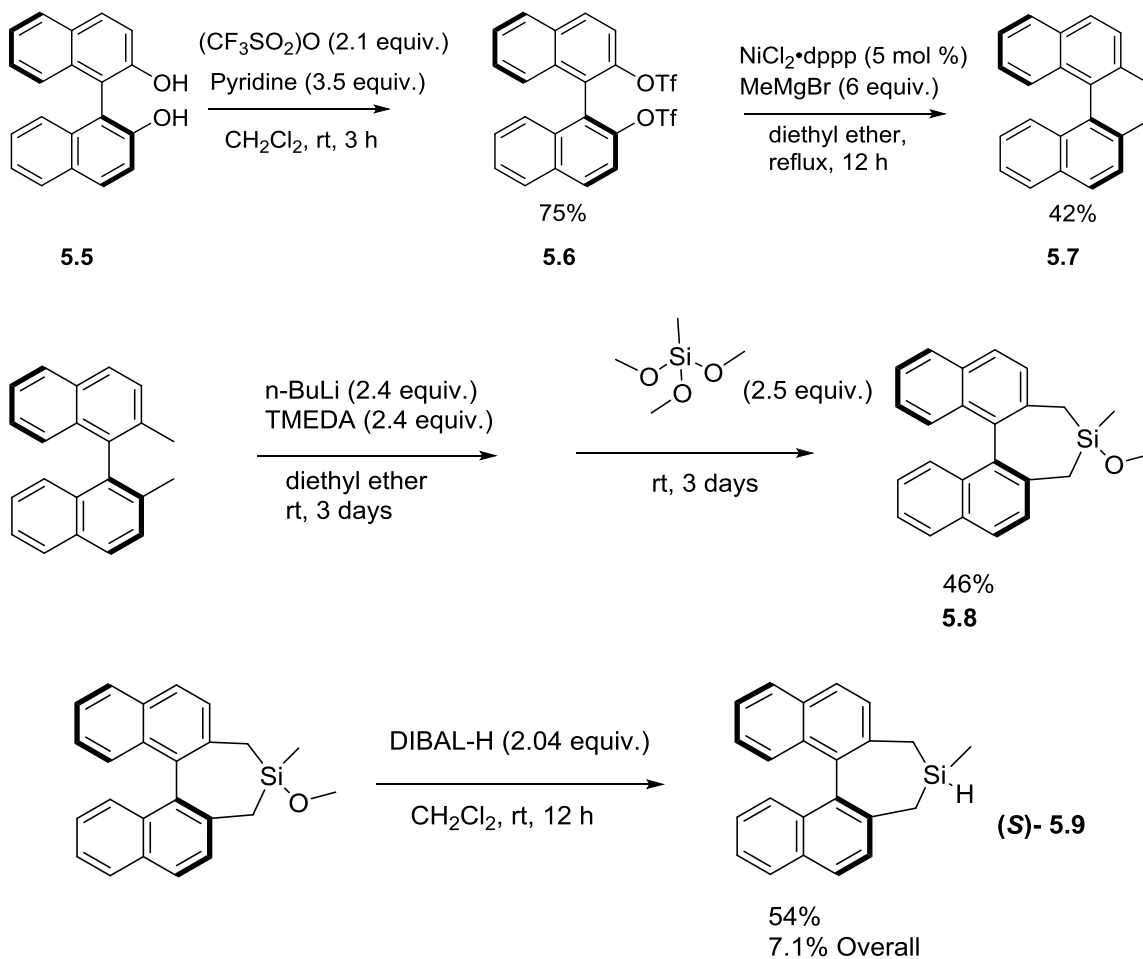
<sup>a</sup>Conversion determined by <sup>1</sup>H NMR. <sup>b</sup>Additional drying step employed

### 5.3 Synthesis of Stereogenic Silanes

There are no chiral silanes commercially available, thus all require synthetic preparation. Recent literature has reported several synthetic routes for obtaining chiral silanes. Two classifications are currently known: silanes stereogenic at silicon<sup>10, 14</sup> and silanes that are achiral at silicon but have chiral substituents.<sup>15</sup> Both classes of chiral silanes were synthesized and utilized in initial investigations.

An initial synthetic goal was silane **5.5**. The starting material (*S*)-BINOL **5.5** is commercially available and was utilized to yield the chiral silane over a five step synthesis with 7.1% overall yield (Scheme 5.2).<sup>15-16</sup> The triflate group is installed on **5.5** with triflic anhydride in presence of pyridine to yield **5.6** in excellent yield. With the appropriate triflate leaving groups installed, a nickel catalyzed Kumada coupling with methylmagnesium bromide yielded the dimethyl substituted binaphthyl **5.7**. Deprotonation of the benzylic protons with *n*-butyllithium-tetramethylethane diamine (TMEDA) and subsequent substitution of trimethoxymethylsilane afforded the methoxy silane **5.8**. A reduction of **5.8** using diisobutylaluminum hydride (DIBAL-H) afforded the

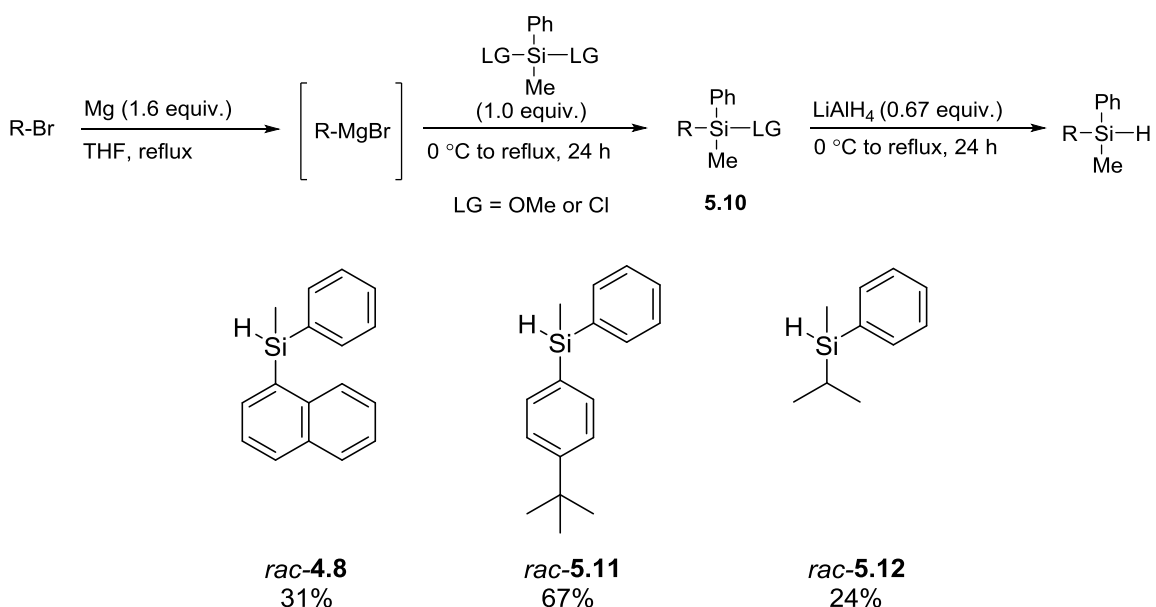
desired stereoenriched silane **5.9**. The stereoenriched silane is not stereogenic at silicon; therefore, the preparation of chiral silanes possessing stereocenters at silicon was next targeted.



### Scheme 5.2 Synthesis of a Stereoenriched Silane from (S)-BINOL

Efforts to synthesize and determine the selectivity of chiral silanes with asymmetry at the silicon atom are paramount to this study and could be more enantioselective in the proposed resolution. Various chiral at silicon silanes were synthetically prepared in order to effectively determine the functionality required to

induce chirality in the dehydrogenative coupling reaction. Silanes *rac*-**4.8**, *rac*-**5.11**, and *rac*-**5.12** were all prepared from reaction between one equivalent of the corresponding Grignard reagent and dimethoxymethylphenyl or dichloromethylphenylsilane (Scheme 5.3).<sup>17</sup> Silane *rac*-**4.8** was prepared from the dimethoxy silane whereas the others *rac*-**5.11**, and *rac*-**5.12** utilized the commercially available dichlorosilane. Reactions bearing a chloro leaving group were not isolated after the Grignard due to the reactivity of chlorosilanes. Intermediate **5.10** was reduced in one pot in this case. All silanes were reduced after the substitution with lithium aluminum hydride (LiAlH<sub>4</sub>) in refluxing THF.

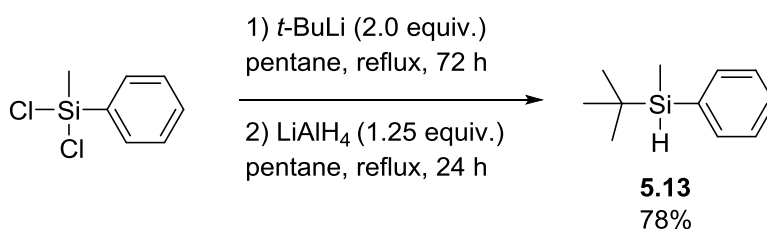


### Scheme 5.3 Synthesis of Stereogenic at Silicon Silanes

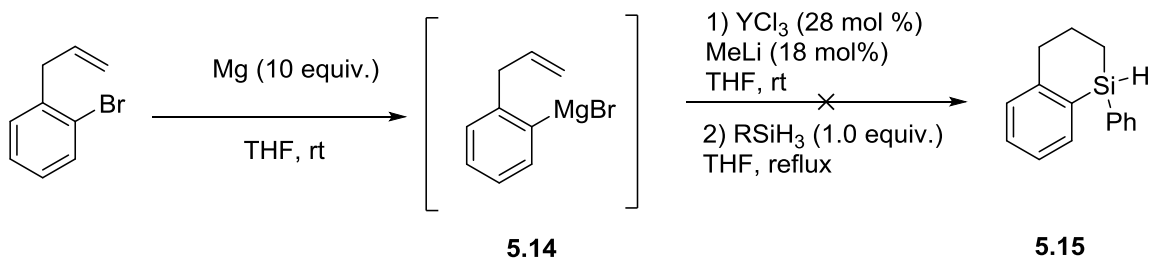
In addition to the three silanes prepared in Scheme 5.3, we also desired to prepare silanes possessing even more sterically demanding groups than the isopropyl group in **5.12**. The added sterics of the *tert*-butyl group were presumed to be close enough to the stereogenic center and thus site of inversion to provide a response in diastereoselectivity (*rac*-**5.13**). This sterically demanding silane was prepared from

dichloromethylphenylsilane in a one pot substitution-reduction method employing *tert*-butyl lithium as the nucleophile to displace a chloro leaving group. The intermediate was immediately reduced with LiAlH<sub>4</sub> to yield the desired silane in 78% overall yield (Scheme 5.4).

Next, a cyclic, chiral silane was targeted for preparation. In transition metal catalyzed hydrosilylation and dehydrogenative silicon-oxygen couplings, cyclic silanes such as *rac*-**5.15** have produced useful selectivities in kinetic resolutions such as those discussed in chapter 1. Oestreich and coworkers previously employed cyclic silane (*R*)-**5.15** (>99% ee) in the related B(C<sub>6</sub>F<sub>5</sub>)<sub>3</sub> hydrosilylation of prochiral ketones and produced moderate enantiomeric excess (up to 38% ee).<sup>8</sup> A method to prepare these silanes in two steps from commercially available starting materials was attempted.<sup>18</sup> The synthesis began with Grignard formation from commercially available *ortho*-allylbromobenzene. The Grignard was then added to a solution of yttrium (III) chloride and methyl lithium to facilitate metal insertion. Finally, phenylsilane was added to cause ring closure in refluxing THF. Unfortunately, the yttrium catalyzed ring closure product from the allylic Grignard **5.14** was never observed after several trials (Scheme 5.5).

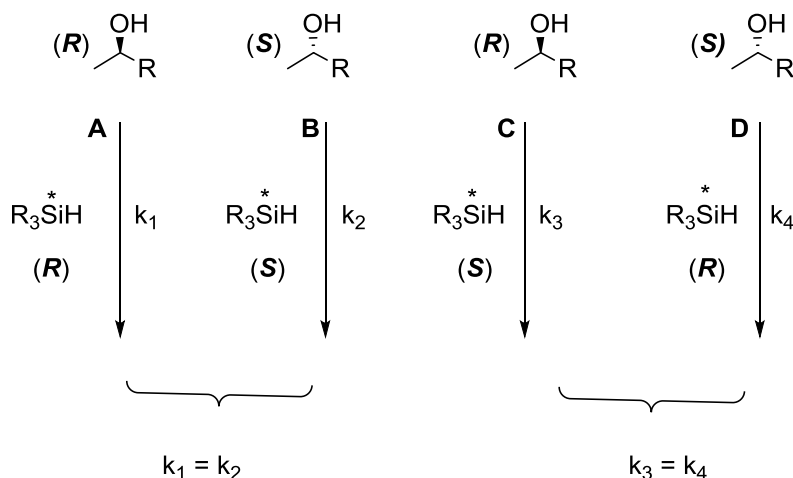


**Scheme 5.4 Preparation of Sterically Hindered *tert*-butylmethylphenylsilane**



**Scheme 5.5 Cyclic Silanes via a Two-Step Protocol**

These silanes were prepared in racemic form to determine the reactivity and diastereoselectivity in subsequent Lewis acid catalyzed resolutions. The diastereomeric ratios of the silyl ethers formed, via reaction of racemic silanes with racemic alcohols, have been demonstrated to predict the selectivity in subsequent kinetic resolutions (Scheme 5.6).<sup>19</sup> Pathways A/B and C/D are in fact enantiomeric and proceed at the same rate when both the silane and alcohol are racemic. These two combined pathways are diastereomeric and is the diastereomeric ratio after reaction completion. It is the ratio of these rates (For example.  $k_2$  and  $k_3$ , Scheme 5.6) that have been utilized to predict selectivity factor in non-racemic reactions. Thus, the racemic silanes were utilized without enantioenrichment which is a distinct advantage for our initial reaction investigations.



**Scheme 5.6 Use of Racemic Silanes in Initial Investigations**

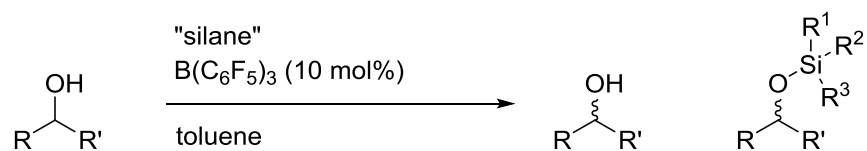
#### 5.4 Substrate Scope Investigations

With a variety of silanes in hand, the scope of compounds amenable to silylation was explored. The initial substrate scope for alcohols was limited to heterocyclic, benzylic and propargylic alcohols. This substrate testing process began by utilizing the silane (*S*)-**5.9** and *rac*-**4.8** (Table 5.2, Entries 1-4) and racemic 4-chromanol. The chiral silane **5.9** was utilized as the only stereoenriched reagent using the conditions in Table 5.2. No product formation was evident via <sup>1</sup>H NMR for the substrates tested presumably due to the steric demands of the silane (Entries 1-3). Extended reaction times did not result in product formation. (Entry 2) The heterocyclic alcohol would not convert even under forcing conditions (Table 5.2, Entry 4). Instead, only degradation products of the 4-chromanol were isolated, which was indicative of Lewis acid mediated ring opening. However, a clear advantage over more reactive silyl chlorides is the recyclability of silanes. Unreacted silane for each run was easily recovered, purified and reused in subsequent studies.



We next focused on other alcohols to test in the reaction to include propargylic alcohols and more simple benzylic alcohols the later was presumed to be less likely to degrade under Lewis acid catalysis. Investigations of propargylic alcohols and (*S*)- **5.9** resulted in no silyl ether formation. The failure of this silane to convert despite other silyl ethers forming more regularly led to (*S*)-**5.9** being abandoned as a viable silane in the transformation. The two propargylic alcohols converted more readily with both *rac*-**4.8** and **5.11**, but demonstrated poor diastereoselectivity with *rac*-**4.8** as the silane source. (Table 5.2, Entries 6 and 8) The diastereomeric ratios for products of a propargylic alcohol and *rac*-**5.11** could not be resolved via <sup>1</sup>H NMR or GC/MS (Table 5.2, Entry 7). A propargylic alcohol possessing bearing a terminal trimethylsilyl group failed to convert under similar conditions with *rac*-**5.6** (Table 5.2, Entry 8). When a simple benzylic alcohol, 1-phenylethanol, was tested the reaction also resulted in poor diastereoselectivity employing *rac*-**4.8**. Employing more bulky silanes **5.11** and **5.13** (Entry 10 and 11) also resulted in poor conversions. Overall, sterically demanding silanes and substrates failed to form silyl ethers under these general reaction conditions.

**Table 5.2 Borane Lewis Acid Catalyzed Silylation of Alcohols**

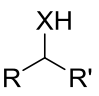
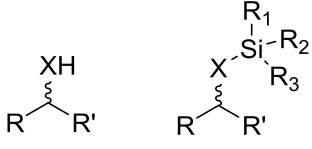
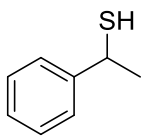
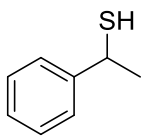
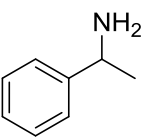
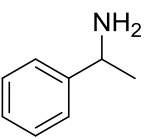


Entry	Substrate	"silane" (equiv.)	T (°C)	t (h)	% conv <sup>a</sup>	d.r. <sup>b</sup>
1		( <i>S</i> )- <b>5.9</b> (0.5)	25	12	--	--
2		( <i>S</i> )- <b>5.9</b> (0.5)	25	48	--	--
3		<i>rac</i> - <b>4.8</b> (1.0)	25	24	--	--
4		<i>rac</i> - <b>4.8</b> (1.0)	60	12	--	--
5		( <i>S</i> )- <b>5.9</b> (0.5)	25	24	--	--
6		<i>rac</i> - <b>4.8</b> (1.0)	25	12	59 (21)	53:47
7		<i>rac</i> - <b>5.11</b> (1.0)	25	12	>90 (68)	-- <sup>c</sup>
8		<i>rac</i> - <b>4.8</b> (1.0)	25	24	--	--
9		<i>rac</i> - <b>4.8</b> (1.0)	rt	12	(76)	41:59
10		<i>rac</i> - <b>5.11</b> (1.0)	rt	12	--	--
11		<i>rac</i> - <b>5.13</b> (1.0)	rt	24	--	--

<sup>a</sup>Conversion determined via <sup>1</sup>H NMR; Isolated yields shown in parenthesis.

<sup>b</sup>Diastereomeric ratios determined from <sup>1</sup>H NMR. <sup>c</sup>Diastereomeric ratio could not be determined from NMR or GC-MS analysis.

**Table 5.3 Further Investigations: Results with Alternate Nucleophiles**

$X = S, NH$ 		"silane" $B(C_6F_5)_3$ (10 mol%) Toluene				
Entry	Substrate	"silane" (equiv.)	T (°C)	t (h)	% conv <sup>a</sup>	d.r.
1		<i>rac</i> - <b>4.8</b> (1.0)	rt	12	--	--
2		<i>rac</i> - <b>4.8</b> (1.0)	60	12	--	--
3		<i>rac</i> - <b>5.13</b> (1.0)	rt	12	--	--
4		Ph <sub>3</sub> SiH (1.0)	rt	12	--	--

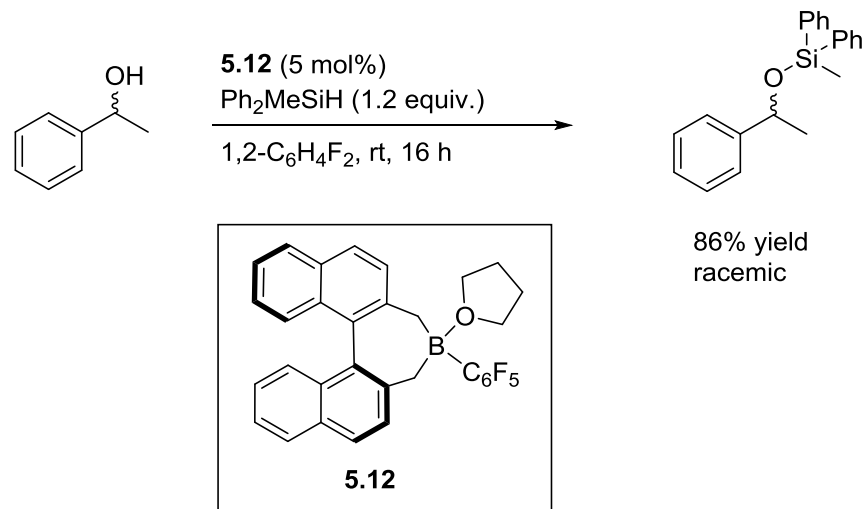
<sup>a</sup>Conversion determined by <sup>1</sup>H NMR.

Research endeavors next focused on substrates other than the alcohols tested previously. Alternate functional groups attempted included thiols and amines. Chiral thiols have been utilized as precursors to valuable catalysts for asymmetric synthesis, however very few studies have successfully produced these enantiopure compounds.<sup>20-21</sup> Recently, silanes in presence of  $B(C_6F_5)_3$  have cleanly silylated thiols. Additionally, the sulfur silicon bond formed in these reactions proved resilient to hydrolysis and solvolysis.<sup>3</sup> We also hypothesized thiols would be less willing to form a complex with the catalyst. The commercially available methylphenyl mercaptan was tested with silanes **4.8** and **5.13** as the silyl sources (Table 5.3, Entries 1-3). These reactions failed to form silicon-sulfur dehydrogenative coupling products. A primary amine, 1-phenylethylamine, was examined with triphenyl silane as the silyl source; however, no product was observed

(Table 5.3, Entry 4). Poor reactivity of amines in the dehydrogenative coupling are most likely due to the strong complexation observed between amines and the  $B(C_6F_5)_3$  catalyst.<sup>22</sup>

### 5.5 Conclusions and Outlook

Generally, these experiments demonstrate a reaction that is not reproducible or general across the substrate scope examined. This is most likely a result of substrate dependence represented by the  $K_{eq}$  between complex **5.1** and free catalyst. The stability of this complex most likely varies widely based upon substrate; therefore, the reactions are highly substrate sensitive. In addition to the problem of generality, the chiral silane may not be the best source of chirality in the  $S_N2$  transition state. The inversion process at silicon in the mechanism would cause the stereocenter to become more planar and less able to affect the approach of chiral nucleophiles. An alternate approach to a borane catalyzed resolution employing a stereo-enriched borane catalyst, has recently been explored.<sup>23</sup> When a bulky borane bearing chiral appendages is utilized a silicon-oxygen coupling with diphenylmethylsilane a non-enantioselective reaction is observed (Scheme 5.8).



**Scheme 5.7 Asymmetric Silicon-Oxygen Coupling Catalyzed by an Axillary Chiral Borane**

The borane catalyst  $\text{B}(\text{C}_6\text{F}_5)_3$  has been demonstrated to be far more useful in the hydrosilylation of  $\pi$  bonds including carbonyls, alkenes and imines.<sup>3, 7</sup> Overall, the results for this approach to the enrichments of alcohol, thiols, or amines do not demonstrate the promising results needed to warrant further investigation.

## 5.6 Experimental

### General Information

All reactions were carried out in oven-dried glassware under nitrogen or argon. Molecular sieves were activated in an oven at 175 °C at least 24 h prior to use. dichloromethane ( $\text{CH}_2\text{Cl}_2$ ), tetrahydrofuran (THF), diethyl ether, and methanol were degassed and passed through a column of activated alumina prior to use. Toluene utilized in kinetic resolutions was passed through a column of activated alumina followed by drying over  $\text{CaH}_2$  and fractional distillation. The thus obtained toluene was stored over 4 angstrom molecular sieves in a desiccator until ready for use. Unless otherwise stated, all

reagents or starting materials were obtained from Aldirch, Acros, TCI, or Alfa Aesar and used without further purification.  $^1\text{H}$  NMR was taken on a Varian Mercury/ VX (300 MHz or 400 MHz).  $^{13}\text{C}$  NMR spectra were taken on a Varian Mercury/ VX (100 MHz). Gas Chromatography/ Mass spectrometry (GC/MS) was submitted to and conducted by the Department of Chemistry and Biochemistry mass spectrometry facility at the University of South Carolina.

### **Synthesis of chiral silane, 5.9**

Silane (*S*)-5.9 was synthesized via a method similar to the literature reference.<sup>15</sup> Commercially available (*S*)-BINOL 5.5 was utilized as starting material in place of the starting material in the reference.

### **(*S*)-Bistriflate 5.6**

(*S*)-BINOL (2.2 g, 8 mmol) was dissolved in 20 mL of dichloromethane in an oven dried 100 mL round bottom flask fitted with septum. Freshly distilled pyridine (2.25 mL, 3.5 mL) was added via syringe with stirring. Triflate anhydride (2.8 mL, 2.1 mmol) was handled under Argon and added to the reaction mixture at 0 °C dropwise. The yellow solution was allowed to warm to room temperature and stirred an addition 3 h. A white precipitate formed. The salts were filtered off and the solvent removed via rotary evaporation. The residue was dissolved in ethyl acetate and washed with 5% HCl followed by sat.  $\text{NaHCO}_3$  and brine. The organic layer was then dried over  $\text{Na}_2\text{SO}_4$ . Volatiles were removed under rotary evaporation to yield a viscous yellow oil. The crude oil was purified via flash chromatography (hexanes) to yield 4.14 g, 75 % of (*S*)-bistriflate as a white solid.  $^1\text{H}$  NMR (300 MHz  $\text{CDCl}_3$ ):  $\delta = 7.25- 7.28$  (m, 3 H), 7.40-7.45 (t, 2 H), 7.57-7.65 (m, 3 H), 8.01- 3.03 (d, 2 H), 8.14- 8.17 (d, 2 H).

### **(S)-2-2'-dimethyl-1-1'-binaphthalene 5.7**

(S)-Bistriflate **5.6** (4.1 g, 7.4 mmol) was dissolved in 30 mL of diethyl ether in an oven dried three necked flask fitted with septum, condenser and stir bar. The NiCl<sub>2</sub> dppp (201 mg, 0.372 mmol, 5 mol %) was weighed under N<sub>2</sub> and added directly to the flask. The mixture was cooled to 0 °C and 14.9 mL of a 3.0 M solution in ether of MeMgBr was added slowly via gastight syringe. The yellow solution was then warmed to room temperature then brought to a gentle reflux for 24 h. The resulting black solution was cooled to 0 °C and the reaction was quenched by careful addition of deionized water followed by 10 mL of a 10% HCl solution. The organic layer was then separated and the aqueous layer was extracted three times with diethyl ether. The volatiles were removed via rotary evaporation to yield a yellow oil. The crude oil was purified on a column (hexanes) to yield the pure product as a white solid, 877 mg, 42%. <sup>1</sup>H NMR (300 MHz CDCl<sub>3</sub>): δ = 2.0 (s 6 H), 7.04-7.07 (d, 2H), 7.19-7.25 (t, 2 H), 7.37-7.43 (t, 2 H), 7.50-7.54 (d, 2H), 7.87-7.92 (m, 4 H).

### **(S)- 4-methoxy-4-methyl-4,5-dihydro-3H-dinaphtho[2,1-c:1',2'-e]silepine 5.8**

A 250 mL oven dried round bottom flask was equipped with stir bar and septum. 500 mg of (S)-2-2'-dimethyl-1-1'-binaphthalene **5.7** was added and dissolved in 50 mL of diethyl ether with stirring. Tetramethylethanediamine (TMEDA, 644 μL, 4.32 mmol) was added via syringe. The solution was then cooled to 0 °C and n-BuLi in hexanes (2.54 mL, 1.7 M, 4.32 mmol) was added dropwise. The solution was then allowed to warm to room temperature and stirred for 2 days obtaining a red-brown coloration. An additional 10 mL of diethyl ether was added to dissolve remaining precipitates. The solution was then

cooled to 0 °C and methyltrimethoxysilane (652  $\mu$ L, 4.57 mmol) was added neat drop wise. The reaction was again allowed to warm to room temperature and allowed to stir 4 days. The solution obtained a grey coloration. The reaction was then carefully quenched by addition of 10 mL of  $\text{NH}_4\text{Cl}$  at 0 °C. The organic layer was removed and the aqueous layer was then extracted three times with diethyl ether. The organic layers were combined washed with brine and dried over  $\text{Na}_2\text{SO}_4$ . Removal of volatiles under rotary evaporation yielded a yellow oil. The crude mixture was purified on a gradient column of hexanes, 3 % diethyl ether: 97 % hexanes. 201 mg of starting material is recovered in initial fractions. The desired product was recovered after increased polarity as a white solid, 175 mg, 27.9 %.  $^1\text{H}$  NMR (400 MHz  $\text{CDCl}_3$ ):  $\delta$  = 0.03 (s, 3H), 1.77-1.81 (d, 1 H), 1.98-2.01 (d, 1H), 2.08- 2.14 (m, 2H), 3.31 (s, 3 H), 6.99-7.16 (m, 4H), 7.27-7.33 (m, 3 H), 7.39-7.42 (d, 1H), 7.74- 7.79 (m, 4 H).

(*S*)-methoxy silane **5.8** (175 mg, 0.494 mmol) is added to an oven dried 4 dram vial fitted with stir bar and septum. The solid was then dissolved in 5 mL of dichloromethane. The solution was then cooled to -78 °C in a dry ice/ acetone bath. DIBAL-H (1.0 mL, 1.0 mmol, 1 M in toluene) was then added drop wise with stirring. The reaction was then allowed to warm to room temperature and stirred 12 h. The solution was cooled to 0 °C and quenched by addition of acetone. After transfer to a separatory funnel, the emulsion formed was broken up by addition of 1 M HCl. The organic layer was separated and the aqueous layer was washed with diethyl ether three times. The organic layers were combined and washed with  $\text{NaHCO}_3$ , brine, and dried of  $\text{Na}_2\text{SO}_4$ . Volatiles were removed under rotary evaporation and the colorless oil was further purified by passage



through a pad of silica gel with hexanes. The desired chiral silane (*S*)-**5.9** was thus acquired as a white solid after removal of volatiles, 93 mg 53.9 %. <sup>1</sup>H NMR (300 MHz CDCl<sub>3</sub>): δ = 0.13-0.14 (d, 3 H), 1.82-1.88 (q, 1 H), 1.94-1.98 (d, 1 H), 2.08- 2.17 (t, 2 H), 7.11-7.22 (m, 4 H), 7.36-7.48 (m, 4 H), 7.85-7.91 (t, 4 H). MS (ESI) [M<sup>+</sup>] = 324

### Synthesis of Racemic Asymmetrically Substituted Silanes- General Procedure

The synthesis of *rac*-**4.8**, **5.11** and **5.12** follow a similar procedure. The electrophile dimethoxy and dichloromethylphenyl silane affords the desired products following the procedure outlined in Scheme 5.5. The procedure for the preparation of **4.8** is shown below and is shown as a representative procedure.

#### Dimethoxymethylphenyl silane

The starting material for many racemic silanes was prepared from dichloromethylphenyl silane. A 100 mL round bottom flask fitted with septum and stir bar was charged with 15 mL of methanol and followed by 3.04 mL (21.9 mmol) of freshly distilled triethylamine. The solution was then cooled to 0 °C with stirring and 1.7 mL (10.45 mmol) dichloromethylphenyl silane was handled under Nitrogen and added to the flask carefully via syringe. The solution was allowed to warm to room temperature and stirred for 4 h. Hexanes was then added to the reaction mixture and the resulting mixture transferred to a separatory funnel. The organic layer was separated and the methanol/ amine layer was washed with hexanes three times. The organic layers were combined and removed of volatiles via rotary evaporation to yield a yellow liquid. The crude liquid was passed through a pad of silica gel with dichloromethane to yield the title compound as a clear

colorless liquid, 1.91g 63.2%.  $^1\text{H NMR}$  (300 MHz  $\text{CDCl}_3$ ):  $\delta$  = 0.0 (s, 3 H), 3.21 (s, 6 H), 7.02-7.04 (m, 3 H), 7.25-7.27 (d, 2 H).

### **methoxymethylnaphthylphenyl silane**

Mg turnings (219.7 mg, 9.04 mmol) were thermally and mechanically activated in a nitrogen flushed 25 mL three-necked round bottom flask fitted with stir bar, septa and condensor. Toluene (0.26 mL), diethyl ether (0.53 mL) and tetrahydrofuran (0.26 mL) was added to the turnings with vigorous stirring. Freshly distilled 1-bromonaphthalene (1.14 mL, 8.22 mmol) was added dropwise. Once the reaction had initiated the dark brown mixture was heated to reflux for 15 min. The grignard was then cooled to room temperature. Dimethoxymethylphenyl silane (1.5 mL, 8.22 mmol) was added neat and the reaction was heated to reflux for 12 h. The mixture was then cooled to 0 °C and quenched slowly with sat.  $\text{NH}_4\text{Cl}$ . Diethyl ether was added and the mixture transferred to a separatory funnel. The organic layer was removed and the aqueous layer was washed with diethyl ether three times. The organic layers were combined, washed with water and brine then dried of  $\text{Na}_2\text{SO}_4$ . Volatiles were removed via rotary evaporation to yield a green oil. The crude oil was passed through a column using 1% diethyl ether to 99% hexanes to yield a pale green solid. The solid was then recrystallized three times from cold pentane to yield the pure product as a white solid, 845 mg 36.9 %.  $^1\text{H NMR}$  (300 MHz  $\text{CDCl}_3$ ):  $\delta$  = 0.80 (s, 3 H), 3.58 (s, 3 H), 7.37-7.48 (m, 6 H), 7.61-7.64 (d, 2 H), 7.77-7.79 (m, 3 H), 8.15-8.18 (d, 1 H).

**Methylphenylnaphthyl silane, *rac*-4.8:**

Methoxymethylnaphthylphenyl silane (150 mg, 0.54 mmol) was added to a 15 mL round bottom flask fitted with stir bar and septum. The flask was then charged with 8 mL of dichloromethane. The solution was then cooled to -78 °C in a dry ice/ acetone bath and 550 µL of diisobutylaluminum hydride (DIBAL-H, 1.0M) in toluene was added slowly. The reaction was allowed to warm to room temperature and a second addition of DIBAL-H (550 µL, 1.0 M) was made. The reaction was allowed to stir for 12 h. The reaction vessel was again cooled to -78 °C and quenched with acetone. The reaction mixture was then transferred to a separatory funnel and the emulsion was broken up with 1 mL of concentrated HCl followed by water ~10 mL. The aqueous layer was washed three times with diethyl ether and the organic layers combined. The organic layers were then washed with NaHCO<sub>3</sub>, brine, and dried over Na<sub>2</sub>SO<sub>4</sub>. Removal of volatiles by rotary evaporation yielded a clear colorless oil. The desired product was further purified by passage through a pad of silica gel with hexanes to yield a clear colorless oil that solidified to a white solid upon freezing, 115.3 mg, 86 %. <sup>1</sup>H NMR (300 MHz CDCl<sub>3</sub>): δ = 0.77- 0.79 (d, 3H), 5.36-5.40 (q, 1 H), 7.34-7.51 (m, 6 H), 7.58-7.61 (d, 2 H), 7.75-7.77 (d, 1 H), 7.87-7.95 (m, 2 H), 8.07-8.09 (d, 1 H). MS (ESI): [M<sup>+</sup>]: 248.

**(4-(*tert*-butyl)phenyl)(methyl)(phenyl)silane, *rac*-5.11:**

Mg turnings (190mg, 1.6 equiv.) were activated by stirring vigorously under argon 6h in an oven dried three-necked flask fitted with oven dried condenser and septa. The magnesium was then covered with THF and 4-*tert*-butylphenyl-1-bromide was added neat (850 µL) dropwise with stirring. Once the reaction had initiated, the solution was

heated to reflux for 1h. The black solution was then cooled to 0 °C and dichloromethylphenylsilane (4.9 mL, 1.0 M in THF) was added dropwise. The solution was again heated to reflux for 18 h. The solution was then cooled to 0 °C and LiAlH<sub>4</sub> (123 mg, 0.67 equiv.) was added directly under a funnel of nitrogen. The reaction was then heated to reflux for 18 h. The LiAlH<sub>4</sub> was carefully quenched with ethyl acetate at 0 °C. The solution was then added to a separatory funnel half filled with crushed ice and 2 mL of concentrated HCl. The organic layer was removed and the aqueous layer was washed three times with diethyl ether. The organic layers were combined, washed with sat. NaHCO<sub>3</sub>, brine, and then dried over Na<sub>2</sub>SO<sub>4</sub>. The solvent was removed and the crude mixture purified via flash chromatography (hexanes) to yield 875 mg of *rac*-**5.13** as a clear colorless liquid, 67.3%. <sup>1</sup>H NMR (300 MHz CDCl<sub>3</sub>): δ = 0.77-0.79 (m, 3 H), 1.46-1.49 (m, 9 H), 5.11-5.13 (q, 1 H), 7.48-7.66 (m, 5 H), 7.68-7.76 (m, 4 H). <sup>13</sup>C NMR: δ = 4.9, 31.2, 34.6, 124.9, 127.9, 129.4, 131.7, 134.7, 135.5, 152.4. MS (ESI): [M<sup>+</sup>]: 254.

### **General procedure for borane catalyzed silicon oxygen couplings with chiral silanes<sup>2</sup>**

The reaction of 1-phenyl-3-propyn-1-ol utilizing *rac*-**4.8** is typical. An oven dried 1 dram vial is equipped with septum and stir bar. The vial is then charged with silane (1.0 equiv., 49.6 mg, 0.2 mmol) followed by addition of (40.8 mg, 42.5 μL, 0.2 mmol) of the alcohol via syringe. The vial was then evacuated and purged with Argon by fitting the vial with a balloon. The mixture was then dissolved in 1 mL of toluene with stirring. 10.2 mg, 0.02 mmol of the B(C<sub>6</sub>F<sub>5</sub>)<sub>3</sub> catalyst was added via gas tight syringe as a 0.2 M solution in toluene. This solution was prepared immediately prior to use. Gas evolution and color change from clear colorless to yellow was clearly evident. The vial was left to stir 12 h at

room temperature. A small sample was removed via syringe and removed of volatiles under vacuum. The crude mixture was analyzed via  $^1\text{H}$  NMR indicating 59.7 % conversion based on the geminal protons to the alcohol and silyl ether at  $\delta = 5.15$  and 6.16 respectively. Diastereomeric ratio was estimated to be 53.3: 46.7 based on integration of baseline separated peaks at  $\delta=2.53$  and 5.53. The reaction mixture was then passed through a pad of silica gel with dichloromethane to remove the catalyst. The volatiles were removed via rotary evaporation followed by high vacuum. The crude mixture is then purified on column using hexanes and dichloromethane (4:1) to yield the protected alcohol as a yellow oil, 16.2 mg, 21.4 %. GC/MS analysis unsuccessfully separated the diastereomeric mixture.

## 5.7 References

1. Keith, J. M.; Larrow, J. F.; Jacobsen, E. N. Practical Considerations in Kinetic Resolution Reactions. *Adv. Synth. Catal.* **2001**, *343*, 5.
2. Denmark, S. E.; Beutner, G. L. Lewis Base Catalysis in Organic Synthesis. *Angew. Chem., Int. Ed.* **2008**, *47*, 1560.
3. Blackwell, J. M.; Foster, K. L.; Beck, V. H.; Piers, W. E. B(C<sub>6</sub>F<sub>5</sub>)<sub>3</sub>-Catalyzed Silylation of Alcohols: A Mild, General Method for Synthesis of Silyl Ethers. *J. Org. Chem.* **1999**, *64*, 4887.
4. Rendler, S.; Auer, G.; Oestreich, M. Kinetic Resolution of Chiral Secondary Alcohols by Dehydrogenative Coupling with Recyclable Silicon-Stereogenic Silanes. *Angew. Chem., Int. Ed.* **2005**, *44*, 7620.
5. Klare, H. F. T.; Oestreich, M. Chiral Recognition with Silicon-Stereogenic Silanes: Remarkable Selectivity Factors in the Kinetic Resolution of Donor-Functionalized Alcohols. *Angew. Chem., Int. Ed.* **2007**, *46*, 9335.
6. Greene, T. W.; Wuts, P. G. M., *Protective Groups in Organic Synthesis*. 3 ed.; John Wiley and Sons: New York, USA, 1999.
7. Piers, W. E.; Marwitz, A. J. V.; Mercier, L. G. Mechanistic Aspects of Bond Activation with Perfluoroarylboranes. *Inorg. Chem.* **2011**, *50*, 12252.
8. Hog, D. T.; Oestreich, M. B(C<sub>6</sub>F<sub>5</sub>)<sub>3</sub>-Catalyzed Reduction of Ketones and Imines Using Silicon-Stereogenic Silanes: Stereoinduction by Single-Point Binding. *Eur. J. Org. Chem.* **2009**, *2009*, 5047.
9. Shinke, S.; Tsuchimoto, T.; Kawakami, Y. Stereochemistry in Lewis Acid-Catalyzed Silylation of Alcohols, Silanols, and Methoxysilanes with Optically Active Methyl(1-naphthyl)phenylsilane. *Silicon Chem.* **2007**, *3*, 243.

10. Oestreich, M. Silicon-Stereogenic Silanes in Asymmetric Catalysis. *Synlett* **2007**, 2007, 1629.
11. Sommer, L. H.; Frye, C. L.; Parker, G. A.; Michael, K. W. Stereochemistry of Asymmetric Silicon. I. Relative and Absolute Configurations of Optically Active  $\alpha$ -Naphthylphenylmethylsilanes. *J. Am. Chem. Soc.* **1964**, 86, 3271.
12. Kagan, H. B.; Fiaud, J. C., In *Topics in Stereochemistry*, L., E.; Wilen, S. H., Eds. John Wiley and Sons: 1988; pp 249.
13. Sheppard, C. I.; Taylor, J. L.; Wiskur, S. L. Silylation-Based Kinetic Resolution of Monofunctional Secondary Alcohols. *Org. Lett.* **2011**, 13, 3794.
14. Corriu, R. J. P.; Guérin, C.; Moreau, J. J. E., Stereochemistry at Silicon. In *Topics in Stereochemistry*, John Wiley & Sons, Inc.: 1984; Vol. 15, pp 43.
15. Johannsen, M.; Jørgensen, K. A.; Helmchen, G. Synthesis and Application of the First Chiral and Highly Lewis Acidic Silyl Cationic Catalyst. *J. Am. Chem. Soc.* **1998**, 120, 7637.
16. Jung, M. E.; Hogan, K. T. Chirality Transfer from Silicon to Carbon: Use of Optically Pure Cyclic Silanes with a Binaphthalene Chiral Unit. *Tetrahedron Lett.* **1988**, 29, 6199.
17. Larson, G. L.; Torres, E. Asymmetric Induction by Chiral Silicon Groups. *J. Organomet. Chem.* **1985**, 293, 19.
18. Oestreich, M.; Königs, C. Shortened Synthesis of a Silicon-Stereogenic Cyclic Silane. *Synthesis* **2011**, 2011, 2062.
19. Rendler, S.; Plefka, O.; Karatas, B.; Auer, G.; Fröhlich, R.; Mück-Lichtenfeld, C.; Grimme, S.; Oestreich, M. Stereoselective Alcohol Silylation by Dehydrogenative Si–O Coupling: Scope, Limitations, and Mechanism of the Cu–H-Catalyzed Non-Enzymatic Kinetic Resolution with Silicon-Stereogenic Silanes. *Chem. – Eur. J.* **2008**, 14, 11512.
20. Strijtveen, B.; Kellogg, R. M. Synthesis of (Racemization Prone) Optically Active Thiols by SN2 Substitution Using Cesium Thiocarboxylates. *J. Org. Chem.* **1986**, 51, 3664.

21. Peschiulli, A.; Procuranti, B.; O' Connor, C. J.; Connon, S. J. Synergistic Organocatalysis in the Kinetic Resolution of Secondary Thiols with Concomitant Desymmetrization of an Anhydride. *Nat. Chem.* **2010**, *2*, 380.
22. Mountford, A. J.; Lancaster, S. J.; Coles, S. J.; Horton, P. N.; Hughes, D. L.; Hursthouse, M. B.; Light, M. E. Intra- and Intermolecular N–H···F–C Hydrogen-Bonding Interactions in Amine Adducts of Tris(pentafluorophenyl)borane and -alane. *Inorg. Chem.* **2005**, *44*, 5921.
23. Mewald, M.; Fröhlich, R.; Oestreich, M. An Axially Chiral, Electron-Deficient Borane: Synthesis, Coordination Chemistry, Lewis Acidity, and Reactivity. *Chem. – Eur. J.* **2011**, *17*, 9406.